Novel Organic Transformations Arising from Gold(I) Chemistry

By

Mathieu André Morin

Thesis submitted to the faculty of Graduate and Postdoctoral Studies

In partial fulfillment of the requirements for the

Ph.D. degree in chemistry

Candidate

Mathieu André Morin

Supervisor

Dr. Louis Barriault

Ottawa-Carleton Chemistry Institute

Faculty of Science

University of Ottawa

Abstract

The use of gold in organic chemistry is a relatively recent occurrence. In addition to being previously considered too expensive, it was also believed to be chemically inert. Soon after the early reports indicating its rich reactivity, the number of reports on chemical transformations involving gold sky rocketed. One such report by Toste and coworkers demonstrated the intramolecular addition of silyl enol ether onto Au(I) activated alkynes, resulting in a 5-*exo dig* cyclization. The first part (Chapter 1) of this thesis discusses the development of a Au(I) catalyzed polycyclization reaction inspired by this transformation. The reaction demonstrated the ability of Au(I) to successfully catalyze the formation of multiple C-C bonds and resulted in the synthesis of benzothiophenes, benzofurans, carbazoles and hydrindene.

With the current resurgence of photochemical transformations being reported in literature, various opportunities for the use of Au(I) complexes arose. The substantial relativistic effect observed in gold which make it a good *soft* Lewis acid also has a significant influence on the redox potential of this metal. Chapter 3 of this thesis discusses the development of a Au(I) photocatalyzed process which benefits from having both a strong oxidation and reduction potential for the reduction of carbon-halide bonds. Radical reductions and cyclizations were accessed with the use of polynuclear Au(I) photocatalysts. In depth analysis of catalytically active Au(I) complexes helped elucidate the mechanism by which this photochemical reaction occurs. This part (Chapter 4) also covers serendipitously discovered uncatalyzed photochemical transformations derived from our work with gold. The halogenation reaction of primary alcohols was successfully achieved and a combination of our developed methods resulted in an efficient dehydroxylation protocol.

Acknowledgement

The time spent working towards this thesis has allowed me the pleasure of interacting with many people who have made this an enriching experience and without whose support this final product would not have been possible. I would like to first thank Prof. Louis Barriault for bringing me into the realm of chemical research. The guidance and experience I have received under his mentorship have been essential to my development as an organic chemist. I am very grateful for his willingness to place such confidence in me and allow me the freedom to pursue this new branch of chemistry with the lab.

I would also like to thank Prof. Derek Pratt for answering my many questions about chemistry. The amount of knowledge he shared with me, especially during the first years of my Ph. D. has been instrumental in solidifying my understanding of chemistry.

Merci à mes parents, Eric et Solange pour leur amour et support pendant toutes ces années. Malgré la distance ils ont toujours été présents en temps de besoin et ont toujours cru en moi.

I would like to thank numerous people both within and outside the lab for their friendship and support; Patrick Levesque for being both a wonderful teacher in the ways of chemistry and a great roommate for several years. Terry McCallum who I was fortunate enough to share many publications and many beers, I am incredibly grateful to have you as a friend and colleague. Gabriel Bellavance for great conversation both about chemistry and literally everything else (I will get to Mars….). Philippe McGee who I was lucky enough to know since my undergraduate studies, who has enriched my experiences in chemistry and taught me so much. Thank you to the

many people I have interacted with throughout these many years, Spencer, J-P, Guillaume, David, Frank, Jason, Joel, Travis, Alex, Colombe, Amandine, Laurie-Anne, Julie, Mike, Huy, Sam.

From outside the lab I would like to thank my friends who had to sometimes remind me that I could talk about things other than chemistry. Jenn, Alex, Dré, J.R., Angie, Gen and Vince, with whom I have shared many great nights and stories. Thank you Alyssa for your love and patience when I go on about chemistry, I am grateful to have you in my life.

Contributions to Research

Refereed Publications:

Tran, H.; McCallum, T.; **Morin**, M.; Barriault, L*. ‘‘Homocoupling of Iodoarenes and Bromoalkanes Using Photoredox Gold Catalysis: A Light Enabled Au(III) Reductive Elimination’’ *Org. Lett.* (2016) 4308 – 4311

McTiernan, S. D.; **Morin, M.**; McCallum, T.; Scaiano, J.C.*; Barriault, L.* ‘‘Polynuclear Gold (I) Complexes in Photoredox Catalysis: Understanding their Reactivity through Characterization and Kinetic Analysis’’ *Catal. Sci. Technol.* (2016) 201 – 207

McCallum, T.; Slavko, E.; **Morin, M.**; Barriault, L.*; ‘‘Light-Mediated deoxygenation of alcohols with a Dimeric Gold Catalyst’’ *Euro. J. Org. Chem.* (2015) 81 – 85

Revol, G.; McCallum, T.; **Morin, M.**; Gagosz, F.*; Barriault, L.*; Photoredox Transformations with Dimeric Gold Complexes*, Angew. Chem. Int. Ed.* (2013),13342 – 13345

Morin, M.; Levesque, P.; Barriault, L.*; Gold(I)-catalyzed domino cyclization for the synthesis of polyaromatic heterocycles, *Beilstein J. Org. Chem.* (2013) 2625 – 2628

Contributing Author:

Barriault, L.; **Morin, M.** (2016) ‘‘The Nazarov Cyclization of Cross-Conjugated Ketones’’, *Cross Conjugation: Modern Dendralene, Radialene and Fulvene Chemistry*, **Wiley-VCH** (Eds. Hopf, H.; Sherburn, M. ISBN: 978-3-527-33437-7)

Oral Presentations:

Revol, G.; McCallum, T.; **Morin, M.***; Gagosz, F.; Barriault, L. (2013) ‘‘Photoredox Transformations with Dimeric Gold Complexes’’ *Centre for Catalysis Research and Innovation* (Regional)

Poster Presentations:

Morin, M.*; McCallum, T.; Barriault, L. (2016) ‘‘Methylating with Methanol’’ *Gordon Research Conference; Natural Products & Bioactive Compounds* (International)

Morin, M.*; McCallum, T.; Barriault, L. (2015) ‘‘Light Initiated Cascade Reaction for the Synthesis of Polycyclic Compounds’’ *International Chemical Congress of Pacific Basin Societies* (International)

Morin, M.*; McCallum, T.; Barriault, L. (2015) ‘‘Light Initiated Radical Polycylization of Cyclopropyl Containing Compounds’’ *98th Canadian Chemistry Conference and Exhibition* (International)

Morin, M.*; McCallum, T.; Barriault, L. (2014) ‘‘Photo-Activated Gold Catalysts: Bridging Bis-Phosphine and Bis-Carbene Ligands’’ *19th International Symposium on Homogeneous Catalysis* (International)

Morin, M.*; McCallum, T.; Barriault, L. (2013) ‘‘Photo-Activated Gold Catalysts: Light Mediated SET for Radical Formation’’ *6th Pacific Symposium on Radical Chemistry* (International)

Morin, M.*; Levesque, P.; Barriault, L. (2012) ‘‘Heterocycle Synthesis via Au(I)/ Prins cyclisation and efforts towards synthesis of dihydrojunenol’’ *Synthesis Day, Université d’Ottawa* (Regional)

Morin, M.*; Levesque, P.; Barriault, L. (2011) ‘‘Synthèse d’hétérocycles par une cascade Au(I)/cyclisation Prins’’ *23e Colloque de Chimie de Sherbrooke* (Provincial)

Table of Contents

Schemes

Tables

Figures

Details of Contributions

Tran, H.; McCallum, T.; Morin, M.; Barriault, L*. *Org. Lett.* (2016) 4308 – 4311

- Supervising student. Mechanistic elucidation. Initial dimerization of alkanes.

McTiernan, S. D.; Morin, M.; McCallum, T.; Scaiano, J.C.*; Barriault, L.* *Catal. Sci. Technol.* (2016) 201-207

- Synthesis and characterization of Au(I) complexes. Evaluation of complexes for catalytic activity.

McCallum, T.; Slavko, E.; Morin, M.; Barriault, L. *Euro. J. Org. Chem.* (2015) 81–85

- Mechanistic elucidation.

Revol, G.; McCallum, T.; Morin, M.; Gagosz, F.*; Barriault, L.* *Angew. Chem. Int. Ed.* (2013),13342–13345

- Intermolecular radical addition optimization, aryl bromide cyclization, lighting system modification and mechanistic elucidation.

Morin, M.; Levesque, P.; Barriault, L. *Beilstein J. Org. Chem.* (2013) 2625–2628

- Synthesis and characterization of all compounds and intermediates.

1 Introduction

Metal catalyzed-processes are immensely important in organic chemistry. More particularly, catalysis using transition metals such as Pd, Ru, Ir and Os (to name a few) is the cornerstone for the development of efficient and reliable synthetic methods for the formation of new C-C, C-O and C-N bonds. Where once only research groups specializing in these reactions would approach them, modern developments have rendered many transition metal reactions almost a mundane occurrence in the daily lives of chemists. Since the year 2000, three Nobel

Scheme 1.1: Nobel prizes awarded for metal-catalyzed transformations

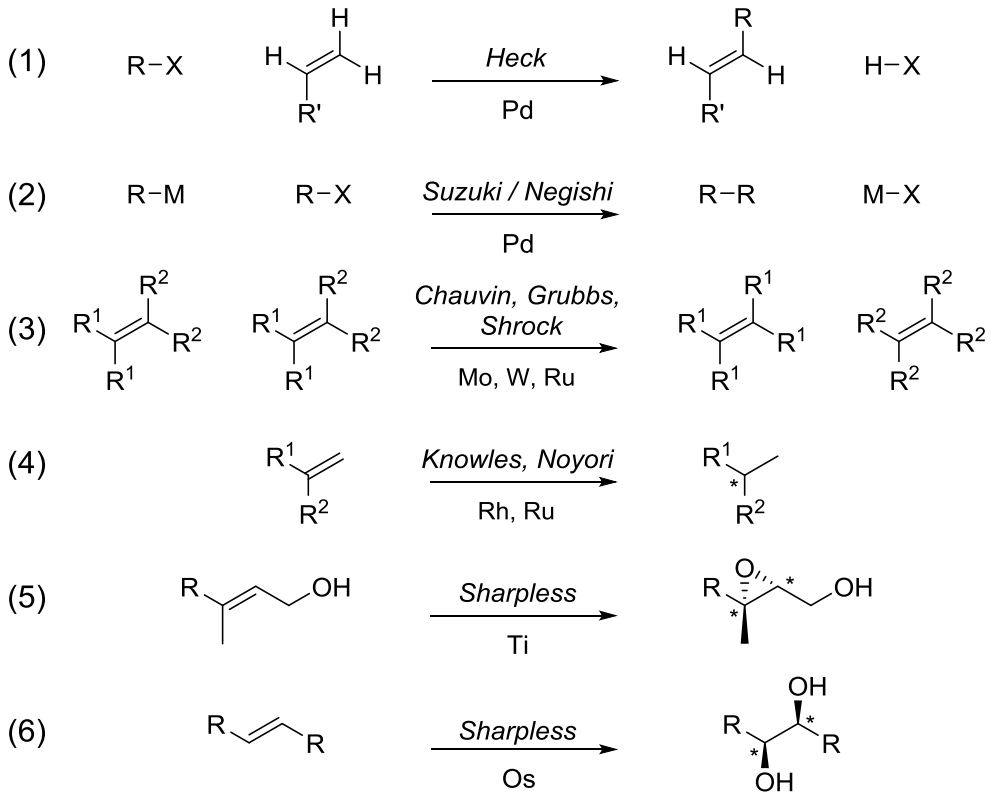

Prizes were awarded for work based on transition metals in organic synthesis (**Scheme 1.1**); Pd-catalyzed cross couplings (2010, Heck, Negishi, Suzuki),[1] olefin metathesis reaction (2005, Chauvin, Grubbs, Schrock),[2] and asymmetric hydrogenation/oxidation (2001, Knowles, Noyori,

Sharpless).[3] These and many other reactions involving transition metals have provided chemists with invaluable tools to approach problems in organic chemistry.

Numerous studies in transition metals often focus on metals such as Pd, Pt, Rh, Ru, and Ti.[4] These offer a diverse range of interesting reactivity and have helped significantly advance the field of chemistry. Interestingly enough, it took a long time for researchers to gain any chemical interest in gold, one of the most widely known metal in the world. Initially believed to be chemically inert for use in chemical synthesis, Ito and Hayashi revealed a different picture of

Scheme 1.2 : First examples of gold-catalyzed transformations

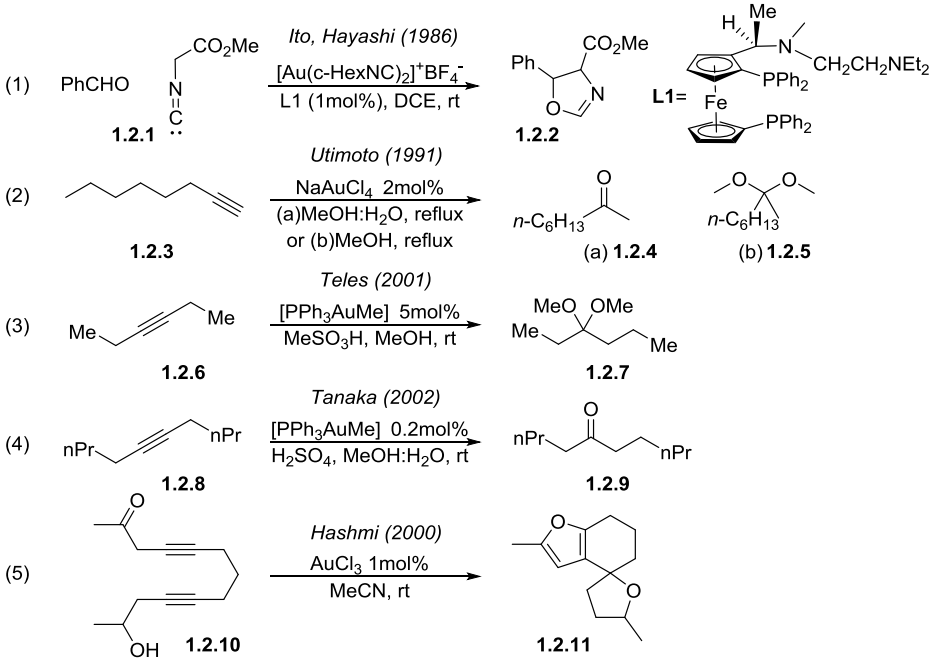

gold (**Scheme 1.2**). In 1986, they developed a Au(I) catalyzed aldol reaction representing the first use of gold in homogeneous catalysis.[5] In 1991 Utimoto reported the formation of acetals and ketones from alkynes by Au(III) catalysis[6]. A decade after their seminal work, Teles reported Au(I) catalyzed addition of alcohols to alkynes,[7] soon followed in 2002 by Tanaka describing the hydration of alkynes with a Au(I) catalyst.[8] The Au(III) catalyzed formation of C-C and C-O bonds was also described by Hashmi in 2000, where cycloisomerization of alkynes and allenes

yielded a variety of furans.[9] What followed could be labelled an avalanche of publications describing Au(I) and Au(III) reactivity.[10-13]

1.1 Relativistic Effect

The theory of relativity proposed by Albert Einstein has helped physicist accurately describing situations involving motion occurring at a significant fraction of the speed of light (relativistic speeds). The many consequences of such velocities are also observed in chemistry and its combined impact is referred to as the relativistic effect. It is considered a direct result of the high velocity of electrons moving near a heavy nucleus.[14] Although technically present in all

Figure 1.1 : Consequences of the relativistic effect on s and d orbitals

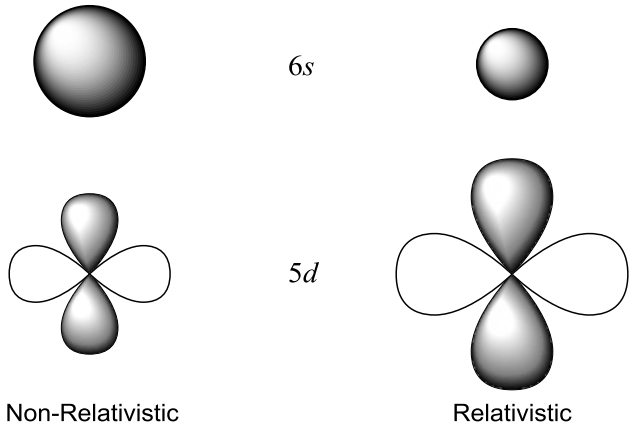

elements, in gold this effect is significant enough to have a profound influence on its observed chemical reactivity.[15] The substantial velocity of the electrons around gold is considered to be of relativistic speed. Thie high velocity causes an increase in mass of the electrons. Since the Bohr radius of an electron is inversely proportional to the mass of the electron, the increase in mass causes the contraction of all *s* and *p* orbitals (**Figure 1.1**). This in turns produces greater screening of nuclear attraction and expands the *d* and *f* orbitals.

Another less mentioned but nonetheless significant effect is called the lanthanide contraction. The effect occurs in lanthanide and actinide transition metals and is responsible for

some of their physical properties.[16] The lanthanide contraction effect is the result of poor shielding of the nucleus by electrons populating the 4*f* orbital because of its geometry which consequently increases orbital contraction of *s* and *p* orbitals. If the relativistic effect is ignored, the lanthanide contraction would cause the *5d* and 6*s* of gold to have very similar orbital energies as the 4*d* and 5*s* of silver. Taking into account the relativistic effect shows a distinct energy difference between these orbital levels, indicating that the entire orbital-energy difference can be attributed to the relativistic effect. The energy difference can be observed in the large first ionisation potential difference between gold and silver (9.22 eV and 7.57 eV respectively) and consequently high electronegativity.

An interesting product of the relativistic effect is a strong aurophilicity between Au(I) atoms. Typically observed Au^{I}-Au^{I} pairs have an interatomic distance on the order of 300±25pm. The strength of such interactions has been measured to be around 29-46 kJ/mol, higher in strength than hydrogen bonds.[17] The source of this attraction has been identified as the hybridization of the filled 5*d* and the empty 6*s* and 6*p* orbitals of Au(I). The aurophilic property of gold has an important role to play in some of the dimeric Au(I) complexes discussed further in the thesis.

1.2 Catalysis by Gold(I) Complex

Cationic Au(I) species are known to be superior soft Lewis acids than other group 11 metals.[18] Gold's strong electronegativity helps justify this, although a better explanation can be derived from the relativistic effect on its 6*s* and 6*p* orbitals. The orbital contraction creates a low-lying LUMO, thus making it a better Lewis acid and promoting activation of π-systems.

The coordination of cationic Au(I) to alkynes makes them susceptible to nucleophilic addition. Although the mechanism is still being studied by many groups, it can be generally described as follows (**Scheme 1.3**).[19] A cationic Au(I) specie **1.3.1** will coordinate a to triple-bond **1.3.2** to form complex **1.3.3** which activates the alkyne for nucleophilic addition. The activation happens via L–Au–S type complexes, where S is an η^2-coordinated alkyne and L is the ancillary ligand.[20] The interaction between the alkyne and the gold center is generally discussed in terms of S→Au σ-donation and Au→S π-back-donation, known as the Dewar-Chatt-Duncanson (DCD) model. Multiple investigations into the mechanism of the reactions use the DCD model to help rationalize activation of the substrate. The consensus achieved by these studies indicate that the σ-donation typically exceeds π-back-donation, resulting in a net

Scheme 1.3: Generalized Au(I) Lewis acid catalytic cycle

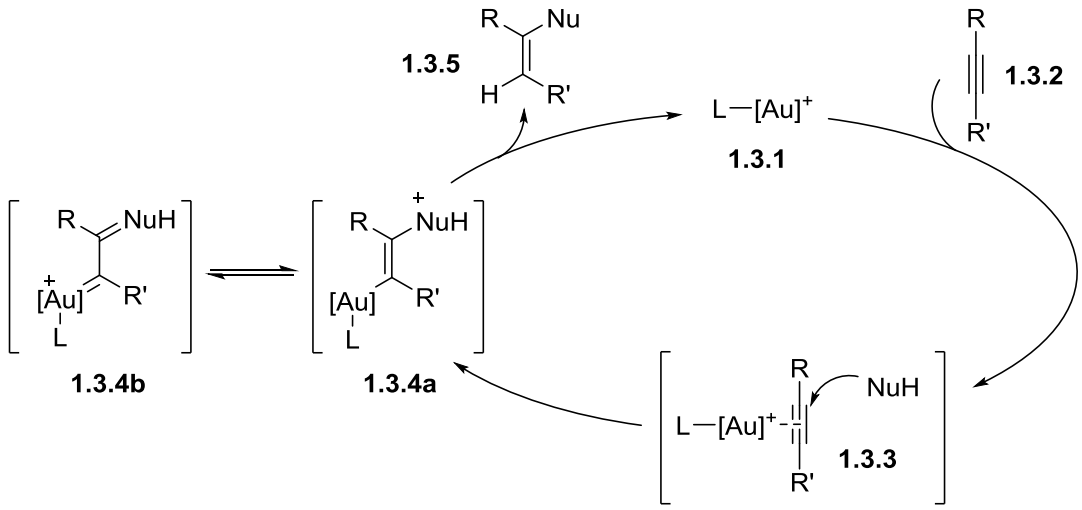

depletion of electronic density from the triple bond region undergoing the nucleophilic attack.[21] Following the activation, nucleophilic addition to the alkyne will occur in a *trans* fashion[22] forming the vinyl gold intermediate **1.3.4a**. Strong σ-donating ligands such as NHCs can help favor the formation of gold carbenes **1.3.4b** from the intermediate **1.3.4a**, opening many other avenues of reactivity. In the presence of water or labile protons, the gold will undergo

protodeauration to form product **1.3.5**, although examples of other electrophiles being used are known.[23,24,25] The cationic Au(I) specie **1.3.1** is released for further activation.

A detailed study by Xu and Hammond showcased the importance of the ligands' electronic properties on Au(I) catalyzed reactions. Most Au(I) catalyzed reaction are thought to go through three stages; alkyne activation, nucleophilic attack, and protodeauration. The study revealed how electron poor ligands will decrease the rate of protodeauration and electron rich ligands increase it.[26] The alkyne activation will be accelerated by electron poor ligands, and slowed by electron rich ones. Degradation of the catalytic complex can also be of concern but seems to depend little on the electronic properties of the ligand. Counter-ion selection can also be crucial in achieving high yields. Au(I) halides are usually not catalytically active for alkyne activation and thus require *in situ* ion exchange, typically with silver(I) salts with anions such as [OTf], [NTf_2], [PF_6], [BF_4], [SbF_6], and [$BAr^F{}_4$].[27] These labile counter-ions help with initial coordination of the cationic Au(I) to the alkyne. There are many combinations possible for the synthesis of an active complex for alkyne activation and the choice depends greatly on the reactions being run and the conditions in which they take place.

Nucleophilic additions to alkynes can form multiple products depending on the regioselectivity of the reaction. In the case of intramolecular reactions, which means the possibility of multiple ring sizes from the same starting material. For C-C anionic reactions, the 5-*exo dig* pathway usually exhibits lower activation barriers over the 6-*endo dig*.[28] It can be explain in part by the 5-*exo* trajectory resembling intermolecular addition angles (between 115°-130°)[29], while the 6-*endo* trajectory approaches but still does not quite achieve the optimal angle of attack for digonal nucleophilic addition. However, structural bias can greatly influence the preference in several ways. For example, orbital polarization can be greatly affected with

appropriately positioned moieties (**Scheme 1.4**), causing one or the other carbon of the alkyne to be a better acceptor for nucleophilic addition.[30]

Orbital distortion can also help favor one transition state over the other by changing the

Scheme 1.4: Example of substituent effect on Au(I) catalyzed on 5-exo/6-endo selectivity

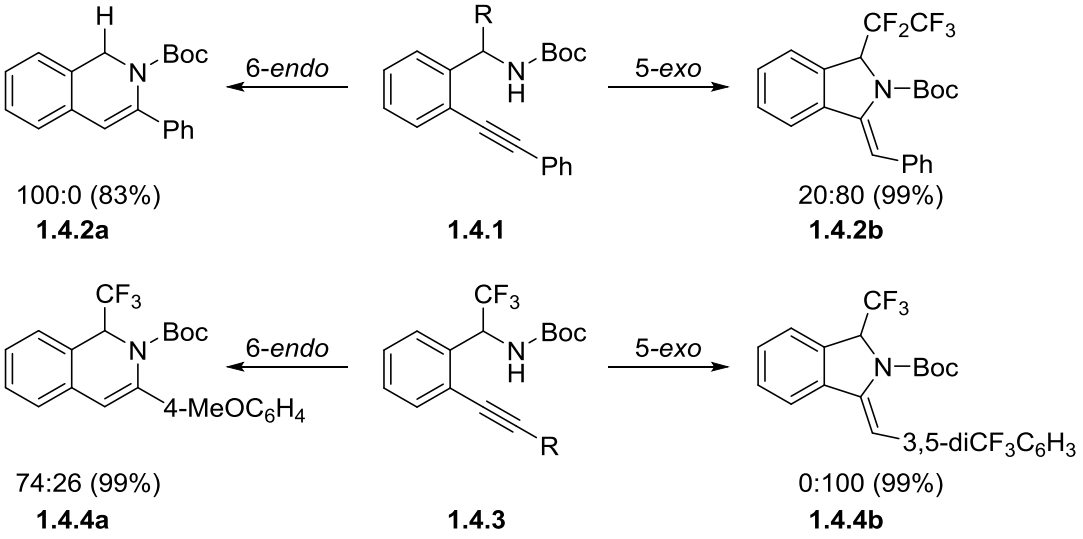

EtOH (5 equiv.) DCE (0.1 M), AuSPhosNTf$_2$ (0.025 equiv.) SPhos = 2-Dicyclohexylphosphino-2',6'-dimethoxybiphenyl

apparent angle of the ideal trajectory for nucleophilic addition (**Scheme 1.5**).[31] In the case of Au(I) catalyzed reactions, some selectivity can be imparted to the reaction based on the ligands used for the catalytic complex.

Scheme 1.5: Substrate dependant 5-exo/6-endo cyclization

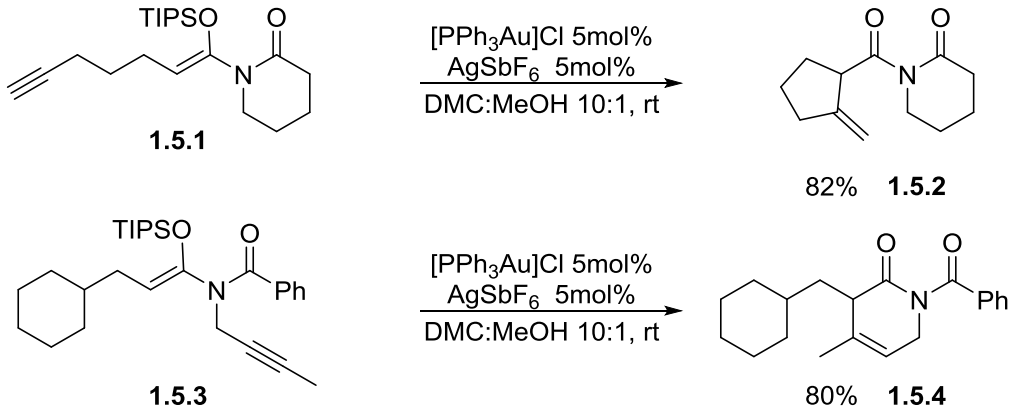

In 2009, Toste and co-workers reported that the ancillary ligand properties could be modulated to selectively discriminate between [4+2] and [4+3] cycloaddition reactions of allene-dienes such as **1.6.1** (**Scheme 1.6**).[32] Using electron rich di-*tert*-butylbiphenyl phosphine **L3** as the gold ligand, the reaction showed strong selectivity for the [4+3] cycloaddition product **1.6.3**. The selectivity seemingly originated from a stabilized cation adjacent to the Au(I). When the relatively electron poor ligand triphenyl phosphite **L2** was used, the reaction showed completed reversal of selectivity, yielding exclusively compound **1.6.2** from the [4+2] cycloaddition.

Scheme 1.6: Ligand induced selectivity of [4+2] vs. [4+3] cycloisomerization

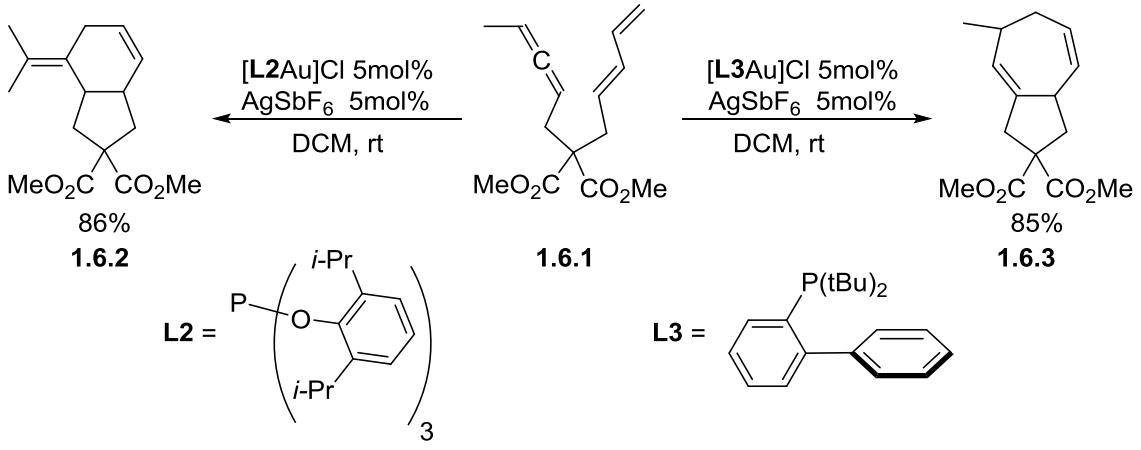

Soon afterwards, Fürstner and co-workers described the use of N-heterocyclic carbenes as ligands for the gold catalyzed [2+2] and [3+2] cycloadditions of eneallenes, along with the [4+2] and [4+3] cycloadditions of allene-dienes (**Scheme 1.7**).[33] Adjusting the π-acceptor properties of the ligand allowed for complete selectivity between each pathway. The stronger net donor [**L5b**Au]$^+$ presumably stabilized an adjacent cation to allow the [3+2] cycloaddition (**1.7.2**), while the better acceptor [**L4**Au]$^+$ disfavoured such a charge build up next to the Au(I), instead generating the formal [2+2] product **1.7.3**. Similar reactivity was observed in the [4+2] and [4+3] cycloadditions. The better donor promoted a 1,2-hydride shift from a common intermediate,

yielding the formal [4+3] cycloaddition product **1.7.5**, whereas the greater π-acceptor instead favored the 1,2-alkyl shift, generating the product from the formal [4+2] cycloaddition **1.7.6**.

Scheme 1.7 : Ligand induced selectivity of [4+2] vs. [4+3] and [2+2] vs. [3+2] cycloaddition

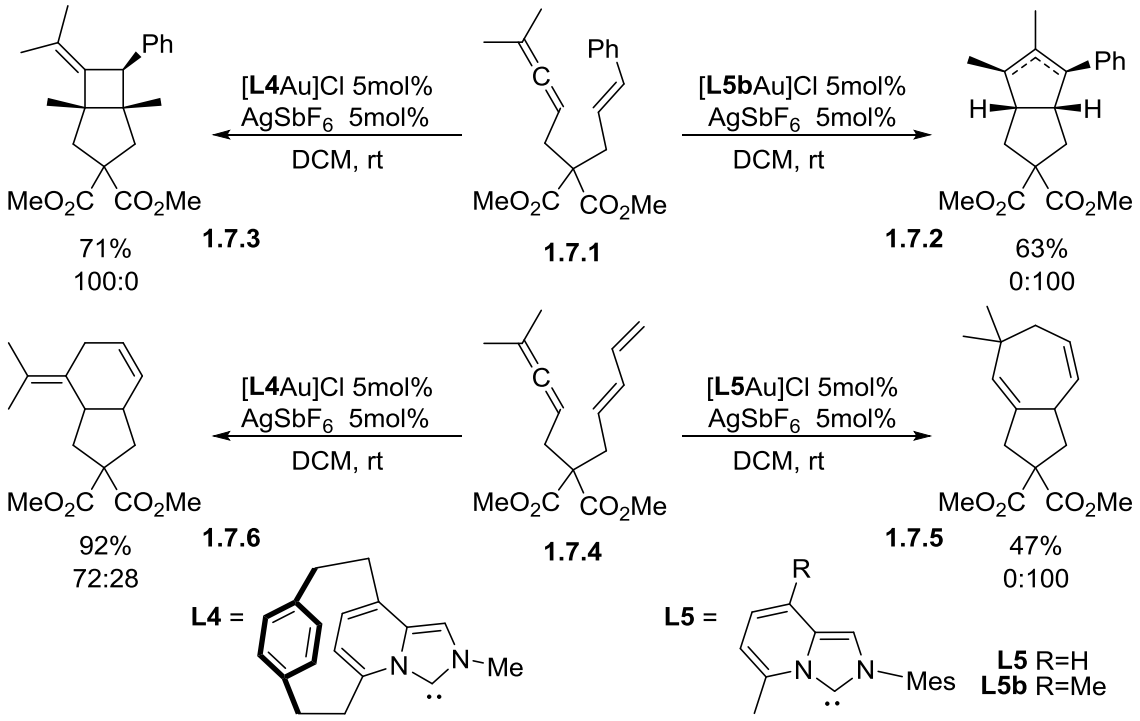

Another example of such ligand based control was described by Barriault *et al.* in 2011,[34] where careful selection of the ligand allowed for the inversion of selectivity in Au(I) catalyzed cyclization. It was found that silyl enol ethers submitted to cyclization conditions using either Me_4XPhos (**L6**) or IPr (**L7**) would yield the 6-*endo dig* or the 5-*exo dig* respectively as the major product (**Scheme 1.8**). In the case of catalyst [**L6**AuNCMe]SbF_6, the selectivity seemed to originate from the increased steric bulk of the ligand which tends to distort the linearity of the L-Au-L' bonds (169.2° for L'= Cl). It was postulated that the distortion caused a positive charge buildup at the C1 carbon in the transition state which would lower the energy of activation for **TS-1** over **TS-2**. The [**L7**AuNCMe]SbF_6 complex on the other hand was most likely near linear

(L-Au-L' angle of 177.1° for L'= Cl)[35] which favored positive charge buildup at the C2 carbon, instead lowering the energy of **TS-2** and resulting in a 5-*exo dig* cyclization.

Scheme 1.8 : Ligand controlled 6-endo vs. 5-exo cyclization of cyclic enol ethers.

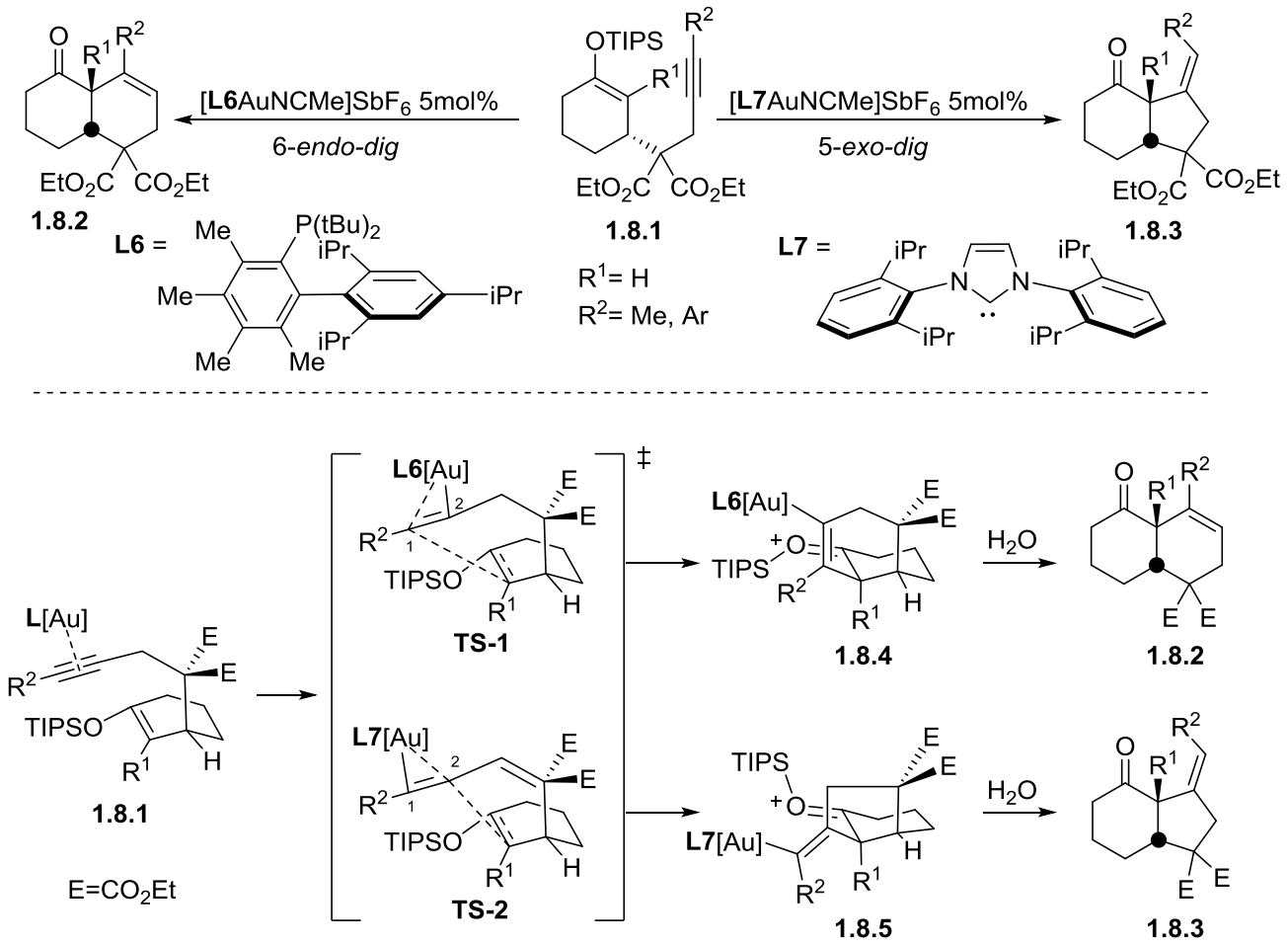

1.3 Initial Contributions in Au(I) Chemistry

During one such selectivity study, compound **1.9.1** proceeded via the 6-*endo-dig* pathway when using Me_4XPhos (**L6**) and formed the cyclic compound **1.9.2** (**Scheme 1.9**). When IPr (**L7**) was used instead, the isolated compound was not the expected 5-*exo-dig* product **1.8.3**, but rather the unforeseen product **1.9.4**.[36] Based on product **1.9.4**, we decided to investigate the scope and limitation of the transformation using an alkyne thiophene moiety.[37]

*Scheme 1.9 : Proposed mechanism for the formation of product **1.9.4***

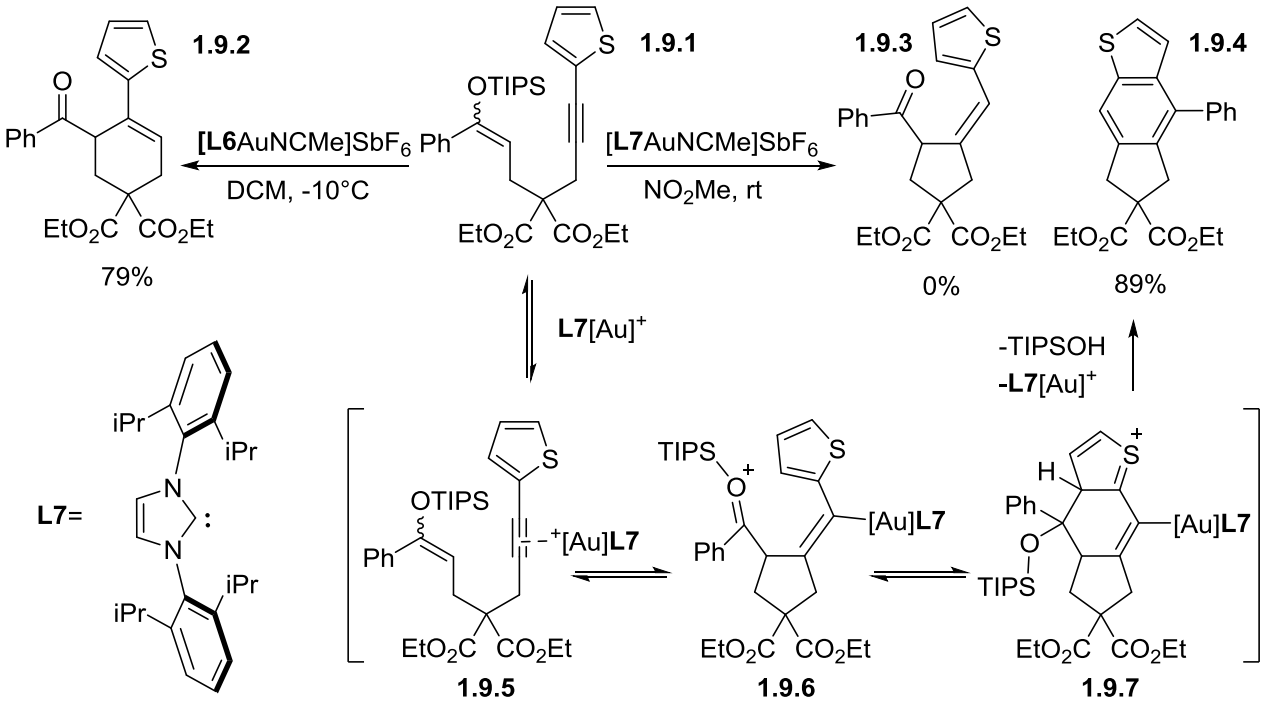

The interesting polycyclic structure afforded by the transformation could potentially be applied to the synthesis of multiple compounds. A similar motif is found in many natural products of known biological activity such as calothrixin B[38] and ellipticine.[39] The mild and efficient nature of Au(I) Lewis acid alkyne activation make it ideal for late stage transformations. High functional group tolerance and selectivity of the Au(I) catalyst could help rapidly expand libraries of compounds and explore many possible synthetic pathways in the synthesis of target molecules.

Analysis of product **1.9.4** allowed us to propose the following mechanism (**Scheme 1.9**). The coordination of Au(I) to the alkyne (**1.9.5**) triggers the 5-*exo-dig* cyclization to produce intermediate **1.9.6**. The subsequent nucleophilic addition of the thiophene to the carboxonium provides the sulfonium intermediate **1.9.7**, which upon protodeauration and aromatization

generates the final product **1.9.4**. The order in which the protodeauration step occurs is not known but is not important in the formation of the product. A solvent scan was performed and nitromethane was found to be the optimal solvent for the transformation. Other classic solvents used in gold catalyzed processes such as methanol almost completely inhibited the second cyclization and acetone provided inconsistent results. The observations could indicate that the second cyclization is less favorable after the hydrolysis of the oxonium. The nitromethane is also believed to help alleviate the charge buildup in the cationic cyclization transition state.

It is worth nothing that the transformation could conceivably go through a gold carbene mechanism as demonstrated by Eschavaren with the cyclization of dienynes.[40] The silyl enol ether would form the cyclopropyl intermediate **1.10.1** (**Scheme 1.10**), and a subsequent Nazarov-like ring expansion could form intermediate **1.9.7**, eventually leading to the same product (**1.9.4**).

*Scheme 1.10 : Alternate mechanism for the formation of **1.9.4***

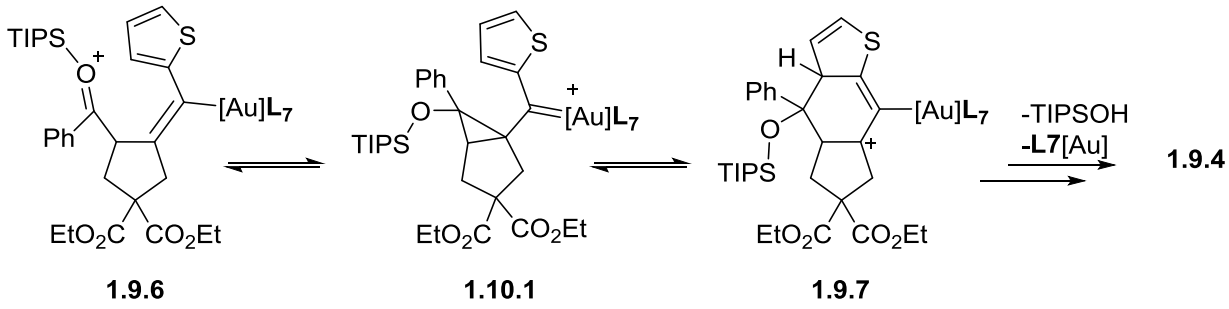

Due to the fundamental importance of aromatic compounds in organic chemistry, we decided to explore the scope of the reaction using various substituted alkynes. Taking advantage of the high regiospecificity of [**L7**AuNCMe][SbF_6], a complimentary approach for substituted aromatic compounds was developed.

The model substrates selected for the study were based on their potential for a second cyclization following the initial silyl enol ether addition to the alkyne. Various substituted alkynes were accessed by using diethyl malonate as a central building block (**Scheme 1.11**). First a monoalkylation with 3-bromo-1-propyne **1.11.2** was performed on large scale and purified by vacuum distillation. A subsequent Sonogashira coupling between **1.11.3** and **1.11.4**, followed by a TIPSOTf promoted 1,4-addition onto unsaturated ketones and aldehydes (**1.11.6**) yielded the model substrates **F1.2.1**. The 1,4-addition reaction yielded a mixture of *cis* and *trans* products. These were not separated knowing that both diastereoisomers would result in the same compound after the gold cyclization.

*Scheme 1.11 : Synthesis of substrates **F1.2.1**.*

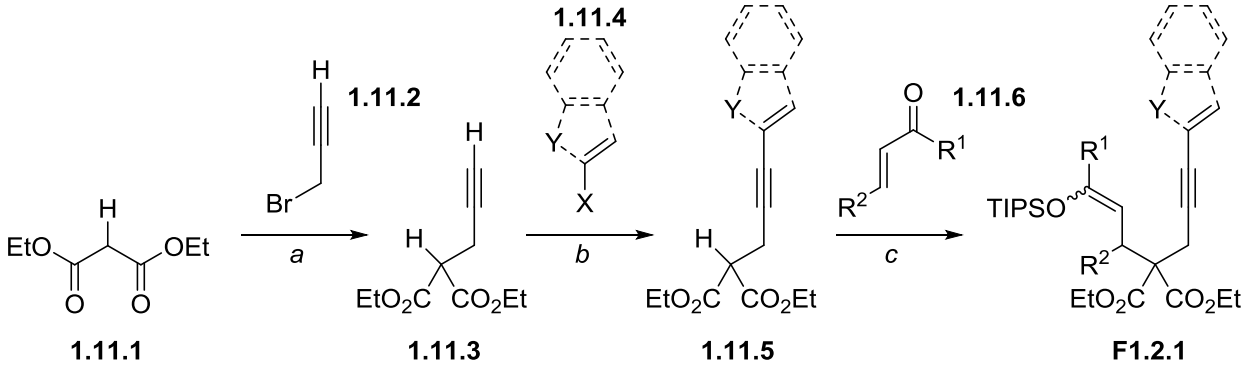

Y = H, O, S, NTs
X = Br, I

*a) NaH(1.1eq) diethyl malonate (1eq) 3-bromo-1-propyne (2eq) NaI (0.5eq) THF. b) $Pd(PPh_3)_4$ (0.05eq) CuI (0.1eq) **1.11.3** (1eq) aryl or vinyl halide (2.5eq) Et_2NH (5eq) Benzene. c) NaH (2eq) **1.11.5** (1.5eq), enone or enal (1eq) TIPSOTf (1.5Eq) DMS (3eq).*

Nine other substrates were prepared using the malonate central building block and submitted to standard reaction conditions (**Figure 1.2**). Gold(I)-catalyzed cyclization of the enol ether **F1.2.1a** (R^1 = *p*-BrC_6H_4, R^2 = H) gave the corresponding benzothiophene **F1.2.2a** in 83% yield. The use of electron-poor silyl enol ether **F1.2.1b** (R^1 = *p*-$NO_2C_6H_4$, R_2 = H) gave the desired product **F1.2.2b**, albeit in lower yield (63%). The synthesis of substituted hydrindene **F1.2.2c** was also achieved in 85% yield from monosubstituted enyne **F1.2.1c** (R_1 = Ph, R_2 = H). Tri- and disubstituted silyl enol ethers **F1.2.1d** (R^1 = H and R^2 = Me) and **F1.2.1e** (R^1 and R^2 = H) were converted to benzothiophenes **F1.2.2d** and **F1.2.2e** in 95% and 82% yield respectively.

Figure 1.2 : Gold-catalyzed 5-exo-dig carbocyclization cascade.

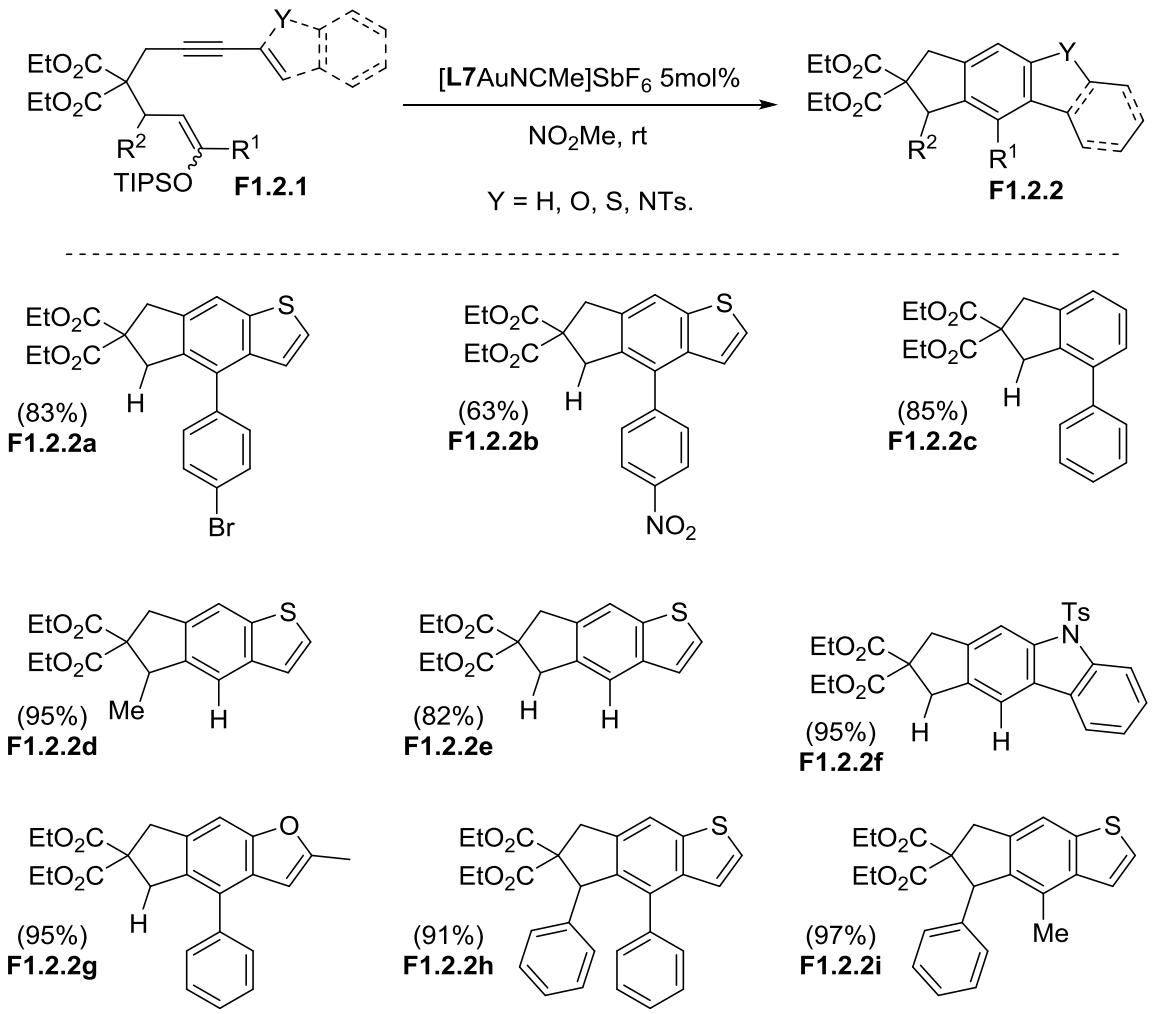

Substituted enynes bearing heterocycles such as indole **F1.2.1f** (R^1 and R^2 = H) and furan **F1.2.1g** (R^1 = Ph and R^2 = H) were both effectively transformed to the desired carbazole **F1.2.2f** and benzofuran **F1.2.2g** in 95% yield. It can be noticed that large substituents at R^1 and R^2 did not affect the efficiency of the reaction. The Au(I)-catalyzed cyclization of **F1.2.1h** (R^1 = R^2 = Ph) and **F1.2.1i** (R^1 = Ph and R^2 = Me) provided the corresponding benzothiophenes **F1.2.2h** and **F1.2.2i** in 91% and 87% yield respectively.

The study resulted in a mild and efficient Au(I) catalyzed 5-*exo dig* polycyclization cascade to prepare a diverse range of aromatic compounds, such as carbazoles, benzofurans, benzothiophenes and hydrindene. The reaction demonstrated the ability of cationic Au(I) complexes to successfully catalyze the formation of multiple C-C bonds. The creation of synthetically useful motifs was made possible by the high regioselectivity imparted by the ancillary IPr ligand (**L7**). These results were my first contribution to the field of gold chemistry. From here I started working with Dr. Guillaume Revol and Terry McCallum on the development of Au(I) photocatalyzed reactions.

---

[1] "The Nobel Prize in Chemistry 2010". *Nobelprize.org.* Nobel Media AB 2014. Web. 28 Mar 2017. <http://www.nobelprize.org/nobel_prizes/chemistry/laureates/2010/>
[2] "The Nobel Prize in Chemistry 2005". *Nobelprize.org.* Nobel Media AB 2014. Web. 28 Mar 2017. <http://www.nobelprize.org/nobel_prizes/chemistry/laureates/2005/>
[3] "The Nobel Prize in Chemistry 2001". *Nobelprize.org.* Nobel Media AB 2014. Web. 28 Mar 2017. <http://www.nobelprize.org/nobel_prizes/chemistry/laureates/2001/>
[4] Ojima, I.; Tzamarioudaki, M.; Li, Z.; Donovan, R. J. *Chem. Rev.* **1996**, *96,* 635 – 662
[5] Ito, Y.; sawamura, M.; Hayashi, T. *J. Am. Chem. Soc.* **1986**, *108*, 6406 – 6407
[6] Fukuda, Y.; Utimoto, K. *J. Org. Chem.* **1991**, *56*, 3729 – 3734
[7] Teles, J. H.; Brode, S.; Chabanas, M. *Angew. Chem. Int. Ed.* **1998**, *37,* 1415 – 1418
[8] Mizushima, E.; Sato, K.; Hayashi, T.; Tanaka, M. *Angew. Chem. Int. Ed.* **2004**, *41*, 4563 – 4565
[9] Hashmi, A. S. K.; Shwarz, L.; Choi, J.-H.; Frost, T. M. *Angew. Chem. Int. Ed.* **2000**, *39*, 2285 – 2288
[10] Hashmi, A. S. K. *Chem. Rev.* **2007**, *107*, 3180 – 3211
[11] Dorel, R.; Echavarren, A. M. *Chem. Rev.* **2015**, *115*,9028 – 9072

[12] Pflästerer, D.; Hashmi, A. S. K. *Chem. Soc. Rev.* **2016**, 45, 1331 – 1367
[13] Miró. J.; del Pozo, C. *Chem. Rev.* **2016**, *116*, 11924 – 11966
[14] Pyykkö, P.; *Angew. Chem. Int. Ed.* **2002**, *41*, 3573 - 3578
[15] Pyykkö, P.; Desclaux, J.-P. *Acc. Chem. Res.* **1979**, *12*, 276 – 281
[16] Pyykkö, P. *Angew. Chem. Int. Ed.* **2004**, *43*, 4412 – 4456
[17] Schmidbaur, H.; Schier, A. *Chem. Soc. Rev.* **2012**, *41*, 370 – 412
[18] Gorin, D. J.; Toste, F. D. *Nature* **2007**, *446*, 395 – 403
[19] Liu, L.-P.; Hammond, G. B. *Chem. Soc. Rev.* **2012**, *41*, 3129 – 3139
[20] Obradors, C.; Echavarren, A. M. *Chem. Commun.* **2014**, *50*, 16 – 28
[21] Bistoni, G.; Belanzoni, P.; Belpassi, L.; Tarantelli, F. *J. Phys. Chem. A* **2016**, *120*, 5239 − 5247
[22] Kennedy-Smith, J. J.; Staben, S. T.; Toste, F. D. *J. Am. Chem. Soc.* **2004**, *126*, 4526 – 4527
[23] Zhang, L. *J. Am. Chem. Soc.* **2005**, *127*, 16804 – 16805
[24] Dubé, P.; Toste, F. D. *J. Am. Chem. Soc.* **2006**, *128*, 12062 – 12063
[25] Miles, D. H.; Veguillas, M.; Toste, F. D. *Chem. Sci.* **2013**, *4*, 3427 – 3431
[26] Wang, W.; Hammond, G. B.; Xu, B. *J. Am. Chem. Soc.* **2012**, *134*, 5697 – 5705
[27] Homs, A.; Obradors, C.; Lebeouf, D.; Echavarren, A. M. *Adv. Synth. Catal.* **2014**, *356*, 221 – 228
[28] Gilmore, K.; Alabugin, I. V. *Chem. Rev.* **2011**, *111*, 6513 – 6556
[29] Alabugin, I. V.; Gilmore, K.; Manoharan, M. *J. Am. Chem. Soc.* **2011**, *133*, 12608 – 12623
[30] Fustero, S.; Ibáñez, I.; Barrio, P.; Maestro, M. A.; Catalán, S. *Org. Lett.* **2013**, *15*, 832 – 835
[31] Minnihan, E. C.; Colletti, S. L.; Toste, F. D.; Shen, H. C. *J. Org. Chem.* **2007**, *72*, 6287 – 6289
[32] Mauleón, P.; Zeldin, R. M.; González, A. Z.; Toste, F. D. *J. Am. Chem. Soc.* **2009**, *131*, 6346 – 6349
[33] Alcarazo, M.; Stork, T.; Anoop, A.; Thiel, W.; Fürstner, A. *Angew. Chem. Int. Ed.* **2010**, *49*, 2542 – 2546
[34] Barabé, F.; Levesque, P.; Korobokov, I.; Barriault, L. *Org. Lett.* **2011**, *13*,5580 – 5583
[35] Fructos, M. R.; Belderrain, T. R.; Frémont, P.; Scott, N. M.; Nolan, S. P.; Dìaz-requejo, M. M.; Pérez, P. J. *Angew.Chem. Int.Ed.* **2005**, *44*, 5284 – 5288
[36] Wessig, P.; Müller, G. *Chem. Rev.* **2008**, *108*, 2051 – 2063
[37] Morin, M.; Levesque, P.; Barriault, L. *Beilstein J. Org. Chem.* **2013**, *9*, 2625 – 2628
[38] Bernardo, P.H.; Chai, C. L. L.; Heath, G. A.; Mahon, P. J.; Smith, G. D.; Waring, P.; Wilkes, B. A. *J. Med. Chem.* **2004,** *47,* 4958 – 4963
[39] Stiborová, M.; Sejbal, J.; Bořek-Dohalská, L.; Aimová, D.; Poljaková, J.; Forsterová, K.; Rupertová, M.; Wiesner, J.; Hudeček, J.; Wiessler, M.; Frei, E. *Cancer Research* **2004** *64*, 8374 – 8380
[40] Nieto-Oberhuber, C.; Pérez-Galán, P.; Herrero-Gómez, E.; Lauterbach, T.; Rodríguez, C.; López, S.; Bour, C.; Rosellón, A.; Cárdenas, D. J.; Echavarren, A. M. *J. Am. Chem. Soc.* **2008** *130*, 269 – 279

2 Organic Photochemistry and Photocatalysis

The photochemistry of organic compounds studies the effect of light in chemical transformations. The first law of photochemistry (the Grotthuss–Draper law) says that *light must be absorbed by a compound in order for a photochemical reaction to take place*. The second law (the Stark-Einstein law) states *for each photon of light absorbed by a chemical system, only one molecule is activated for a subsequent reaction*. These two principles guide any chemist's approach to photochemical transformations.

2.1. Photochemical Excitation

To properly understand the behavior of photoexcited compounds, it is necessary to first look at the consequences of absorbing a photon (Figure 2.1**a**).[41] After initial absorption, an electron is promoted from the highest occupied (HO) molecular orbital to the lowest unoccupied (LU) molecular orbital in the singlet state, where the electron settles in the most stable vibrational level (S_1, *cf* Kasha's rule). The electron can then lose energy through fluorescence (**F**), emitting a photon and returning to the singlet ground state. This energy loss can also be achieved through non-emissive vibrational relaxation (internal conversion, **IC**). Alternatively, the electron can undergo intersystem crossing (**ISC**) via a spin flip to reach the triplet state of the molecule. From here the molecule can emit a photon by phosphorescence (**P**), or undergo non-emissive energy loss through vibrational relaxation to reach the singlet ground state once again (**ISC**). Since phosphorescence requires the electron to undergo a spin flip, it is a slower and less energetic process than fluorescence. According to the Franck-Condon principle and the Born-Oppenheimer approximation, these phenomena generally occur in the same molecular structure as the ground state since the movement of the electrons happens on a much shorter timescale

than atomic reorganisation. Other photochemical processes can also occur, but the ones described above are sufficient to discuss the results in the thesis.

Figure 2.1 : (a) Simplified Jablonski diagram (b) Effect of excitation on ionisation potential (IP) and electron affinity (EA)

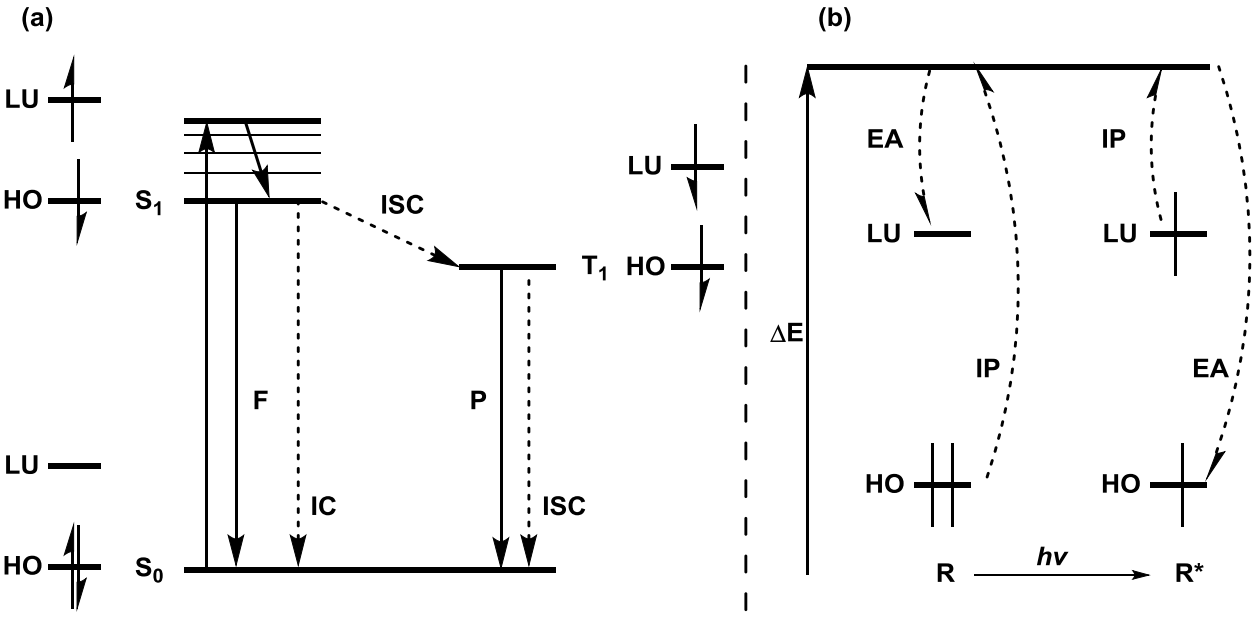

Based on these observations, an interesting property of all excited compounds become apparent: every excited molecule is both a better oxidizer and a better reducer than the parent ground state molecule (Figure 2.1**b**). The claim may seem strange, but it becomes apparent when looking at the principles guiding the two processes. The ionization potential (**IP**) is the energy needed to remove an electron from a molecule. In other words, the reduction potential is inversely proportional to the IP. An electron in the ground state sits in a low energy orbital, and thus requires a large amount of energy to be removed from the molecule. However in the excited state of the same molecule, the electron sits in a higher energy orbital and consequently requires less energy to be removed. The electron affinity (EA) is affected in the same way. In the ground state, a new electron would be added to a high energy orbital, with little energy gain.

Alternatively, the excited state of the molecule would be able to accept an electron into a lower energy orbital, thus making it a stronger oxidizer.

The most visible instance of this property can be seen in the leaves of trees. Chlorophyll contains a magnesium atom at its core which gets excited by the absorption of a photon from sunlight. The excited magnesium atom undergoes an oxidative quench process, losing an electron to the electron transport chain in the photosystem. The magnesium can then act as an oxidizing agent, stripping away an electron from water through various intermediates and returns to its ground state. The ultimate goal of the system is to form monosaccharides and oxygen from carbon dioxide and water molecules. This process would not be possible without the photoexcitation of the magnesium atom which significantly alters its oxidation and reduction potential when compared to its ground state.[42,43]

Sunlight would be the ideal source of energy for photochemistry, given its sustainability and accessibility. Therefore, it is no surprise that many photochemical transformations currently being studied focus on visible light. Nevertheless, as so wonderfully put to words by Dr. Neil Degrasse Tyson in the award winning documentary *Cosmos* "Confining our perception of Nature to visible light is like listening to music in only one octave".[44] As such, we would be remiss as chemists to only study visible light photochemistry.

2.2. Photocatalysis

Small organic molecules do not always absorb the correct wavelengths to produce any meaningful chemical transformation. The photons at the required wavelength for absorption often can be too energetic and lead to the decomposition of the substrate or even of the product being formed. To solve the issue, chemists use intermediary molecules (photocatalysts) to

convert lower energy photons into useful chemical transformation in a second molecule. The field of photocatalysis has recently undergone revived interest in chemical research and many recent developments have yielded interesting reactions using various catalysts.[45,46]

Figure 2.2 : Common catalysts in recent photoredox reactions.

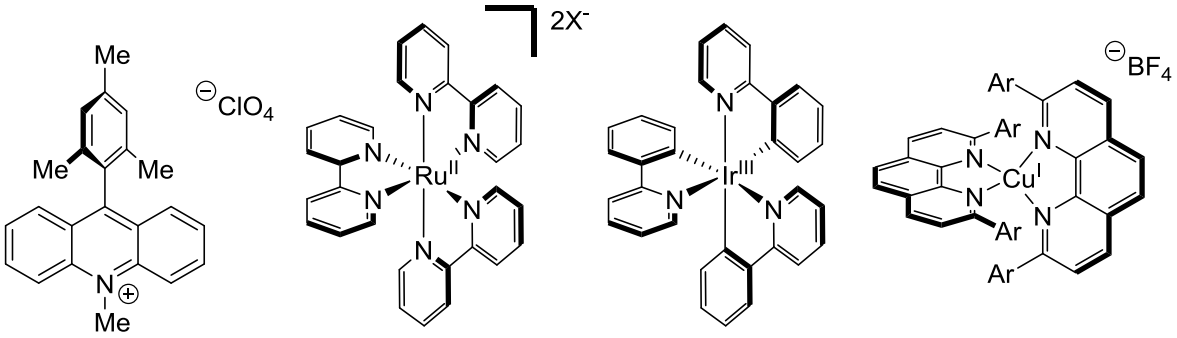

9-mesityl-10-methylacridinium

F2.2.1

$Ru(bpy)_3X_2$

F2.2.2

fac-$Ir(ppy)_3$

F2.2.3

$Cu(dap)_2BF_4$
Ar=*p*-anisyl

F2.2.4

Popular transformations catalyzed by photocatalysts often involve reduction/oxidation processes through single electron transfers. The approach has been used in several novel systems in order to generate carbon centred radical for the purpose of forming new C-C, C-O, and C-N bonds. Once formed, the radical intermediates behave the same way as if they were generated through radical chain processes. They will undergo cyclization, radical addition, atom transfer reactions or eventually a second oxidation or reduction. Contrary to the classical systems, most of the recent photoredox processes offer an attractive alternative to hazardous conditions previously associated with radical chemistry. In addition, photoredox process conditions tend to have a high degree of chemoselectivity and avoid certain complications such as premature reduction of radicals, and temperature sensitive reagents.

Photoredox transformations which perform single electron transfer (SET) from the catalyst usually proceed via one of two pathways (**Scheme 2.1**). First, the ground state

photocatalyst (PC) absorbs a photon and becomes excited. The excited catalyst then transfers an electron to an acceptor (A) in a process called oxidative quenching. The electron deficient catalyst must then receive an electron from a donor (D) to return to its native form and start another cycle.

Scheme 2.1 : Generalized photoredox catalytic cycle.

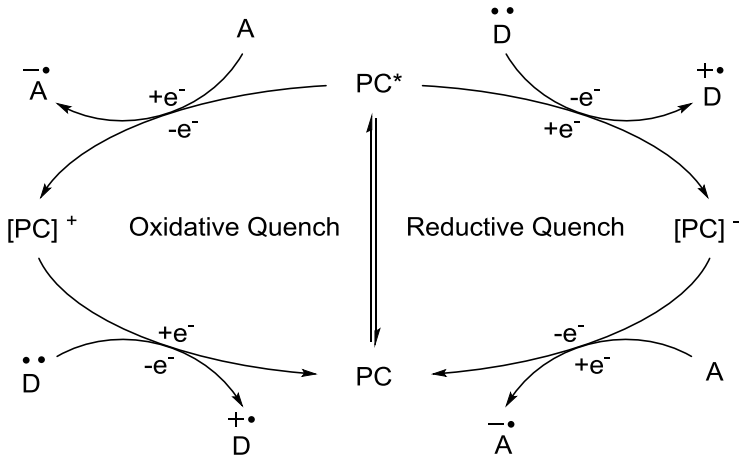

Alternatively, the excited catalyst receives an electron from a donor (reductive quenching), and a subsequent electron transfer to an acceptor regenerates the catalyst. In most cases, the donor/acceptor pair must not be able to directly interact with each other and must use the catalyst as an intermediate between the two. The substrate of the transformation usually plays the role of the donor or acceptor and sometimes both, although there are examples where the photoredox cycle does not necessarily interact with the substrate itself, but instead is used as an oxidant or reductant for a second catalyst.[47]

2.3. Photocatalytic Systems

2.3.1. Single catalyst systems

An interesting example of photoredox catalysis was reported by Nicewicz in 2014 using an organic dye (**Scheme 2.2**).[48] It is only one of the many examples in the field of

organophotocatalysis.[49] Using the acridine derived photocatalyst [Mes-Acr-Me]ClO_4 **F2.2.1** they perform a SET to oxidize an alkene via a reductive quenching reaction, forming the radical cation **2.2.2**. A subsequent addition from a pendant nucleophile forms a furan ring containing a stabilized tertiary radical **2.2.4**. The radical abstracts a hydrogen atom from the donor **2.2.6** to form the benzyl radical **2.2.7**. The reduced catalyst **F2.2.1**$^{1-}$ returns to its native state by reducing **2.2.7** to the carbanion **2.2.8** which deprotonates substrate **2.2.4** and regenerates the hydrogen donor **2.2.6** and forms the desired product **2.2.5**.

Scheme 2.2 : Proposed photocatalytic cycle for the hydrofunctionalization of alkenes.

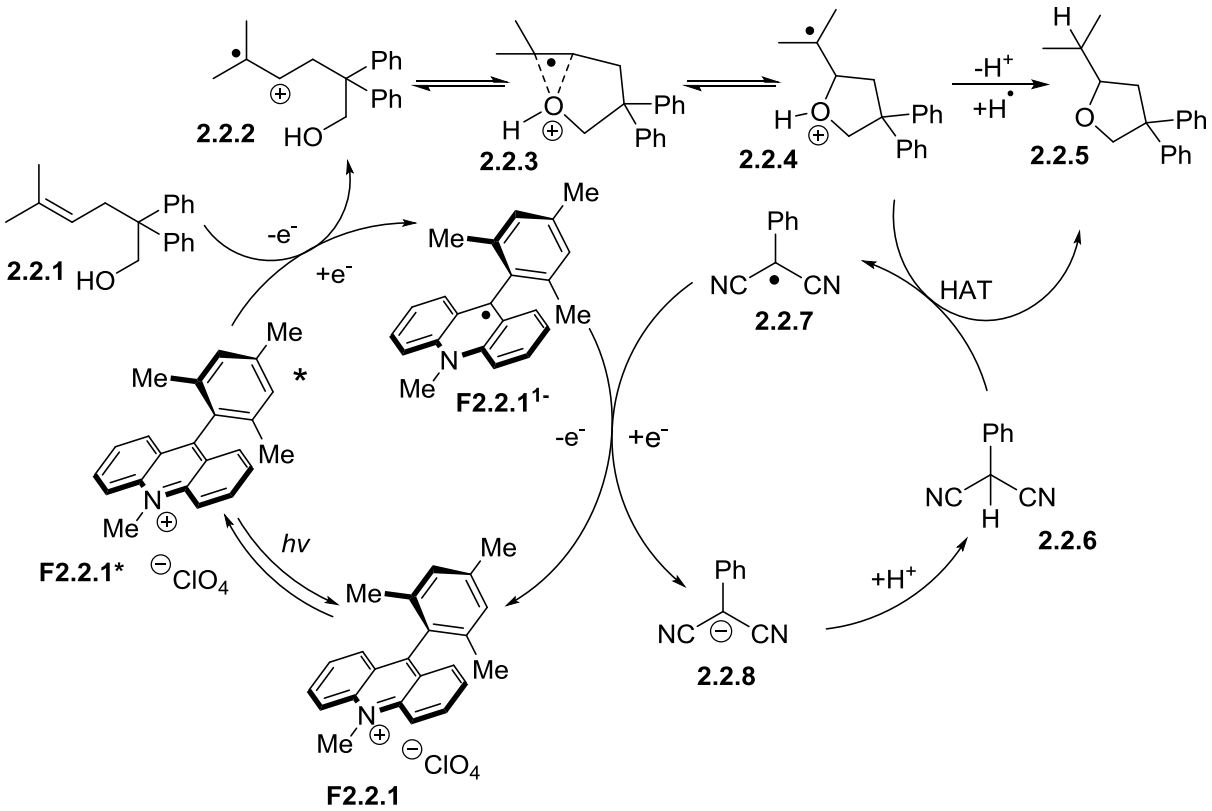

Two photocatalyzed reactions were reported by Yoon where the metal organic complex $[Ru(bpy)_3]^{2+}$ (**F2.2.2**) reduced enones through single electron transfer reactions (**Scheme 2.3**). The systems involves the reductive quenching of the excited $[Ru(bpy)_3]^{2+*}$ by *i*Pr_2NEt via a metal to ligand charge transfer (MLCT) to generate $[Ru(bpy)_3]^{+}$. Iridium complexes similar to

ruthenium complexes also undergo a MLCT following excitation, causing electron transfers to occur by the means of an outer-sphere mechanism. The reducing complex **F2.2.2^{1-}** can then perform an SET to the acid activated enone **2.3.1**, forming the carbon centered radical **2.3.2**. If a Lewis acid such as $LiBF_4$ is used for the carbonyl activation, the reduction forms a radical anion which proceeds through a formal [2+2] cycloaddition, yielding product **2.3.3a**.[50] If on the other hand a Bronsted acid is used, the compound forms a neutral radical species, and a subsequent 5-*exo trig* cyclization yields product **2.3.3b**.[51]

Scheme 2.3: Proposed mechanism for the photocatalyzed reduction of enones.

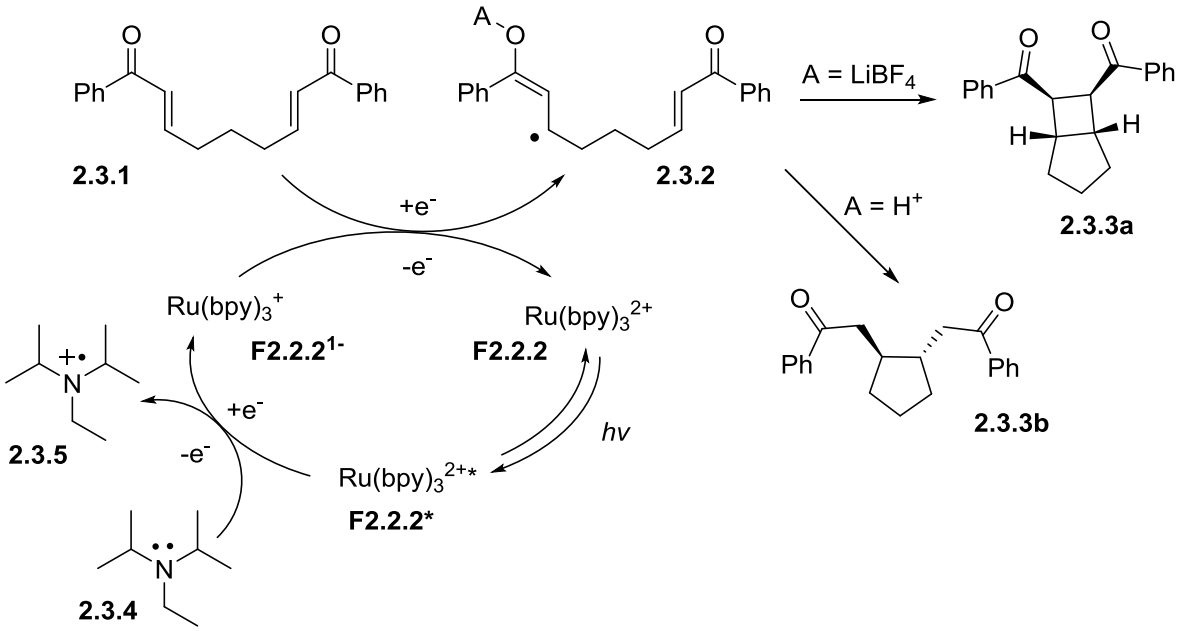

The reduction of unactivated carbon-iodide bonds was reported by the group of Stephenson, using the [*fac*-Ir(ppy)$_3$] complex (**Scheme 2.4a**).[52] The proposed mechanism involves an oxidative quench by alkyl or aryl iodides (**2.4.1**). Through a single electron transfer mechanism, the reduction of the carbon-iodide bond forms a carbon centered radical (**2.4.2**). The radical intermediate generated can then undergo cyclization (**2.4.3**) prior to H abstraction from the hydrogen donors (either Bu_3N or HCO_2H) to form the final product (**2.4.4**). The regeneration

of the **F2.2.3** catalyst proceeds via single electron transfer from the trialkylamine base (**2.4.5**). It is worth noting that the catalyst may instead undergo a reductive quench by the trialkylamine first (**Scheme 2.4b**), generating the reduced complex [*fac*-Ir(ppy)$_3$]$^{-1}$ (**F2.3.3^{1-}**), followed by a subsequent SET to the carbon-iodide bond which regenerates the Ir complex **F2.2.3** and forms the carbon centered radical **2.4.2**. Both pathways may even be in play simultaneously.

Scheme 2.4 : Proposed mechanism for the reduction of carbon iodide bonds.

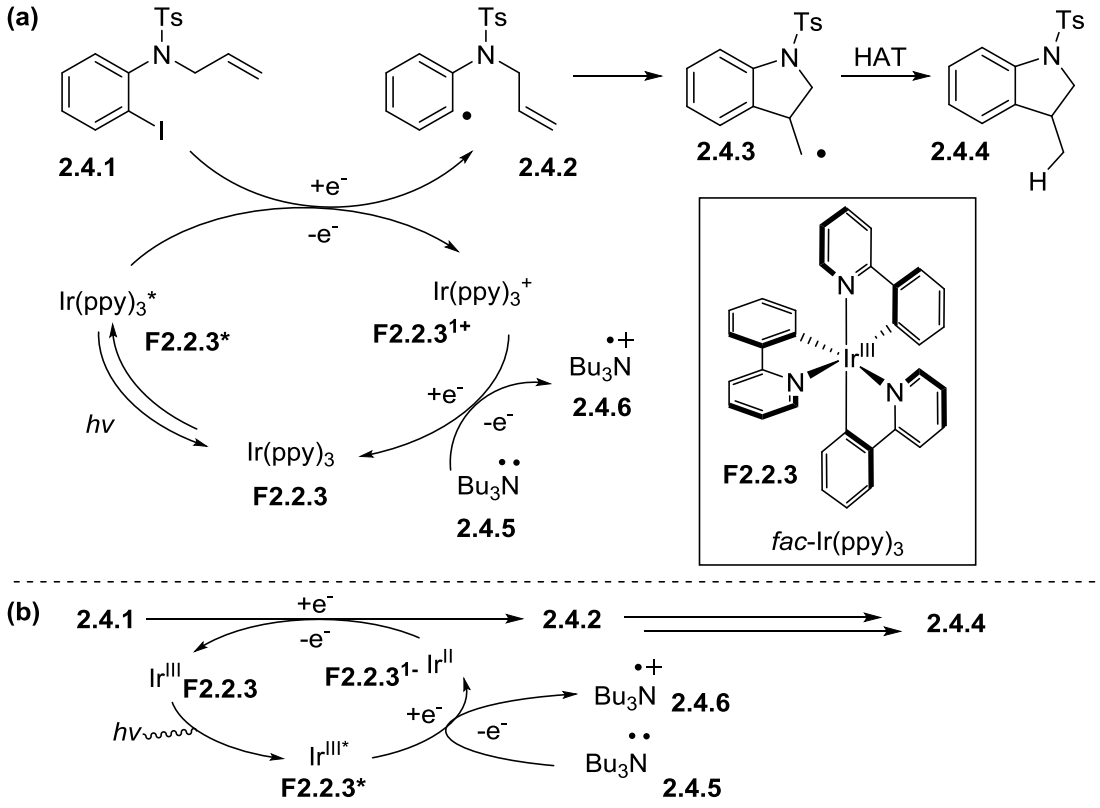

Copper can also be used in similar types of transformations. It has previously been demonstrated that rigid and encasing ligands can promote a long metal to ligand charge transfer in Cu(I).[53,54] Sauvage later described the use one of the copper complexes in the photoredox reaction of *p*-nitrobenzyl bromide (**Scheme 2.5**).[55] Complex **F2.2.4** is irradiated by >350 nm light to generate the excited Cu(I) species **F2.2.4***, which undergoes an oxidative quench in the presence of 4-nitrobenzyl bromide **2.5.1** to generate the benzylic radical **2.5.2**. Concomitant

radical fragment recombination and reduction of $Cu(dap)^{2+}$ with triethylamine **2.5.4** give dimer **2.5.3** and photocatalyst **F2.2.4**.

Scheme 2.5 : Proposed mechanism for the reduction of 4-nitrobenzyl bromide.

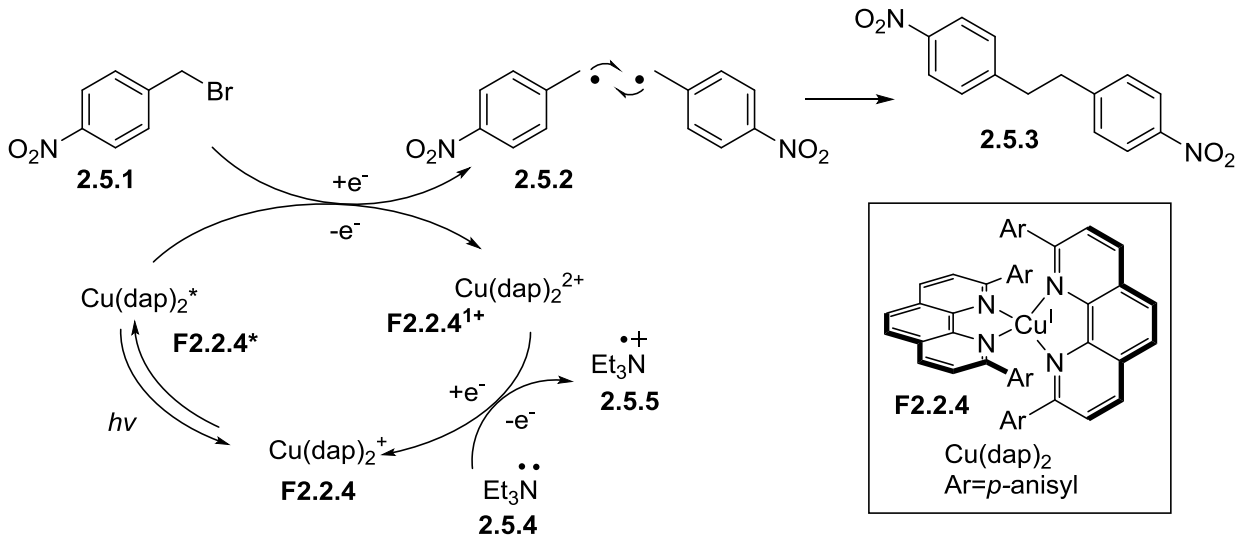

2.3.2. Dual catalytic photochemical processes

As mentioned previously, certain dual catalytic systems might not contain any direct interaction between the substrates and the photocatalyst, relying instead on another intermediary molecule for the generation of the desired product. The method described by the group of MacMillan represents a clever example (**Scheme 2.6a**).[47] They used a Ni(0) species (**2.6.1**) to perform an oxidative addition to a C-Br aryl bond (**2.6.3**), followed by a ligand exchange to generate Ni(II) aryl alkoxide **2.6.5**. The complex cannot reductively eliminate on its own. Instead, the photoexcited iridium catalyst **2.6.12*** oxidizes the Ni(II) **2.6.5** to the Ni(III) complex **2.6.6**, which promptly undergoes reductive elimination to form the aryl ether product **2.6.7**, and Ni(I) complex **2.6.8**. Both catalysts are regenerated through a single electron transfer from the Ir^{II} to the Ni^{I} complex, completing both catalytic cycle. They were also able to replace the use of $Ni(COD)_2$ by the bench stable $NiCl_2(dtbbpy)$ (pre-catalyst) as a source of Ni(0). The

quinuclidine acts as a sacrificial electron donor and allows two consecutive SET from the Ir complex **2.6.12** to take place to generate the active Ni(0) catalyst (**Scheme 2.6b**).

Scheme 2.6 : Proposed mechanism for the dual catalytic Ni/Ir system.

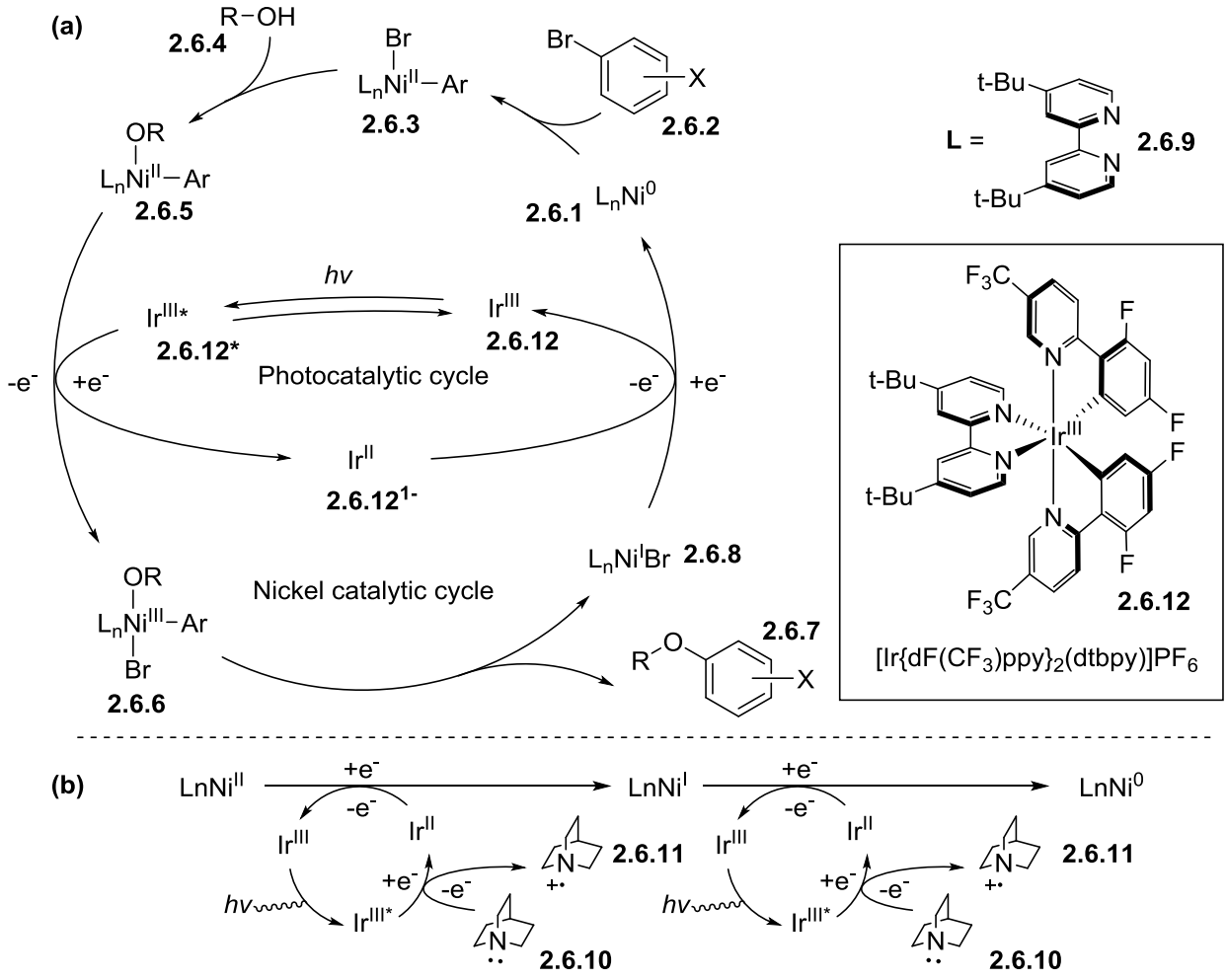

A dual photoredox reaction involving a Au(I) catalyst for the oxyarylation of alkenes has been reported by Glorius.[56] The proposed mechanism described in **Scheme 2.7** reveals that the cationic PPh_3AuNTf_2 (**2.7.1**) catalyzes the addition of methanol onto the alkene to give intermediate **2.7.4**. At the same time, the diazo compound **2.7.5** is reduced through an oxidative quench cycle by the Ir(III) catalyst **2.7.10** to form an aryl radical (**2.7.6**). The latter adds to the alkyl gold intermediate **2.7.4**, forming the Au(II) specie **2.7.7** which is oxidizes by the Ir(IV)

complex **2.7.10**$^{1+}$ to generate the Au(III) organometallic specie **2.7.8**. The complex then undergoes reductive elimination to afford the desired product **2.7.9** and regenerate the cationic Au(I) catalyst **2.7.1**.

Scheme 2.7 : Proposed dual catalytic cycle for the Au/Ir system.

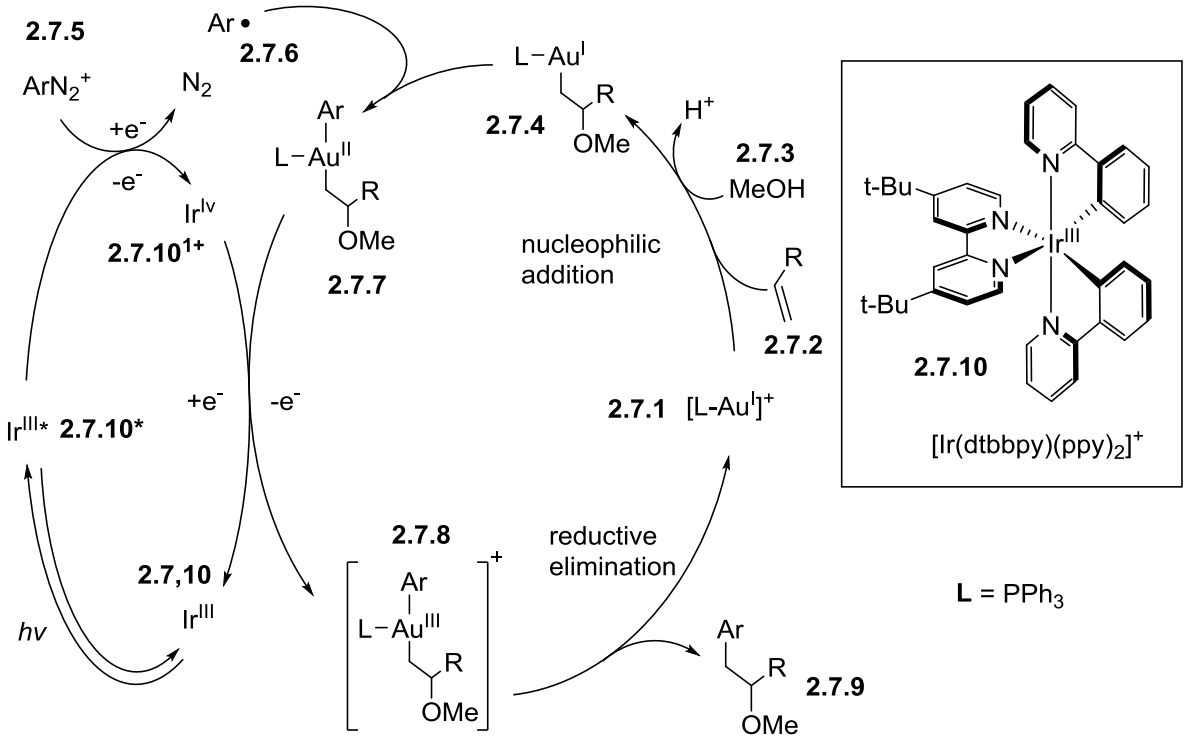

Analogous reactivity has been reported by Toste involving the use of a Ru(II) photocatalyst **F2.2.2** and PPh_3AuCl (**Scheme 2.8**).[57] The proposed mechanism first involves the reduction of the diazoaryl **2.8.2** to an aryl radical through oxidative quenching of the excited complex **F2.2.2*** to Ru(III) **F2.2.2**$^{1+}$. The aryl radical **2.8.3** generated is trapped by the Au(I) chloride **2.8.1**, forming Au(II) complex **2.8.4**. A single electron transfer from **F2.2.2**$^{1+}$ to **2.8.4** regenerates the Ru(II) photocatalyst and yields the Au(III) complex **2.8.5**. The Au(III) complex

coordinates to the alkene **2.8.6** and causes a subsequent ring expansion to **2.8.8**. The following reductive elimination regenerates the Au(I) catalyst and forms the desired product **2.8.9**.

Scheme 2.8 : Proposed mechanism for the semi-pinacol rearrangement in the dual catalytic Au/Ru system.

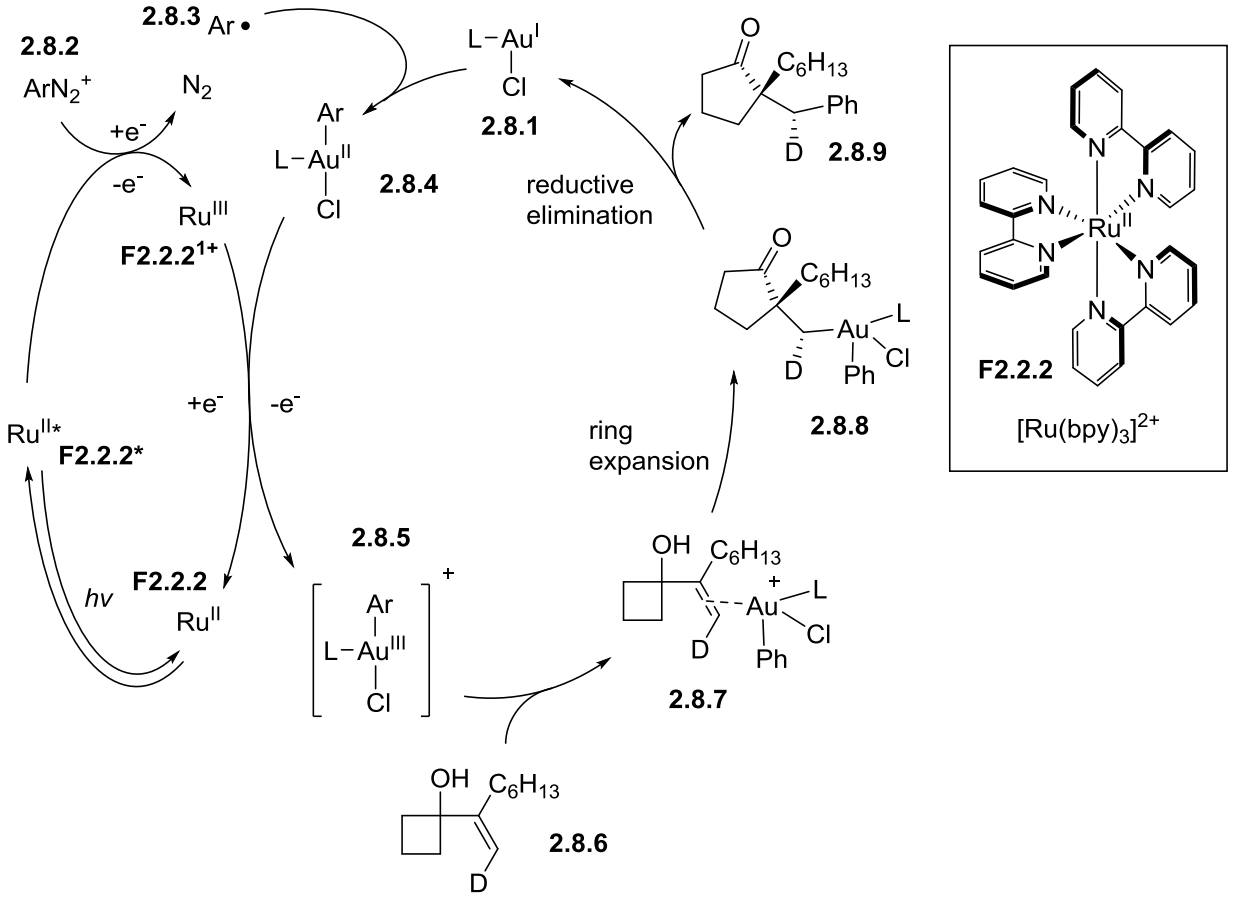

An elegant photocatalyzed reaction was demonstrated by Hashmi by using a simple tris(4-trifluoromethylphenyl)phosphine Au(I) complex **2.9.1** (**Scheme 2.9**).[58] The complex itself is not photoactive, however Hashmi proposed that the reaction of the Au(I) complex with an aryl diazonium (**2.9.2**) salt produces the light absorbent gold complex **2.9.5**. The organogold intermediate undergoes a light-enabling extrusion of N_2 to form the aryl Au(III) Lewis acid catalyst **2.9.7** which catalyzes the nucleophilic addition of methanol to an alkyne and generates the vinyl Au(III) specie **2.9.8**. Reductive elimination provides the arylated silyl enol ether **2.9.9**

which upon hydrolysis gives the desired ketone **2.9.10**. It is worth nothing the lack of a dedicated photocatalytic complex in the reaction. Preliminary iteration of the transformation were performed using Ir(III), Ru(II), and Au(I) photocatalysts in addition to PPh_3AuCl. They were believed necessary to generate an aryl radical from the aryl diazonium salt via a photomediated SET reaction. Although light was found to be crucial for the reaction, further investigation demonstrated successful conversion to the desired compound without any photocatalyst other than the tris(4-trifluoromethylphenyl)phosphine Au(I) complex.

Scheme 2.9 : Proposed mechanism of Au(I) catalyzed light mediated 1,2-difunctionalization of alkyne

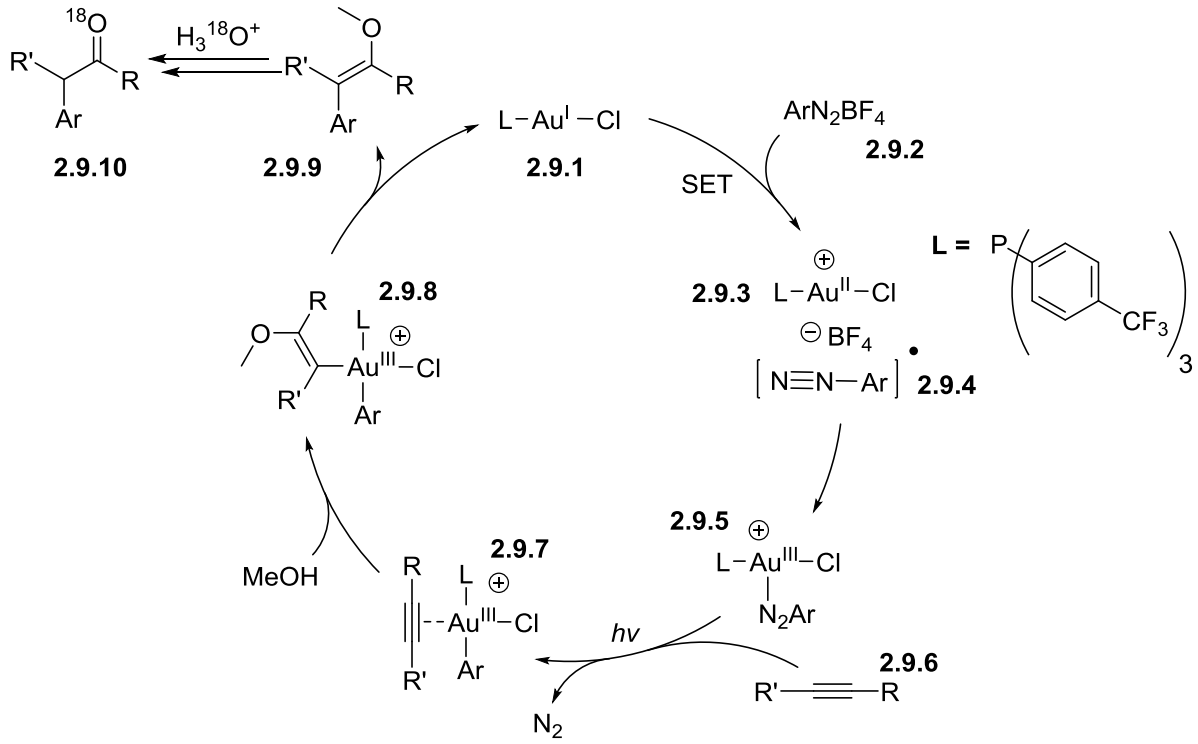

The examples above represent a small sampling of the recent developments in photocatalyzed chemistry. The renewed interest has caused many research groups to look more diligently at the possibilities offered by photocatalytic systems, which include in many ways revisiting well known radical transformations. The rapid progress in the field can be in part

attributed to technological advances in lighting systems. Specific wavelengths are now more accessible than ever before with the development of LEDs, which in many cases help avoid the need for large or powerful lasers. High intensity lights can be bought from non-specialty stores and can produce great results at low-costs. In hindsight, with today's interest placed on sustainability and efficiency, the revival of photochemistry does not only seem appropriate, it almost seems inevitable.

Many of the reactions described above inspired our development of the dimeric Au(I) mediated photochemistry, and others were often reported during our own concurrent research into the subject. The research avenues that opened to us seemed to parallel other research groups in a logical pathway towards novel reactivity. Nevertheless, all the recent advances are due in part to the previous efforts of researchers in the fields of photochemistry, radical chemistry, electrochemistry and even organometallic chemistry. The results described in the following chapters are no exception, and like the recent ruthenium photochemistry,[59] the development began with a complex synthesized many years earlier.

---

[41] Turro, N. J.; Ramamurthy, V.; Scaiano, J. C. *Modern Molecular Photochemistry of Organic Molecules*; University Books, Sausalito, CA, **2010**.
[42] Shen, J.-R. *Annu. Rev. Plant Biol.* **2015,** *66*, 23 – 48
[43] Vinyard, D. J.; Ananyev, G. M.; Dismuke, G. C. Annu. Rev. Biochem. **2013,** *82*, 577 – 606
[44] Dr. Neil Degrasse Tyson (Hanich, L.; Holtzman, S.; Pope, B.; Braga, B.; Tyson, N. G.; Silvestri, A.; Sagan, C.; Druyan, A.; Soter, S. *Twentieth Century Fox Home Entertainment Ltd.* **2014**, *Cosmos: A Spacetime Odyssey*)
[45] Fukuzumi, S.; Kotani, H,; Ohkubo, K.; Ogo, S.; Tkachenko, N. V.; Lemmetyinen, H. *J. Am. Chem. Soc.* **2004**, *126,* 1600 – 1601
[46] Prier, C. K.; Rankic, D. A.; MacMillan, D. W. C. *Chem. Rev.* **2013**, *113*, 5322 – 5363
[47] Terrett, J. A.; Cuthbertson, J. D.; Shurtleff, V. W.; MacMillan, D. W. C. *Nature* **2015**, *524*, 330 – 334
[48] Nicewicz, D. A.; Hamilton, D.S. *Synlett* **2014**, *25*, 1191 – 1196
[49] Romero, N. A.; Nicewicz, D. A. *Chem. Rev.* **2016**, *116*, 10075 − 10166
[50] Ischay, M. A.; Anzovino, M. E.; Du, J.; Yoon, T. P. *J. Am. Chem. Soc.* **2008**, *130*, 12886 – 12887

[51] Du, J.; Ruiz Espelt, L.; Guzei, I. A.; Yoon, T. P. *Chem. Sci.* **2011**, *2*, 2115 – 2119
[52] Nguyen, J. D.; D'Amato, E. M.; Narayanam, J. M. R.; Stephenson, C. R. J. *Nature Chemistry* **2012**, *4*, 854 – 859
[53] Edel, A.; Marnot, P. A.; Sauvage, J. P. *Nouv. J. Chim.* **1984**, *8* , 495 – 498
[54] Dietrich-Buchecker, C. O.; Marnot, P. A.; Sauvage, J.-P.; Kirchoff, J. R.; McMillin, D. R. *J. Chem. Soc. Chem. Commun.* **1983**, *9*, 513 – 515
[55] Kern, J.-M.; Sauvage, J.-P. *J. Chem. Soc. Chem. Commun.* **1987**, *8*, 546 – 548
[56] Hopkinson, M. N.; Sahoo, B.; Glorius, F. *Adv. Synth. Catal.* **2014**, *356*, 2794 – 2800
[57] Shu, X.-Z.; Zhang, M.; He, Y.; Frei, H.; Toste, D. F. *J. Am. Chem. Soc.* **2014**, *136*, 5844 − 5847
[58] Juang, L.; Rudolph, M.; Rominger, F; Hashmi, A. S. K. *Angew. Chem. Int. Ed.* **2016**, *55*, 4808 – 4813
[59] Paris, J. P.; Brandt, W. W. *J. Am. Chem. Soc.* **1959**, *81*, 5001 – 5002

3 Bi-nuclear Au(I) Photocatalysis

3.1 $Au_2dppm_2Cl_2$

In 1977, Schmidbaur described the synthesis and structure of a dimeric Au(I) complex which would become important in the development of our photochemical research, the complex $[Au_2(\mu\text{-dppm})_2]Cl_2$ (**Figure 3.1**). The X-ray crystallography of the complex revealed an eight

Figure 3.1 : $[Au_2(\mu\text{-dppm})_2]^{2+}$

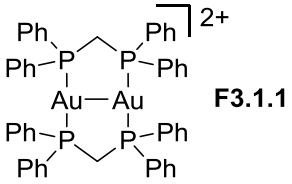

F3.1.1

membered metallocycle formed by the two bridging bisphosphane ligands and the two Au(I) atoms.[60] Schmidbaur remarked that these gold atoms formed a surprisingly short axis (296pm) which sat perpendicular to the P_2AuCl planes, indicating a possible transannular metal-metal

Table 3.1: Rate constants for quenching of $[Au_2(\mu\text{-dppm})_2](ClO_4)_2$.

Entry	Quencher	$k_q(M^{-1}s^{-1})^a$
1	Tetrabromomethane	8.90×10^9
2	Bromoform	8.70×10^9
3	Tetrachloromethane	3.37×10^9
4	Ethyl iodide	1.73×10^9
5	Methy iodide	1.00×10^9
6	Allyl bromide	7.58×10^8
7	Chloroform	4.59×10^7
8	*n*-Butyl bromide	2.85×10^6
9	Benzyl chloride	1.85×10^6

[a] Obtained from Stern-Volmer analysis where $\tau_0/\tau = 1 + k_q\tau_0[Q]$

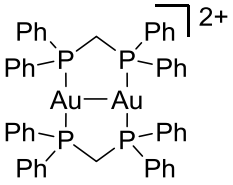

$[Au(\mu\text{-dppm})_2]^{2+}$

F3.1.1

interaction. Another study of a perchlorate analog of this complex by Che focused more on some of its photophysical properties.[61] It was shown that irradiation at 290-320 nm resulted in photoluminescence. The long lived emission band at 565 nm was attributed to a low lying phosphorescence state as suggested by the large Stokes shift. The study also showed that this photoluminescence could be quenched by various by haloalkanes including benzyl chloride, *n*-butyl bromide and ethyl iodide (**Table 3.1**).

Particular attention was given to the nature of the orbitals forming the suspected Au-Au interaction previously mentioned by Schmidbaur. Through photophysical studies, the Che group was able to determine the nature of the transition in the excited state by using the analogous complex **F3.2.1** bearing the UV-silent ligand DCPM (**F3.2.2**).

Figure 3.2 : Binuclear Au(I) complex bearing UV silent ligand DCPM.

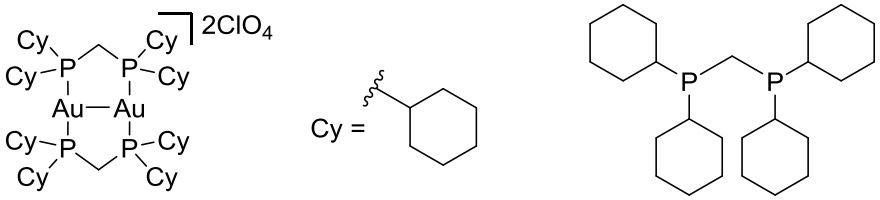

[Au(μ-dcpm)$_2$](ClO$_4$)$_2$ **F3.2.1** DCPM **F3.2.2**

In various solvents and phase conditions, absorption of a photon was shown to promote a metal centered 5dσ*→6pσ transition, which causes an electron to be excited from the anti-bonding 5d$_{z^2}$ to the bonding combination 6s/6p$_z$ orbital (Au-Au axis defined as z). The ground state metal-metal interaction shows a formal bond order of 0 which is enhanced in the ^{1}5dσ*6pσ excited state, leading to a formal bond order of 1.[62] Although this suggests that photoexcitation increases the bond order between the two gold atoms, there is a large amount of evidence indicating the presence of a Au(I) aurophilic interaction in the ground state.[63] This particular aurophilic binding is said to be "fully supported" (**Figure 3.3**), where two bridging ligands

connect the Au(I) atoms together. Such interactions can have binding energies between 5 and 15 kcal mol^{-1} which play a significant role in the molecular structure adopted by the binuclear Au(I) complex in solution.

Figure 3.3 : Aurophilic interactions.

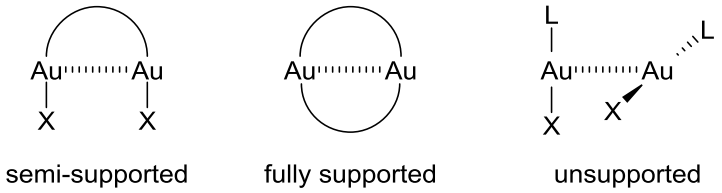

3.2 Photocatalyzed Reduction of Halocarbon Bonds

The photochemical activity shown by the binuclear Au(I) complex inspired us to develop an efficient photocatalytic system for the reduction of haloalkanes to easily access carbon centered radicals. The initial observations made by Che involving the quenching of the complex by unactivated bromoalkanes helped put together the pieces required for a complete catalytic cycle (**Scheme 3.1**). First, excitation of the $[Au_2(\mu\text{-dppm})_2]^{2+}$ would lead to the higher energy $^3[Au_2(\mu\text{-dppm})_2]^{2+*}$. Oxidative quenching by a haloalkane would lead to the formation of a carbon centered radical, a halide anion, and $[Au_2(\mu\text{-dppm})_2]^{3+}$. The reduction of the complex

Scheme 3.1 : Proposed photocatalyzed reduction of haloalkanes.

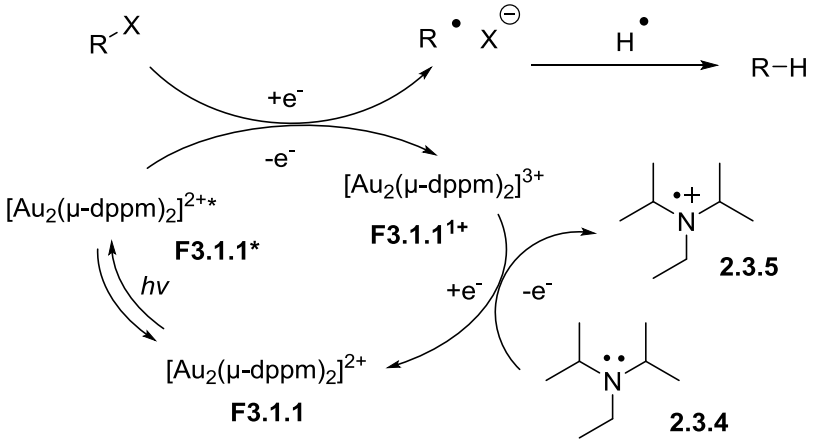

back to its ground state would require a sacrificial electron donor, and the carbon centered radical would require a hydrogen donor to achieve full reduction. We postulated that the role of electron donor and hydrogen donor could be filled by a trialkylamine in both cases.

To probe the transformation, a simple bromoalkene constructed from diethyl malonate was used (**T3.2.1a**).[64] In combination with a trialkylamine base as a sacrificial electron donor,

Table 3.2 : Optimization of photocatalyzed cyclization of bromoalkenes.

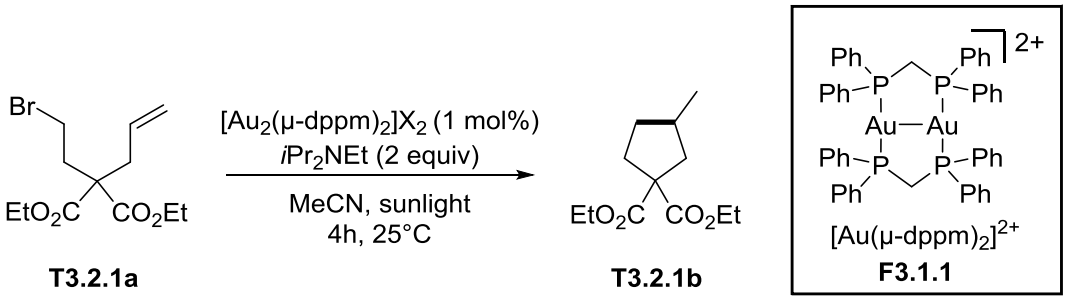

T3.2.1a **T3.2.1b** **F3.1.1**

Entry	Catalyst	Light Source	Yield [%]
1[b]	$[Au_2(\mu\text{-dppm})_2](OTf)_2$	Sunlight	20
2	$[Au_2(\mu\text{-dppm})_2](OTf)_2$	Sunlight	94
3	$[Au_2(\mu\text{-dppm})_2](NTf_2)_2$	Sunlight	72
4	$[Au_2(\mu\text{-dppm})_2](BF_4)_2$	Sunlight	70
5	$[Au_2(\mu\text{-dppm})_2](SbF_6)_2$	Sunlight	90
6	$[Au_2(\mu\text{-dppm})_2]Cl_2$	Sunlight	86
7	$[Au_2(\mu\text{-dppm})_2]Cl_2$	UVA(315-400 nm)	74
8[c]	–	Sunlight / UVA	s.m.
9[d]	$[Au_2(\mu\text{-dppm})_2]Cl_2$	–	s.m.
10[e]	$[Ru(bpy)_3]Cl_2$	23 W CFL / LEDs	s.m.
11[e]	$[Ir(ppy)_2(dtbbpy)]PF_6$	23 W CFL / LEDs	s.m.
12[e]	*fac*-$[Ir(ppy)_3]$	23 W CFL / LEDs	<5%

[a] All reactions were performed in degassed solvent with Pyrex glassware. [b] Et_3N was used instead of iPr_2NEt. [c] The reaction mixture was irradiated for 18h. [d] The reaction mixture was heated at 60°C for 24h. [e] The reaction mixture was irradiated for 36h.

the binuclear Au(I) complex $[Au_2(\mu\text{-dppm})_2]^{2+}$ was able to convert compound **T3.2.1a** to **T3.2.1b** in excellent yield when under irradiation. A short optimization indicated that *i*Pr_2NEt in acetonitrile (MeCN) and sunlight gave the highest yields (up to 94%, entry 2).

The different counterions only slightly affected the conversion of **T3.2.1a** to **T3.2.1a** (entry 2-6). The difference was attributed mainly to the overall stability of the dimeric gold complex under the reaction conditions. As such, complex **F3.1.1**Cl_2 was selected because of its high stability and overall robustness for further exploration of the reaction scope. In anticipation for the reduced sunlight of Canadian winters, UVA (315-400 nm) lamps were tested and proven to be decent surrogates for sunlight in the reaction. Control experiments showed complete recovery of starting material in the absence of light or catalyst (entry 8 and 9). Other common photocatalytic systems were compared and proved unable to efficiently catalyze the cyclization (entry 10-12).

3.2.1 Reduction of unactivated bromoalkanes

An expanded look into bromoalkenes provided further insight into the reaction (**Table 3.3**). Trisubstituted alkenes **T3.3.1a and T3.3.2a** proved suitable for both 5-*exo* and 6-*exo* cyclization and showed excellent conversion (entry 1-4). Interestingly, two products were recovered from those reactions; the isopropyl and the isopropenyl substituted product. The formation of the alkene was attributed to the dimeric gold complex oxidizing the tertiary radical to a carbocation and a subsequent deprotonation.[65] The monosubstituted alkene **T3.3.3a** showed lower yield then the equivalent 5-*exo* reaction (entry 5-6). The reaction also proved successful when cyclizing onto an alkyne instead of an alkene (**T3.3.4a**, entry 7-8). Replacing the *gem*-diethyl ester moiety from the substrate with a sulfonyl protected nitrogen (**T3.3.5a**) caused a

Table 3.3 : Photocatalyzed cyclization of unactivated bromoalkanes.

Entry	Substrate	Product	Procedure [a] (type of light)	Yield [%] (ratio)[b]
1[b]	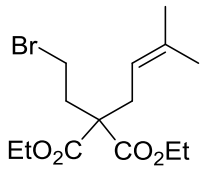 **T3.3.1a**	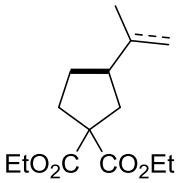 **T3.3.1b,c**	A (UVA)	81 (73:27)
2			A (Sunlight)	92 (65:35)
3	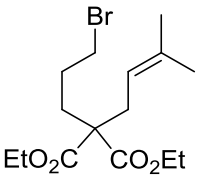 **T3.3.2a**	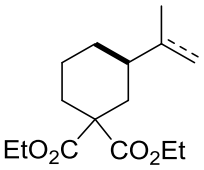 **T3.3.2b,c**	A (UVA)	58 (84:16)
4			A (Sunlight)	81 (86:14)
5	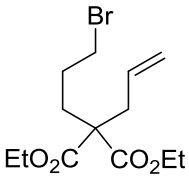 **T3.3.3a**	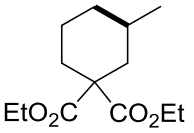 **T3.3.3b**	A (UVA)	58
6			A (Sunlight)	60
7	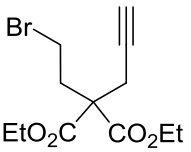 **T3.3.4a**	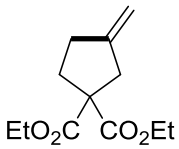 **T3.3.4b**	A (UVA)	93
8	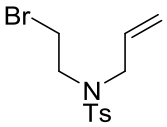 **T3.3.5a**	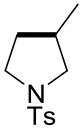 **T3.3.5b**	A (UVA)	63
9			B (UVA)	66[c]
10	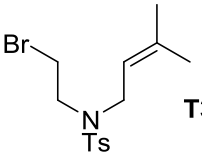 **T3.3.6a**	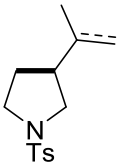 **T3.3.6b,c**	B (UVA)	86 (50:50)[c]
11	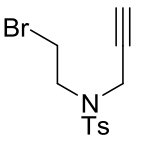 **T3.3.7a**	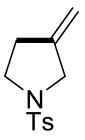 **T3.3.7b**	B (UVA)	63[c]

[a] Procedure A: $[Au_2(\mu\text{-dppm})_2]Cl_2$ (2.5 mol%), *i*Pr_2NEt (2 equiv), MeCN, 2-8 h; Procedure B: $[Au_2(\mu\text{-dppm})_2]Cl_2$ (2.5 mol%), *i*Pr_2NEt (5 equiv), HCO_2H (2 equiv), MeCN, 1-4 h. [b] Ratio of the isopropyl to the isopropenyl substituted product. [c] The reaction was completed in 1h.

substantial reduction in the overall rate of reaction. The irradiation was extended to 36 h to achieve full conversion and a 63% yield of the corresponding pyrrolidine (**T3.3.5b,** entry 8). A short screen of compatible electron donors demonstrated that the addition of formic acid alongside *i*Pr_2NEt greatly enhanced the rate of reaction. Full conversion was achieved in one hour and yielded 66% of pyrrolidine (**T.3.3.5b**, entry 9). The conditions were applied to substrates **T3.3.6a** and **T3.3.7a** to yield the corresponding pyrrolidines in 86% and 63% yield respectively (entries 10-11).

Labeling experiments using deuterated formic acid (DCO_2D) led to a 20% incorporation of deuterium in the final product, which seemed to indicate that *i*Pr_2NEt is still the major source of hydrogen atom in the reaction. Although the increased reactivity caused by the addition of formic acid is undisputable, there is currently insufficient data to fully explain the phenomenon.

3.2.2 Reduction of bromoarenes

Bromoarenes were submitted to the same reaction conditions and performed similarly (**Table 3.4**). Phenolic ether **T3.4.1a** yielded a mixture of isopropyl and isopropenyl substituted dihydrobenzofuran in 74% yield, again indicating that the oxidation of the tertiary radical to a carbocation is non negligible (entry 1). Biaryl compounds **T3.4.2a** and **T3.4.3a** yielded the biphenyl compounds **T3.4.2b** and **T3.4.3b** in excellent yields. It should be noted that the oxidation levels of the starting materials are the same as the final products. Similar to compounds **T3.3.1c** and **T3.3.2c**, the net reaction from the starting material is redox neutral, indicating that the substrate itself can become a source of electron for the reduction of the gold complex. It is also observed in compound **T3.4.4c**, one of the two products recovered from the reaction of sulfonamide **T3.4.4a** (entry 6). Interestingly, the other compound recovered (**T3.4.4b**) is

Table 3.4: Photocatalyzed cyclization of bromoarenes.

Entry	Substrate	Product	Procedure [a] (type of light)	Yield [%] (ratio)
1	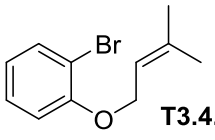 **T3.4.1a**	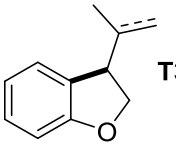 **T3.4.1b**	A (Sunlight)	74 (71:29)[b]
2	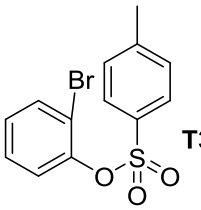 **T3.4.2a**	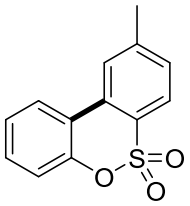 **T3.4.2b**	A (UVA)	75[c]
3			A (Sunlight)	80
4	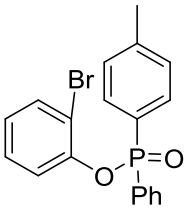 **T3.4.3a**	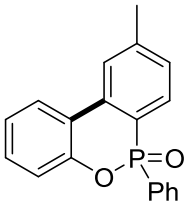 **T3.4.3b**	A (UVA)	90[c]
5			A(Sunlight)	91
6	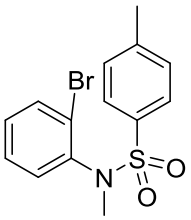 **T3.4.4a**	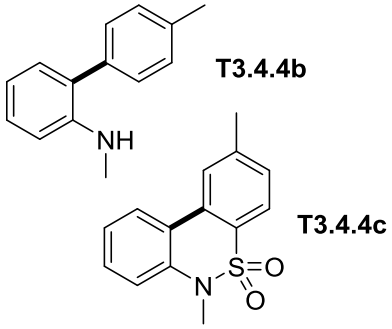 **T3.4.4b** **T3.4.4c**	A (UVA)	93[c] (63:37)[d]
7	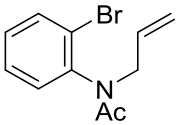 **T3.4.5a**	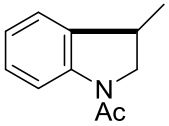 **T3.4.5b**	B (UVA)	90[c]
10	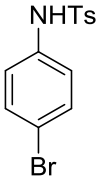 **T3.4.6a**	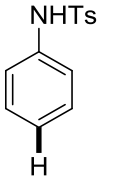 **T3.4.6b**	B (UVA)	94[c]

[a] Procedure A: $[Au_2(\mu\text{-dppm})_2]Cl_2$ (2.5 mol%), *i*Pr_2NEt (2 equiv), MeCN, 2-8 h; Procedure B: $[Au_2(\mu\text{-dppm})_2]Cl_2$ (2.5 mol%), *i*Pr_2Net (5 equiv), HCO_2H (2 equiv), MeCN, 1-4 h. [b] Ratio of the isopropyl to the isopropenyl substituted product. [c] The reaction was irradiated 8-16 h; $[Au_2(\mu\text{-dppm})_2]Cl_2$ (5 mol%). [d] Ratio of **T3.4.4b** to **T3.4.4c**.

believed to arise from an *ipso*-substitution and a subsequent fragmentation of the sulfonyl moiety as demonstrated by the work of Motherwell.[66] **T3.4.5a** was submitted to the modified conditions using formic acid to achieve the desired indoline **T3.4.5b** in 90% yield (entry 9), and the same conditions successfully catalyzed the full reduction of bromoaniline **T3.4.6a** (entry 10).

3.2.3 Photocatalyzed intermolecular radical addition

Preliminary extension of this method to intermolecular addition reactions were met with some success (**Scheme 3.2**). The conveniently available diethyl diallylmaloate **3.2.2** and 1-bromopropanol **3.2.1** successfully yielded the monoaddition/cyclization product **3.2.3** in 77% yield. N-chloromethylphtalimide **3.2.4** also productively added to the diallyl acceptor to form compound **3.2.5**, albeit in lower yield.

Scheme 3.2 : Photocatalyzed intermolecular radical addition of haloalkanes.

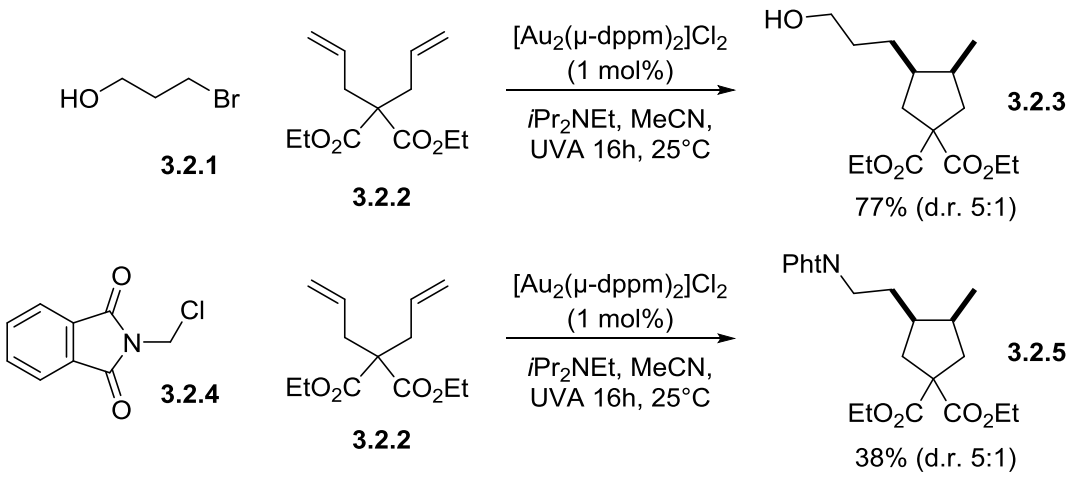

The 2-bromobenzylbromide **3.3.1** was an interesting case (**Scheme 3.3**). Under the reaction conditions, it yielded dihydrophenanthrene **3.3.3** in 44% yield. It was postulated that the benzylic C-Br bond could undergo homolytic cleavage when subjected to UVA light, and subsequently dimerize to the bibenzyl product **3.3.2** prior to the formation of the final product. In order to test the hypothesis, **3.3.1** was irradiated with UVA in MeCN and in the presence of

*i*Pr$_2$NEt. The reaction resulted in the successful isolation of compound **3.3.2** which was submitted to the Au(I) photocatalyzed conditions, yielding the dihydrophenanthrene **3.3.3** as expected.

Scheme 3.3 : Photocatalyzed dimerization of bromobenzyl bromide.

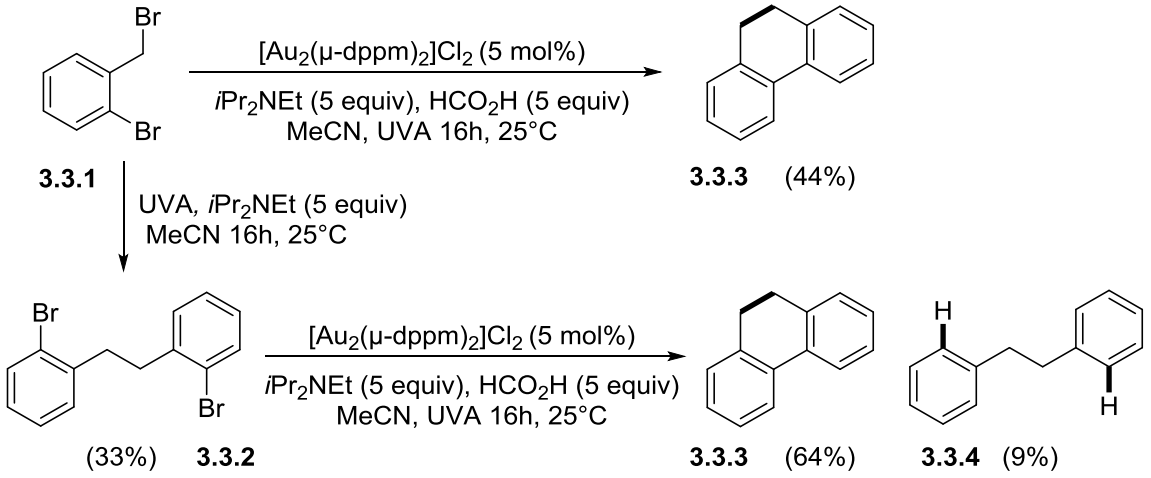

The results above described the first procedure for reductive radical reactions of unactivated bromoalkanes and bromoarenes using dimeric gold catalysts. The initial results showcased the viability of the catalytic system for both intra and intermolecular processes. The mechanism was so far not fully elucidated, however sufficient understanding of the reaction supported its synthetic potential.[67]

The initial data gathered by Che pointed to an oxidative quenching pathway, but the reductive quenching by the *i*Pr$_2$NEt was still considered a possibility under the reaction conditions. This would suggest the formation of the same carbon centered radical from two different oxidation states of the photocatalyst. Therefore, the excited photocatalyst **F3.1.1*** could undergo a reductive quench through a single electron transfer from *i*Pr$_2$NEt, yielding the reduced complex **F3.1.1^{1-}**, followed by a subsequent single electron transfer reaction to the carbon bromide bond to yield the carbon centered radical (**Scheme 3.4**). Alternatively, the excited

photocatalyst **F3.1.1*** could go through an oxidative quench, directly reducing the carbon bromide bond via a single electron transfer reaction to generate the carbon centered radical and form the oxidized complex **F3.1.1**$^{1+}$. The complex would then be reduced by *i*Pr_2NEt and return to its ground state.

Scheme 3.4 : Possible quenching pathways of $Au_2(dppm_2)Cl_2$ in the photocatalyzed reduction of carbon bromide bonds.

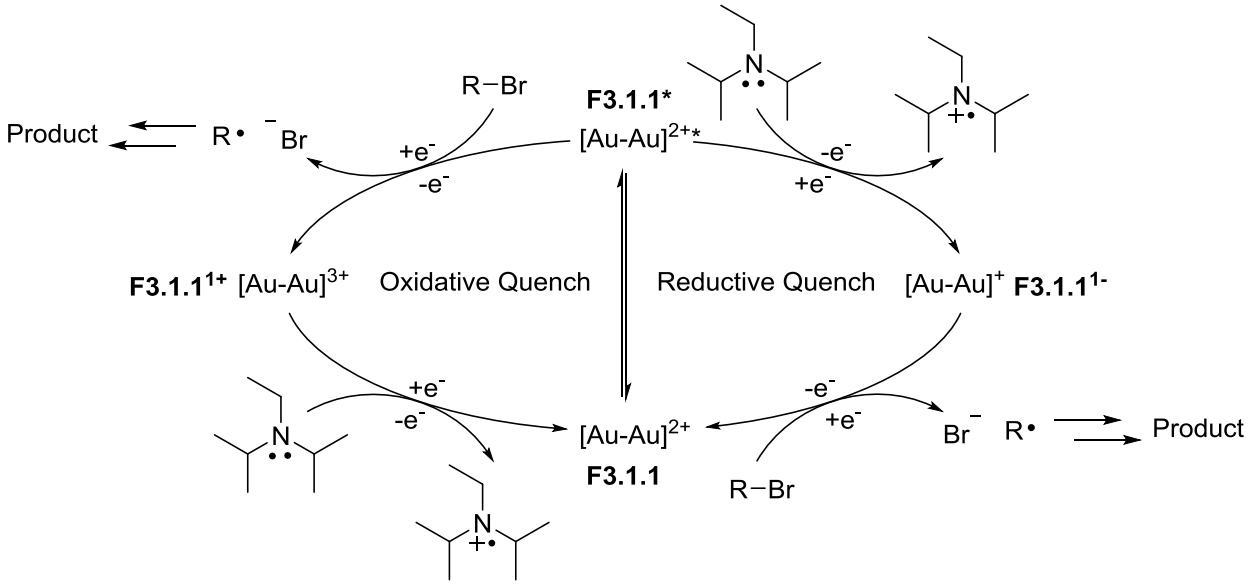

3.3 Further Development of Au(I) Photochemical Reduction

The development of the method did emphasize the need for a consistent and uniform lighting system which would provide more accurate control of the reaction. Consequently, we evaluated various light sources and elected to use high powered UVA (365 nm) light emitting diodes (LEDs). Initial results demonstrated that irradiation using 365 nm UV LEDs gave better

Scheme 3.5 : Appearance of new product under 365nm LED irradiation.

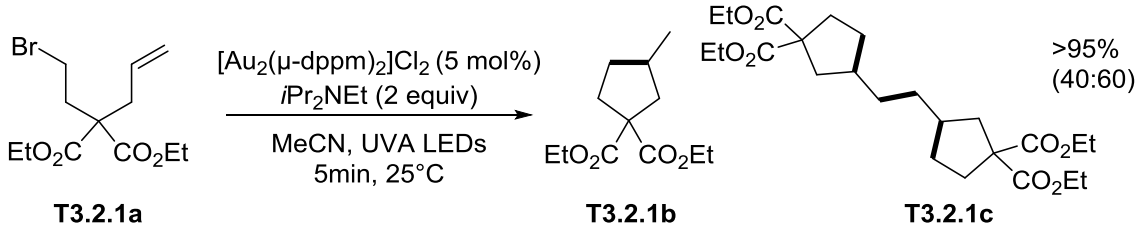

results and shorter irradiation times were required for the full conversion of **T3.2.1a** (from 4 h under sunlight to 5 min with LEDs). However, the increased rate of the reaction translated into the formation of dimer **T3.2.1c** in significant amounts.

Originally, we proposed that compound **T3.2.1c** originated from a rapid reduction of the carbon-bromide bond relative to the original conditions, causing an increase in the population of radical species available for head to head termination. One can see this as a result of a relatively

Table 3.5 : Optimization of bromoalkane dimerization.

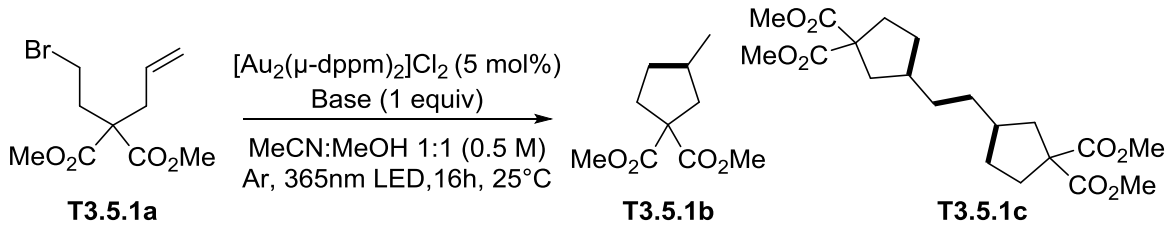

T3.5.1a **T3.5.1b** **T3.5.1c**

Entry	Base	Yield [%] **T3.5.1a**	Yield [%] **T3.5.1b**	Yield [%] **T3.5.1c**
1	Et_3N	0	24	75
2	d_{15}-Et_3N	0	20	72
3	Et_3N[b]	0	7	66
4	d_{15}- Et_3N[b]	0	9	89 (53)
5	Et_3N[d]	0	95 (68)	0
6	Et_3N[e]	100	0	0
7	–	100	0	0
8	Et_3N[f]	100	0	0
9	Et_3N[g]	100	0	0

[a] **T3.5.1a** (0.2 mmol), [Au(μ-dppm)$_2$]Cl$_2$ (5 mol%), base (1 equiv), 1:1 MeCN:MeOH (0.5 M), Ar degas, UVA LED irradiation for 16h at room temperature. Yields determined by ^{1}H NMR analysis using an internal standard of mesitylene (isolated). [b] Deuterated solvents used (CD_3OD and CD_3CN). [c] Produces corresponding deuterated **T3.5.1b** as byproduct. [d] 1,4-cyclohexadiene (3 equiv) was added. [e] TEMPO (3 equiv) was added. [f] Absence of [Au(μ-dppm)$_2$]Cl$_2$. [g] Absence of UVA LED irradiation.

slower rate for hydrogen atom abstraction from the *i*Pr_2NEt compared to the recombination of the carbon centered radicals. As part of another project, summer student Huy Tran (under my supervision) synthesized the dimethylmalonate **T3.5.1a** and submitted it to similar conditions (**Scheme 3.5**). To our surprise, the replacement of *i*Pr_2NEt by Et_3N led to the formation of **T3.5.1c** as the major product (entry 1). In an attempt to slow down the hydrogen abstraction, we envisioned performing the reaction in the presence of triethylamine-*d15.* It caused practically no change in yield or product ratio (entry 2). The reaction was then performed in deuterated acetonitrile-*d3* and methanol-*d4* and demonstrated an increase in ratio favoring dimer **3.5.1c** (entry 3). Optimal conditions for the formation of **3.5.1c** (89% yield) consisted of using deuterated Et_3N-*d15* in addition to deuterated solvents in order to reduce the rate of hydrogen abstraction from both the solvent and the sacrificial electron donor (entry 4). The addition of 1,4-cyclohexadiene as a hydrogen atom source completely reversed the product selectivity, forming **T3.5.1b** as the sole product in 95% yield (entry 5). One can argue that the results would support the hydrogen atom transfer process as the rate determining step. Although the hydrogen atom transfer could explain the mechanism by which the reduced compound **T3.5.1c** is formed, it does not discard the hypothesis that the dimerized product could arise from a mechanism other than radical recombination. (see **Section 3.5**)

Another interesting compound was discovered when testing new conditions with the LED illumination system. In an attempt to find other sacrificial electron donors, compound **T3.2.1a** was combined with ammonium formate and photocatalyst **F3.1.1**Cl_2 in a mixture of 10% water in MeCN, and submitted to 1.5 h of UVA irradiation (**Table 3.6**, entry 1). Despite product **T3.2.1b** only forming in minimal amounts (<10%), the unexpected bromoalkane **T3.2.1d** was present in 22% yield, the rest being starting material. Using sodium bicarbonate instead of

ammonium formate increased the yield to 31% (entry 2). Omitting both additives and changing the ratio of MeCN:H_2O to 7:3 eventually yielded **T3.2.1d** in 67% yield (entry 7), the mass balance being starting material and less than 10% of **T3.2.1b**.

*Table 3.6 : Formation of brominated compound **T3.2.1d**.*

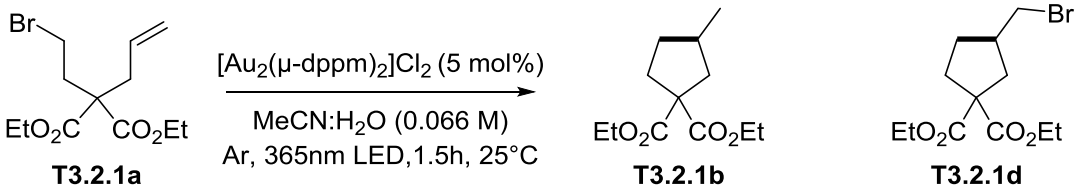

Entry	MeCN:H_2O (3 mL)	**T3.2.1b** [%]	**T3.2.1d** [%]
1[a]	9:1	11	22
2[b]	9:1	11	31
3	9:1	11	35
4[c]	9:1	13	34
5	10:0	9	6
6	8:2	10	47
7	7:3	8	67
8	6:4	10	59
9	5:5	9	53

[a] With NH_4OAc (5 equiv). [b] With $NaHCO_3$ (5 equiv). [c] Reaction run for 16 h.

Despite the reaction not achieving full conversion within 90 minutes, it provided us clues about the reaction mechanism and possible intermediates. Using the standard condition, we closely monitored the reaction and found that after 1 min of irradiation, **T3.2.1d** was observed, along with **T3.2.1b**, dimer **T3.2.1c** and starting material **T3.2.1a**. Further irradiation of the reaction mixture led to a full conversion of both **T3.2.1a** and **T3.2.1d** into products **T3.2.1b** and **T3.2.1c**. These results suggest that **T3.2.1d** is either an intermediate or a reactive side product to the reduction reaction of **T3.2.1a**

Although a full disclosure of the reaction mechanism is not yet possible, one could envisage many possible scenarios (**Scheme 3.6**). After reduction of **T3.2.1a** to **3.6.1**, the radical intermediate could bind to a Au(II) species (**3.6.5**), forming Au(III) complex **3.6.3** (path **A**). A subsequent intramolecular Au(III) mediated carboauration would generate intermediate **3.6.4** which could undergo either a nucleophilic substitution by a bromide anion or a reductive elimination of a C-Br bond to form the observed product **T3.2.1d** (path **C**). The intermediate

*Scheme 3.6 : Potential pathways for the formation of compound **T3.2.1d**.*

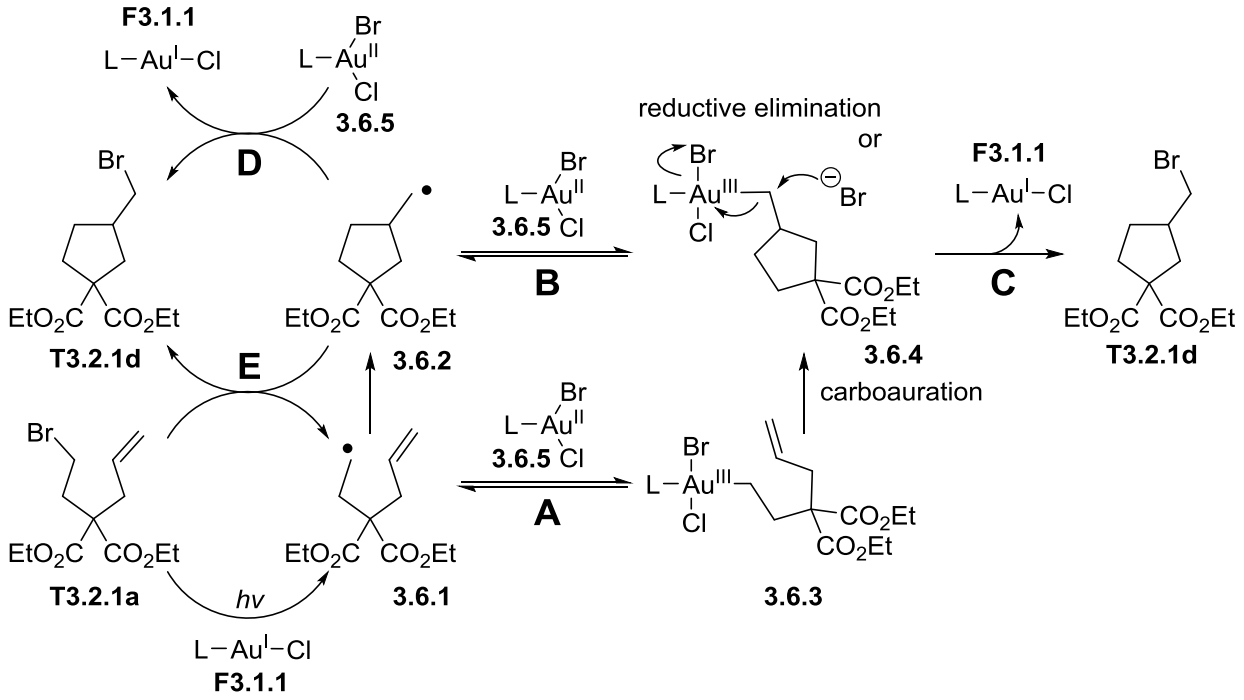

3.6.4 could also be accessed via radical **3.6.1** first undergoing a 5-*exo trig* cyclization to form intermediate **3.6.2** prior to binding with the Au(II) specie **3.6.5**. Alternatively, intermediate **3.6.2** could participate in a chain propagation reaction with the starting material **T3.2.1a**, forming **T3.2.1d** and **3.6.1**, or perhaps even abstract a bromine atom from Au(II) species **3.6.5,** regenerating the catalyst and forming the observed product **T3.2.1d**.

Scheme 3.7: Reductive elimination of carbon iodide bond.

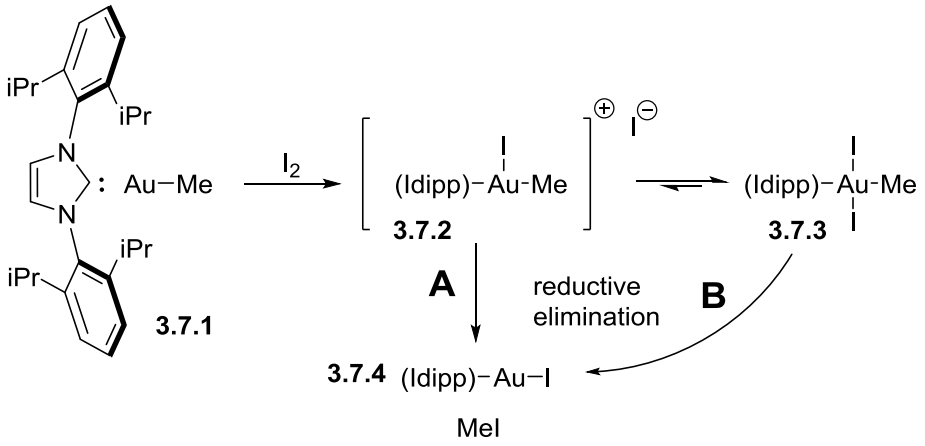

An example of reductive elimination of a carbon iodide bond by a Au(III) species has previously been reported.[68] As shown in **Scheme 3.7**, the oxidation of the Au(I) complex **3.7.1** with I_2 caused the formation of trans-(Idipp)AuI_2Me (**3.7.3**). According to Bercaw, the complex is converted to **3.7.4** and methyl iodide overtime. The mechanistic information indicates that the major route for the formation of MeI is a reductive elimination from a three coordinate cation **3.7.2** (**Scheme 3.7** path **A**) rather than from complex **3.7.3** (**Scheme 3.7** path **B**) or than an intermolecular nucleophilic attack. While the study mainly focused on results for a carbon iodide bond, it mentions that the oxidation of (Idipp)AuMe (**3.7.1**) with Cl_2 and Br_2 "appears to proceed similarly to I_2, although less cleanly", which could indicate the possibility of reductive elimination from a similar Au(III) intermediate in the reaction shown in **Scheme 3.6**.

3.4 Mechanistic Investigation

All the new results kept underlining the need for a more accurately described mechanism. If certain aspects of the mechanism could be formalized, we could better inform the decision making process for the improvement and extension of the method. This was accomplished through a collaboration with the Scaiano research group to study the photophysical properties of our catalytic system in regards to the reagents being used.[69] Including complex **F3.1.1** originally

used in the development of our method, five polynuclear Au(I) complexes were studied (**Figure 3.4**). They included the electron rich **F3.4.1** and electron deficient **F3.4.2**, a trinuclear gold analog **F3.4.3** and the N-heterocyclic biscarbene analog **F3.4.4**.

Figure 3.4 : Photoactive multinuclear Au(I) complexes.

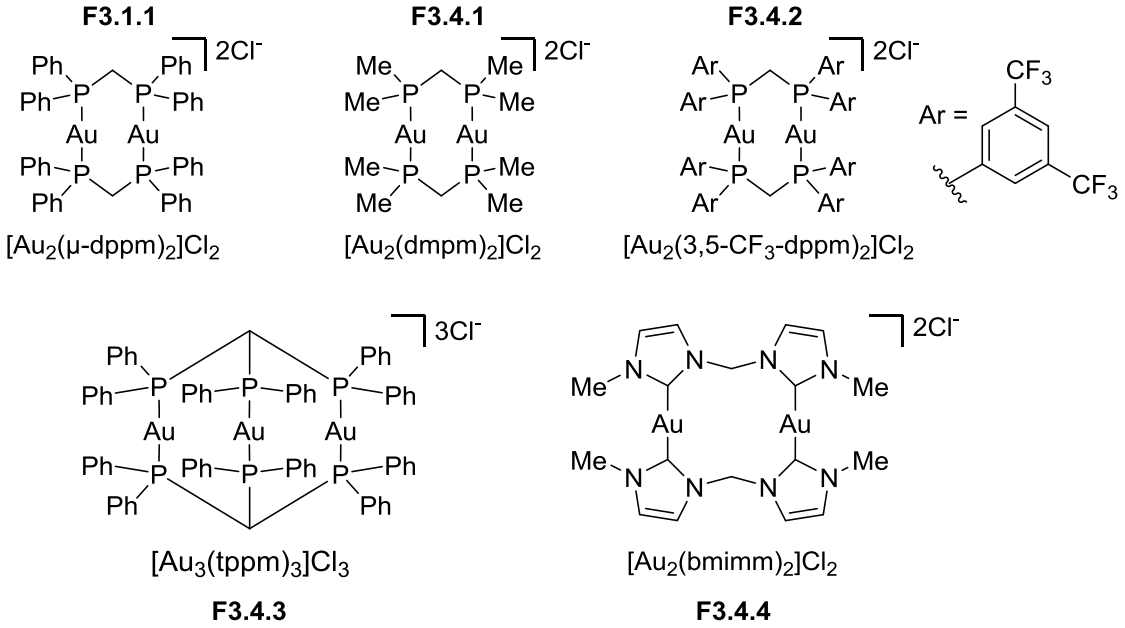

3.4.1 Chemical compatibility of polynuclear Au(I) complexes

First and foremost, the complexes studied had to be kinetically competent for the photochemical reduction of carbon bromide bonds. While all the complexes selected for the study were able to catalyze the reduction, initial results for the cyclization of **T3.2.1a** to **T3.2.1b+c** immediately highlighted an inherently different activity between the complexes (**Table 3.7**).

Conditions for the reactions were altered slightly to solve solubility issues with some complexes when using only acetonitrile. The conditions were kept uniform for all catalytic systems to permit proper comparison and do not necessarily represent the optimal reaction conditions of each system (**Table 3.7**). As it was in the previous conditions, **F3.1.1** still showed

full conversion within 5 min to the desired products (entry 1). Electron rich complex **F3.4.1** and trinuclear Au(I) complex **F3.4.3** required 2 h to achieve a full conversion (entry 4 and 12) whereas electron deficient gold complex **F3.4.2** only led to 82% conversion despite prolonged irradiation (entry 9). A complete conversion was achieved using the NHC analog **F3.4.4** although 20 h of irradiation were required (entry 17). One might be prone to attribute the different efficiency of each catalyst to their capacity of absorbing the fraction of light provided. However, this scenario would be a grave oversimplification of the reaction mechanism. In fact,

*Table 3.7 : Photoreduction of **T3.2.1a** using polynuclear Au(I) complexes.*

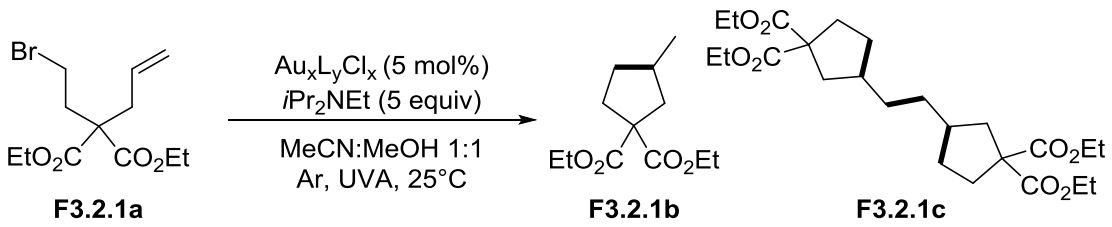

F3.2.1a **F3.2.1b** **F3.2.1c**

Entry	$Au_xL_yCl_x$ Complex	Time (h)	% Conversion (**T3.2.1b**:**T3.2.1c**)[a]
1	$Au_2(dppm)_2Cl_2$ (**F3.1.1**)	0.1	>95(40:60)
2	$Au_2(dmpm)_2Cl_2$ (**F3.4.1**)	0.1	21
3	$Au_2(dmpm)_2Cl_2$ (**F3.4.1**)	0.5	56
4	$Au_2(dmpm)_2Cl_2$ (**F3.4.1**)	2.0	>95(73:27)
5	$Au_2(3,5\text{-}CF_3\text{-}dppm)_2Cl_2$ (**F3.4.2**)	0.1	<5
6	$Au_2(3,5\text{-}CF_3\text{-}dppm)_2Cl_2$ (**F3.4.2**)	0.5	11
7	$Au_2(3,5\text{-}CF_3\text{-}dppm)_2Cl_2$ (**F3.4.2**)	2.0	27
8	$Au_2(3,5\text{-}CF_3\text{-}dppm)_2Cl_2$ (**F3.4.2**)	8.0	55
9	$Au_2(3,5\text{-}CF_3\text{-}dppm)_2Cl_2$ (**F3.4.2**)	20.0	82 (54:46)
10	$Au_3(tppm)_2Cl_3$ (**F3.4.3**)	0.1	12
11	$Au_3(tppm)_2Cl_3$ (**F3.4.3**)	0.5	41
12	$Au_3(tppm)_2Cl_3$ (**F3.4.3**)	2.0	>95 (63:37)
13	$Au_2(bmimm)_2Cl_2$ (**F3.4.4**)	0.1	<5

14	$Au_2(bmimm)_2Cl_2$ (**F3.4.4**)	0.5	28
15	$Au_2(bmimm)_2Cl_2$ (**F3.4.4**)	2.0	35
16	$Au_2(bmimm)_2Cl_2$ (**F3.4.4**)	8.0	67
17	$Au_2(bmimm)_2Cl_2$ (**F3.4.4**)	20.0	>95 (80:20)

[a] % conversion by ^{1}H NMR.

complexes **F3.4.1** and **F3.4.3** have drastically different absorption spectra (**Figure 3.5**) and yet catalyze the full conversion of **T3.2.1a** to **T3.2.1b+c** within approximately the same timeframe. Therefore, the observations seem to indicate that the thermodynamic and kinetic properties of the reaction, as well as other photophysical properties of the catalysts such as triplet quantum yield and lifetime are likely culprits for much of the observed differences in reactivity.

Figure 3.5 : Absorption spectra of polynuclear gold complexes.

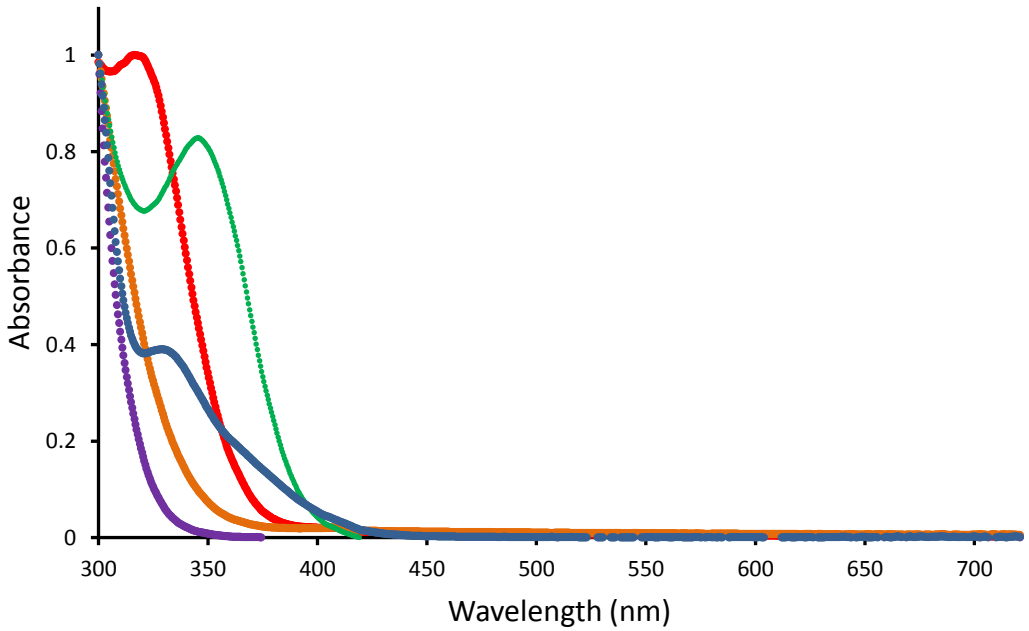

*Red = **F3.1.1** [Au_2dppm_2]Cl_2 ; Orange = **F3.4.1** [$Au_2(dmpm)_2$]Cl_2 ; Green = **F3.4.2** [Au_2(3,5-CF_3-dppm)$_2$]Cl_2 ; Blue = **F3.4.3** [$Au_3(tppm)_2$]Cl_3 ; Purple = **F3.4.4** [$Au_2(bmimm)_2$]Cl_2*

3.4.2 Oxidation and reduction potentials

The catalytic cycle shown in Scheme 3.4 : Possible quenching pathways of Au2(dppm2)Cl2 in the photocatalyzed reduction of carbon bromide bonds. **Scheme 3.4** outlines the plausible mechanistic steps for the oxidative and reductive quenching pathway of the reduction of a carbon bromide bond. It is essential to examine the thermodynamic and kinetic properties of each step to gain a better understanding of the contributing factors. The first step after initial excitation in the catalytic cycle involves a single electron transfer, either to or from the catalyst (reductive and oxidative quench respectively). The Gibbs free energy associated with the two process can help determine what pathway is preferred over the other. Calculating the value requires knowledge of many factors, such as the ground state oxidation and reduction potential of the metal complexes as well as their corresponding triplet energy, along with the

Figure 3.6: Cyclic voltammogram of polynuclear gold complexes (Anodic Scan).

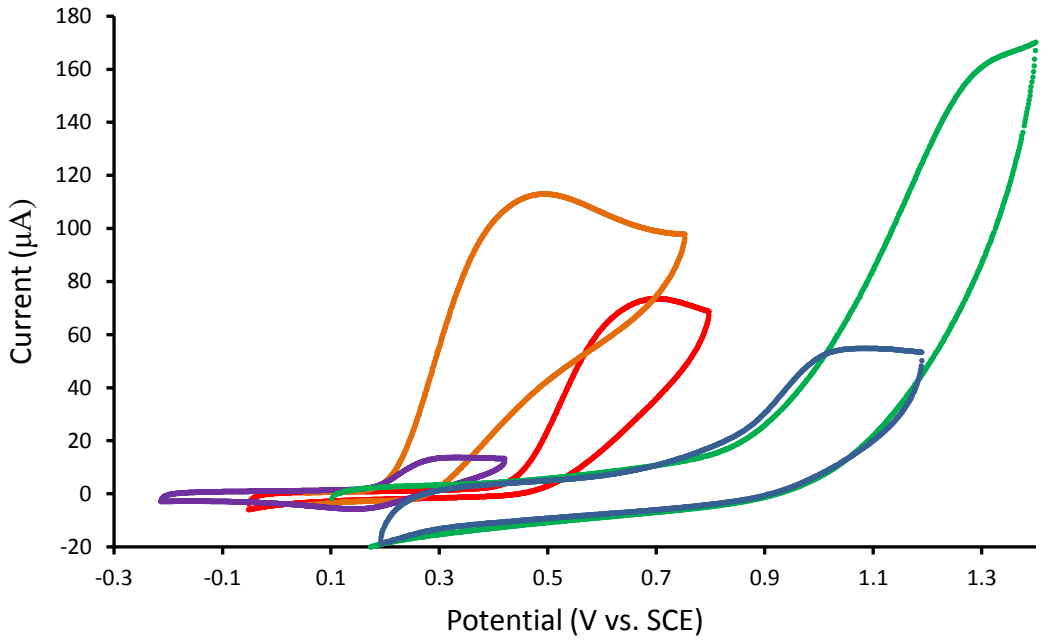

*Red = **F3.1.1** [Au_2dppm_2]Cl_2 ; Orange = **F3.4.1** [$Au_2(dmpm)_2$]Cl_2 ; Green = **F3.4.2** [Au_2(3,5-CF_3-dppm)$_2$]Cl_2 ; Blue = **F3.4.3** [$Au_3(tppm)_2$]Cl_3 ; Purple = **F3.4.4** [$Au_2(bmimm)_2$]Cl_2*

reduction potential of the acceptor molecule (**T3.2.1a**) and the oxidation potential of the acceptor molecule (**2.3.4**, *i*Pr$_2$NEt).

The values for oxidation and reduction potential of the metal complexes in their ground state were measured by Chris McTiernan (Scaiano group) using cyclic voltammetry (CV). Since all Au(I) complexes exhibited irreversible oxidation and reduction waves, the peak anodic (E_{pa}, **Figure 3.6**) and the peak cathodic ($E_{pc,}$ **Figure 3.7**) potentials were used as approximations of the oxidation and reduction potentials respectively. They are reported alongside measurements for the absorption coefficient (ε_{ex}), emission wavelength (λ_{em}), quantum yield ($\Phi_{em}{}^{b}$), triplet state lifetime ($^{3}\tau_0{}^{c}$) and triplet state energy (E_T^*) in **Table 3.8**. Timed studies of the model reaction in deuterated solvents using ^{1}H and ^{31}P NMR monitoring showed that the fate of the gold catalyst was more complicated than previously believed. The electrochemical irreversibility of the gold catalysts suggests that the complex introduced to the reaction might merely be a precatalyst,

Figure 3.7 : Cyclic voltammogram of polynuclear gold complexes (Cathodic scan).

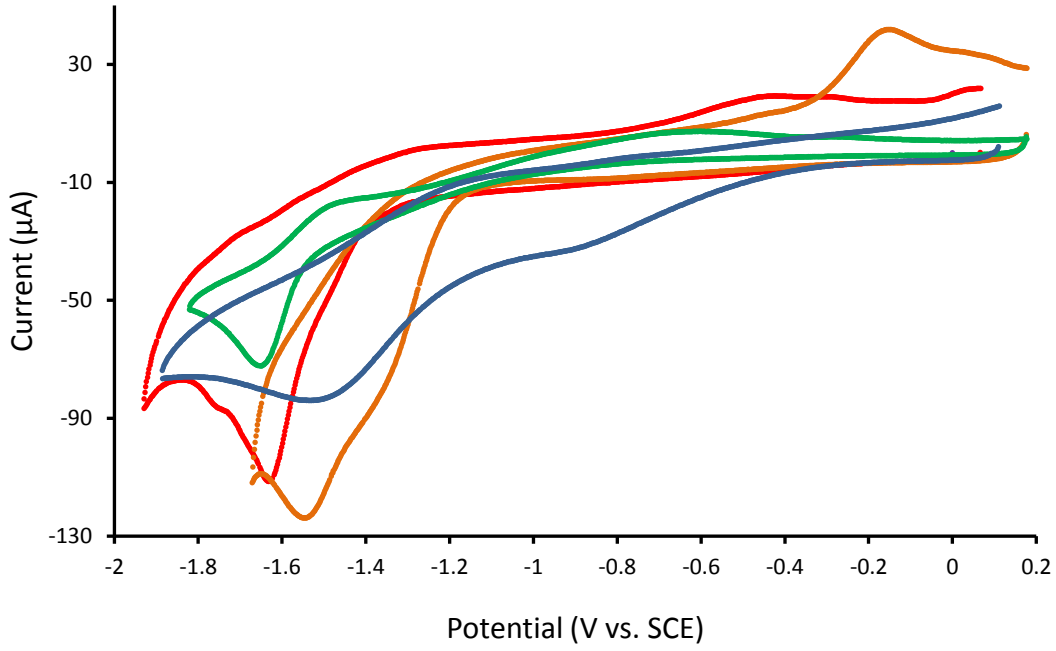

*Red = **F3.1.1** [Au$_2$dppm$_2$]Cl$_2$; Orange = **F3.4.1** [Au$_2$(dmpm)$_2$]Cl$_2$; Green = **F3.4.2** [Au$_2$(3,5-CF$_3$-dppm)$_2$]Cl$_2$; Blue = **F3.4.3** [Au$_3$(tppm)$_2$]Cl$_3$*

although further studies are necessary to conclude the true identity of the reactive intermediates.

Figure 3.8 : 77K phosphorescence spectrum of gold complexes.

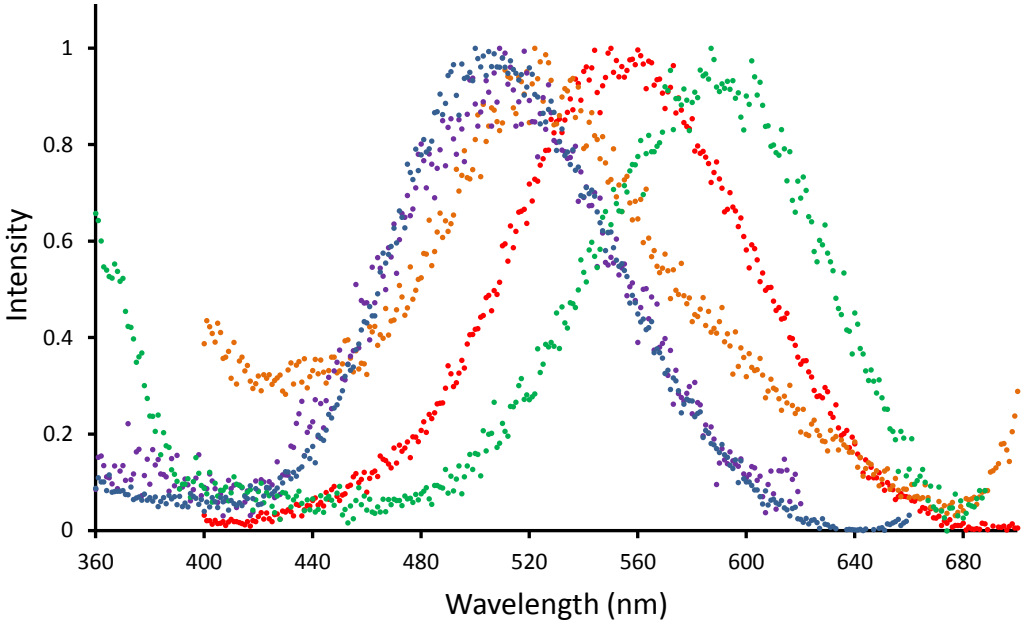

*Red = **F3.1.1** [Au2dppm2]Cl2 ; Orange = **F3.4.1** [Au2(dmpm)2]Cl2 ; Green = **F3.4.2** [Au2(3,5-CF3-dppm)2]Cl2 ; Blue = **F3.4.3** [Au3(tppm)2]Cl3 ; Purple = **F3.4.4** [Au2(bmimm)2]Cl2*

Table 3.8 : Photophysical and electrochemical data of the polynuclear Au(I) complexes.

Catalyst	λ_{ex}[a]	ε_{ex} (M^{-1} cm^{-1})[a]	λ_{em}[a]	Φ_{em}[b]	$^3\tau_0$[c]	E_T^* (kJ mol−1)[d]	E_{pa} (V vs. SCE)[e]	E_{pc} (V vs. SCE)[e]
F3.1.1 $Au_2(dppm)_2Cl_2$	355 nm	73 163	560 nm	0.137	850 ns	215	0.70	−1.63
F3.4.1 $Au_2(dmpm)_2Cl_2$	308 nm	3813	525 nm	0.028	400 ns	228	0.49	−1.77
F3.4.2 $Au_2(3,5\text{-}CF_3\text{-}dppm)_2Cl_2$	355 nm	6539	590 nm	0.006	10 µs	203	1.41	−1.65
F3.4.3 $Au_3(tppm)_2Cl_3$	355 nm	3780	545 nm	0.028	1.5 µs	220	1.09	−1.54
F3.4.4 $Au_2(bmimm)_2Cl_2$	308 nm	491	510 nm	0.017	20 ns	235	0.34	—

[a] Measured in MeCN at 298 K. [b] Photoluminescence quantum yield determined relative to $Ru(bpy)_3Cl_2$ as standard (ΦMeCN = 0.095).60 [c] Triplet lifetime measured in N_2 degassed MeCN after 10 mJ laser pulse at λex. [d] Triplet-state energy determined from the low temperature (77 K) phosphorescence spectra. [e] Determined using cyclic voltammetry. Conditions: scan rate = 100 mV s−1; 0.5–2.0 mM Au(I) complex in Ar degassed MeCN containing 100 mM Bu_4NClO_4 supporting electrolyte; Pt wire working electrode; Pt wire counter electrode; Ag wire pseudo-reference electrode; Fc/Fc+ redox couple as internal reference (0.41 V vs. SCE); oxidation and reduction potential reported as peak anodic (E_{pa}) and peak cathodic (E_{pc}) potentials due to their irreversible nature.

Triplet energies (E_T^*) of the Au(I) catalysts were obtained from their phosphorescence spectra at 77 K (**Figure 3.8**). With the use of equation (**1**) and equation (**2**), we calculated their oxidation (E_{ox}^*) and reduction (E_{red}^*) potentials in their excited state (**Table 3.9**). In the case of **F3.1.1**, the calculated values found were (E_{ox}^*) = -1.53 V *vs.* SCE and (E_{red}^*) = 0.60 V *vs.* SCE (entry 1). This (E_{ox}^*) value was in good agreement with the literature value of 1.6 ± 0.1 V *vs.* SCE obtained through excited state quenching using a series of pyridinium acceptors of known reduction potential.[70]

$$E_{ox}^* = E_{pa} - E_T^* \quad (1)$$

$$E_{red}^* = E_{pc} + E_T^* \quad (2)$$

Table 3.9 : Excited state redox potentials of the polynuclear Au(I) complexes.

Entry	Catalyst	E_T^* (V)	E_{pa} (V vs. SCE)[e]	E_{pc} (V vs. SCE)[e]	E_{ox}^* (V vs. SCE)	E_{red}^*(V vs. SCE)
1	**F3.1.1** $Au_2(dppm)_2Cl_2$	2.23	0.70	-1.63	-1.53	0.60
2	**F3.4.1** $Au_2(dmpm)_2Cl_2$	2.36	0.49	-1.77	-1.87	0.59
3	**F3.4.2** $Au_2(3,5\text{-}CF_3\text{-}dppm)_2Cl_2$	2.10	1.41	-1.65	-0.69	0.45
4	**F3.4.3** $Au_3(tppm)_2Cl_3$	2.28	1.09	-1.54	-1.19	0.74
5	**F3.4.4** $Au_2(bmimm)_2Cl_2$	2.44	0.34	—	-2.10	—

3.4.3 Oxidative *vs* reductive quenching

Using equation (**3**) and (**4**) along with the measured reduction potential of **T3.2.1a** (E_{red} = -1.90 V *vs.* SCE) and the oxidation potential of *i*Pr$_2$NEt (E_{ox} = 0.50 V *vs.* SCE), we determined the Gibbs free energy associated with either pathway of the gold catalyst quenching.

$$\Delta G_{eT}^{\text{ox quenching}} = E_{ox}^*(\text{Au}) - E_{red}(\mathbf{T3.2.1}\boldsymbol{a}) \quad (3)$$

$$\Delta G_{eT}^{\text{red quenching}} = E_{ox}(i\text{Pr}_2\text{NEt}) - E_{red}^*(Au) \quad (4)$$

The reductive quenching of catalyst **F3.3.1** by *i*Pr$_2$NEt was found to be thermodynamically favorable by -0.1 eV. On the other hand, the oxidative quenching of **F3.1.1** by the malonate derived bromoalkane **T3.2.1a** is thermodynamically uphill by 0.37 eV. It would suggest that **F3.1.1** undergoes reductive quenching in the photocatalytic system, but it is worth noting that the thermodynamics of a reaction only determine if a reaction can take place, and there are examples in photoredox literature of reactions with significant free energy barriers proceeding efficiently. All the complexes used for the study have only minor differences in their E^*_{red}, however they vary significantly in their E^*_{ox}, particularly **F3.4.1** and **F3.4.4** (**Table 3.9** entry 2 and 5). Their oxidation potentials are negative enough to make the oxidative quenching by **F3.2.1a** thermodynamically favorable. To determine which of the two pathways actually takes place, the kinetics of the reactions have to be analyzed.

To that end, time-resolved transient spectroscopy was performed on the gold complexes, using nanosecond laser flash photolysis (LFP) to determine the rate of triplet quenching by each different component. The data used to determine the rate of quenching of **F3.1.1** by 1-bromobutane is shown in **Figure 3.10**, **Figure 3.9** and **Figure 3.11**. The quenching of the excited catalyst with different compounds at varying concentrations allowed for the determination of the bimolecular rate constant for the reaction. The method was applied to all quenchers and all complexes.

Figure 3.10 Transient spectrum showing $[Au_2(dppm)_2]Cl_2$ emission signal at 560 nm from laser pulse excitation (355 nm, 10 mJ)

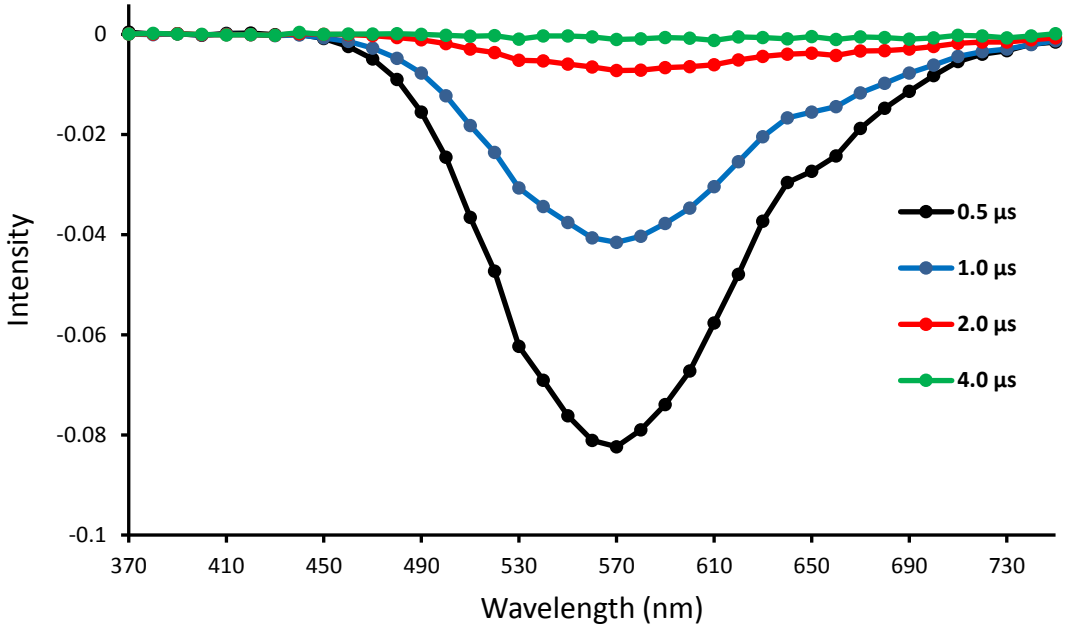

Figure 3.9 : Corresponding decay trace of $[Au_2(dppm)_2]Cl_2$ at 560 nm.

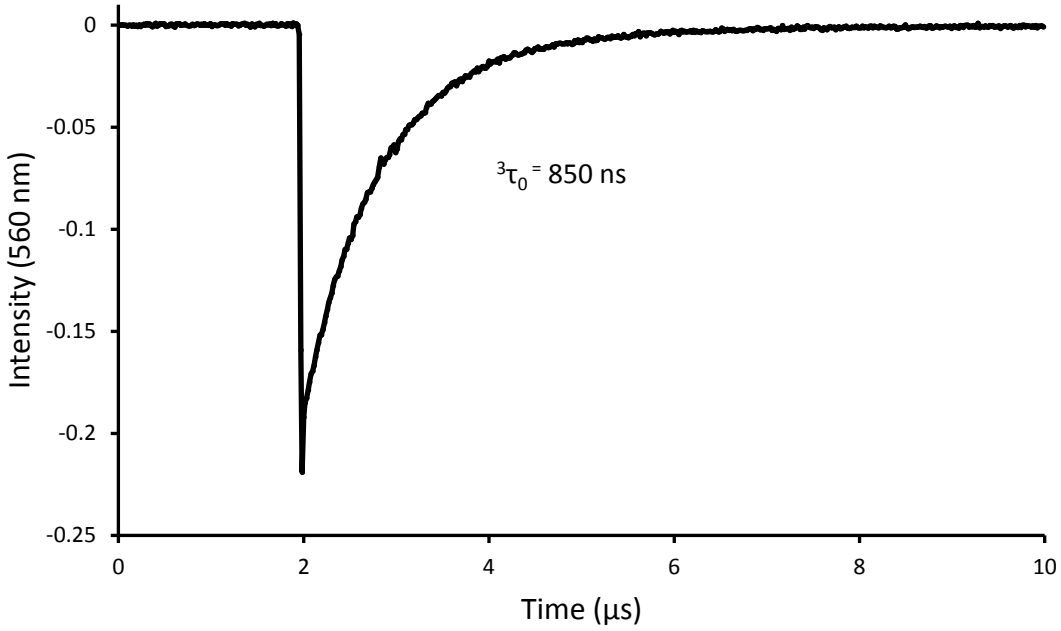

Figure 3.11 : Kinetic quenching plot showing the rate of $[Au_2(dppm)_2]Cl_2$ quenching as a function of [1-bromobutane]

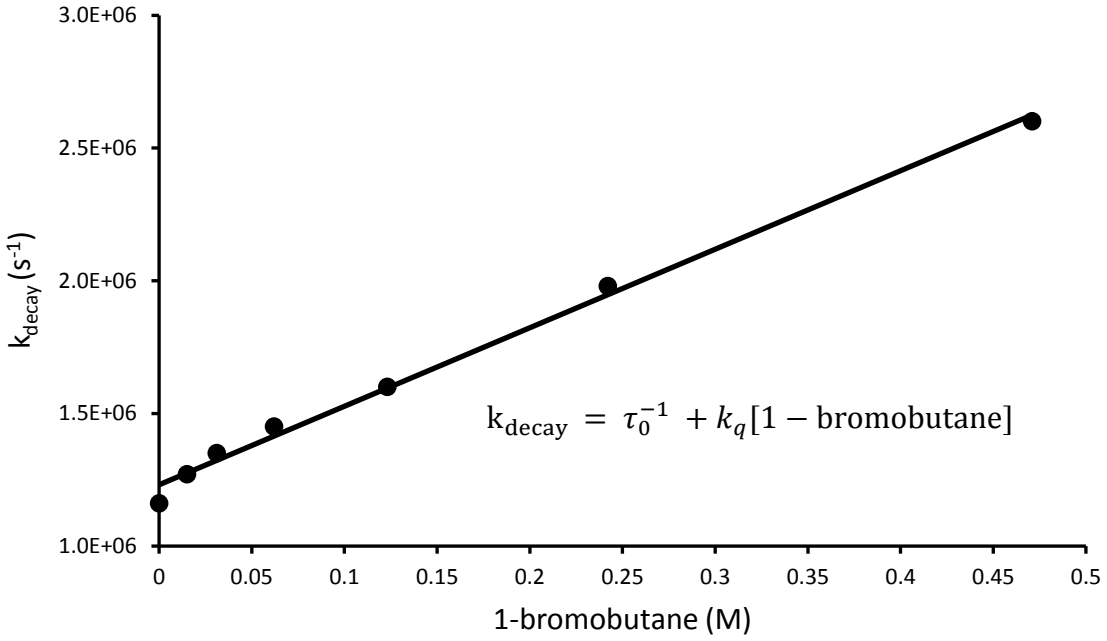

Table (**Table 3.10**) summarizes the bimolecular rate constants measured for the quenching of each complex in the presence of **T3.2.1a**, 1-bromobutane and *i*Pr$_2$NEt. The 1-bromobutane ($E_{1/2}^{red}$ = −2.5 V *vs.* SCE) was known to reduce to butane under the reaction conditions and was included as a reference. When looking at the results, a strong relationship between the redox potential of the quenchers and the Au(I) complexes became very evident. Compound **T3.2.1a** consistently had a greater rate of quenching than the harder to reduce 1-bromobutane regardless of catalyst. It was also observed that the rate of quenching with *i*Pr$_2$NEt varied significantly between catalysts; up to three orders of magnitude. The reduction potential of each complexes corroborated well with the relative rates of quenching between the catalysts, with complexes **F3.1.1** and **F3.4.1** being the hardest to reduce and having the lowest rates, and complex **F4.3.2** being the easiest to reduce and having the fastest rate.

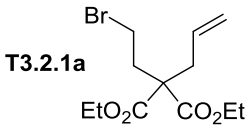

Table 3.10 : Triplet quenching of polynuclear Au(I) complexes

	k_q ($M^{-1}s^{-1}$)[a]				
Quencher	$Au_2(dppm)_2Cl_2$ **F3.1.1**	$Au_2(dmpm)_2Cl_2$ **F3.4.1**	$Au_2(3,5\text{-}CF_3\text{-}dppm)_2Cl_2$ **F3.4.2**	$Au_3(tppm)_2Cl_3$ **F3.4.3**	$Au_2(bmimm)_2Cl_2$ **F3.4.4**
1-Bromobutane	2.9×10^6	1.1×10^9	4.8×10^5	4.5×10^6	1.2×10^9
T3.2.1a	3.1×10^7	1.7×10^9	5.1×10^6	2.8×10^7	1.3×10^9
iPr_2NEt	2.7×10^7	2.1×10^7	1.1×10^9	1.6×10^9	1.6×10^8

[a] Determined from the slope of the corresponding kinetic quenching plot (kdecay vs. [Q])

Despite having the slowest measured rate constants in table **Table 3.10**, complex **F3.1.1** is the most efficient for the conversion of **T3.2.1a**. This demonstrates that the overall efficiency of the reaction requires considering other factors, such as the excited state lifetime of the catalyst as well as the relative concentration of each quencher present under the standard reaction conditions. Equation (**5**) and (**6**) allow us to better interpret the data from table **Table 3.10**. The equations calculate the percentage of catalyst undergoing triplet quenching by either reagent. Both equations contain a term corresponding to oxygen quenching of the Au(I) catalyst ($k_q^{O_2}$ $^3[Au_2(dppm)_2]^{2+}$ = 2.0×10^9 M^{-1} s^{-1}) for completeness,[70] although the argon purging of the reactions prior to irradiation allowed us to eliminate it when performing the calculation. It is worth nothing that the high solubility of oxygen in acetonitrile (approx. 1.6 mM under air)[71] means that inefficient purging could lead to highly reduced yield caused by non-productive quenching of the Au(I) catalysts by oxygen.

$$\%\ Quenched\ by\ (\boldsymbol{T3.2.1a}) = \frac{100 \times k_q^6[6]}{\tau_0^{-1} + k_q^6[6] + k_q^{iPr_2NEt}[iPr_2NEt] + k_q^{O_2}[O_2]} \qquad (5)$$

$$\%\ Quenched\ by\ (i\mathrm{Pr_2NEt}) = \frac{100 \times k_q^{iPr_2NEt}[i\mathrm{Pr_2NEt}]}{\tau_0^{-1} + k_q^6[6] + k_q^{iPr_2NEt}[i\mathrm{Pr_2NEt}] + k_q^{O_2}[O_2]} \qquad (6)$$

Using equation (**5**) and (**6**) on catalyst **F3.1.1** had interesting results. It was found that as much as 18% of the catalyst undergoes oxidative quenching by **T3.2.1a** under the reaction conditions, while 78% reductively quench with *i*Pr_2NEt. The remaining 4% emit a photon in a non-productive pathway. Despite the similar quenching constants (**Table 3.10**), the preferential quenching by *i*Pr_2NEt is due to the excess used in the reaction, 5 times as much as compound **T3.2.1a**. The results combined with the 5 min of irradiation required to achieve full conversion would indicate that the major pathway to product formation for catalyst **F3.1.1** is the reductive quenching. However, the conclusion is not the same for each complex. While the percentage of triplet quenched by *i*Pr_2NEt for complexes **F3.4.2** and **F3.4.3** is greater than 99% for both and most likely indicates reductive quenching as the major pathway to product formation, complex **F3.4.1** is significantly different. Up to 93% of triplets for catalyst **F3.4.2** are quenched by bomoalkane **T3.2.1a**, while only 6% are quenched by *i*Pr_2NEt indicating that the major product forming pathway could be the oxidative quenching. For complex **F3.4.4** it becomes slightly more difficult to determine the major product forming pathway. Up to 55% of triplets are quenched by bromoalkane **T3.2.1a** while 34% are quenched by *i*Pr_2NEt. Even if we generously assume that all quenching events lead to product formation (which it most likely does not), the extended reaction time of complex **F3.4.4** most likely comes from its poor absorption and very short excited state lifetime causing a significant fraction of the triplet state complex to escape quenching. On the other hand, the extended reaction time of complex **F3.4.2** should increase the amount of productive quenching events. However the complex suffers from a low quantum yield, and in turn the reaction times are significantly increased. Consequently, the results allowed us to conclude that both quenching pathways are kinetically competitive. The complexity of the

transformation becomes quickly apparent when considering that both pathways also lead to the same product and are highly dependent on the reduction potential of the bromoalkane substrate.

3.4.4 Substrate pre-association

The intricacies of the mechanism are also made evident when considering that despite the large energy barrier for the electron transfer reaction between **T3.2.1a** and complex **F3.1.1**, the reaction still occurs. Two possible explanations can be put forward; 1) Much of the energy barrier would be eliminated when using the onset outer sphere potentials in place of the peak potentials for our calculations or; 2) An interaction between the Au(I) complex and the bromoalkane activates the substrate and lowers the free energy of the reaction. Similar interactions between $[Au_2(dppm)_2]^{2+}$ with LiBr and LiCl salts have previously been described by Che. To further explore the possibility of such a binding occurring, the chiral bromoalkane **F3.12.1** was introduced to a solution of complex **F3.1.1**.

One could imagine that the binding interaction between the achiral Au(I) catalyst and a chiral bromoalkane could induce asymmetry which would be visible in circular dichroism (CD) measurements. The two components were analyzed individually and in combination. Since complex **F3.1.1** is achiral, no signal was observed on its circular dichroism CD spectra (**Figure 3.12**, black trace). The chiral bromoalkane **F3.12.1** did exhibit the expected signal around 265nm (**Figure 3.12,** red trace). Interestingly, the solution of both bromoalkane **F3.12.1** and complex **F3.1.1** clearly showed a new signal centered at 312 nm which we attributed to the induction of chirality by compound **F3.12.1** with Au(I) through some form of halogen binding (**Figure 3.12**, blue trace) . These results lead us to propose that an inner-sphere mechanism is responsible for the reduction of the carbon-bromide bond.

*Figure 3.12 : Circular dichroism (CD) spectra. $[Au_2(dppm)_2]Cl_2$ alone (black), chiral Br (**F3.12.1**) alone (red),and $[Au_2(dppm)_2]Cl_2$ in the presence of chiral Br (**F3.12.1**) (blue) at 20 °C.*

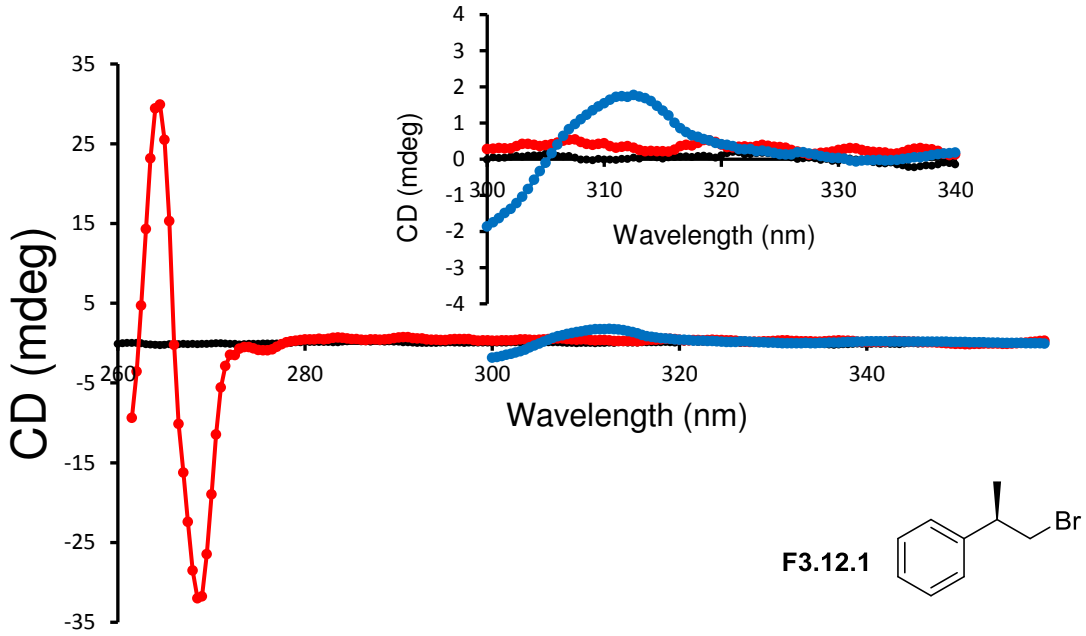

During the reaction, *i*Pr$_2$NEt is converted into its radical cation through single electron transfer, and is rapidly deprotonated to a strongly reducing α-aminoalkyl radical (**2.3.5**, $E_{1/2}^{ox}$= -1.12 V *vs.* SCE).[72] Although such intermediates have been known to participate in a variety of redox reactions, their reduction potentials are not sufficient enough to reduce unactivated bromoalkanes and bromoarenes ($E_{1/2}^{ox}$= -1.9 to -2.5 V *vs.* SCE).

The photophysical and electrochemical properties of the polynuclear Au(I) complexes highlight the mechanistic complexity of the reaction. The new data gathered from the study gave us of glimpse of the possible pathways accessed during the transformation. The identity of intermediates throughout the reaction still need to be elucidated. The fate of the carbon centered radical postulated to form after reduction of the carbon bromide bond can be quite complex. On the one hand, it seems to behave like a classic carbon centered radical in certain cases, such as

the cyclization onto arenes or alkenes, and yet can produce unexpected compounds, such as dimer **F3.2.1c** and bromoalkane **F3.2.1d**. There exists the likelihood of a metal bound radical, increasing further the complexity of the reaction and possibly allowing for additional reactivity to be developed. The metal bound radicals could possibly explain the formation of compounds **F3.2.1c** and **F3.2.1d** through reductive elimination pathways. The possibility was explored further by studying the homocoupling reaction between various iodoarenes and bromoalkanes.

3.5 Homocoupling of Halocarbons

Symmetrical biaryls are an important class of natural products and are often the subject of research interest, be it in pharmaceutical exploration, medicinal chemistry or total synthesis.[73,74,75] Transition metals are often used to create biaryl linkages, with the classical Ullman coupling being one of the most practical method when using haloarene substrates (**Scheme 3.8**).[76,77] As the use of stoichiometric transition metals became less desirable, variations emerged to resolve the issue, often opting for a catalytic transition metal and a stoichiometric reductant.[78]

Scheme 3.8 : Methods of homocoupling reactions

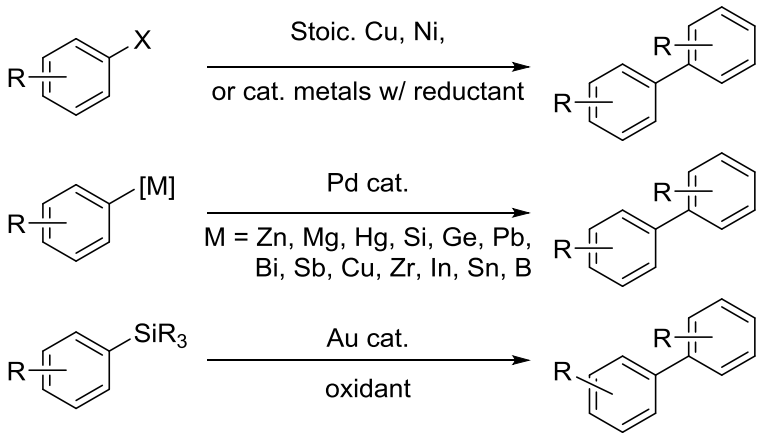

Gold catalysts have also shown some potential for aryl coupling reactions, using silyl-functionalized arenes and stoichiometric oxidant to turn over catalytic amounts of Au(I) complexes.[79,80] Similar types reactions for the homocoupling of haloalkanes are lacking in organic synthesis and research towards mild, efficient and convenient methods could be beneficial. The currently described alkane homocoupling are often limited to benzylic compounds, taking advantage of their stability and propensity to dimerize.[81,82] With our recently described Au(I) photoredox system for reduction of carbon-halide bonds, we developed a protocol for the homocoupling of iodoarenes and bromoalkanes.[83] Most of the following reactions were performed by Huy Tran, an undergraduate student under my supervision.

3.5.1 Photocatalytic arene dimerization

To begin expanding the previous methodology, we attempted the homocoupling of compound **T3.11.1** (**Table 3.11**). Optimization of the reaction conditions showed that a 1:1 mixture of acetonitrile and methanol seemed to be optimal for the transformation, yielding 75% of product **T3.11.2** (entry 1). Addition of K_2HPO_4 gave quantitative conversion to the desired product (entry 2). One equivalent of Et_3N was optimal to promote the reductive quenching pathway for the Au(I) complex without acting as a source of hydrogen thus avoiding premature reduction of the aryl radical. UVA was essential to product formation, and the absence of photocatalyst caused significant degradation (entry 5 and 6). The corresponding methyl 4-bromobenzoate yielded less than 20% of the desired product under similar conditions.

Table 3.11 : Optimization of iodoarene coupling.

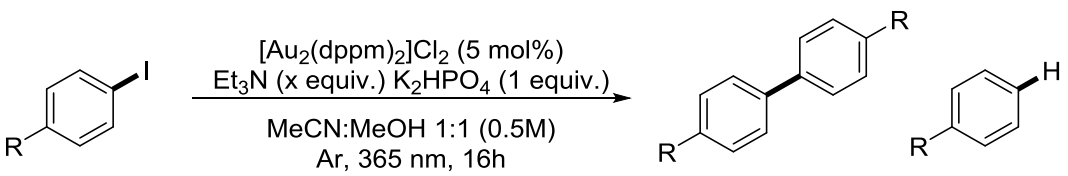

T3.11.1 R = CO_2Me **T3.11.2** **T3.11.3**

entry	Et_3N (equiv.)	T3.11.1 (%)	T3.11.2 (%)	T3.11.3 (%)
1[a]	1	0	75	25
2[a]	2	0	69	11
3	1	0	98 (91)	2
4	–	70	22	8
5[b]	1	22	2	8
6[c]	1	99	0	0

[a] no K_2HPO_4. [b] no $Au_2(dppm)_2Cl_2$. [c] no UVA.

Expanding the scope of the reaction to other iodoarenes gave the following results (**Figure 3.13**). Electron poor substrate **F3.13.1a** dimerized in 60% yield. Iodoarene **F3.13.1b** and **F3.13.1c** formed the desired products in 66% and 14% yield respectively, demonstrating that steric effects could significantly hinder the formation of the new bond. Compounds **F3.13.1d** to **F3.13.1l** gave the corresponding dimers **F3.13.2d** to **F3.13.2l** in yield ranging from 31% to 63%. N-acetyl functionalized **F3.13.1m** did not yield any dimerized product, but instead exclusively formed the coresponding dehalogenated product, showing that hydrogen atom transfer is a competing process. Alkyl substituted iodoarenes **F3.13.1n** to **F3.13.1p** gave modest yields of 34-53%, while ethyl phenylether **F3.13.1q** gave compound **F3.13.2q** in 29% yield. Phenylalanine analog **F3.13.1r** desmonstrated compatibility with amino acids, forming the desired compound **F3.13.2r** in 66% yields. Estrone derivative **F3.13.1s** also showed compatibility, converting to the desired dimer **F3.13.2s** in 28% yield.

Figure 3.13 : Homocoupling of iodoarenes.

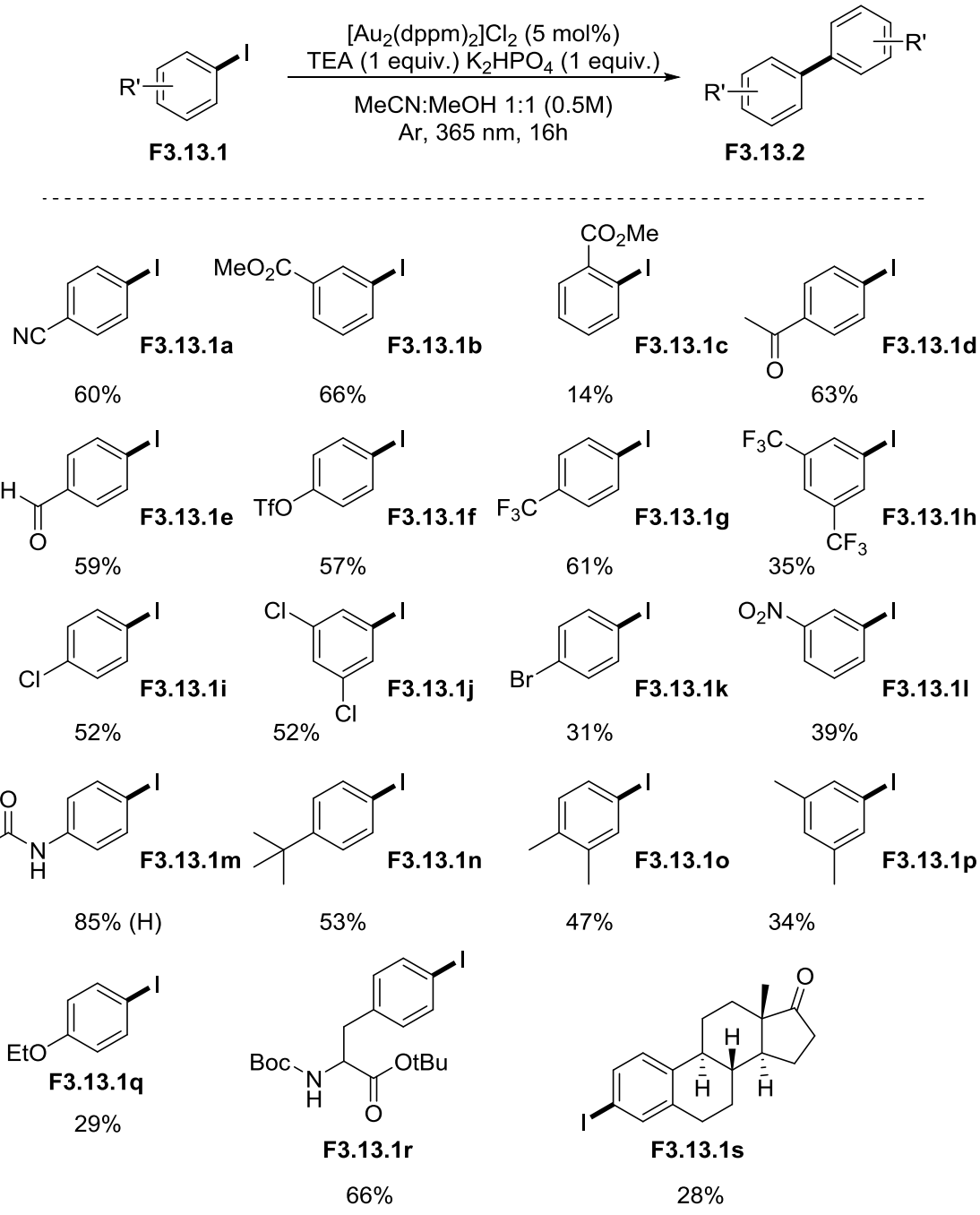

Scheme 3.9 : Cyclization vs arene dimerization.

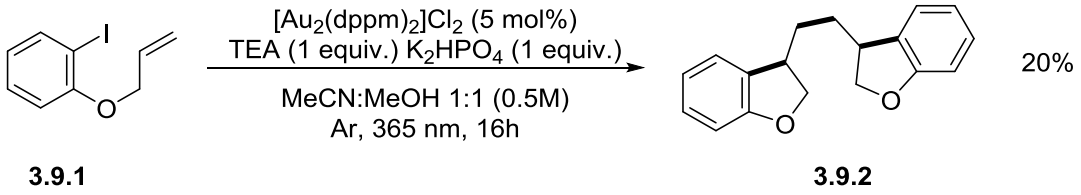

Substrate **3.9.1** was submitted to the reaction conditions to garner further mechanistic information (**Scheme 3.9**). The product originating from the transformation would help determine whether the cyclization or the homocoupling occurred at a faster rate under the reaction conditions. Interestingly, only compound **3.9.2** was isolated from the reaction. The product arises from the cyclization of **3.9.1** prior to homocoupling. Based on the premise that the homocoupled products are formed from a gold bound carbon radical, it could indicate an equilibrium between the free aryl/alkyl radical and the addition to a gold center.

As mentioned above, we had previously observed the formation of alkyl dimers arising in our photoredox reactions (**Table 3.5**). Compound **3.9.2** can be seen as another such product of alkyl dimerization. After 5-*exo trig* cyclization of the aryl radical, the resulting primary alkyl radical can then go through the same dimerization mechanism to afford product **3.9.2**. The reaction was revisited with compounds **F3.14.1a-d** in order to form the corresponding dimers **F3.14.2a-d** (**Figure 3.14**). The use of deuterated solvent was necessary in order to supress the hydrogen atom transfer reaction and achieve acceptable conversion to the dimerize compounds. For compound **F3.14.2d**, the benzyl chloride was instead used for the reaction since benzyl bromide was known to undergo homolysis under the irradiation conditions.

Figure 3.14 : Dimerization of haloalkanes

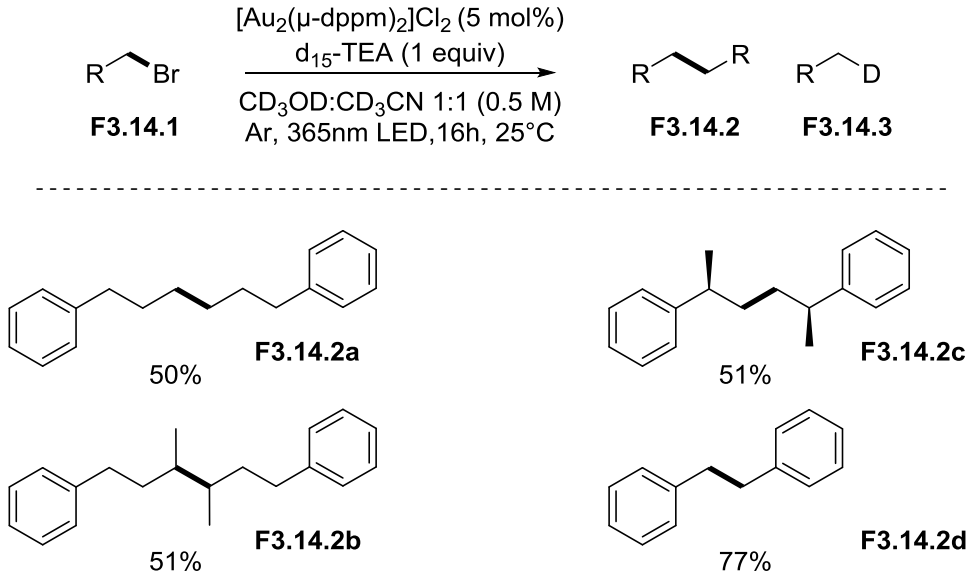

Using the accumulated information from the obtained results, we proposed the following catalytic cycle for the transformation (**Scheme 3.10**). After irradiation, the excited **F3.1.1*** undergoes a reductive quench to form the reduced complex **F3.1.1**$^{1-}$. A subsequent SET to the iodoarene/bromoalkane yields a carbon centered radical and a bromide ion while at the same time returning the catalyst to its ground state (**F3.1.1**). The free radical can reversibly binds to gold, forming complex **3.10.1**. A second addition of a carbon centered radical yields complex **3.10.2**, which undergoes reductive elimination to yield the observed product and regenerate the photocatalyst **F3.1.1**.

The above homocoupling reaction showcases even more of the complexity of the dimeric Au(I) complex. The reactivity has the potential to help develop further dimerization procedures, and even other types of Au(I)/Au(III) coupling reactions.

Scheme 3.10 : Mechanism of Au(I) photocatalyzed homocoupling of halocarbons.

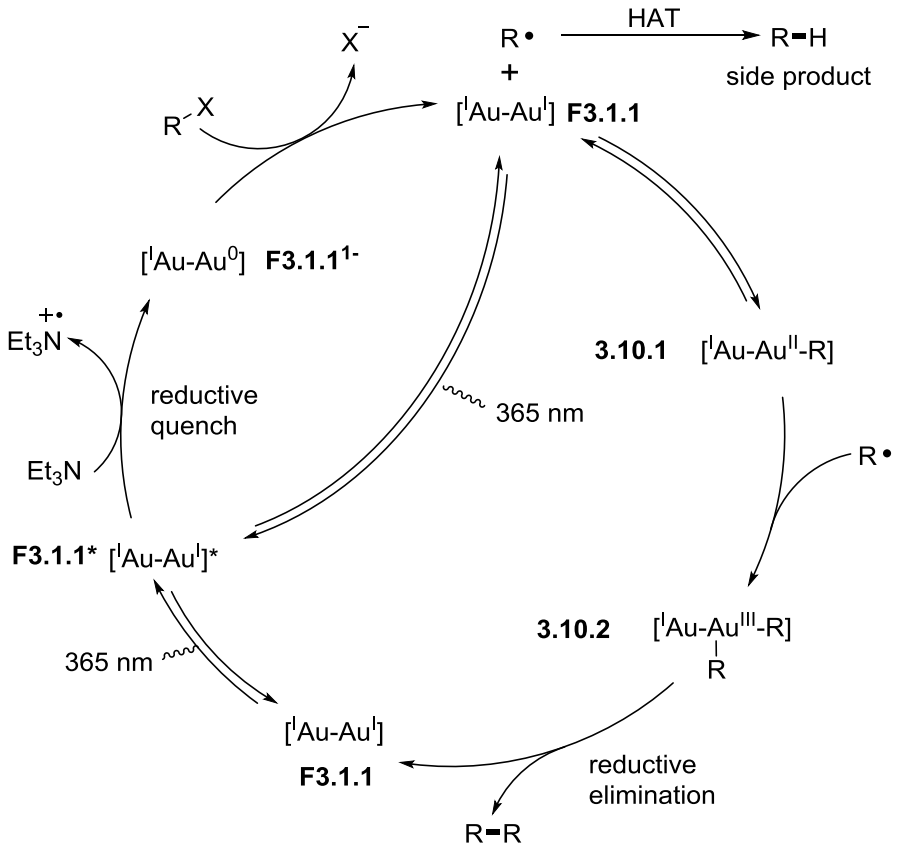

3.6 Summary of findings in polynuclear Au(I) Photocatalysis

The information gathered from the work on polynuclear Au(I) complexes will allow future work to be more pointed and in all likelihood, more successful. The construction of new photocatalysts now comes with the first few pages of the instruction booklet. For strong σ-donating ligands such as NHC-carbenes, excited dinuclear Au(I) complexes will tend to be highly reducing. Electron rich phosphine ligands will also generate highly reducing complexes. Accordingly, it is no surprise that electron poor phosphine ligands tend to be less reducing. It is worth noting that despite the significant variances in excited state oxidation potentials caused by the different ligands (**Table 3.9**), the excited state reduction potentials of the complexes are very

similar. The only exception to this rule seems is the bis-carbene bridging ligands which was too high to measure. Modifying this property might require combining Au(I) with another metal, but it may one day lead to new reactivity for polynuclear metal complexes.

The absorption wavelengths of the complexes can also be varied. Almost the entirety of their relevant absorbance arises from the aurophilic interaction between the two Au(I) atoms. Their proximity is directly responsible for the absorbance. For example, the bis-carbene complex **F3.4.4** ($Au_2(bmimm)_2Cl_2$) has an interatomic Au-Au distance of about 3.47 Å and, under reaction conditions, barely has any absorption above 350 nm. On the other hand, **F3.1.1** ($Au_2(dppm)_2Cl_2$) which has a Au-Au distance of around 2.97 Å, absorbs light up to 410 nm. Any efforts to create a visible light absorbing catalyst based on a dinuclear Au(I) structure should focus on achieving a ligand geometry that encourages short Au-Au distances. For dppm type ligands, two main areas of substitution are important; the groups on the phosphorus atoms, and the CH_2 linker. Modifications at these two sites would have the greater impact on the geometry of the whole complex.

The initial purpose of the tri-nuclear Au(I) complex $Au_3(tppm)_2Cl_3$ (**F3.4.3**) was to achieve a higher absorption wavelength by increasing the amount of Au-Au interactions present in the complex. Despite not resulting in such and increase, the complex is still catalytically active, and quite efficient. In addition, it does have the highest excited state reduction potential. The tri-nuclear structure could be a useful model for the incorporation of mix metal catalysts.

The proposed inner sphere mechanism by which the polynuclear Au(I) complexes operate have other implications as well. The pre-association demonstrated with bromoalkane **F3.12.1** (**Figure 3.12**) could possibly be replicated with other functional groups. By moving away from

chloride counterions and making the Au(I) complexes cationic with the help of labile anions, pre-association could be achieved with carbonyls, alkenes, alkynes, or even allenes. The subsequent oxidation or reduction of these groups constitute another avenue of research for Au(I) photochemical systems.

The inner sphere mechanism is also important with regards to metal-bound radicals. Details about such species will be harder to gather, but their importance must be recognized. The Au(I) metal-bound radicals effectively resulted in examples of $sp^3 - sp^3$ and $sp^2 - sp^2$ couplings between alkyl and aryl bromides. Understanding the mechanism fully would help expand the scope of reactivity accessible to polynuclear Au(I) complexes. The results could yield asymmetric reaction and or even new cross-coupling conditions between non-classical partners.

The results described above help glimpse the potential of polynuclear Au(I) complexes in photochemistry. The nature of the complexes allow for many modifications, and in turn open a variety of reactive pathways to choose from. The broad compatibility with functional groups, as well as with many solvents and additives make these types of systems candidates for one-pot procedures or even multi-catalyst reactivity. Potential improvement through ligand modifications has only been broached and many other photoactive Au(I) complexes are sure to be discovered.

---

[60] Schmidbaur, H.; Wohlleben, A.; Schubert, U.; Frank, A.; Huttner, G. *Chem. Ber.* **1977**, *110*, 2751 – 2757

[61] Che, C.-M.; Kwong, H.-L.; Yam, V.W.-W.; Cho, K.-C. *J. Chem. Soc. Chem. Commun.* **1989**, *13*, 885 – 886

[62] Ma, C.; Chan, C.T.-L.; To, W.-P.; Kwok, W.-M.; Che, C.-M. *Chem. Eur. J.* **2015**, *21*, 13888 – 13893

[63] Schmidbaur, H.; Schier, A. *Chem. Soc. Rev.* **2012**, *41*, 370 – 412
[64] Revol, G.; McCallum, T.; Morin, M.; Gagosz, F.; Barriault, L. *Angew. Chem. Int. Ed.* **2013**, *52*, 13342 – 13345
[65] Maity, S.; Zheng, N. *Angew. Chem., Int. Ed.* **2012**, *51*, 9562 – 9566
[66] Motherwell, W. B.; Pennell, A. M. K. *J. Chem. Soc. Chem. Commun.* **1991**, *13*, 877 – 879
[67] Yoon, T. P.; Ischay, M. A.; Du, J. *Nature Chemistry* **2010**, *2*, 527 – 532
[68] Scott, V. J.; Labinger, J. A.; Bercaw, J. E. *Organometallics* **2010**, *29*, 4090 – 4096
[69] Mctiernan, C. D.; Morin, M.; McCallum, T.; Scaiano, J. C.; Barriault, L. *Catal. Sci. Technol.* **2016**, *6*, 201 – 207
[70] C.-M. Che, H.-L. Kwong, C.-K. Poon and V. W.-W. Yam, *J. Chem. Soc. Dalton Trans*. **1990**, *11*, 3215 – 3219.
[71] Coetzee, J. F.; Kolthoff, I. M. *J. Am. Chem. Soc.* **1957**, *79*, 6110 – 6115
[72] Jonsson, M.; Wayner, D. D. M.; Lusztyk, J. *J. Phys. Chem.* **1996**, *100*, 17539 – 17543.
[73] Baudoin, O.; Gueritte, F. *Stud. Nat. Prod. Chem.* **2003**, *29*, 355 – 417
[74] Ghera, E.; Ben-David, Y. *J. Chem. Soc. Chem. Commun.* **1978**, *11*, 480 – 481
[75] Warshawsky, A. M.; Meyers, A. I. *J. Am. Chem. Soc.* **1990**, *112*, 8090 – 8099
[76] Kozlowski, M. C.; Morgan, B. J.; Linton, E. C. *Chem. Soc. Rev.* **2009**, *38*, 3193 – 3207
[77] Bringmann, G.; Gulder, T.; Gulder, T. A. M.; Breuning, M. *Chem. Rev.* **2011**, *111*, 563 – 639
[78] Hassan, J.; Sevignon, M.; Gozzi, C.; Schulz, E.; Lemaire, M. *Chem. Rev.* **2002,** *102*, 1359 – 1470
[79] Ball, L. T.; Green, M.; Lloyd-Jones, G. C.; Russell, C. A. Org. Lett. **2010**, 12, 4724 – 4724
[80] Ball, L. T.; Lloyd-Jones, G. C.; Russell, C. A. *Chem. Eur. J.* **2012**, *18*, 2931 – 2937
[81] Hironaka, K.; Fukuzumi, S.; Tanaka, T. *J. Chem. Soc. Perkin Trans.* **1984**, *2*, 1705 – 1709
[82] Lanterna, A. E.; Elhage, A.; Scaiano, J. C. *Catal. Sci. Technol.* **2015**, *5*, 4336 – 4340
[83] Tran, H.; McCallum, T.; Morin, M.; Barriault, L. *Org. Lett.* **2016**, *18*, 4308 – 4311

4 Uncatalyzed Photoactivation

Despite all the existing chemistry describing the reduction of halocarbon bonds in literature,[84-89] accessing certain halocarbons can be impractical in some cases, and impossible in others. Multiple steps may be necessary to transform other functional groups into the appropriate halide, functional groups may be incompatible with the transformation, or in many cases the halocarbon in question may be very difficult to incorporate into a reaction because of its instability or volatility. Photochemistry can help solve some of the problems as it offers alternate synthetic strategies to classic thermal chemistry and can often be combined with other existing methods.

4.1 Bromination of Alcohols

The radical reduction of alcohols has been extensively studied since the pioneering work of Barton and McCombie.[90] A multitude of reactions conditions exist in which the alcohol is transformed into other functional groups such as xanthates, phosphites, and benzoyl esters in preparation for a subsequent radical reduction (**Scheme 4.1**).[91-94] This usually involves radical initiators such as AIBN, peroxides, or trialkylborane, and hydrogen donors like organostannanes, or often stoichiometry amounts of metals (SmI_2) are necessary to achieve good conversion.[95] Catalytic variations do exist but still contain toxic reagents such as alkyl tin species.[96]

The reaction conditions for transforming the alcohols to the appropriate functional group are rarely compatible with the subsequent radical reduction which prevents one-pot procedures from being developed. Furthermore, competitive fragmentation pathways exist between the desired products and by-products, limiting the types of substrates that can be efficiently used to secondary and tertiary alcohols.[97] The side reactions emphasize the need for a more efficient

reaction for the radical reduction of primary alcohols. By merging a photo mediated bromination of alcohols with our previously developed dimeric Au(I) photoreduction of halocarbons, we were successful in achieving the deoxygenation of alcohols in a one-pot process (**Scheme 4.1**).[98]

Scheme 4.1: Protocol for reductive deoxygenation.

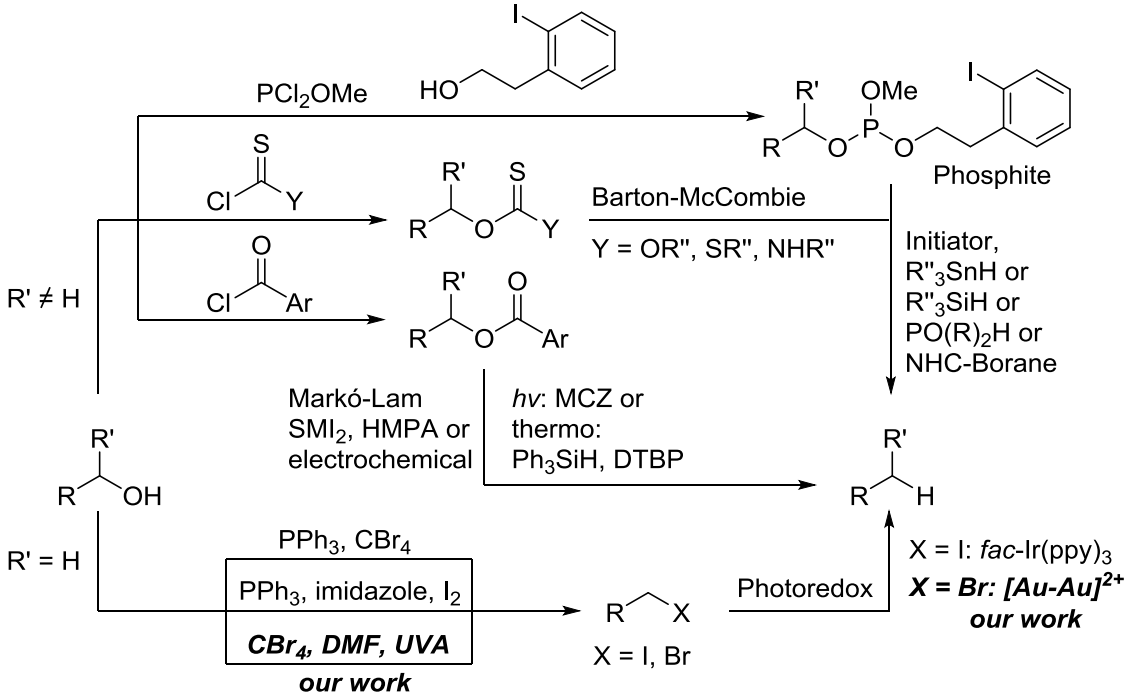

4.1.1 Photolysis of CBr_4

Alcohols are usually considered good substrates for organic synthesis because of their abundance and diversity, and are often converted to other functional groups to obtain the desired reactivity. In addition to the functional groups mentioned above, alcohols are commonly transformed into halides, and often by arguably one of the most efficient and reliable method, the Appel Reaction (CX_4 and PPh_3).[99] Unfortunately, the by-product triphenyl phosphine oxide and any remaining triphenyl phosphine can render the reaction incompatible with many metal catalyzed photoredox processes, and thus prevent it from being combined in one-pot procedures.

The group of Stephenson reported a novel development on this method by using tetrabromomethane or iodoform alongside NaBr or NaI, and replacing the triphenyl phosphine by a Ru(II) photocatalyst (**Scheme 4.2**).[100] From these conditions, many primary and secondary alcohols were transformed into bromo and iodoalkanes.

Scheme 4.2: Proposed mechanism for the photocatalytic halogenation of alcohols.

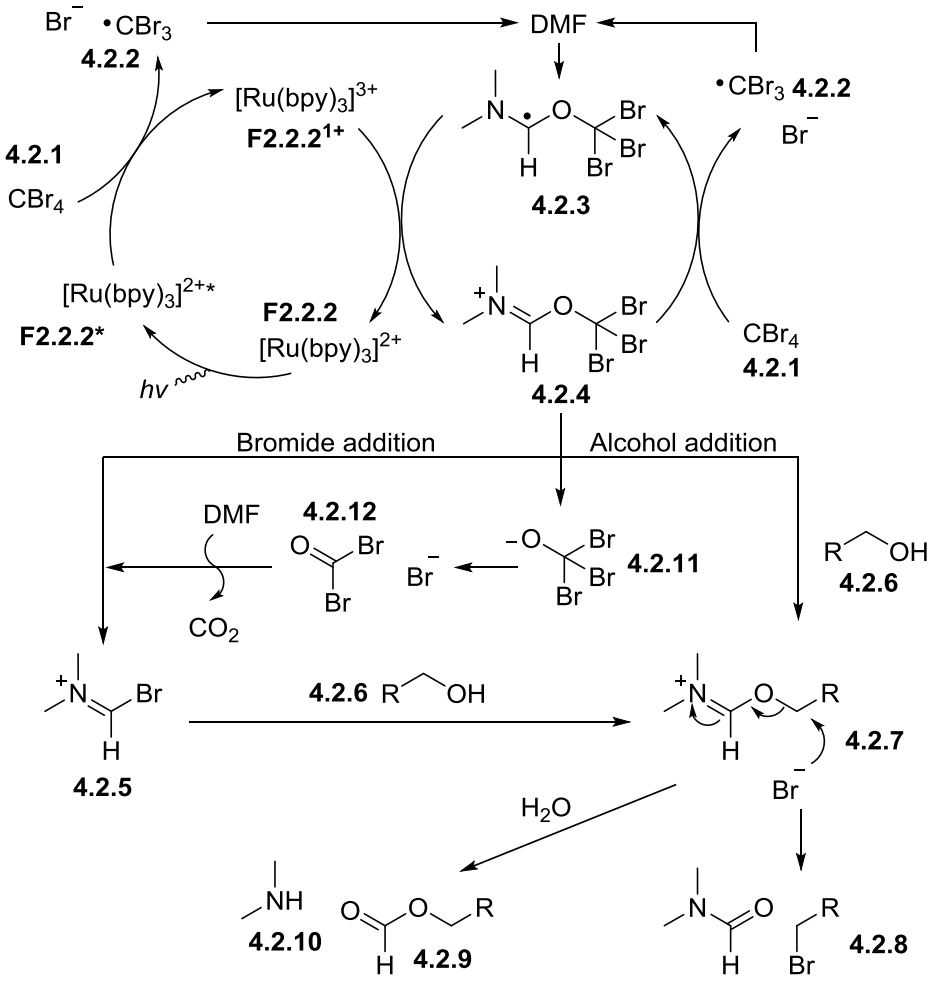

Upon irradiation with visible light, the Ru(II)* complex **F2.2.2*** undergoes oxidative quenching by the tetrabromomethane (**4.2.1**), forming a bromide anion and a tribromomethyl radical (**4.2.2**). The addition of the radical to a molecule of the DMF (solvent) leads to intermediate **4.2.3**. The latter can be oxidized by the Ru(III) complex (**F2.2.2^{1+}**), thus

regenerating the catalyst, or alternatively it can reduce another molecule of CBr_4, creating a radical chain reaction concurrently with the photoredox cycle, both pathways generating intermediate **4.2.4**. This intermediate will form the iminium **4.2.7**, either directly through a nucleophilic addition of an alcohol (**4.2.6**) and subsequent elimination of CBr_3O^- (**4.2.11**), or first through the addition of a bromide, forming the Vilsmeier Haack reagent **4.2.5**, after which a nucleophilic addition by an alcohol will take place. From iminium **4.2.7**, the nucleophilic substitution yields the final product **4.2.8**.

From this development, we postulated that a one-pot reduction of alcohols could be developed from our previously reported radical reduction of halocarbons by $[Au_2(dppm)_2]Cl_2$.[101] Our hypothesis was based on previous observations revealing that CBr_4 can oxidatively quench the dimeric Au(I) complex,[102] while the same complex can also reduce unactivated C-Br bonds. Combining the two processes should yield the desired deoxygenated product.

Scheme 4.3: Initial attempt at Au(I) photoreduction of alcohols.

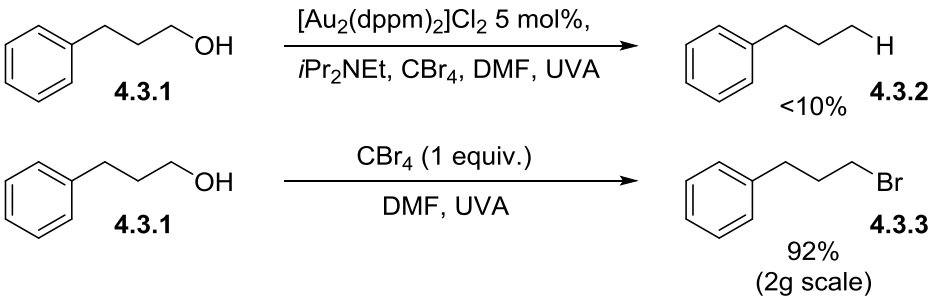

To validate our hypothesis, 3-phenyl-propanol **4.3.1** was irradiated in the presence of $[Au_2(dppm)_2]Cl_2$ (5 mol%), *i*Pr_2NEt (5 equiv.) and CBr_4 (1 equiv.) in DMF (**Scheme 4.3**). To our dismay, the desired product (propylbenzene, **4.3.2)** was observed in very low yields (<10%). While exploring new reaction conditions, we performed a series of control experiments. We were please to find that upon UVA irradiation (365 nm) and in the absence of the Au(I) complex

and *i*Pr$_2$NEt, the alcohol **4.3.1** was converted into 1-bromo-3-phenylpropane **4.3.3** in 92% yield. To demonstrate its robustness, the metal-free reaction was performed on gram-scale (2 g) yielding 2.69 g of the corresponding bromoalkane **4.3.3.** The results demonstrated the possibility of forming the Vilsmeier-Haack reagent from CBr_4 and DMF directly from UVA without the need for any photocatalyst. It prompted us to investigate the applicability of the light-enabled bromination to a wider range of alcohols.

Using a single equivalent of DMF or a substoichiometric amount in acetonitrile showed sluggish reactivity, and using dimethyl acetamide (DMA) instead of the formamide yielded no product. With optimized conditions, we investigated a wide range of primary alcohols (Figure 4.1). Primary aliphatic bromides such as **F4.1.2a** and **F4.1.2b** were obtained in excellent yields.

Figure 4.1: Photomediated bromination products of various alcohols.

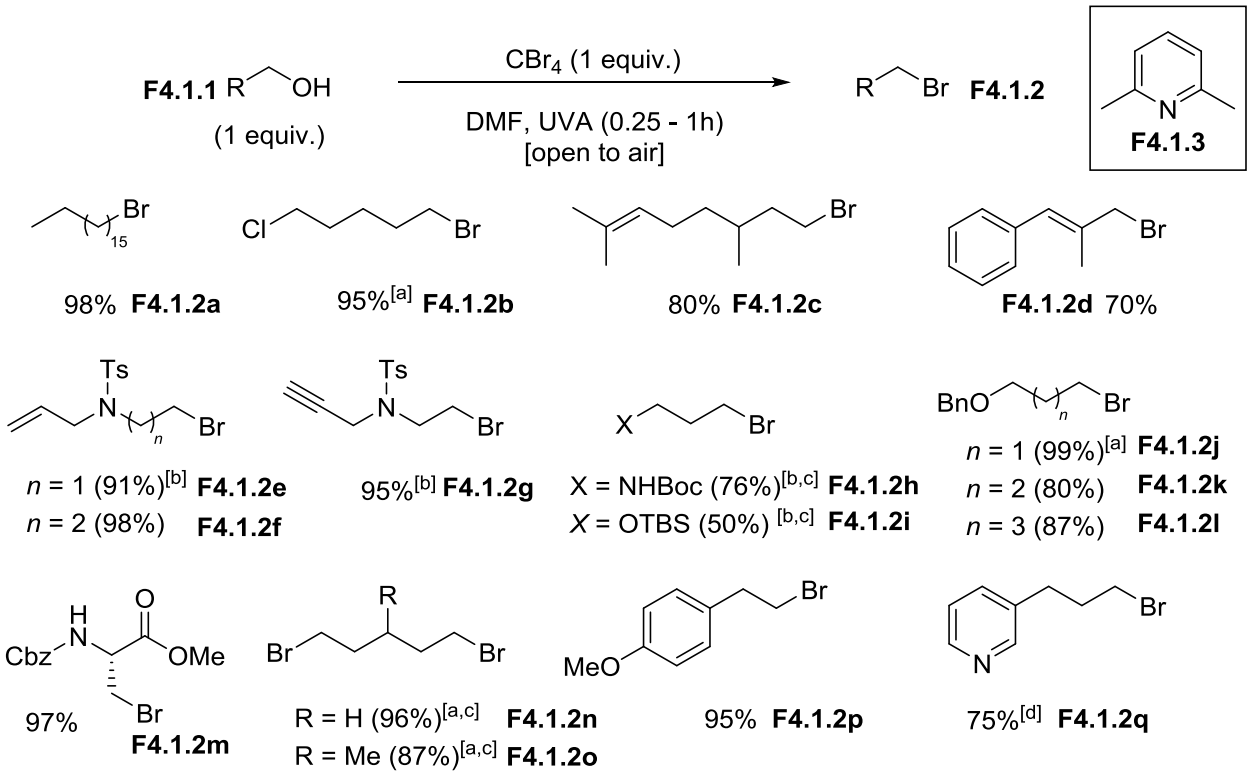

[a] Yield determined by ^{1}H NMR spectroscopy with mesitylene as standard. [b] NaBr (2-3 equiv.) was added after irradiation and the mixture was stirred overnight in the absence of light. [c] 2,6-lutidine (3 equiv.) added, 6h irradiation. 16h irradiation with NaBr (3 equiv.).

These conditions were compatible with multiple functionalities including alkenes (**F4.1.2c-f**), alkynes (**F4.1.2g**), *O*-benzyl protecting groups (**F4.1.2j-l**), and *N*-carboxybenzyl (**F4.2.1m**). Substrates containing acid sensitive groups such as *N-tert*-butoxycarbonyl (Boc) and *O-tert*-butyldimethylsilyl (TBS) required the presence of 2,6-lutidine (**F4.1.3**) to prevent substrate degradation. The substrates (**F4.1.1h** and **F4.1.1i**) afforded the desired bromide in 76% and 50% yield respectively. This method also was compatible with diols by using 2 equivalents of CBr_4, affording the dibromoalkanes **F4.1.2n** in 96% and **F4.1.2o** in 87%. The pyridine substituted propanol **F4.1.2q** was also compatible with the halogenation reaction, although a 16 h reaction time was required along with 3 equivalents of NaBr. Other than for product **F4.1.2q**, the reactions achieved full conversion between 15 min and 1 h.

Interestingly, the primary alcohols showed comparable reactivity when the CBr_4 was replaced with iodoform (CHI_3) (**Figure 4.2**). Just as with 365 nm light and CBr_4, 400 nm light is of sufficient energy to cause the photolysis of the iodoform but not energetic enough to degrade

Figure 4.2 : Photomediated iodination products of various alcohols.

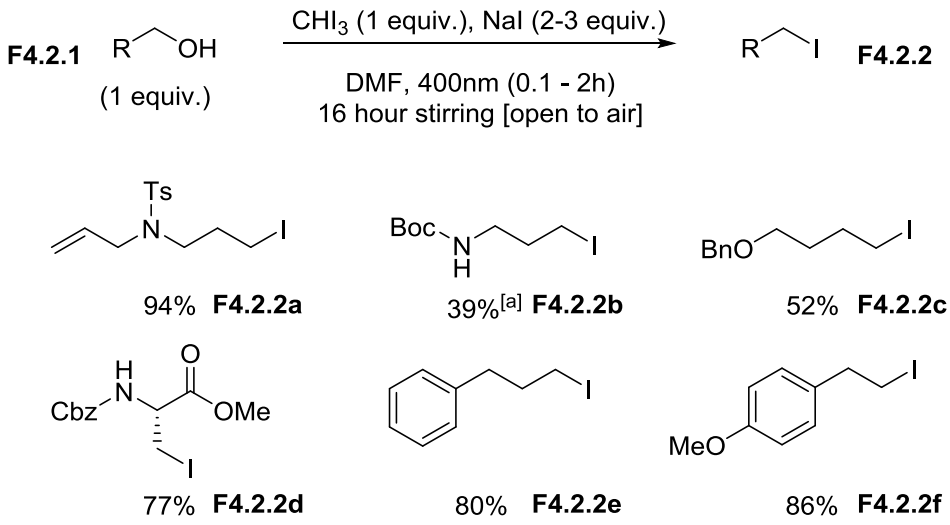

[a] 2,6-lutidine (3 equiv.) added, 6h irradiation, CHI_3 (1.5 equiv.)

the products **(F4.2.2a-f**), enabling a simple synthesis of both bromoalkanes and iodoalkanes from primary alcohols without the need for any photocatalyst. Unfortunately in both sets of conditions, secondary alcohols suffered from considerably reduced yields.

4.1.2 One-Pot Radical Reduction

With an efficient and reliable method of synthesizing bromoalkanes in hand, we proceeded with the development of a one-pot method for the radical reductions of primary alcohols. Initial results showed the addition of $[Au_2(dppm)_2]Cl_2$ (5 mol%) to the reaction vessel after the initial bromination step led to low or inconsistent yields of the reduced product. We postulated that either a by-product of the bromination or potential remaining CBr_4 could be causing issues with the photoredox process. After an extensive solvent screen and experimentation, it was discovered that the addition of *i*PrOH prior to the addition of $[Au_2(dppm)_2]Cl_2$ and *i*Pr_2NEt provide good and reproducible yields of the desired product. The optimized conditions were employed to investigate the scope of the reaction using primary alcohols (**Figure 4.3**).

Figure 4.3 : One-pot deoxygenation of alcohols

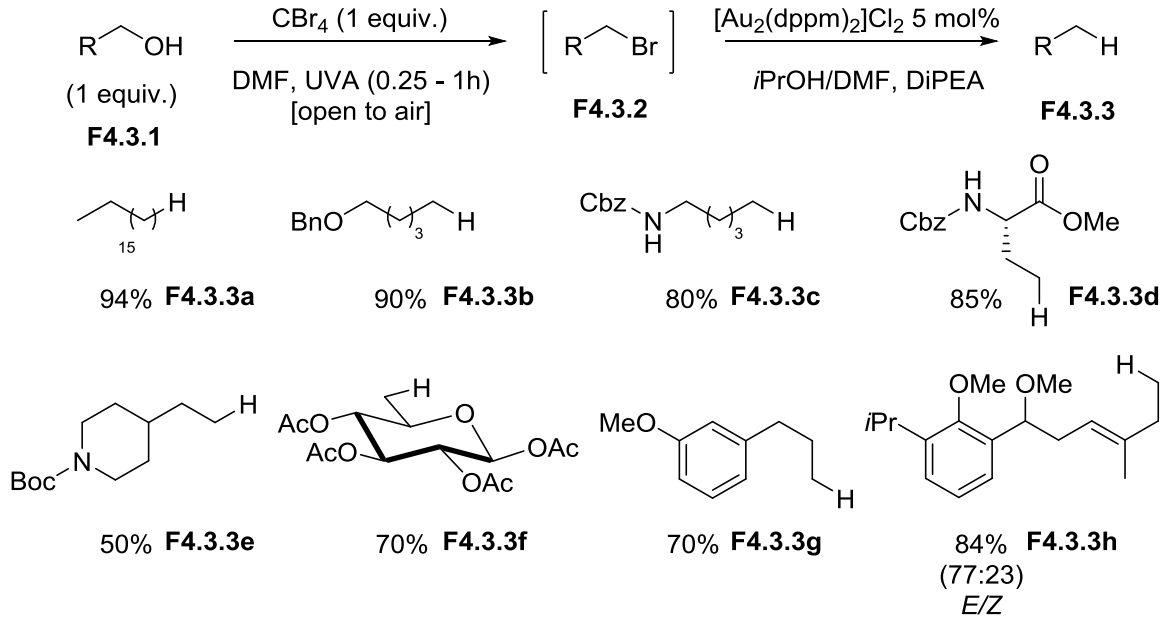

Heptadecanol was successfully reduced to the corresponding heptadecane **F4.3.3a** in excellent yield (94%). Alcohol **F4.3.1b** and **F4.3.1c** showed compatibility with *O*-benzyl (Bn) and *N*-carboxybenzyl (Cbz) groups and afforded the desired reduced products **F4.3.3b** and **F4.3.3c** in 90% and 80% yields respectively. The amino acid surrogate **F4.3.1d** was efficiently converted to compound **F4.3.3d** in 85% yield. Substrate **F4.3.1e** containing an acid-sensitive Boc group was reacted in the presence of 3 equivalents 2,6-lutidine and NaBr to produce **F4.3.3e** in 50% yield. The deoxygenation reaction showed compatibility with acetyl protected pyranose, with tetra-*O*-acetylated glucose **F4.3.1f** yielding the 6-deoxyglucose **F4.3.3f** in 70% yield over a 16 hour irradiation. Aryl substituted alcohols **F4.3.1g** and **F4.3.1h** were converted to the corresponding alkanes **F4.3.3g** and **F4.3.3h** in 70% and 84% yields respectively. It is worth nothing that when the bromination reaction was performed on alcohol **F4.3.1h**, the bromoalkane **F4.3.2h** was isolated as a single *E* isomer, although when the one-pot deoxygenation was performed, the alkane **F4.3.3h** showed a 3:1 mixture of the *E/Z* isomers.

Scheme 4.4: One-pot deoxygenation/cyclization of alcohols

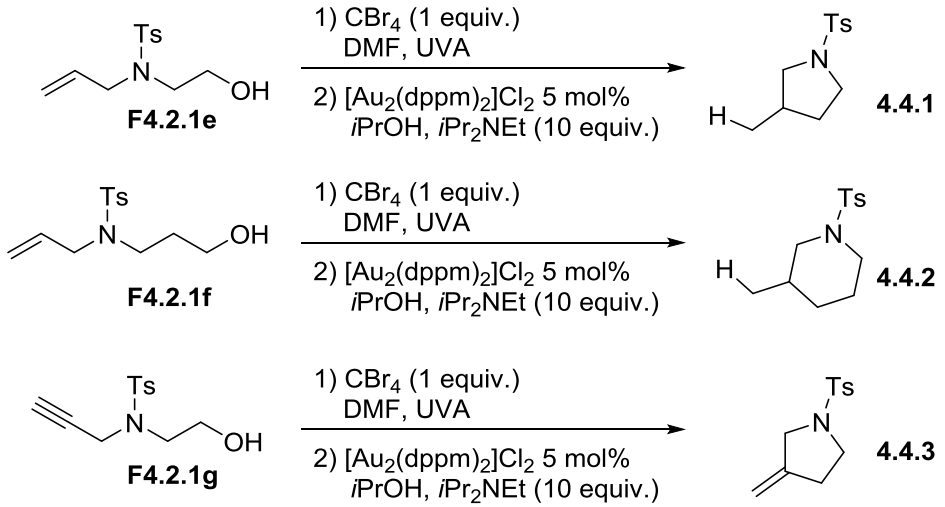

As shown in **Scheme 4.4**, the method is not limited to deoxygenation reactions and can also be employed in radical cyclizations. Alcohols **F4.2.1e** and **F4.2.1f** containing alkene groups underwent 5-*exo* and 6-*exo trig* cyclization to give the cyclic compounds **4.4.1** and **4.4.2** in 77% and 76% yield respectively. The reaction conditions were also compatible with a 5-*exo dig* cyclization onto an alkyne as demonstrated by the conversion of alcohol **F4.2.1g** to the sulfonyl protected pyrrolidine **4.4.3** in 84% yield.

The mechanism for the reaction seems to be the as shown in **Scheme 4.5**. As demonstrated by Nishima in a previous study, the CBr_4 **4.5.1** can be homolytically cleaved by irradiation with UV light, generating a bromide radical and a tribromomethyl radical **4.5.2**.[103] As proposed by Stephenson, the tribromomethyl radical can be trapped by a molecule of DMF

Scheme 4.5 : Proposed mechanism for one-pot deoxygenation process

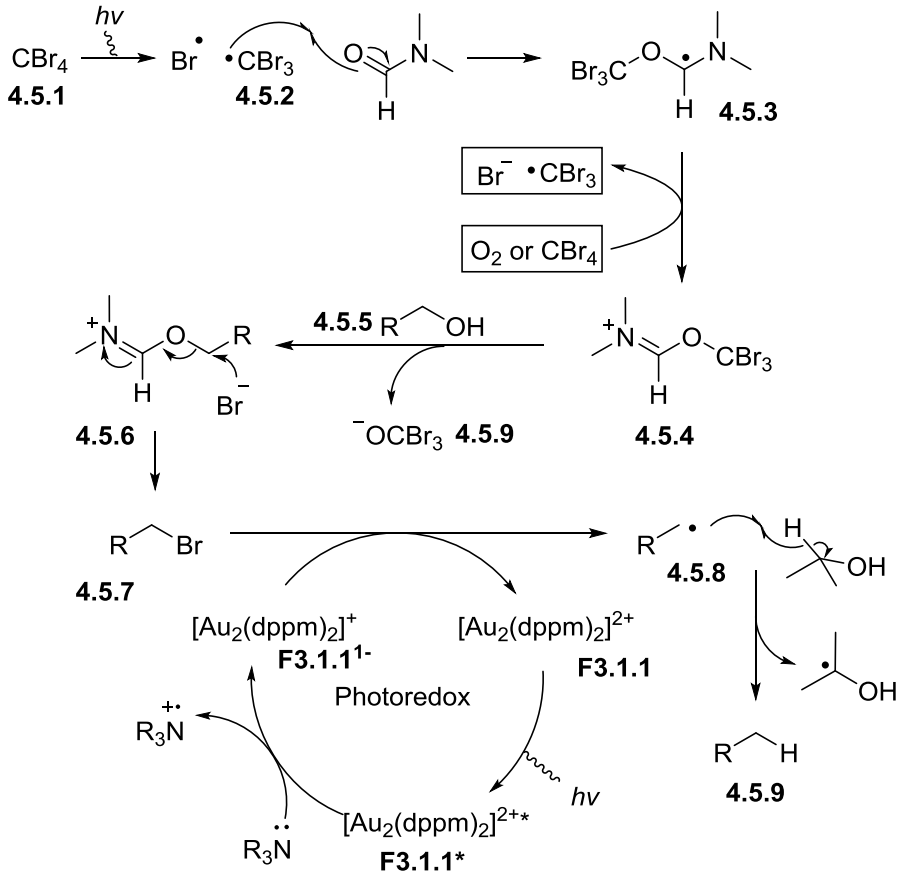

(solvent) forming intermediate **4.5.3**. The intermediate is oxidized by CBr_4 or O_2 to generate a Vilsmeier-Haack like intermediate **4.5.4**. The addition of an alcohol (**4.5.5**) and the subsequent elimination of tribromomethoxide **4.5.9** yields intermediate **4.5.6**, which can then undergo nucleophilic substitution to yield the corresponding bromide **4.5.7**. After the addition of *i*Pr_2NEt, *i*PrOH and the Au(I) photocatalyst **F3.1.1**, the newly formed C-Br bond is then reduced via a SET process to generate a carbon centered radical **4.5.8**, which undergoes hydrogen abstraction from either *i*Pr_2NEt or *i*PrOH to yield the reduced product **4.5.9**.

The overall process showed great complementarity with pre-existing deoxygenation reactions; since the older reactions performed well with secondary and tertiary alcohols but more poorly with primary alcohols, the procedure filled a niche for the efficient deoxygenation of these primary alcohols. In addition, the development of a very simple halogenation procedure demonstrates that uncatalyzed photochemical transformations are still relevant in organic chemistry.[104]

4.2 Methylation with Methanol

Our work with Au(I) mediated photocatalysis has opened unexpected avenues of analogous reactivity via uncatalyzed photoactivation of compounds. In some cases, this even helped solve unexpected problems that arose from the typical Au(I) photoredox reaction conditions. Thorough investigations of a reaction mechanism should always be prioritized while developing new reactivity. Correctly understanding the role of each component of a reaction and identifying deficiencies can properly guide the optimization of reaction conditions. Furthermore, investigating the role and fate of each component in a reaction can often lead to the discovery of unexpected reactivity.

4.2.1 Photo-mediated alkylation of heterocycles

Following the development of our Au(I) mediated radical reduction of bromoalkanes, we began exploring further types of reactions that could be enabled by the facile generation of carbon centered radicals. Our method benefitted from the ability to successfully reduce unactivated C-Br bonds to generate 1°, 2° and 3° alkyl radicals which are known to add to heterocycles. In general, these types of radicals possess a high energy singly occupied molecular orbital (SOMO) which interacts best with a double bond having a lower energy LUMO (lowest unoccupied molecular orbital). Taking advantage of this, my colleague Terry McCallum developed a system to efficiently alkylate heterocycles in an intermolecular fashion (**Figure 4.4**).[105]

The procedure looks deceptively simple but required many iterations prior to achieving optimal conditions. The final product is essentially a formal C-H functionalization of heteroarenes, although several mechanistic steps are required to achieve the alkylation (**Scheme**

Figure 4.4: Selected examples of photomediated alkylation of heterocycles

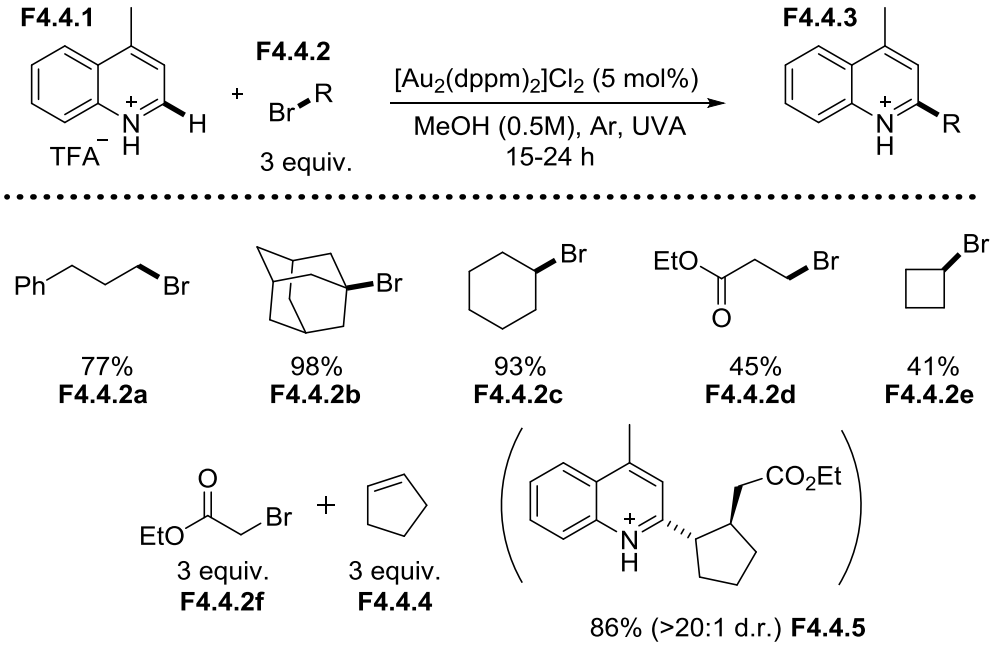

4.6). First, the bromoalkane **4.6.1** has to be reduced to the carbon centered radical **4.6.2** by our previously develop Au(I) photoredox process, albeit without any trialkylamine, which causes the reduction of the C-Br bond to occur via an oxidative quenching of the photoexcited $[Au_2(dppm)_2]^{2+*}$ (**F3.1.1***) complex and limits the premature reduction of the alkyl radical by hydrogen abstraction. The nucleophilic carbon centered radical can then add to the heteroarene **4.6.3** to form **4.6.4**. A subsequent SET to the $[Au_2(dppm)_2]^{3+}$ and the loss of a proton yields the final product **4.6.5** while simultaneously regenerating the photocatalyst **F3.1.1**.

Scheme 4.6 : Proposed mechanism in the photocatalyzed alkylation of heteroarenes

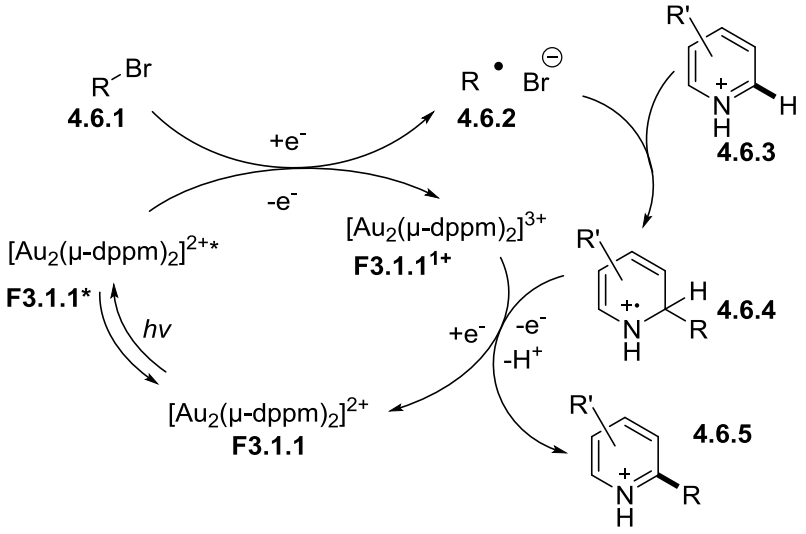

The reaction was successfully applied to a variety of bromoalkanes and heteroarenes, achieving excellent yields in many instances and even showcasing the importance of proper bond polarization through polarity reversal additions (**F4.4.5**). But despite its versatility, the low boiling points and high volatility of short chained bromoalkanes required for the addition caused some issues. In the case of bromomethane, which becomes gaseous at room temperature, it was unusable for the methodology. Thus, a surrogate had to be found.

4.2.2 Sulfonyl chloride and sulfonic acid

To find an eventual surrogate, we initially looked towards methylsulfonyl chloride. Our intention was to reduce the S-Cl bond with the $[Au_2(dppm)_2]Cl_2$ complex and form a chloride anion and a sulfinyl radical. The sulfinyl radical **4.7.4** could fragment to form SO_2 and a methyl radical **4.7.5** which could potentially undergo radical addition to the heteroarenes. When the reaction was performed, we were pleased to see the formation of the methylated product **4.7.2** we had expected in relatively good yields (**Scheme 4.7**) (**1**).

Scheme 4.7: Initial methylation of 4-methylquinoline by sulfonyl chlorides

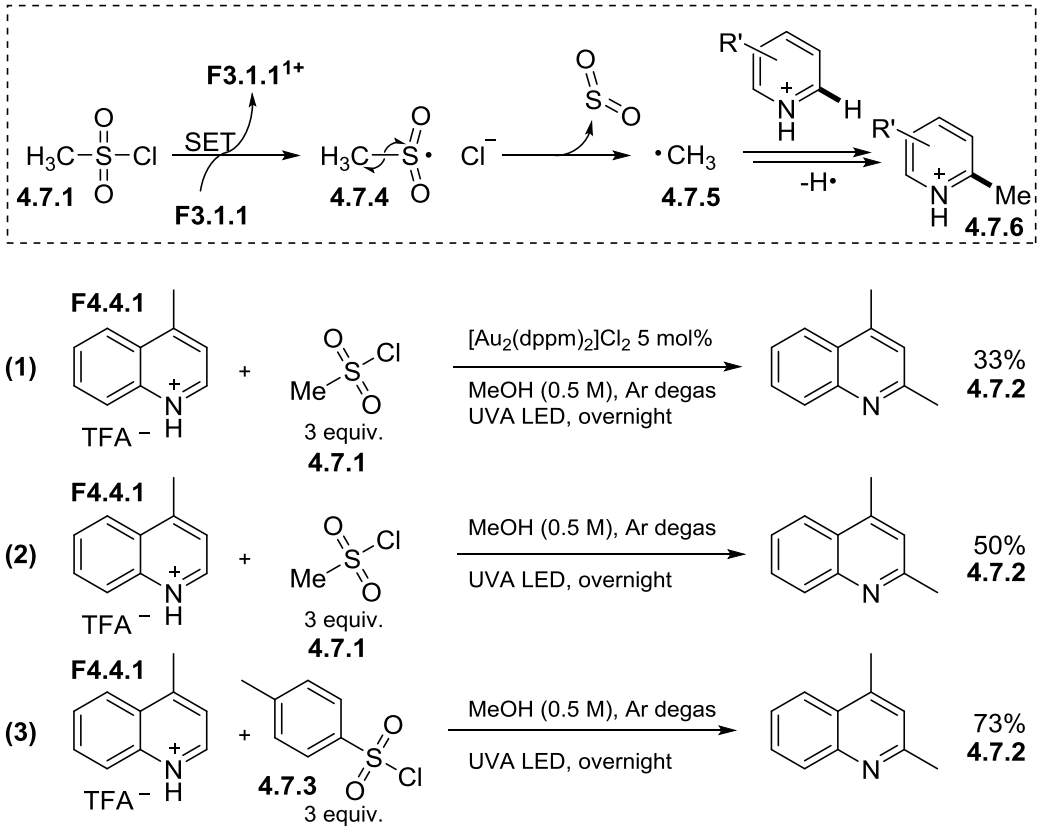

The reaction was also performed in the absence of the $[Au_2(dppm)_2]Cl_2$ complex in order to observe any potential background reactivity caused by the substitution of bromoalkanes by a sulfonyl chloride (**2**). Interestingly, the desired product **4.7.2** was formed despite the lack of

photocatalyst, something which was not observed when bromoalkanes were used. This seemed to indicate that a different reactivity was at play under the reaction conditions. The source of the reactivity was still uncertain but the assumption that a methyl radical was formed still held at the time. We postulated that *p*-toluenesulfonyl chloride could fragment in a similar fashion, generating an aryl radical and subsequently adding to heteroarenes. To our surprise, it generated the methylated product **4.7.2** once again and no arylated product was observed.

Startled by the result, we postulated that perhaps the methanol used as the solvent might be sulfonated under the reaction conditions and generate the active reagent, in this case methyl *p*-toluenesulfonate **4.8.1a** (**Scheme 4.8**). This would cause the fragmentation of a methyl radical from C-O bond instead of the C-S bond. Although the formation of the radical from the hemolysis of the C-O bond is unlikely, quinoline **F4.4.1** was irradiated in the presence of methyl *p*-toluenesulfonate in MeOH. To our surprise, the desired product was obtained in 90% yield. With this interesting result in hand, we decided to use other alkyl *p*-toluenesulfonates (**4.8.1b-e**)

Scheme 4.8 : Methylation of 4-methylquinoline with various alkyl sulfonates.

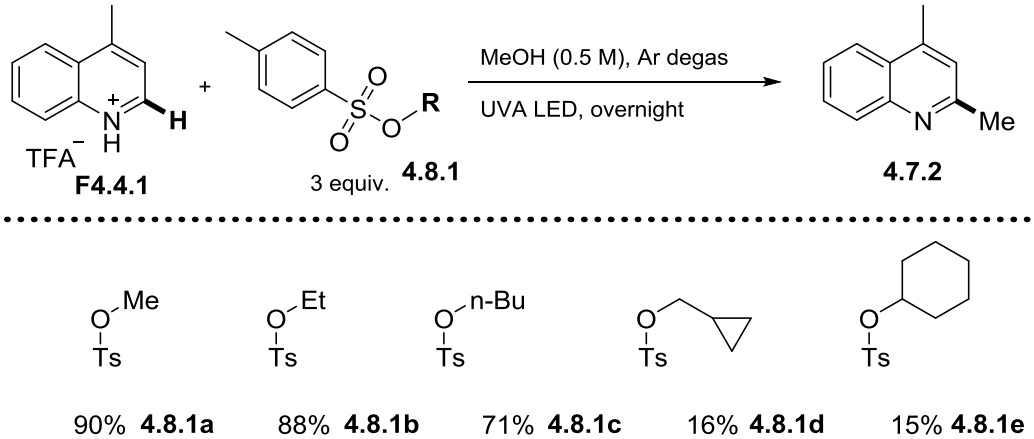

to explore the substrate scope of this reactivity. Remarkably, regardless of the alkyl sulfonate used, the only observed product was the methylated quinoline **4.7.2,** which was obtained in all

cases. In fact, when methyl sulfonate **4.8.1a** was used in a solvent other than methanol, no product was observed. The results prompted us to heavily revise our original hypothesis.

4.2.3 Alpha-hydroxy radical

The methylation results mentioned above were obtained in a short time span. Taken together, they painted a very different picture than what we had initially predicted. The formation of the expected product skewed our understanding of the mechanism, which in hindsight was flawed to begin with. With methanol as the solvent, the presence of any methyl radical would have resulted in hydrogen abstraction from the solvent, forming methane and preventing any direct methylation from occurring. In addition, if such a radical addition was formed in methanol, we should have observed some product in other solvents such as acetonitrile. Therefore it seems likely that the methylation is originated from the solvent, and that the radical

Scheme 4.9: Proposed mechanism for the Ir catalyzed alkylation of heteroarenes.

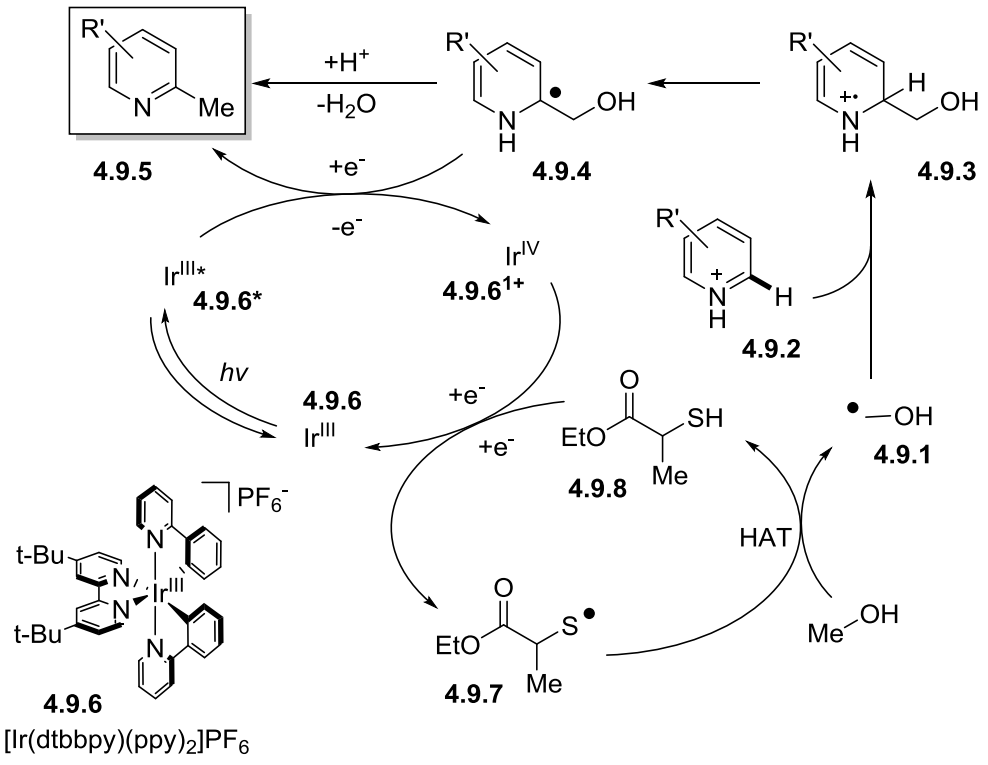

was derived from it. On the assumption that the reaction was still a radical process, we proposed the formation of an alpha hydroxy radical from the methanol which would subsequently add to the protonated quinoline and eventually generate the observed methylated product **4.7.2**.

A recent report at the time by MacMillan and co-workers proposed the formation of an alpha hydroxy radical from alcohols by using a combination of PTSA, an Ir(III) photocatalyst, and a thiol co-catalyst in a 1:1 mixture of DMSO and the desired alcohol (**Scheme 4.9**).[106] The transformation resulted in the alkylation of various heterocycles in very good yields with reaction times between 20 and 48 hours. Despite the report showing evidence of quenching of the iridium catalyst by PTSA, such quenching is not incorporated in the proposed mechanism.

Table 4.1: Co-solvent screen for photomediated methylation of 4-methylquinoline.

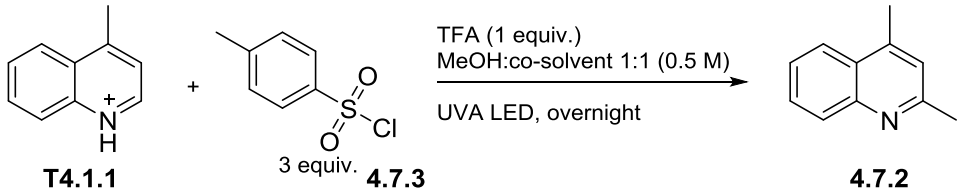

T4.1.1 **4.7.3** **4.7.2**

Entry	Co-solvent (1:1 methanol, 0.5M)	Conversion
1	ACN	38%
2	DMF	20%
3	DCE	38%
4	Acetone	25%
5	DMSO	<5%
6	DMSO[a]	20%
7	H_2O	72%
8	H_2O[b]	78%
9	H_2O[b,c]	80%

[a] Without p-*toluenesulfonyl chloride. [b] with PTSA instead of* p-*toluenesulfonyl chloride [c]1.5* Water to :1 Methanol

The authors proposed a Spin-Centered-Shift mechanism to explain the formation of **4.9.5** from the radical specie **4.9.4.** In addition, one can suggest that the formation of the α-alkoxy radical **4.9.1** via the hydrogen abstraction on methanol (**4.9.7 → 4.9.8**) could be an uphill process.

First, we screened various co-solvents aiming to reduce the amount of alcohol and to solubilize larger and more viscous alcohols. Acetonitrile, DMF, DCE and acetone considerably reduced the conversion of **T4.1.1** to **4.7.2** when used in combination with methanol (**Table 4.1**, entry 1-4). DMSO almost completely stopped the reaction when combine with the *p*-toluenesulfonyl chloride, but showed a 20% conversion in the absence of the latter (entry 5 and 6). Fortunately water did demonstrate good compatibility with the reaction, causing a 72% conversion of **T4.1.1** to **4.7.2** with *p*-toluenesulfonyl chloride.

In a concurrent optimization of our conditions, we demonstrated that many sulfonyl analogues in addition to the ones already tested were successful in catalysing the conversion of **F4.4.1** to **4.7.2** (**Figure 4.5**). Electron deficient and electron rich analogs **F4.5.1a** and **F4.5.1b** showed good conversion to the desired product. PTSA (**F4.5.1c**) also showed decent conversion to the desired product. Dimethyl sulfone **F4.5.1e** showed very low conversion and sulfuric acid

Figure 4.5 : Compatible sulfonates for the photomediated methylation.

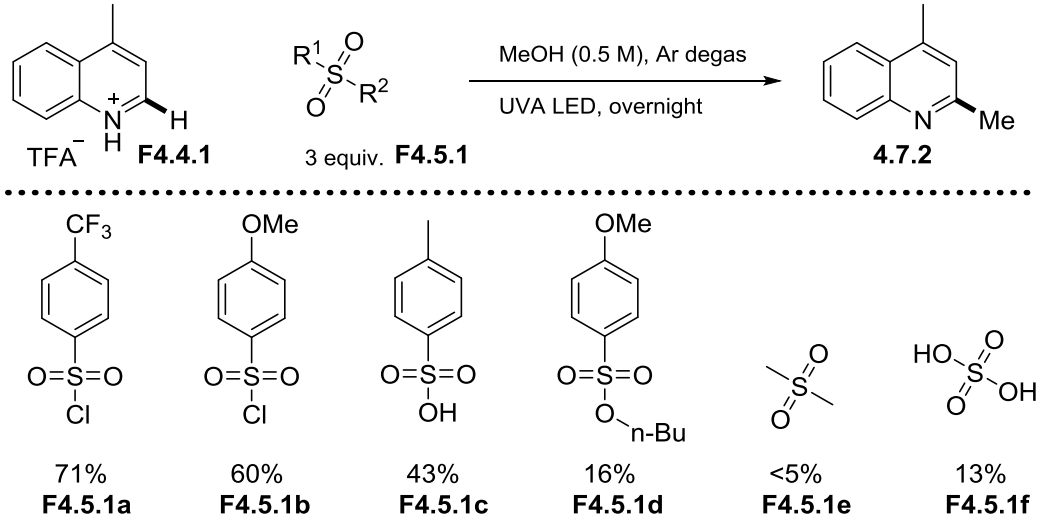

F4.5.1f afforded low and inconsistent results. *P*-toluenesulfonyl chloride was a very attractive reagent because of its availability and affordability. After discovering that water was an efficient co-solvent, we decided to start using PTSA instead for similar reasons in addition to its increased conversion (80%) and high solubility in the reaction mixture (**Table 4.1**, entry 9).

4.2.4 C-O Bond Reduction

If indeed our observed product arises from the addition of an α-hydroxy radical, one of the reactive intermediates must then contain an extraneous C-O bond. The reduction of the bond to a C-H bond is necessary to yield the final product. The reduction mechanism could conceivably occur via either a radical pathway or an ionic pathway. To help determine which pathway is more likely, compound **4.10.1** was submitted to the reaction conditions to act as surrogate of such an intermediate (**Scheme 4.10**). The compound was successfully reduced to the desired compound **4.7.2** in quantitative yield (**1**). With the assumption that compound **4.10.1** underwent reduction via the same reaction pathway than the radical addition substrate, it offered the possibility that **4.10.1** was either an intermediate in the reaction, or could enter the reaction at a different step in the mechanism.

Scheme 4.10 : Photomediated reduction of quinoline methanol.

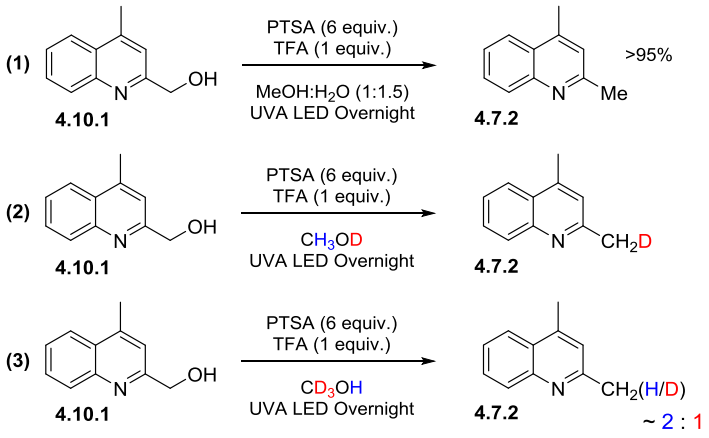

Deuterated experiments were performed with compound **4.10.1** to determine the origin of the hydrogen of the C-H bond derived from the C-O bond. When mono-deuterated methanol CH_3OD was used (**Scheme 4.10**) (**2**), the reaction exclusively incorporated a single deuterium to the final product **4.7.2(D_1)**. If the methylation occurs via de the same types of intermediates, it would indicate that the final hydrogen in the methylation process comes from the proton on the methanol. It is worth nothing that a deuteron-proton exchange with the PTSA and TFA could occur with the solvent during the reaction, which would create a source of acidic deuterons that might not come directly from the methanol but rather from deuterated PTSA and TFA. The result suggested that the final protonation in the dehydroxylation was an ionic process.

When tris-deuterated methanol CD_3OH was used (**Scheme 4.10**) (**3**), the major product formed contained no deuterium atom. Although monodeuterated **4.7.2(D_1)** should not be observed based on the proposed ionic protonation step, it was nevertheless present in the reaction mixture. We believe the deuterium comes from the erosion of the C-D bonds in the methanol via a radical process, creating a source of acidic deuteron. It is unavoidable and is inherent to the mechanism.

The results were followed by deuterated experiments of the methylation process in the hopes of corroborating the results obtained from compound **4.10.1** (**Scheme 4.11**). Unsurprisingly, when fully deuterated solvents CD_3OD and D_2O were used, the tris-deuterated **4.7.2(D_3)** was observed. In addition to supporting the solvent as the source of the methyl group and final protonation, it also eliminates the possibility that a hydrogen originating from a C-H bonds of the heterocycle would be responsible for the dehydroxylation. As expected, when D_2O and mono-deuterated methanol CH_3OD were used, the major product was the CH_2D methylated product **4.7.2(D_1)**, again supporting an ionic protonation for the final step. Unfortunately, the

non-deuterated product was also observed and could not be avoided since the PTSA and TFA used in the reaction were non-deuterated. Most interestingly of all, when tris-deuterated methanol CD_3OH was used, the expected compound **4.7.2(D_2)** was the only observed product in the reaction mixture, which supports both assertions that the methyl group originates from the methanol through a hydrogen abstraction of a C-H bond, and ultimately an ionic protonation to form the final product.

Scheme 4.11 : Methylation of quinoline with methanol

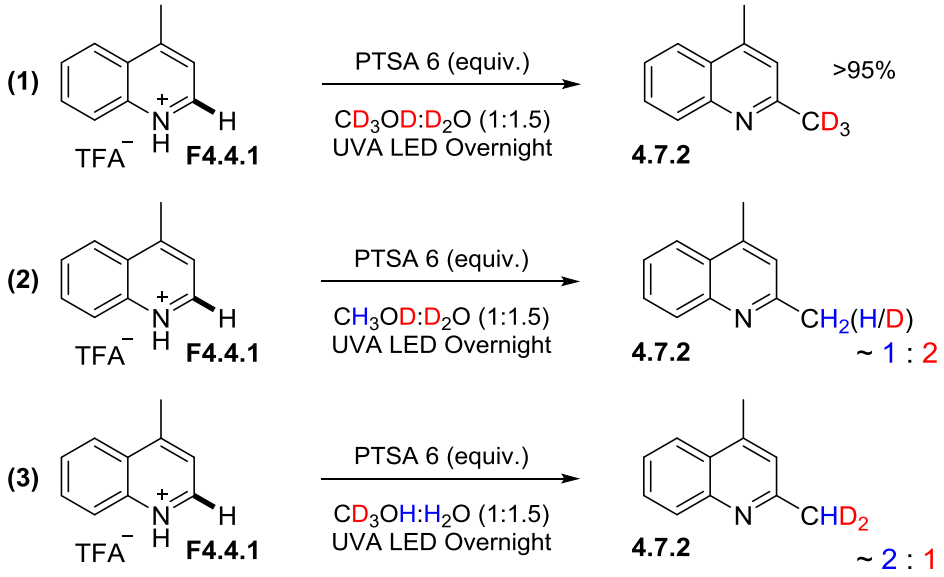

The combination of the results allowed us to propose the two following mechanisms (**Scheme 4.12**, trifluoroacetate omitted for clarity). The TFA quinoline adduct **F4.4.1** can be irradiated by UVA light, forming the corresponding excited quinoline **F4.4.1***. An energy transfer between **F4.4.1*** and PTSA would lead to the diradical intermediate **F4.5.1c***, which would subsequently undergo a hydrogen atom transfer (HAT) from methanol to form the alpha hydroxy radical **4.12.4** and intermediate **4.12.5**. We believe the HAT reaction could also be the source of the deuterium incorporation when CD_3OH is used for the reduction of **4.10.1** (**Scheme**

Scheme 4.12: Proposed mechanism for methylation of 4-methylquinoline via energy transfer

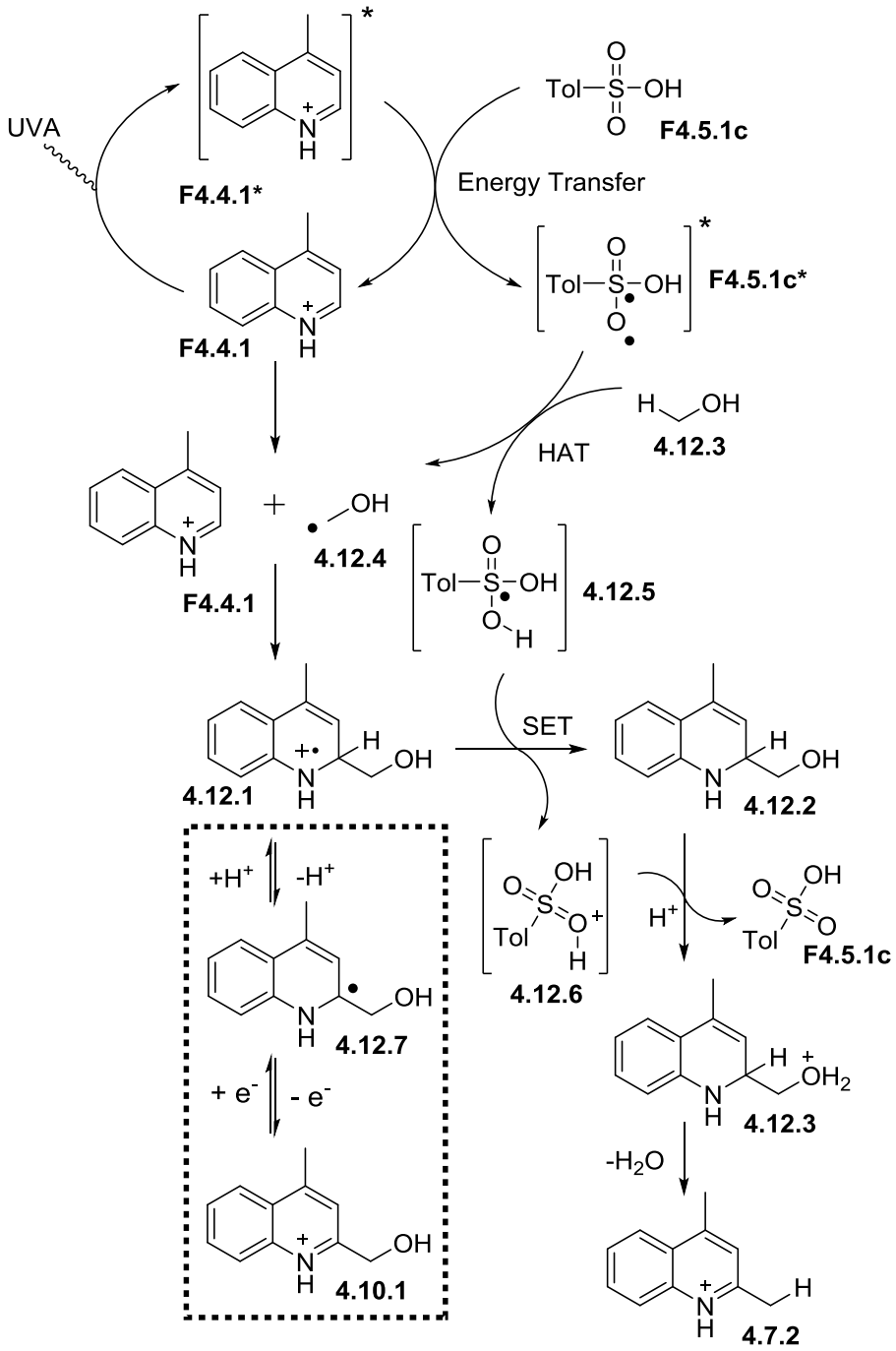

4.10). Intermediate **4.12.4** would then undergo radical addition reaction to a protonated quinoline, forming the hydroxymethylated radical cation **4.12.1**. A subsequent electron transfer

(possibly via **4.12.5** formed from the HAT between PTSA and methanol) would generate the neutral intermediate **4.12.2**. A subsequent protonation of the hydroxyl group (**4.12.3**), followed by elimination and tautomerization would lead to the final product **4.7.2**. The mechanism also accounts for the reduction of compound **4.10.1**. The intermediate could undergo a SET reaction to form the alpha amino radical **4.12.7**. The alpha amino radical is in equilibrium with the radical cation **4.12.1** and would be the common intermediate in both transformation.

Alternatively, the excited quinoline could undergo an oxidative quenching event (**Scheme 4.13**), transferring an electron and a proton to PTSA and forming intermediate **4.13.2** and the radical cation **4.13.1**. Intermediate **4.13.2** would then undergo the elimination of a water molecule, forming the sulfinic acyl radical **4.13.3**. A subsequent HAT with methanol would form the alpha hydroxy radical **4.12.4** and sulfinic acid **4.13.4**. The oxidized quinoline **4.13.1** would reform **F4.4.1** via the oxidation of methanol, and subsequently undergo a radical addition from the hydroxymethyl radical **4.12.4** to intercept intermediate **4.12.1**. The rest of the transformation would be identical to what was discussed in **Scheme 4.12**. We know from initial kinetic quenching studies of **F4.4.1*** that PTSA does indeed participate in the quenching event, although whether it is an oxidative or reductive quench or even an energy transfer is still unclear. The origins of the electrons in the SET steps are also uncertain. They most likely originate from the methanol, however if this occurs directly or via PTSA derived intermediates is unknown at this time.

Scheme 4.13 : Proposed mechanism for methylation of 4-methylquinoline via oxidative quenching cycle

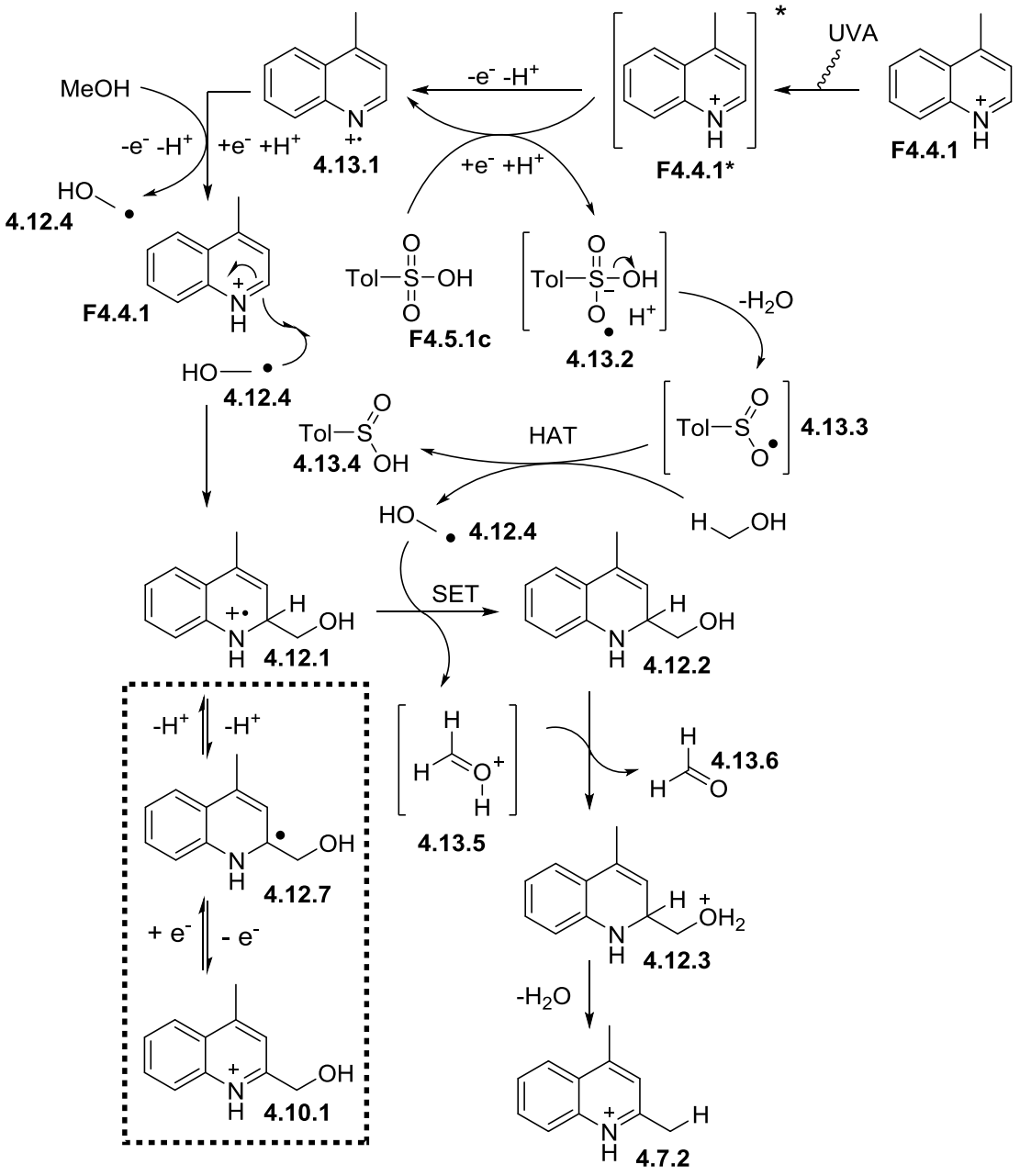

4.2.5 Searching for solutions with flow chemistry

Despite our initial accomplishments with methanol and 4-methylquinoline, incorporating other alcohols to the reaction system was met with only mild success. The reaction mixture which was initially transparent became colored during the irradiation and it reduced the depth at which the light could effectively penetrate the solution. The issue was evident when we looked at the conversion of the starting material overtime. More than 50% of the starting material was consumed within the first 8 h of irradiation, however full conversion was not achieved after an additional 8 h. We postulated that the conversion could be improved if the light had better penetration of the overall solution.

The conditions we had developed with PTSA along with water as a co-solvent guaranteed that all the reagents were soluble in the reaction mixture (**Table 4.1**, entry 9). Nonetheless, the coloration of the reaction still could not be avoided and thus the light could not be made to penetrate any deeper into the reaction vessel. However the reaction vessel could be changed, and since the reaction mixture was a homogeneous solution, flow chemistry through UVA transparent tubbing was performed. A simple set-up was constructed using PTFE tubing and a syringe pump. The 0.3 mm thick wall and 0.8mm inner diameter of the tubing allowed light to fully penetrate the reaction despite the coloration. In addition, the flow of the reaction also allowed for overall shorter exposure, limiting potential degradation of the product. We successfully applied the methodology to the alkylation of 4-methylquinoline with methanol, ethanol and *n*-butanol.

During a 16 h irradiation in standard batch reactions, the methylation achieved 80% conversion (**Table 3.3**, entry 1). The corresponding alkylation using EtOH and *n*-BuOH achieved 40% and 7% respectively (entry 3 and 5). Under flow conditions, the conversion of

each of these reactions was significantly improved. The methylation achieved full conversion (entry 2) and both the ethylation and butylation were improved, achieving 61% and 60% conversion respectively (entry 4 and 6). This seemed to represent a model example where flow chemistry would impart a significant advantage to the reaction conditions relative to standard batch conditions. Unfortunately because of the very primitive style of flow system, the injection speeds had to be abysmally slow in order achieve the desired exposure time. Work towards improving the reaction with the aid of a recirculating pump is currently underway. The device should allow for a faster flow rate by continuously pumping a batch solution through a coiled PTFE tubing irradiated by UVA which would create a high penetration window for the reaction to occur while simultaneously facilitating higher scale reactions.

Table 4.2 : Modified conditions for alkylation of 4-methylquinoline in flow

Entry	Alcohol	Product	Procedure [a]	Conversion [%]
1[b]	Methanol	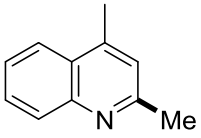 **T4.2.1**	A (Batch)	80
2			B (Flow)	>99
3	Ethanol	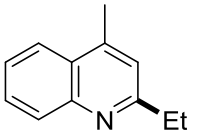 **T4.2.2**	A (Batch)	40
4			B (Flow)	61
5	*n*-Butanol	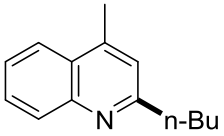 **T4.2.3**	A (Batch)	7
6			B (Flow)	60

[a] Procedure A: Screw-top reaction flask, MeOH:H_2O (1:1.5, 3ml) **F4.4.1** (1 equiv.) PTSA (6 equiv.) UVA, 16 h; Procedure B: Syringe injected flow (PTFE tubing, 0.3 mm wall, 0.8 mm ID, MeOH:H_2O (1:1.5, 3ml) **F4.4.1** (0.2 mmol, 1 equiv.) PTSA (1.2 mmol, 6 equiv.) UVA, 10 h. The reaction was prepared in a vial, loaded in a syringe and injected through a 2.1 ml volume coil of PTFE exposed to UVA over 10 h.

4.2.6 Ongoing work on methylating with methanol

The novel reactivity described above shows promise for methylation of heteroarene. Preliminary results with other alcohols and heteroarenes are encouraging although ample work is needed to develop a highly generalized alkylation of heteroarenes. Certain parts of the mechanism are currently being investigated. The type of quenching by the PTSA either via energy transfer or electron transfer still needs to be elucidated. The role of the PTSA needs to be properly understood from initial quenching to final by-product. Whether it also plays the role of electron donor or acceptor, or perhaps is regenerated or turns into another reagent is still unclear. The details of C-O bond reduction along with the nature of the electron donors should be elucidated. In addition to help improve this method, they might also reveal a novel reduction pathway. Many questions still need to be answered if this method is ever to effectively be extended to a wider variety of alcohols and heteroarenes. Nevertheless, the potential application of such a methodology could have a significant impact on how these kinds of reactions are performed in the future and allow easier access to previously difficult to synthesize or even unattainable compounds.

---

[84] Sibi, M. P.; Yang, Y.-H.; Lee, S. *Org. Lett.* **2008**, *10*, 5349 – 5352
[85] Schultz, D. M.; Yoon, T. P. *Science* **2014**, *343*, 985 – 995
[86] Discekici, E. H.; Treat, N. J.; Poelma, S. O.; Mattson, K. M.; Hudson, Z. M.; Luo, Y.; Hawker, C. J.; de Alaniz, J. R. *Chem. Commun.* **2015**, *51*, 11705 – 11708
[87] Bailey, W. F.; Patricia, J. J. *J. Organomet. Chem.* **1988**, *352*, 1 – 46
[88] Pan, X.; Lacôte, E.; Lalevée, J.; Curran, D. P. *J. Am. Chem. Soc.* **2012**, *134*, 5669 - 5674
[89] Narayanam, J. M. R.; Tucker, J. W.; Stephenson, C. R. J. *J. Am. Chem. Soc.* **2009**, *131*, 8756 – 8757
[90] Barton, D. H. R.; McCombie, S. W.; *J. Chem. Soc. Perkin Trans. 1* **1975**, 1574 – 1585
[91] Park, H. S.; Lee, H. Y.; Kim, Y. H. *Org. Lett.* **2005**, *7*, 3187 – 3190
[92] Dolan, S. C.; MacMillan, J. *J. Chem. Soc. Chem. Commun.* **1985**, *22,* 1588 – 1589
[93] Zhang, L.; Koreeda, M. *J. Am. Chem. Soc.*, **2004**, *126*, 13190 – 13191
[94] Lam, K.; Markó, I. E. *Org. Lett.* **2008**, *10*, 2773 – 2776
[95] Girard, P.; Namy, J. L. Kagan, H. B. *J. Am. Chem. Soc.*, **1980**, *102*, 2693 – 2698
[96] Lopez, R. M.; Hays, D. S.; Fu, G. C. *J. Am. Chem. Soc.*, **1997**, *119*, 6949 – 6950

[97] McCombie, S. W.; Motherwell, W. B.; Tozer, M. J. *Organic Reactions* (Ed.: S. E. Denmark), Wiley, Hoboken, **2012**, *77*, 161 – 432, online.
[98] McCallum, T.; Slako, E.; Morin, M.; Barriault, L. *Eur. J. Org. Chem.* **2015**, *1*, 81 – 85
[99] Appel, R. *Angew. Chem. Int Ed.* **1975**, *14*, 801 – 811
[100] Dai, C.; Narayanam, J. M. R.; Stephenson, C. J. *Nat. Chem.* **2011**, *3*, 140 – 145
[101] Revol, G.; McCallum, T.; Morin, M.; Gagosz, F.; Barriault, L. *Angew. Chem. Int. Ed.* **2013**, *52*, 13342 – 13345
[102] Che, C.-M.; Kwong, H.-L.; Yam, V.W.-W.; Cho, K.-C. *J. Chem. Soc. Chem. Commun.* **1989**, *13*, 885 – 886
[103] Nhishina, Y.; Ohtani, B.; Kikushima, K. *Beilstein J. Org. Chem.* **2013**, *9,* 1663 – 1667.
[104] McCallum, T.; Barriualt, L. *J. Org. Chem.* **2015**, *80*, 2874 − 2878
[105] McCallum, T.; Barriault, L. *Chem. Sci.* **2016**, *7*, 4754 – 4758
[106] Jin, J.; MacMillan, D. W. C. *Nature* **2015**, *525*, 87 – 90

5 Supplemental Information (by Chapter)

5.1 General Information

All reactions were performed under argon atmosphere in flame-dried glassware equipped with a magnetic stir bar and a rubber septum, unless otherwise indicated. Most solvents were filtered using LC Technology Solutions INC. Solvent Systems. All other commercial reagents were used without further purification, unless otherwise noted. Reactions were monitored by thin-layer chromatography (TLC) analysis of aliquots using glass sheets precoated (0.2 mm layer thickness) with silica gel 60 F254 (E. Merck). Thin-layer chromatography plates were viewed under UV light and stained with potassium permanganate or p-anisaldehyde staining solution. Column chromatography was carried out with silica gel 60 (230–400 mesh, Merck). Yields refer to products isolated after this purification, unless otherwise stated. Proton nuclear magnetic resonance (^{1}H NMR) spectra were recorded on Bruker AMX 300 MHz and Bruker AMX 400 MHz. NMR samples were dissolved in $CDCl_3$ (unless specified otherwise) and chemical shifts are reported in ppm referenced to residual undeuterated solvent. Data are reported as follows: chemical shift, multiplicity, coupling, integration, where multiplicity (s = singlet, d = doublet, dd = doublet of doublets, ddd = doublet of doublets of doublets, dt = doublet of triplets, ddt = doublet of doublets of triplets, dq = doublet of quartets, br = broad signal, t = triplet, td = triplet of doublets, tt = triplet of triplets, tquin = triplet of quintets, q = quartet, qd = quartet of doublets, quin = quintet, m = multiplet, or otherwise noted), coupling constant. Carbon nuclear magnetic resonance (13C NMR) spectra were recorded same Bruker instruments as in 1H NMR using 75 MHz or 100 MHz. IR spectra were recorded with a Bomem Michaelson 100 FTIR spectrometer. HRMS were obtained on a Kratos Analytical Concept instrument (University of Ottawa Mass

Spectrum Centre). UV-Vis absorption spectra were recorded on a Cary-100 spectrophotometer, using MeCN as solvent in a 1 cm x 1cm quartz cuvette. Optical rotations were measured using an Anton Paar MCP 500 Modular Circular Polarimeter at 589 nm with 0.1 dm/2 mL sample cell.

5.2 Supplemental Information Chapter 1

(*GP5.2.1*) General procedure for the formation of 1.11.5a-d

To a flame-dried round- bottom flask equipped with a magnetic stirrer under argon atmosphere was added $Pd(PPh_3)_4$ (0.063 mmol, 0.05 equiv.) and CuI (0.126 mmol, 0.10 equiv.). Benzene (12.6 mL, 0.1 M) was added and the mixture was degassed (sparged) for 15 min. During the degassing, the aryl (or vinyl) halide **1.11.4a-d** (1.89 mmol, 1.5 equiv.) was added followed by diethyl 2-(prop-2-yn-1-yl)malonate **1.11.3** (1.26 mmol, 1.0 equiv.). Once the degassing is finished, diethylamine (6.31 mmol, 5 equiv.) was added and the solution was stirred at room temperature overnight. After workup and evaporation of the solvent, the residue was purified by column chromatography and gave the desired product (**1.11.5a-d**).

(*GP5.2.2*) General procedure for the formation of 1.9.1, F1.2.1a-i

Solution 1: To a flame-dried round- bottom flask equipped with a magnetic stirrer under argon atmosphere was added NaH (7.13 mmol, 2 equiv.) in THF (17 mL) followed by the addition of compound **1.11.5** (5.35 mmol, 1.5 equiv.) dropwise and the reaction was stirred for 30 min at room temperature.

Solution 2: In a separate round- bottom flask equipped with magnetic stirrer under argon atmosphere was added the enone **1.11.6** (3.57 mmol, 1 equiv.) followed by THF (17 mL). The solution was cooled to −78 °C and TIPSOTf (5.35 mmol, 1.5 equiv.) was added slowly. The reaction mixture was stirred for 5 min, after which Me_2S (10.7 mmol, 3 equiv.) was added to the

solution drop wise along the side of the flask, and the solution is stirred for 25 min at −78 °C. *Solution 1* was added via cannula to *solution 2* in a dropwise manner. The mixture was then stirred for 1 h as the bath warmed to room temperature. The reaction mixture was quenched with a saturated aqueous $NaHCO_3$ and extracted with EtOAc. The fractions were concentrated *in vacuo* and the residue was purified by column chromatography (EtOAc/hexanes) to give the desired product (**1.91, F1.21a-i**).

(***GP5.2.3***) **General procedure for the formation of 1.9.4, F1.2.2a-i (Au(I)-catalyzed cyclization)**

In a flask equipped with a magnetic stirrer was added the silyl enol ether **F1.2.1a-i** (0.10 mmol) followed by nitromethane (1 mL) and [**L7**AuNCMe][SbF_6] (0.005 mmol). After stirring overnight, the reaction mixture was concentrated *in vacuo* and the crude mixture was purified by column chromatography (1–5% ethyl acetate/hexanes) and gave the desired cyclized product (**1.9.4**, **F1.2.2a-i**).

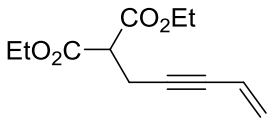

1.11.5a: ^{1}H NMR (400MHz, CHLOROFORM-d) δ ppm = 5.69 (tdd, *J* = 17.5, 11.1, 2.1 Hz, 1 H), 5.51 (dd, *J* = 17.5, 2.1 Hz, 1 H), 5.37 (dd, *J* = 11.0, 2.2 Hz, 1 H), 4.19 (q, *J* = 7.2 Hz, 4 H), 3.52 (t, *J* = 7.7 Hz, 1 H), 2.86 (dd, *J* = 7.7, 1.9 Hz, 2 H), 1.24 (t, *J* = 7.2 Hz, 6 H) ^{13}C NMR (101MHz, CHLOROFORM-d) δ ppm = 168.0 (2 X C), 126.6 (CH_2), 117.0 (CH), 86.1 (C), 81.1 (C), 61.7 (2 X CH_2), 51.3 (CH), 19.3 (CH_2), 14.0 (2 X CH_3). IR (neat, cm^{-1}): 2984, 1732; HRMS (EI) m/z calculated for $C_{12}H_{14}O_4$ $[M]^+$: 224.1049, found: 224.1010. 5.01g, 89% yield.

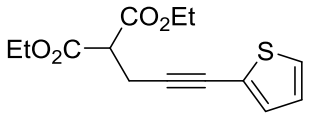

1.11.5b: ^{1}H NMR (400MHz, CHLOROFORM-d) δ ppm = 7.16 (dd, *J* = 5.2, 1.1 Hz, 1 H), 7.09 (dd, *J* = 3.5, 0.9 Hz, 1 H), 6.90 (dd, *J* = 5.2, 3.6 Hz, 1 H), 4.22 (q, *J* = 7.1 Hz, 4 H), 3.61 (t, *J* = 7.7 Hz, 1 H), 3.00 (d, *J* = 7.7 Hz, 2 H), 1.27 (t, *J* = 7.2 Hz, 6 H). ^{13}C NMR (101MHz, CHLOROFORM-d) δ ppm = 168.0 (2 X C), 131.6 (CH), 126.8 (CH), 126.5 (CH), 123.3 (C), 89.5 (C), 75.6 (C), 61.8 (2 X CH_2), 51.2 (CH), 19.7 (CH_2), 14.1 (2 X CH_3). IR (neat, cm^{-1}): 2980, 1732; HRMS (EI) m/z calculated for $C_{14}H_{16}O_4S$ $[M]^+$: 280.7069, found: 280.0753. 5.30g, 75% yield.

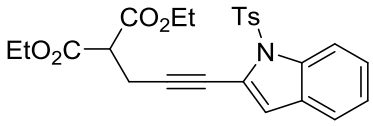

1.11.5c ^{1}H NMR (400MHz, CHLOROFORM-d) δ ppm = 8.16 (qd, *J* = 8.5, 0.7 Hz, 1 H), 7.86 - 7.78 (m, 2 H), 7.40 (td, *J* = 7.8, 0.9 Hz, 1 H), 7.32 (ddd, *J* = 8.5, 7.2, 1.3 Hz, 1 H), 7.23 - 7.18 (m, 3 H), 6.76 (s, 1 H), 4.31 - 4.18 (m, 4 H), 3.73 (t, *J* = 7.6 Hz, 1 H), 3.13 (d, *J* = 7.6 Hz, 2 H), 2.33 (s, 3 H), 1.27 (t, *J* = 7.2 Hz, 6 H). ^{13}C NMR (101MHz, CHLOROFORM-d) δ ppm = 168.0 (2 X C), 144.9 (C), 136.2 (C), 135.7 (C), 129.7 (2 X CH), 128.9 (C), 127.1 (2 X CH), 125.7 (CH), 123.8 (CH), 120.9 (CH), 120.7 (C), 117.0 (CH), 114.7 (CH), 93.7 (C), 73.4 (C), 62.0 (2 X CH_2), 51.0 (CH), 21.6 (CH_3), 19.9 (CH_2), 14.1 (2 X CH_3). IR (neat, cm^{-1}): 2986, 1733; HRMS (EI) m/z calculated for $C_{25}H_{25}O_6NS$ $[M]^+$: 467.1403, found: 467.1374. 1.69g, 65% yield.

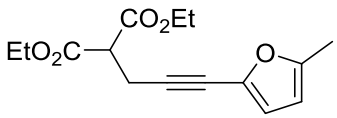

1.11.5d: ^{1}H NMR (400MHz, CHLOROFORM-d) δ ppm = 6.34 (d, *J* = 3.1 Hz, 1 H), 5.88 (qd, *J* = 3.1, 1.1 Hz, 1 H), 4.20 (q, *J* = 7.2 Hz, 4 H), 3.59 (t, *J* = 7.7 Hz, 1 H), 2.99 (d, *J* = 7.7 Hz, 2 H), 2.23 (s, 3 H), 1.25 (t, *J* = 7.2 Hz, 6 H). ^{13}C NMR (101MHz, CHLOROFORM-d) δ ppm = 167.9 (2 X (C), 153.1 (C), 135.1 (C), 115.7 (CH),

106.7 (CH), 89.4 (C), 73.1 (C), 61.8 (2 X CH_2), 51.1 (CH), 19.5 (CH_2), 14.0 (2 X CH_3), 13.7 (CH_3). IR (neat, cm^{-1}): 2988, 1733; HRMS (EI) m/z calculated for $C_{15}H_{18}O_5$ $[M]^+$: 278.1154, found: 278.1147. 1.39g, 84% yield.

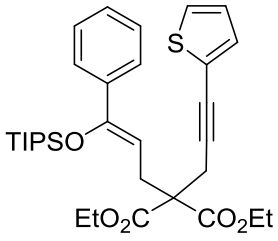

1.9.1: ^{1}H NMR (400MHz, CHLOROFORM-d) δ ppm 7.40 (dd, *J* = 7.8, 1.7 Hz, 2 H) 7.17 - 7.35 (m, 3 H) 7.15 (dd, *J* = 5.2, 1.08 Hz, 1 H) 7.06 (dd, *J* = 3.52, 1.0 Hz, 1 H) 6.90 (dd, *J* = 5.14, 3.7 Hz, 1 H) 4.84 (t, *J* = 7.0 Hz, 1 H) 4.04 - 4.29 (m, 4 H) 3.06 (s, 2 H) 3.04 (d, *J* = 7.0 Hz, 2 H) 1.24 (t, *J* = 7.1 Hz, 6 H) 0.98 - 1.05 (m, 21 H). ^{13}C NMR (101MHz ,CHLOROFORM-d) δ ppm = 170.2 (2 X C), 153.4 (C), 139.9 (C), 131.5 (CH), 127.9 (2 X CH), 127.8 (CH), 126.7 (CH), 126.3 (CH), 126.2 (2 X CH), 123.5 (C), 103.7 (CH), 89.1 (C), 76.3 (C), 61.6 (2 X CH_2), 57.3 (C), 29.7 (CH_2), 24.5 (CH_2), 17.9 (6 X CH_3), 14.1 (2 X CH_3), 12.3 (3 X CH). IR (neat, cm^{-1}): 2942, 2865, 1733; HRMS (EI) m/z calculatedd for $C_{32}H_{44}O_5SSi$ $[M]^+$: 568.2679, found: 568.2657. 725mg, 36% yield.

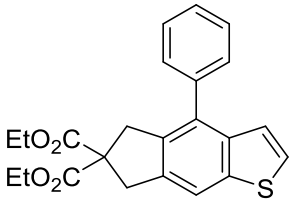

1.9.4: 1H NMR (400MHz, CHLOROFORM-d) δ ppm 7.66 (s, 1 H) 7.33 - 7.52 (m, 5 H) 7.27 (d, *J* =5 .6 Hz, 1 H) 7.09 (dd, *J* = 5.56, 0.7 Hz, 1 H) 4.16 (qd, *J* = 7.1, 0.6 Hz, 3 H) 3.72 (s, 2 H) 3.51 (s, 2 H) 1.20 (t, *J* =7.15 Hz, 6 H). 13C NMR (101MHz ,CHLOROFORM-d) δ ppm = 171.5 (2 X C), 139.5 (C), 139.0 (C), 138.1 (C), 137.5 (C), 135.2 (C), 133.3 (C), 129.3(2 X CH), 128.4 (2 X CH), 127.4 (CH), 125.3 (CH), 123.1 (CH), 117.0 (CH), 61.7 (2 X CH2), 61.0 (C), 40.4 (CH2), 39.3 (CH2), 14.0 (2 X CH3). IR (neat, cm^{-1}): 2360, 1733; HRMS (EI) m/z calculated for $C_{23}H_{22}O_4S$ $[M]^+$: 394.1239, found: 394.1246. 62mg, 89% yield.

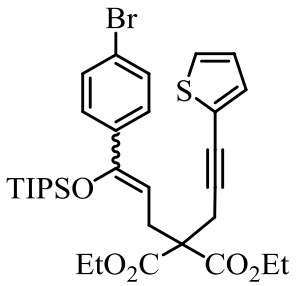

F1.2.1a: Characterized as E/Z mixture. **Major Isomer**: ^{1}H NMR (400MHz, CHLOROFORM-d) δ ppm = 7.46 - 7.37 (m, 2 H), 7.34 - 7.23 (m, 2 H), 7.17 (dd, *J* = 5.2, 1.2 Hz, 1 H), 7.06 (dd, *J* = 3.5, 1.1 Hz, 1 H), 6.91 (dd, *J* = 5.2, 3.5 Hz, 1 H), 4.89 (t, *J* = 7.0 Hz, 1 H), 4.30 - 4.08 (m, 4 H), 3.07 (s, 2 H), 3.04 (d, *J* = 7.0 Hz, 2 H), 1.25 (t, *J* = 7.1 Hz, 6 H), 1.14 - 0.98 (m, 21 H) ^{13}C NMR (101MHz ,CHLOROFORM-d) δ ppm = 170.1 (2 X C), 152.4 (C), 138.9 (C), 131.6 (CH), 131.2 (2 X CH), 130.2 (CH), 127.8 (2 X CH), 126.8 (CH), 126.4 (CH), 123.5 (C), 121.8(C), 104.6 (CH), 89.0 (C), 76.5 (C), 61.7 (CH_2), 57.3 (C), 29.9 (CH_2), 24.6 (CH_2), 18.0 (6 X CH_3), 13.5 (2 X CH_3), 12.6 (3 X CH).

Minor Isomer: ^{1}H NMR (400MHz, CHLOROFORM-d) δ ppm = 7.46 - 7.37 (m, 2 H), 7.34 - 7.23 (m, 2 H), 7.17 (dd, *J* = 5.2, 1.2 Hz, 1 H), 7.06 (dd, *J* = 3.5, 1.1 Hz, 1 H), 6.91 (dd, *J* = 5.2, 3.5 Hz, 1 H), 4.79 (t, *J* = 7.7 Hz, 1 H), 4.30 - 4.08 (m, 4 H), 3.00 (s, 2 H), 2.93 (d, *J* = 7.7 Hz, 2 H), 1.22 (t, *J* = 7.1 Hz, 6 H), 1.14 - 0.98 (m, 21 H) ^{13}C NMR (101MHz, CHLOROFORM-d) δ ppm = 169.9 (2 X C), 152.5 (C), 136.4 (C), 131.7 (CH), 131.2 (2 X CH), 129.8 (CH), 127.8 (2 X CH), 126.8 (CH), 126.5 (CH), 123.2 (C), 122.1 (C), 102.3 (CH), 88.4 (C), 76.6 (C), 61.7 (CH_2), 57.6 (C), 30.5 (CH_2), 23.8 (CH_2), 18.1 (6 X CH_3), 14.2 (2 X CH_3), 12.3 (3 X CH). IR (neat, cm^{-1}): 3103, 1732. HRMS (EI) m/z calculated for $C_{32}H_{43}BrO_5SSi$ $[M]^+$, 646.1784, found 646.1741. 655mg, 34% yield.

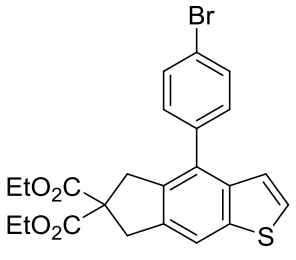

F1.2.2a: ^{1}H NMR (400MHz, CHLOROFORM-d) δ ppm = 7.69 (d, *J* = 0.5 Hz, 1 H), 7.61 (td, *J* = 8.6, 2.4 Hz, 2 H), 7.32 (td, *J* = 8.5, 2.3 Hz, 2 H), 7.31 (s, 1 H), 7.07 (dd, *J* = 5.5, 0.7 Hz, 1 H), 4.18 (ddd, *J* = 14.2, 7.2, 0.7 Hz, 4 H), 3.73 (s, 2 H), 3.50 (s, 2 H), 1.23 (t, *J* = 7.1 Hz, 6 H).

^{13}C NMR (101MHz, CHLOROFORM-d) δ ppm = 171.3 (2 X C), 139.6 (C), 137.9 (C), 137.8 (C), 137.5 (C), 135.2 (C), 131.9 (2 X CH), 131.7 (2 X CH), 131.0 (CH), 125.8 (CH), 122.7 (CH), 121.5 (C), 117.3 (CH), 61.8 (2 X CH_2), 61.0 (C), 40.3 (CH_2), 39.2 (CH_2), 14.0 (2 X CH_3). IR (neat, cm^{-1}): 1733; HRMS (EI) m/z calculated for $C_{23}H_{21}O_4SBr$ $[M]^+$: 472.0344, found: 472.0361. 61mg, 83% yield.

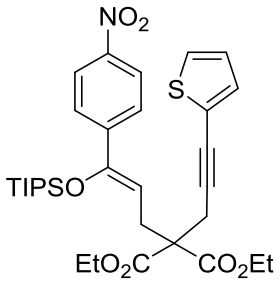

F1.2.1b: ^{1}H NMR (400MHz, CHLOROFORM-d) δ ppm = 8.13 (d, *J* = 8.9 Hz, 2 H), 7.55 (d, *J* = 8.9 Hz, 2 H), 7.16 (dd, *J* = 2.3, 1.2 Hz, 1 H), 7.05 (dd, *J* = 3.6, 1.1 Hz, 1 H), 6.89 (t, *J* = 3.7 Hz, 1 H), 5.11 (t, *J* = 7.0 Hz, 1 H), 4.29 - 4.11 (m, 4 H), 1.27 (t, *J* = 7.2 Hz, 6 H), 1.04 - 1.00 (m, 21 H). ^{13}C NMR (101MHz, CHLOROFORM-d) δ ppm = 169.9 (C), 168.0 (C), 151.4 (C), 147.2 (C), 146.1 (C), 131.6 (CH), 129.2 (CH), 126.8 (CH), 126.4 (2 X CH), 123.5 (2 X CH), 108.0 (CH), 89.5 (C), 88.6 (C), 75.6 (C), 61.8 (2 X CH_2), 57.0 (C), 30.0 (CH_2), 24.7 (CH_2), 17.9 (6 X CH_3), 14.1 (2 X CH_3), 12.3 (3 X CH). IR (neat, cm^{-1}): 3105, 1734; HRMS (EI) m/z calculated for $C_{32}H_{43}NO_7SSi$ $[M]^+$: 613.2529, found: 613.2537. 2.30g, 70% yield.

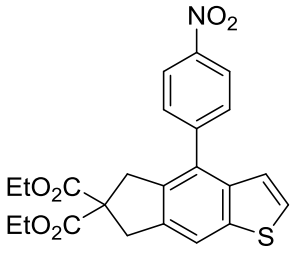

F1.2.2b: ^{1}H NMR (400MHz, CHLOROFORM-d) δ ppm = 8.37 (td, *J* = 9.0, 2.2 Hz, 2 H), 7.76 (s, 1 H), 7.64 (td, *J* = 9.0, 2.2 Hz, 2 H), 7.39 (d, *J* = 5.5 Hz, 1 H), 7.05 (dd, *J* = 5.6, 0.8 Hz, 1 H), 4.19 (q, *J* = 7.1 Hz, 4 H), 3.76 (s, 2 H), 3.50 (s, 2 H), 1.24 (t, *J* = 7.1 Hz, 6 H). ^{13}C NMR (101MHz, CHLOROFORM-d) δ ppm = 171.2 (2 X C), 147.2 (C), 145.9 (C), 139.8 (C), 137.6 (C), 137.4 (C), 135.3 (C), 130.8 (C), 130.3 (2 X CH), 126.6 (CH), 123.8 (2 X CH), 122.1 (CH), 118.2 (CH), 61.9 (2 X CH_2), 61.0 (C), 40.2 (CH_2), 39.2 (CH_2), 14.0 (2 X CH_3). IR (neat, cm^{-1}):

1733; HRMS (EI) m/z calculated for $C_{23}H_{21}NO_6S$ $[M]^+$: 439.1090, found: 439.1104. 45mg, 63% yield.

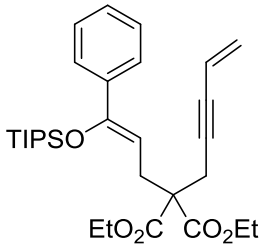

F1.2.1c: ^{1}H NMR (400MHz, CHLOROFORM-d) δ ppm = 7.62 - 7.25 (m, 5 H), 5.75 - 5.64 (m, 1 H), 5.58 - 5.47 (m, 1 H), 5.34 (s, 1 H), 4.79 (t, *J* = 7.0 Hz, 1 H), 4.29 - 4.00 (m, 4 H), 3.07 - 2.83 (m, 4 H), 1.22 (t, *J* = 6.8 Hz, 6 H), 1.13 - 0.97 (m, 21 H). ^{13}C NMR (101MHz, CHLOROFORM-d) δ ppm = 170.2 (2 X C), 153.3 (C), 139.9 (C), 127.9 (2 X CH), 127.8 (CH), 126.3 (CH_2) 126.2 (2 X CH), 117.2 (CH), 103.7 (CH), 85.6 (C), 81.9 (C), 61.5 (2 X CH_2), 57.2 (C), 29.5 (CH_2), 24.0 (CH_2), 17.9 (6 X CH_3), 14.1 (2 X CH_3), 13.5 (3 X CH). IR (neat, cm^{-1}): 2943, 1733; HRMS (EI) m/z calculated for $C_{30}H_{44}O_5Si$ $[M]^+$: 512.2958, found: 512.2919. 2.19g, 72% yield.

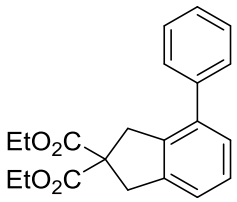

F1.2.2c: ^{1}H NMR (400MHz, CHLOROFORM-d) δ ppm = 7.46 - 7.38 (m, 4 H), 7.37 - 7.29 (m, 1 H), 7.27 - 7.21 (m, 0 H), 7.20 - 7.13 (m, 2 H), 4.16 (ttd, *J* = 10.6, 7.0, 3.5 Hz, 4 H), 3.63 (d, *J* = 4.8 Hz, 4 H), 1.21 (t, *J* = 7.1 Hz, 6 H). ^{13}C NMR (101MHz, CHLOROFORM-d) δ ppm = 171.6 (2 X C), 140.7 (C), 140.7 (C), 138.4 (C), 137.7 (C), 128.5 (2 X CH), 128.4 (2 X CH), 127.5 (2 X CH), 127.1 (CH), 123.2 (CH), 61.7 (2 X CH_2), 60.3 (C), 40.6 (CH_2), 40.2 (CH_2), 14.0 (2 X CH_3). IR (neat, cm^{-1}): 2984, 1734; HRMS (EI) m/z calculated for $C_{21}H_{22}O_4$ $[M]^+$: 338.1518, found: 338.1519. 56mg, 85%

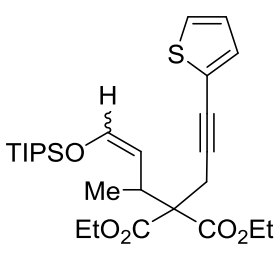

F1.2.1d : ^{1}H NMR (400MHz ,CHLOROFORM-d) δ ppm = 7.15 (dd, *J* = 5.1, 1.0 Hz, 1 H), 7.06 (d, *J* = 3.5 Hz, 1 H), 6.90 (dd, *J* = 5.1, 3.6 Hz, 1 H), 6.47 (d, *J* = 11.7 Hz, 1 H), 4.84 (dd, *J* = 11.6, 10.4 Hz, 1 H), 4.20 (q, *J* = 7.1 Hz, 4 H), 3.00 (q, *J* = 17.1 Hz, 2 H), 3.08 - 2.90 (m, 1 H), 1.25 (t, *J* = 7.4 Hz, 6 H), 1.16 (d, *J* = 6.9 Hz, 3 H), 1.14 - 0.98 (m, 21 H). ^{13}C NMR (101MHz,

CHLOROFORM-d) δ ppm = 170.0 (C), 169.6 (C), 142.7 (CH), 131.3 (CH), 126.7 (CH), 126.2 (CH), 123.6 (C), 110.6 (CH), 89.6 (C), 76.3 (C), 61.3 (2 X CH_2), 60.8 (C), 36.3 (CH), 25.4 (CH_2), 18.7 (CH_3) 17.7 (6 X CH_3), 14.1 (2 X CH_3) , 12.0 (3 X CH). IR (neat, cm_{-1}): 2942, 2866, 1728; HRMS (EI) m/z calculated for $C_{27}H_{42}O_5SSi$ $[M]^+$: 506.2522, found: 506.2526. 2.07g, 69% yield.

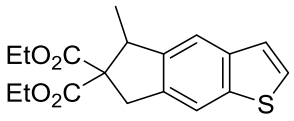

F1.2.2d ^{1}H NMR (400MHz, CHLOROFORM-d) δ ppm = 7.64 (s, 1 H), 7.58 (s, 1 H), 7.33 (d, *J* = 5.4 Hz, 1 H), 7.24 (d, *J* = 5.5 Hz, 1 H), 4.27 - 4.12 (m, 4 H), 4.08 (q, *J* = 7.2 Hz, 1 H), 3.84 (d, *J* = 16.7 Hz, 1 H), 3.38 (d, *J* = 16.6 Hz, 1 H), 1.30 (d, *J* = 7.2 Hz, 3 H), 1.24 (dt, *J* = 7.1, 1.4 Hz, 6 H). ^{13}C NMR (101MHz, CHLOROFORM-d) δ ppm = 171.6 (C), 170.2 (C), 143.0 (C), 139.1 (C), 138.9 (C), 136.5 (C), 125.6 (CH), 123.6 (CH), 118.0 (CH), 117.6 (CH), 65.3 (C), 61.5 (CH_2), 61.3 (CH_2), 44.3 (CH), 38.6 (CH_2), 16.9 (CH_3), 14.2 (CH_3), 14.1 (CH_3). IR (neat, cm^{-1}): 2977, 1725; HRMS (EI) m/z calculated for $C_{18}H_{20}O_4S$ $[M]^+$: 332.1082, found: 332.1085. 63mg, 95% yield.

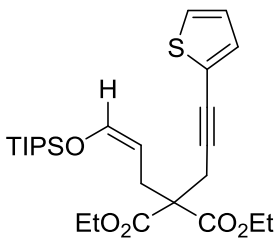

F1.2.1e: ^{1}H NMR (400MHz ,CHLOROFORM-d) δ ppm = 7.17 (dd, *J* = 5.2, 1.2 Hz, 1 H), 7.09 (dd, *J* = 3.6, 1.2 Hz, 1 H), 6.92 (dd, *J* = 5.2, 3.6 Hz, 1 H), 6.45 (d, *J* = 11.7 Hz, 1 H), 4.80 (td, *J* = 11.7, 8.1 Hz, 1 H), 4.29 - 4.13 (m, *J* = 2.8, 7.1, 7.1, 7.1 Hz, 4 H), 3.02 (s, 2 H), 2.69 (dd, *J* = 1.0, 8.0 Hz, 2 H), 1.26 (t, *J* = 7.2 Hz, 6 H), 1.17 - 1.09 (m, 3 H), 1.06 (d, *J* = 6.7 Hz, 18 H). ^{13}C NMR (101MHz ,CHLOROFORM-d) δ ppm = 170.1 (2 X C), 144.5 (CH), 131.6 (CH), 126.9 (CH), 126.5 (CH), 123.6 (C), 103.2 (CH), 88.9 (C), 76.5 (C), 61.7 (2 X CH_2), 57.5 (C), 30.7 (CH_2),

23.7 (CH_2), 17.8 (6 X CH_3), 14.2 (2 X CH_3), 12.1 (3 X CH). IR (neat, cm^{-1}): 3108, 1734; HRMS (EI) m/z calculated for $C_{26}H_{40}O_5SSi$ $[M]^+$: 492.2366, found: 492.2385. 662mg, 45%

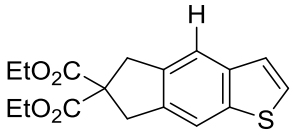

F1.2.2e: ^{1}H NMR (400MHz, CHLOROFORM-d) δ ppm = 7.68 (s, 1 H), 7.62 (s, 1 H), 7.35 (d, *J* = 5.4 Hz, 1 H), 7.24 (dd, *J* = 5.5, 0.7 Hz, 1 H), 4.21 (q, *J* = 7.1 Hz, 4 H), 3.67 (d, *J* = 3.2 Hz, 4 H), 1.26 (t, *J* = 7.1 Hz, 6 H). ^{13}C NMR (101MHz, CHLOROFORM-d) δ ppm = 171.6 (2 X C), 139.1 (C), 139.0 (C), 137.4 (C), 137.2 (C), 125.8 (CH), 123.4 (CH), 118.8 (CH), 117.8 (CH), 61.8 (2 X CH_2), 61.2 (C), 40.0(CH_2), 39.9 (CH_2), 14.2 (2 X CH_3). IR (neat, cm^{-1}): 1734; HRMS (EI) m/z calculated for $C_{17}H_{18}O_4S$ $[M]^+$: 318.0926, found: 318.0926. 53mg, 82% yield.

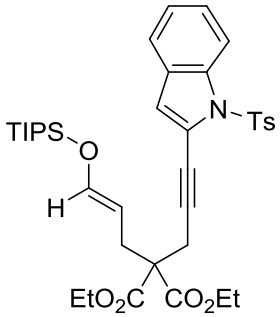

F1.2.1f: ^{1}H NMR (400MHz, CHLOROFORM-d) δ ppm = 8.15 (d, *J* = 8.5 Hz, 1 H), 7.82 (d, *J* = 8.3 Hz, 2 H), 7.39 (d, *J* = 7.7 Hz, 1 H), 7.35 - 7.28 (m, 1 H), 7.23 - 7.15 (m, 3 H), 6.75 (s, 1 H), 6.55 (d, *J* = 11.7 Hz, 1 H), 4.82 (d, *J* = 11.7 Hz, 1 H), 4.22 (dq, *J* = 2.7, 7.1 Hz, 4 H), 3.16 (s, 2 H), 2.80 (d, *J* = 7.9 Hz, 2 H), 2.32 (s, 3 H), 1.25 (t, *J* = 7.1 Hz, 6 H), 1.17 - 0.98 (m, 21 H). ^{13}C NMR (101MHz, CHLOROFORM-d) δ ppm = 170.0 (2 X C), 144.8 (C), 144.7 (CH), 136.0 (C), 135.7 (C), 129.7 (2 X CH), 128.9 (C), 127.1 (2 X CH), 125.7 (CH), 123.7 (CH), 120.8 (CH), 117.2 (CH), 114.7 (CH), 103.1 (CH), 93.0 (C), 74.2 (C), 61.7 (2 X CH_2), 57.5 (C), 30.6 (CH_2), 23.8 (CH_2), 21.6 (C), 17.7 (6 X CH_3), 14.1 (2 X CH_3), 12.3 (CH_3), 11.9 (3 X CH). IR (neat, cm^{-1}): 3109, 1731; HRMS (EI) m/z calculated for $C_{37}H_{49}NO_7SSi$ $[M]^+$: 679.2999, found: 679.2974. 616.9mg, 46% yield.

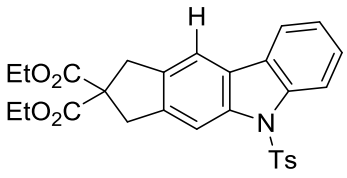

F1.2.2f: ^{1}H NMR (400MHz, CHLOROFORM-d) δ ppm = 8.25 (d, *J* = 8.3 Hz, 1 H), 8.12 (s, 1 H), 7.80 (d, *J* = 7.3 Hz, 1 H), 7.65 (d, *J* = 8.5 Hz, 3 H), 7.41 (dt, *J* = 1.2, 7.9 Hz, 1 H), 7.33 - 7.26 (m, 1 H), 7.08 (d, *J* = 8.0 Hz, 2 H), 4.20 (q, *J* = 7.2 Hz, 4 H), 3.73 (s, 2 H), 3.65 (s, 2 H), 2.24 (s, 3 H), 1.34 - 1.17 (m, 6 H). ^{13}C NMR (101MHz, CHLOROFORM-d) δ ppm = 171.5 (2 X C), 144.8 (C), 140.2 (C), 138.6 (C), 138.1 (C), 136.1 (2 X C), 135.0 (C), 129.7 (2 X CH), 127.0 (CH), 126.5 (2 X CH), 126.0 (C), 123.8 (CH), 119.7 (CH), 115.3 (CH), 115.2 (CH), 110.9 (CH), 61.8 (2 X CH_2), 61.0 (C), 40.8(CH_2), 40.0 (CH_2), 31.0, 21.5 (CH_3), 14.1(2 X CH_3). IR (neat, cm^{-1}): 1733; HRMS (EI) m/z calculated for $C_{28}H_{27}NO_6S$ $[M]^+$: 505.1559, found: 505.1561. 71mg, 95% yield.

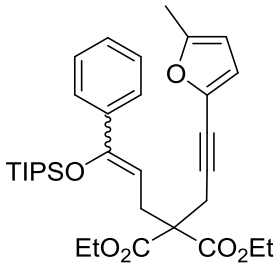

F1.2.1g: Characterized as E/Z mixture. **Major Isomer** ^{1}H NMR (400MHz, CHLOROFORM-d) δ ppm = 7.46 - 7.33 (m, 2 H), 7.31 - 7.16 (m, 3 H), 6.31 (d, *J* = 3.1 Hz, 1 H), 5.89 (dd, *J* = 3.2, 0.9 Hz, 1 H), 4.82 (t, *J* = 7.0 Hz, 1 H), 4.30 - 4.00 (m, 4 H), 3.06 (s, 2 H), 3.03 (d, *J* = 7.1 Hz, 2 H), 2.24 (s, 3 H), 1.23 (t, *J* = 7.1 Hz, 6 H), 1.14 - 0.95 (m, 21 H). ^{13}C NMR (101MHz ,CHLOROFORM-d) δ ppm = 170.1 (2 X C), 153.4 (C), 152.9 (C), 139.9 (C), 135.4 (C), 127.9 (2 X CH), 127.8 (CH), 126.2 (2 X CH), 115.6 (CH), 106.6 (CH), 103.7 (CH), 88.8 (C), 73.9 (C), 61.6 (2 X CH_2), 57.2 (C), 29.6 (CH_2), 24.3 (CH_2), 17.9 (6 X CH_3), 14.0 (2 X CH_3), 13.4 (CH_3), 12.3 (3 X CH).

Minor Isomer ^{1}H NMR (400MHz ,CHLOROFORM-d) δ ppm = 7.46 - 7.33 (m, 2 H), 7.31 - 7.16 (m, 3 H), 6.18 (d, *J* = 3.1 Hz, 1H), 5.86 (dd, *J* = 3.2, 0.9 Hz, 1 H), 4.77 (t, *J* = 7.7 Hz, 1 H), 4.30 - 4.00 (m, 4 H), 3.01 (s, 2 H), 2.92 (d, *J* = 7.7 Hz, 2 H), 2.24 (s, 3 H), 1.17 (t, *J* = 7.1 Hz, 6

H), 1.14 - 0.95 (m, 21 H). ^{13}C NMR (101MHz ,CHLOROFORM-d) δ ppm = 169.9 (2 X C), 153.4 (C), 152.8 (C), 137.4 (C), 135.2 (C), 128.5 (2 X CH), 128.1 (CH), 127.8 (2 X CH), 115.6 (CH), 106.6 (CH), 101.6 (CH), 88.3 (C), 74.0 (C), 61.8 (2 X CH_2), 57.4 (C), 30.4 (CH_2), 23.7 (CH_2), 17.7 (6 X CH_3), 14.0 (2 X CH_3), 13.8 (CH_3), 12.6 (3 X CH). IR (neat, cm^{-1}): 3106, 1734; HRMS (EI) m/z calculated for $C_{33}H_{46}O_6Si$ $[M]^+$: 566.3064, found: 566.3080. 603mg, 36% yield.

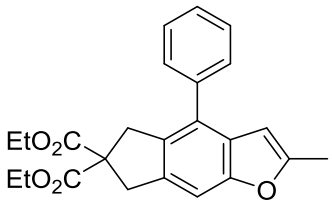

F1.2.2.g: ^{1}H NMR (400MHz, CHLOROFORM-d) δ ppm = 7.49 - 7.39 (m, 4 H), 7.39 - 7.30 (m, 1 H), 7.20 (d, *J* = 0.5 Hz, 1 H), 6.25 (t, *J* = 1.0 Hz, 1 H), 4.23 - 4.09 (m, 4 H), 3.68 (s, 2 H), 3.57 (s, 2 H), 2.38 (d, *J* = 0.9 Hz, 3 H), 1.21 (t, *J* = 7.2 Hz, 6 H). ^{13}C NMR (101MHz, CHLOROFORM-d) δ ppm = 171.6 (2 X C), 155.4 (C), 154.7 (C), 138.7 (C), 136.0 (C), 132.0 (C), 129.7 (C), 129.1 (2X CH), 128.4 (2 X CH), 127.7 (C), 127.1 (CH), 105.7 (CH), 102.1 (CH), 61.7(2 X CH_2), 61.1(C), 40.5(CH_2), 39.3 (CH_2), 17.7 (CH_3), 14.0 (2 X CH_3). IR (neat, cm^{-1}): 1736; HRMS (EI) m/z calculated for $C_{24}H_{24}O_5$ $[M]^+$: 392.1624, found: 392.1642. 67mg, 95% yield.

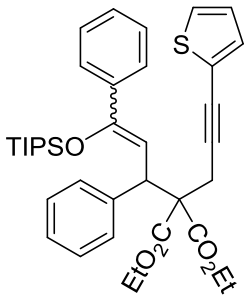

F1.2.1h: Characterized as E/Z mixture. **Major Isomer :** ^{1}H NMR (400MHz, CHLOROFORM-d) δ ppm = 7.48 - 7.38 (m, 1 H), 7.35 (s, 1 H), 7.34 - 7.16 (m, 8 H), 7.13 (t, *J* = 3.2 Hz, 1 H), 6.88 (q, *J* = 3.0 Hz, 2 H), 5.88 (d, *J* = 11.1 Hz, 1 H), 4.39 (d, *J* = 11.1 Hz, 1 H), 4.28 - 4.04 (m, 4 H), 2.95 (d, *J* = 17.0 Hz, 1 H), 2.80 (d, *J* = 17.0 Hz, 1 H), 1.22 (t, *J* = 7.2 Hz, 6 H), 1.10 - 0.95 (m, 21 H). ^{13}C NMR (101MHz, CHLOROFORM-d) δ ppm = 169.5 (C), 169.3(C), 152.1 (C), 140.8 (C), 137.7 (C), 131.5 (CH), 129.3 (2 X CH), 128.4 (CH), 128.1 (2 X CH), 128.1 (2 X CH), 127.9 (CH), 127.8 (CH), 126.9 (CH), 127.6 (2 X CH), 123.5 (C), 106.8

(CH), 89.4 (C), 76.9 (C), 62.2 (C), 61.4 (CH_2), 61.4 (CH_2), 46.7 (CH), 26.2 (CH_2), 18.0 (6 X CH_3), 14.0 (CH_3), 14.0 (CH_3), 12.7 (3 X CH).

Minor Isomer : ^{1}H NMR (400MHz, CHLOROFORM-d) δ ppm = 7.48 - 7.38 (m, 1 H), 7.35 (s, 1 H), 7.34 - 7.16 (m, 8 H), 7.13 (t, *J* = 3.2 Hz, 1 H), 6.88 (q, *J* = 3.0 Hz, 2 H), 5.78 (d, *J* = 10.4 Hz, 1 H), 4.87 (d, *J* = 10.5 Hz, 1 H), 4.28 - 4.04 (m, 4 H), 3.10 (d, *J* = 17.0 Hz, 1 H), 3.02 (d, *J* = 17.0 Hz, 1 H), 1.12 (t, *J* = 7.2 Hz, 6 H), 1.10 - 0.95 (m, 21 H). ^{13}C NMR (101MHz, CHLOROFORM-d) δ ppm = 169.5 (C), 169.3 (C), 151.6 (C), 140.5 (C), 139.9 (C), 131.4 (CH), 129.7 (2 X CH), 128.4 (CH) , 128.1 (2 X CH), 127.8 (CH), 127.8 (CH), 126.6 (CH), 126.6 (2 X CH), 126.1 (2 X CH), 123.8 (C), 108.7 (CH), 90.1 (C), 76.3 (C), 62.5 (C), 61.4 (CH_2), 61.4 (CH_2), 44.8 (CH), 25.5 (CH_2), 18.0 (6 X CH_3), 14.0 (CH_3), 14.0 (CH_3), 12.7 (3 X CH). IR (neat, cm^{-1}): 2942, 2866 1734; HRMS (TOF MS EI+) m/z calculated for $C_{38}H_{48}O_5SSi$ $[M]^+$: 644.2992, found: 644.3011. 1.83g, 48% yield.

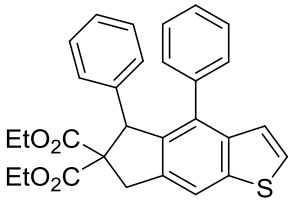

F1.2.2h ^{1}H NMR (400MHz, CHLOROFORM-d) δ ppm = 7.77 (s, 1 H), 7.54 (d, *J* = 7.5 Hz, 1 H), 7.43 (t, *J* = 7.4 Hz, 1 H), 7.27 - 7.21 (m, 1 H), 7.08 - 6.88 (m, 5 H), 6.65 (dd, *J* = 7.9, 1.5 Hz, 2 H), 6.53 (d, *J* = 7.5 Hz, 1 H), 5.21 (s, 1 H), 4.26 (d, *J* = 17.1 Hz, 1 H), 4.25 (qd, *J* = 10.8, 7.2 Hz, 1 H), 4.12 (qd, *J* = 10.8, 7.1 Hz, 1 H), 3.80 (qd, *J* = 10.8, 7.2 Hz, 1 H), 3.63 (qd, *J* = 10.8 7.2 Hz, 1 H), 3.53 (d, *J* = 17.2 Hz, 1 H), 1.21 (t, *J* = 7.1 Hz, 3 H), 0.91 (t, *J* = 7.2 Hz, 3 H). ^{13}C NMR (101MHz, CHLOROFORM-d) δ ppm = 171.8 (C), 168.8 (C), 140.0 (C), 139.7 (C), 139.6 (C), 138.9 (C), 138.4 (C), 136.8 (C), 134.4 (C), 129.2 (CH), 129.1 (CH), 128.9 (2 X CH), 128.2 (CH), 127.7 (2 X CH), 127.1 (CH), 126.7 (CH), 125.3 (CH), 123.3 (CH), 117.1 (CH), 66.5

(C), 61.8 (CH_2), 61.3 (CH_2), 54.9 (CH), 39.0 (CH_2) , 14.0 (CH_3), 13.7 (CH_3). IR (neat, cm-1): 2933, 2863, 1732; HRMS (EI) m/z calculated for $C_{29}H_{26}O_4S$ $[M]^+$: 470.1552, found: 470.1542. 67mg, 91% yield.

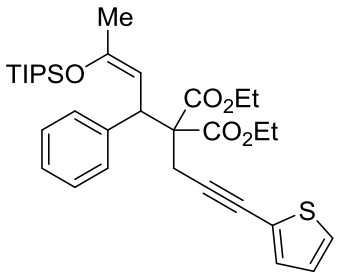

F1.2.1i: ^{1}H NMR (400MHz, CHLOROFORM-d) δ ppm = 7.24 - 7.20 (m, 4 H), 7.19 - 7.13 (m, 2 H), 7.13 - 7.07 (m, 1 H), 6.92 (dd, *J* = 5.1, 3.6 Hz, 1 H), 5.36 (d, *J* = 10.7 Hz, 1 H), 4.30 (d, *J* = 10.8 Hz, 1 H), 4.27 - 4.01 (m, 4 H), 3.02 (d, *J* = 17.1 Hz, 1 H), 2.85 (d, *J* = 17.1 Hz, 1 H), 1.82 (s, 3 H), 1.25 (t, *J* = 7.2 Hz, 3 H), 1.18 (t, *J* = 7.1 Hz, 3 H), 1.08 - 1.00 (m, 21 H). ^{13}C NMR (101MHz, CHLOROFORM-d) δ ppm = 169.6 (C), 169.4 (C), 150.6 (C), 140.6 (C), 131.3 (CH), 129.1 (2 X CH), 128.0 (2 X CH), 126.8 (CH), 126.8 (CH), 126.3 (CH), 123.7 (C), 105.3 (CH), 89.7 (C), 76.9 (C), 61.8(C), 61.4 (2 X CH_2), 47.0 (CH), 26.3 (CH_2), 18.2 (CH_3), 18.0 (6 X CH_3), 14.0 (CH_3), 14.0 (CH_3), 12.6 (3 X CH). IR (neat, cm^{-1}): 2943, 2866, 1725; HRMS (EI) m/z calculated for $C_{33}H_{46}O_5SSi$ $[M]^+$: 582.2835, found: 582.3091. 1.80g, 52% yield.

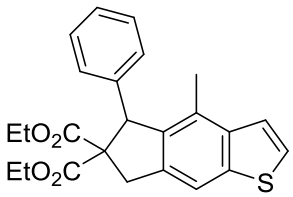

F1.2.2i: ^{1}H NMR (400MHz ,CHLOROFORM-d) δ ppm = 7.61 (s, 1 H), 7.30 (dd, *J* = 19.2, 5.6 Hz, 2 H), 7.21 - 7.09 (m, 3 H), 7.01 - 6.95 (m, 2 H), 5.34 (s, 1 H), 4.21 (qd, *J* = 10.8, 7.2 Hz, 1 H), 4.17 (d, *J* = 17.0 Hz, 1 H), 4.10 (qd, *J* = 10.8, 7.2 Hz, 1 H), 3.85 (qd, *J* = 10.8, 7.1 Hz, 1 H), 3.67 (qd, *J* = 10.8, 7.2 Hz, 1 H), 3.47 (d, *J* = 17.0 Hz, 1 H), 2.25 (s, 3 H), 1.21 (t, *J* = 7.1 Hz, 3 H), 1.01 (t, *J* = 7.2 Hz, 3 H). ^{13}C NMR (101MHz ,CHLOROFORM-d) δ ppm = 171.7 (C), 168.9 (C), 139.6 (C), 139.6 (C), 139.2 (C), 139.1 (C), 136.9 (C), 129.1 (2 X CH), 128.9 (C), 128.1 (2 X CH), 127.1 (CH), 125.1 (CH), 121.9 (CH), 115.3 (CH), 66.6 (C), 61.9 (CH_2), 61.3 (CH_2), 54.9 (CH), 38.9 (CH_2), 15.9

(CH_3), 14.0 (CH_3), 13.8 (CH_3). IR (neat, cm^{-1}): 2982, 1733; HRMS (EI) m/z calculated for $C_{24}H_{24}O_4S$ $[M]^+$: 408.1395, found: 408.1411. 61mg, 87% yield.

5.3 Supplemental Information Chapter 3

5.3.1 Compounds and supplemental information Chapter 3.2

(***GP5.3.1***) **General procedure for the formation of T3.2.1a, T3.3.1a-4a, T3.4.1a.**

Preparation of halogenated alkyl malonates and alkyl aryl ethers. To a flamed dried round-bottom flask under argon atmosphere was added NaH (1.01 equiv.; 60% in mineral oil), followed by dry THF (0.1-1.0 M). The suspension was cooled to 0^{o}C in an ice bath prior to the dropwise addition of diethyl malonate or the corresponding aryl phenols (1.00 equiv.). The reaction was allowed to stir for 30 minutes and in this time the solutions became transparent. The corresponding alkyl bromide or the substituted allyl bromide (0.90-3.00 equiv.) was then added and the reaction mixture was allowed to stir overnight at ambient temperature. After being judged complete by TLC, the resulting reaction mixture was quenched with a saturated aqueous solution of ammonium chloride. The aqueous mixture was extracted with DCM, dried with $MgSO_4$, and concentrated *in vacuo*. The crude product was further purified by column chromatography (2-20% EtOAc:Hex) and gave the desired product (**T3.2.1a, T3.3.1a-4a, T3.4.1a.**). Compounds **T3.3.1a-3a** were further purified by Kugelrohr distillation between 50-70°C.

(***GP5.3.2***) **General procedure for the formation of T3.3.5a-7a.**

Allyl, dimethylallyl, or propargyl amine (50.0mmol, 1.00 equiv.) was solvated in DCM (250 mL), to which Et_3N (3.00 equiv.) and 4-(dimethylamino)pyridine (DMAP, 0.05 equiv.) were added. The solution was cooled to 0°C using an ice bath and allowed to stir for 15 minutes at which time *p*-toluenesulfonyl chloride was added (1.10 equiv.) in several portions. The reaction was allowed to stir overnight and subsequently quenched by a saturated aqueous solution of ammonium chloride when deemed complete by TLC. The aqueous mixture was extracted with

DCM, dried with $MgSO_4$, and concentrated *in vacuo*. The crude product was further purified by column chromatography (25% EtOAc:Hex). The resulting N-tosyl-N-allyl or N-propargyl amine was then submitted to Hassner's conditions[107] to yield the corresponding N-tosyl-N-allyl-N-alkyl bromide or N-tosyl-N-propargyl-N-alkyl bromide.

(***GP5.3.3***) **General procedure for the formation of T3.2.1b, T3.3.1b-7b, T3.4.1b-6b, 3.2.3, 3.2.5, 3.3.4.** (**Photocatalyzed Cyclization/Reduction/Addition).**

To an oven-dried 8 mL pyrex screw-top reaction vessel was added $[Au_2(m\text{-}dppm)_2][X]_2$ (1.0-5.0 mol%), the corresponding alkyl or aryl bromide (0.2-0.4 mmol, 1.00 equiv.), acetonitrile (2-3 mL), base (2.00-5.00 equiv.) (Procedure A), formic acid additive if necessary (2.00-6.13 equiv.) (Procedure B), and degassed under argon by sparging. The reaction mixtures were then placed under sunlight or in a UVA photoreactor for 2-24 hours. After few hours of irradiation, the solution becomes dark yellow, red, or brown. Upon reaction completion, the resulting mixture was concentrated *in vacuo*, and the crude mixture was purified by flash chromatography (1-25% EtOAc:Hex) to yield the final product.

(GP5.3.4) **General procedure for the formation of $[Au_2(\mu\text{-}dppm)_2][X]_2$ (F3.1.1 $[X]_2$)**

Commercially available (chloro(dimethylsulfide)gold(I)) was obtained from Glove-box under argon atmosphere (0.34-2.58 mmol, 1.00 equiv.) and placed in solution with DCM under argon at room temperature. To this solution the bis(diphenylphosphino)methane ligand (dppm, 1.00 eq) was added and allowed to stir for 1 hours. After this time, the solution was concentrated *in vacuo* and the complex was precipitated out by the addition of ether. The white powder was isolated and washed by filtration using ether, yields ranging from 40-85%. *Complexes **F3.1.1 $[OTf]_2$, $[BTf_2]_2$, $[BF_4]_2$** and **$[SbF_6]_2$** were obtained from $[Au_2(\mu\text{-}dppm)_2][Cl]_2$ by solvation of the

complex (0.08-0.16 mmol) in DCM (2 mL) and adding the corresponding silver salt, AgX (0.16-0.32 mmol, 2 equiv.) to the solution (X = OTf, NTf_2, BF_4, and SbF_6). After 1 h the solutions were concentrated *in vacuo* and the complexes were precipitated out by the addition of ether. The white powders were isolated and washed by filtration using ether.

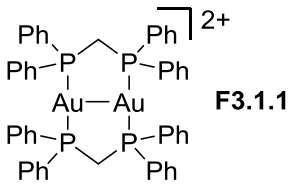

F3.1.1

F3.1.1 [Cl]$_2$: ^{1}H NMR (400MHz, DMSO-d_6): δ ppm = 7.98-7.82 (m, 16 H), 7.49 (t, *J* = 7.33 Hz, 8 H), 7.41 (t, *J* = 7.46 Hz, 16 H), 4.95 (m, 4 H). ^{13}C NMR (101MHz, DMSO-d_6): δ ppm = 134.80-132.04 (m, 16 C), 131.97 (s, 8 X C), 129.02 (s, 16 X C), 128.34 (td, *J* = 30.05, 15.08 Hz, 8 X C), 27.30 (dd, *J* = 30.08, 14.80 Hz, 2 X C). ^{31}P NMR (121MHz, CHLOROFORM-d) δ ppm = 33.28 (s, 4 X P). *^{31}PNMR was standardized using 85% phosphoric acid as reference. IR (neat, cm^{-1}): 1485, 1434, 1266, 1188, 1099, 783, 725, 678. HRMS calculated for $C_{50}H_{44}Au_2P_4Cl$ [M – Cl]: 1197.1413, found: 1197.1451. *(characterized by Guillaume Revol)*

F3.1.1[OTf]$_2$: ^{1}H NMR (400MHz, CHLOROFORM-d): δ ppm = 7.75-7.63 (m, 16 H), 7.45-7.34 (m, 24 H), 4.50 (4 H). ^{13}C NMR (101MHz, CHLOROFORM-d): δ ppm = 133.70 (dd, *J* = 4.20, 3.68 Hz), 132.52, 129.77 (td, *J* = 5.67, 2.95 Hz), 126.59 (m). ^{31}P NMR (121MHz, DMSO-d_6) δ ppm = 36.83 (s, 4 X P). *^{31}PNMR was standardized using 85% phosphoric acid as reference. IR (neat, cm^{-1}): 1436, 1350, 1257, 1188, 1157, 1103, 1029, 740, 690, 636.HRMS calculated for $C_{51}H_{44}Au_2P_4SO_3F_3$ [M – OTf]: 1311.1245, found: 1311.1226. *(characterized by Guillaume Revol)*

F3.1.1[NTF$_2$]$_2$: ^{1}H NMR (400MHz, DMSO-d_6): δ ppm = 7.99-7.78 (m, 16 H), 7.54 (t, *J* = 7.25 Hz, 8 H), 7.46 (t, *J* = 7.42 Hz, 16 H), 4.99 (td, *J* = 9.98, 5.17 Hz, 4 H).^{13}C NMR (101MHz,

DMSO-d_6): δ ppm = 133.71-133.09 (m), 132.33 (s), 129.46-129.01 (m), 127.90 (m). ^{31}P NMR (121 MHz, DMSO-d_6) δ ppm = 36.01 (s, 4 X P). *^{31}PNMR was standardized using 85% phosphoric acid as reference. IR (neat, cm^{-1}): 1436, 1346, 1180, 1134, 1049 (bs), 736, 673. HRMS calc. for $C_{52}H_{44}Au_2P_4NS_2O_4F_6$ [M – NTf_2]: 1442.0897, found: 1442.0693. *(characterized by Guillaume Revol)*

F3.1.1 $[BF_4]_2$: ^{1}H NMR (400MHz, DMSO-d_6): δ ppm = 7.99-7.80 (m, 16 H), 7.55 (t, *J* = 7.29 Hz, 8 H), 7.47 (t, *J* = 7.45 Hz, 16 H), 5.01 (td, *J* = 10.51, 5.29 Hz, 4 H). ^{13}C NMR (101MHz, DMSO-d_6) δ ppm = 133.86-133.20 (m), 132.45, 129.49-129.13 (m), 127.78 (td, *J* = 31.63, 15.88 Hz,1C). ^{31}P NMR (121MHz, DMSO-d_6) δ ppm = 36.57 (s, 4 X P). *^{31}PNMR was standardized using 85% phosphoric acid as reference. IR (neat, cm^{-1}): 1701, 1434, 1365, 1099, 1053 (bs), 786, 686.HRMS calculated for $C_{50}H_{44}Au_2P_4BF_4$ [M – BF_4]: 1249.1763, found: 1249.1744. *(characterized by Guillaume Revol)*

F3.1.1 $[SbF_6]_2$: ^{1}H NMR (400MHz, DMSO-d_6) δ ppm = 7.88 (m, 16 H), 7.54 (t, *J* = 7.28 Hz, 8 H), 7.46 (t, *J* = 7.42 Hz, 16 H), 4.99 (m, 4 H). ^{13}C NMR (400MHz, DMSO-d_6) δ ppm = 139.03-138.52 (m), 137.67 (s), 134.94-134.15 (m), 133.23 (m). ^{31}P NMR (121MHz, DMSO-d_6) δ ppm = 36.27 (s, 4 P). *^{31}PNMR was standardized using 85% phosphoric acid as reference. IR (neat, cm^{-1}): 1438, 1360 (bs), 1191, 1103, 1056 (bs), 732 (bs), 702 (bs). HRMS calculated for $C_{50}H_{44}Au_2P_4SbF_6$ [M – SbF_6]: 1397.0668, found: 1397.0687. *(characterized by Guillaume Revol)*

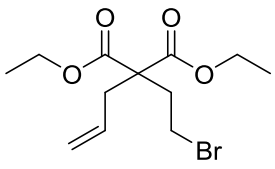

T3.2.1a: Diethyl (+/-)-(2-bromoethyl)(2-propenyl)propanedioate

Synthesized according to ***GP5.3.1*** and spectral data was consistent with literature.[108]

^{1}H NMR (400MHz, CHLOROFORM-d) δ ppm = 5.73 - 5.58 (m, 1 H), 5.21 - 5.11 (m, 2 H), 4.21 (qd, *J* = 7.2, 0.7 Hz, 4 H), 3.37 (t, *J* = 8.2 Hz, 2 H), 2.67 (d, *J* = 7.3 Hz, 2 H), 2.45 (t, *J* = 8.3 Hz, 2 H), 1.27 ppm (t, *J* = 7.1 Hz, 6 H), ^{13}C NMR (101MHz, CHLOROFORM-d) δ ppm = 170.2 (2 X C), 131.8 (CH), 119.7 (CH_2), 61.6 (2 X CH_2), 57.5 (C), 37.7 (CH_2), 36.2 (CH_2), 27.1 (CH_2), 14.0 (2 X CH_3).

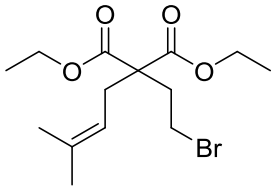

T3.3.1a: Diethyl (+/-)-(2-bromoethyl)(2-prenyl)propanedioate

Synthesized according to ***GP5.3.1***.

^{1}H NMR (400MHz, CHLOROFORM-d) δ ppm = 4.95 (tquin, *J* = 7.4, 1.4 Hz, 1 H), 4.20 (q, *J* = 7.2 Hz, 4 H), 3.38 - 3.30 (m, 2 H), 2.62 (d, *J* = 7.5 Hz, 2 H), 2.47 - 2.39 (m, 2 H), 1.70 (d, *J* = 1.0 Hz, 3 H), 1.63 (s, 3 H), 1.26 (t, *J* = 7.2 Hz, 6 H). ^{13}C NMR (101MHz, CHLOROFORM-d) δ ppm = 170.6 (2 X C), 136.2 (C), 117.1 (CH), 61.5 (2 X CH_2), 57.7 (C), 36.2 (CH_2), 31.9 (CH_2), 27.4 (CH_2), 26.0 (CH_3), 17.9 (CH_3), 14.0 (2 X CH_3). IR (neat, cm^{-1}): 2995 (m), 2927 (m), 2359 (m), 1728 (s), 1445 (m), 1367 (s), 1180 (s). HRMS (EI) m/z calculated for $C_{14}H_{23}O_4Br$ $[M]^+$: 334.0780, found: 334.0737. *(characterized by Terry McCallum)*

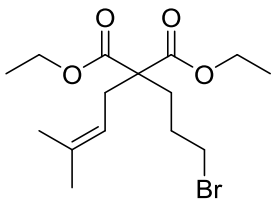

T3.3.2a: Diethyl (+/-)-(2-bromopropyl)(2-prenyl)propanedioate

Synthesized according to ***GP5.3.1***.

^{1}H NMR (400MHz, CHLOROFORM-d) δ ppm = 4.96 (tquin, *J* = 7.4, 1.5 Hz, 1 H), 4.18 (qd, *J* = 7.3, 2.1 Hz, 4 H), 3.38 (t, *J* = 6.6 Hz, 2 H), 2.61 (d, *J* = 7.4 Hz, 2 H),

1.93 - 2.04 (m, 2 H), 1.72 - 1.83 (m, 2 H), 1.70 (d, *J* = 1.1 Hz, 3 H), 1.62 (d, *J* = 0.7 Hz, 3 H), 1.25 (t, *J* = 7.2 Hz, 6 H). ^{13}C NMR (101MHz, CHLOROFORM-d) δ ppm = 171.3 (2 X C), 135.7 (C), 117.4 (CH), 61.2 (2 X CH_2), 57.1 (C), 33.3 (CH_2), 31.3 (CH_2), 31.0 (CH_2), 27.7 (CH_2), 26.0 (CH_3), 18.0 (CH_3), 14.1 (2 X CH_3) IR (neat, cm^{-1}): 2978 (m), 2920 (m), 1724 (s), 1447 (m), 1366 (s), 1235 (s). HRMS (EI) m/z calculated for $C_{15}H_{25}O_4Br$ $[M]^+$: 348.0936, found: 348.0954.

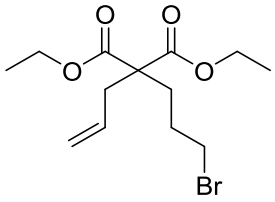

<u>T3.3.3a</u>: Diethyl (+/-)-(2-bromopropyl)(2-propenyl)propanedioate

Synthesized according to ***GP5.3.1***.

^{1}H NMR (400MHz, CHLOROFORM-d) δ ppm = 5.65 (ddt, *J* = 17.1, 9.9, 7.5 Hz, 1 H), 5.17 - 5.06 (m, 2 H), 4.20 (q, *J* = 7.1 Hz, 4 H), 3.39 (t, *J* = 6.5 Hz, 2 H), 2.65 (d, *J* = 7.4 Hz, 2 H), 2.06 - 1.95 (m, 2 H), 1.85 - 1.74 (m, 2 H), 1.26 (t, *J* = 7.1 Hz, 6 H), ^{13}C NMR (101MHz, CHLOROFORM-d) δ ppm = 170.9 (2 X C), 132.1 (CH), 119.2 (CH_2), 61.4 (2 X CH_2), 56.8 (C), 37.1 (CH_2), 33.2 (CH_2), 31.0 (CH_2), 27.5 (CH_2), 14.1 (2 X CH_3). IR (neat, cm^{-1}): 2978 (m), 1724 (s), 1447 (m), 1366 (s), 1230 (s). HRMS (EI) m/z calculated for $C_{13}H_{21}O_4Br$ $[M]^+$: 320.0623, found: 320.0599. *(characterized by Terry McCallum)*

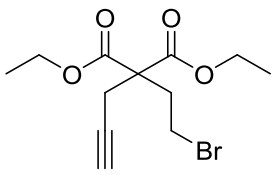

<u>T3.3.4a</u>: Diethyl (+/-)-(2-bromoethyl)(2-propynyl)propanedioate

Synthesized according to ***GP5.3.1.***

^{1}H NMR (400MHz, CHLOROFORM-d) δ ppm = 4.23 (qd, *J* = 7.1, 3.1 Hz, 4 H), 3.35 - 3.45 (m, 2 H), 2.85 (d, *J* = 2.7 Hz, 2 H), 2.61 - 2.69 (m, 2 H), 2.06 (t, *J* = 2.7 Hz, 1 H), 1.28 (t, *J* = 7.2 Hz, 6 H), ^{13}C NMR (101MHz, CHLOROFORM-d) δ ppm = 169.3 (2 X C), 78.2 (C), 72.0 (CH), 62.0 (2 X CH_2), 56.7 (C), 35.7 (CH_2), 26.9 (CH_2), 23.3 (CH_2), 14.0 (2 X

CH_3). IR (neat, cm^{-1}): 3290 (s), 2982 (m), 2357 (w), 1724 (s), 1447 (m), 1369 (s), 1196 (s). HRMS (EI) m/z calculated for $C_{12}H_{17}O_4Br$ $[M]^+$: 304.0310, found: 304.0298

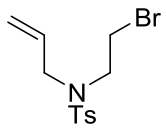

T3.3.5a: ***N*-Allyl-*N*-(2-bromoethyl)-4-methylbenzenesulfonamide**

Synthesized according to ***GP5.3.2*** and spectral data was consistent with literature.[109] ^1H NMR (400MHz, CHLOROFORM-d) δ ppm = 7.72 (dt, *J* = 8.2, 1.9 Hz, 2 H), 7.33 (dd, *J* = 8.5, 0.7 Hz, 2 H), 5.58 - 5.77 (m, 1 H), 5.22 (dq, *J* = 6.3, 1.3 Hz, 1 H), 5.19 (t, *J* = 1.3 Hz, 1 H), 3.82 (dt, *J* = 6.5, 1.2 Hz, 2 H), 3.37 - 3.53 (m, 4 H), 2.45 (s, 3 H). ^{13}C NMR (101MHZ, CHLOROFORM-d) δ ppm = 143.7 (C), 136.3 (C), 132.9 (CH), 129.9 (2 X CH), 127.2 (2 X CH), 119.7 (CH_2), 52.0 (CH_2), 48.9 (CH_2), 29.2 (CH_2), 21.5 (CH_3). *(characterized by Terry McCallum)*

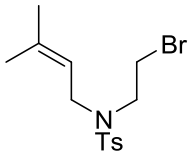

T3.3.6a: ***N*-(3-methyl-but-2-en-1-yl)-*N*-(2-bromoethyl)-4-methylbenzene sulfonamide**

Synthesized according to ***GP5.3.2***.

^1H NMR (400MHz, CHLOROFORM-d) δ ppm = 7.66 - 7.75 (m, 2 H), 7.28 - 7.36 (m, *J* = 7.9 Hz, 2 H), 5.03 (tquin, *J* = 7.3, 1.5 Hz, 1 H), 3.81 (d, *J* = 7.2 Hz, 2 H), 3.36 - 3.49 (m, 4 H), 2.44 (s, 3 H), 1.70 (d, *J* = 0.9 Hz, 3 H), 1.64 (s, 3 H). ^{13}C NMR (101MHz, CHLOROFORM-d) δ ppm = 143.5 (C), 138.1 (C), 136.5 (C), 129.7 (2 X CH), 127.2 (2 X CH), 118.6 (CH), 48.9 (CH_2), 46.7 (CH_2), 29.6 (CH_2), 25.8 (CH_3), 21.5 (CH_3), 17.8 (CH_3). IR (neat, cm^{-1}): 2913 (s), (m), 2368 (w), 1597 (s), 1447 (m), 1339 (s), 1153 (s). HRMS (EI) m/z calculated for $C_{12}H_{17}O_4Br$ $[M]^+$: 345.0398, found: 345.0419. *(characterized by Terry McCallum)*

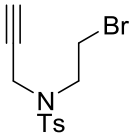

T3.3.7a: ***N*-(2-bromoethyl)-4-methyl-*N*-(prop-2-yn-1-yl)benzenesulfonamide**

Synthesized according to ***GP5.3.2*** and spectral data was consistent with literature.[109] ^{1}H NMR (400MHz, CHLOROFORM-d) δ ppm = 7.74 (dt, *J* = 8.3, 1.9 Hz, 2 H), 7.32 (dd, *J* = 8.5, 0.6 Hz, 2 H), 4.18 (d, *J* = 2.4 Hz, 2 H), 3.49 - 3.62 (m, 4 H), 2.44 (s, 3 H), 2.12 (t, *J* = 2.5 Hz, 1 H), ^{13}C NMR (101MHz, CHLOROFORM-d) δ ppm = 144.0 (C), 135.4 (C), 129.7 (2 X CH), 127.6 (2 X CH), 76.6 (C), 74.2 (CH), 48.3 (CH_2), 37.9 (CH_2), 29.0 (CH_2), 21.5 (CH_3). *(characterized by Terry McCallum)*

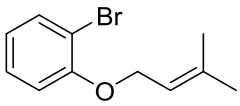

T3.4.1a: **2-bromophenyl 3-methyl-2-propenyl ether (21)**

Synthesized according to ***GP5.3.1*** and spectral data was consistent with literature.[110]

^{1}H NMR (400MHZ, CHLOROFORM-d) δ ppm = 7.54 (dd, *J* = 7.8, 1.6 Hz, 1 H), 7.25 (ddd, *J* = 8.2, 7.5, 1.8 Hz, 1 H), 6.92 (dd, *J* = 8.3, 1.3 Hz, 1 H), 6.83 (td, *J* = 7.6, 1.2 Hz, 1 H), 5.52 (tquin, *J* = 6.5, 1.3 Hz, 1 H), 4.61 (d, *J* = 6.7 Hz, 2 H), 1.80 (s, 3 H), 1.76 (s, 3 H), ^{13}C NMR (101MHz, CHLOROFORM-d) δ ppm = 155.2 (C), 138.1 (C), 133.3 (CH), 128.3 (CH), 121.7 (CH), 119.4 (CH), 113.7 (CH), 112.4 (C), 66.1 (CH_2), 25.8 (CH_3), 18.3 (CH_3). *(characterized by Terry McCallum)*

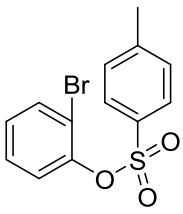

T3.4.2a: **2-bromophenyl 4-methylbenzenesulfonate**

Synthesized by standard tosylation procedure using White's method[111] and spectral data was consistent with literature.[112]

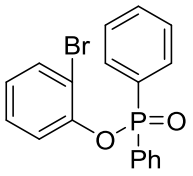

T3.4.3a: 2-bromophenyl diphenylphosphinate

Synthesized using Heller's method for phosphonation starting from 2-bromophenol.[113]

^{1}H NMR (400MHz, CHLOROFORM-d) δ ppm = 7.94 - 8.01 (m, 23 H), 7.91 - 8.06 (m, 4 H), 7.60 (dt, *J* = 8.2, 1.4 Hz, 6 H), 7.40 - 7.55 (m, 7 H), 7.14 (ddd, *J* = 8.2, 7.5, 1.7 Hz, 1 H), 6.92 (td, *J* = 7.7, 1.2 Hz, 1 H). ^{13}C NMR (101MHz, CHLOROFORM-d) δ ppm = 148.4 (d, $J_{(C-P)}$=7.34 Hz, C), 133.5 (CH), 132.6 (d, $J_{(C-P)}$=2.94 Hz, 2 X CH), 131.9 (d, $J_{(C-P)}$=10.64 Hz, 4 X CH), 130.6 (d, $J_{(C-P)}$=138.65 Hz, 2 X C), 128.6 (CH), 128.6 (d, $J_{(C-P)}$=13.57 Hz, 4 X CH), 125.55 (CH), 121.6 (d, $J_{(C-P)}$=4.03 Hz, CH), 114.3 (d, $J_{(C-P)}$=7.34 Hz, C). IR (neat, cm^{-1}): 3075 (w), 2920 (w), 1710 (br), 1591, 1478 (s), 1438 (s), 1219 (br), 1125 (s), 917, 724. HRMS (EI) m/z calculated for $C_{18}H_{14}BrO_2P$ $[M]^+$: 371.9915, found: 371.9908.

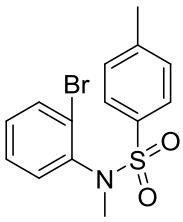

T3.4.4a: *N*-(2-bromophenyl)-*N*-methyl-*p*-toluenesulfonamide

Synthesized according to Hiroi's method and spectral data was consistent with literature.[114]

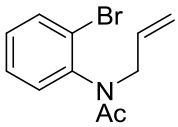

T3.4.5a: *N*-allyl-N-(2-bromophenyl)acetamide

To a mixture of 2-bromoaniline (3.20 mmol, 1.00 eq) and DMAP (0.16 mmol, 0.05 eq) solvated in DCM (25 mL), was added acetic anhydride (3.2 mmol, 1.00 eq). The reaction was allowed to stir for 2 h, and was quenched with a saturated aqueous solution of ammonium chloride when judged complete by TLC. The mixture washed with DCM, the organic fractions were combined and the solvent evaporated *in vacuo*. The crude product was then isolated by column chromatography (30% EtOAc:Hex). The resulting N-Acetyl-2-bromo-aniline

was isolated as an off-yellow solid in quantitative yield. The resulting material was then submitted to Hassner's conditions[107] to yield the corresponding N-Acetyl-N-allylbromoaniline as yellow oil (87%). Spectral data was consistent with literature.[115]

^{1}H NMR (400MHz, CHLOROFORM-d) δ ppm = 7.70 (dd, *J* = 8.0, 1.3 Hz, 1 H), 7.37 (td, *J* = 7.5, 1.5 Hz, 1 H), 7.19 - 7.27 (m, 2 H), 5.84 - 5.94 (m, 1 H), 5.10 (dq, *J* = 10.1, 1.2 Hz, 1 H), 5.06 (dq, *J* = 17.0, 1.4 Hz, 1 H), 4.78 (ddt, *J* = 14.7, 5.6, 1.3 Hz, 1 H), 3.73 (dd, *J* = 14.7, 7.6 Hz, 1 H), 1.82 (s, 3 H). ^{13}C NMR (101MHz, CHLOROFORM-d) δ ppm = 170.1 (C), 141.4 (C), 133.8 (CH), 132.8 (CH), 131.1 (CH), 129.7 (CH), 128.5 (CH), 123.9 (C), 118.5 (CH_2), 50.9 (CH_2), 22.4 (CH_3).

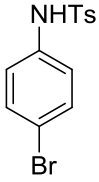

T3.4.6a: ***N*-(4-bromo-phenyl)-4-methyl-benzenesulfonamide**

To a mixture of 4-bromoaniline (4.65 mmol, 1.00 eq) and pyridine (14.0 mmol, 3.00 eq) solvated in DCM (30 mL), was added Tosyl chloride (5.12 mmol, 1.1 eq) in portions. The reaction was allowed to stir for 2 h and was quenched with a saturated aqueous solution of ammonium chloride when judged complete by TLC. The mixture was washed with DCM and the organic fractions were combined and the solvent evaporated *in vacuo*. The crude product was then isolated by column chromatography (30% EtOAc:Hex). The resulting N-tosyl-4-bromo-aniline was isolated as an off-yellow powder in quantitative yield. Spectral data was consistent with literature.[116]

^{1}H NMR (300MHz, CHLOROFORM-d) δ ppm = 7.58 - 7.70 (m, 2 H), 7.32 - 7.41 (m, 2 H), 7.25 (dd, *J* = 8.6, 0.6 Hz, 2 H), 6.91 - 7.05 (m, 2 H), 6.82 (br. s., 1 H), 2.40 (s, 3 H).

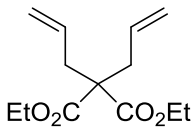

3.2.2: **α,α-diallyl-malonic acid diethyl ester**

Allyl malonate isolated from ***GP5.3.1*** underwent another round of alkylation with allyl bromide to give pure diallylated product. Spectral data was consistent with literature.[117]

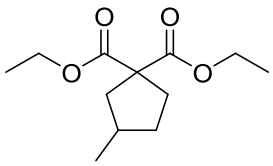

<u>T3.2.1b:</u> 3-methyl-cyclopentane-1,1-dicarboxylic acid diethyl ester

Synthesized according to ***GP5.3.3***.

^{1}H NMR (400MHz, CHLOROFORM-d) δ ppm = 4.17 (q, *J* = 7.1 Hz, 4 H), 2.44 (dd, *J* = 13.2, 7.1 Hz, 1 H), 2.36 - 2.26 (m, 1 H), 2.19 - 2.08 (m, 1 H), 2.08 - 1.98 (m, 1 H), 1.90 - 1.78 (m, 1 H), 1.66 (dd, *J* = 13.4, 10.0 Hz, 2 H), 1.24 (t, *J* = 7.1 Hz, 6 H), 1.01 (d, *J* = 6.7 Hz, 3 H). ^{13}C NMR (101MHz, CHLOROFORM-d) δ ppm = 172.8 (2 X C), 61.2 (2 X CH_2), 60.3 (C), 42.5 (CH_2), 34.4 (CH), 34.1 (CH_2), 34.0 (CH_2), 19.6 (CH_3), 14.0 (2 X CH_3). IR (neat, cm^{-1}): 2955 (m), 1724 (s), 1447 (m), 1366 (s), 1254 (s). HRMS (EI) m/z calculated for $C_{12}H_{20}O_4$ $[M]^+$: 228.1362, found: 228.1320.

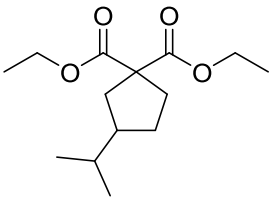

<u>T3.3.1b:</u> 3-isopropyl-cyclopentane-1,1-dicarboxylic acid diethyl ester

Synthesized according to ***GP5.3.3***.

^{1}H NMR (400MHz, CHLOROFORM-d) δ ppm = 4.18 (qd, *J* = 7.0, 2.6 Hz, 4 H), 2.39 - 2.46 (m, 1 H), 2.28 (ddd, *J* = 13.5, 8.7, 3.3 Hz, 1 H), 2.08 - 2.18 (m, 1 H), 1.80 - 1.91 (m, 1 H), 1.71 - 1.79 (m, 1 H), 1.65 - 1.69 (m, 1 H), 1.37 - 1.47 (m, 1 H), 1.28 - 1.36 (m, 1 H), 1.25 (td, *J* = 6.9, 0.9 Hz, 6 H), 0.90 (dd, *J* = 7.9, 6.9 Hz, 6 H). ^{13}C NMR (101MHz, CHLOROFORM-d) δ ppm = 172.8 (C), 172.8 (C), 61.2 (2 X CH_2), 60.0 (C), 47.3 (CH), 39.1 (CH_2), 33.9 (CH_2), 33.2 (CH), 30.3 (CH_2), 21.5 (CH_3), 21.4 (CH_3), 14.0 (2 X CH_3). IR (neat, cm^{-1}): 2870 (m), 1724 (s), 1462 (m), 1447 (m), 1366 (s), 1250 (s). HRMS (EI)

m/z calculated for $C_{14}H_{24}O_4$ $[M]^+$: 256.1675, found: 256.1704. *(characterized by Terry McCallum)*

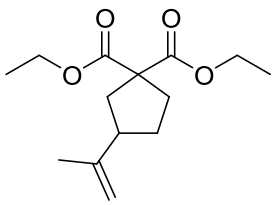

<u>T3.3.1c:</u> 3-isopropenyl-cyclopentane-1,1-dicarboxylic acid diethyl ester

Synthesized according to ***GP5.3.3.***

^{1}H NMR (400MHz, CHLOROFORM-d) δ ppm = 4.73 (dd, *J* = 6.9, 0.7 Hz, 2 H), 4.19 (qd, *J* = 7.3, 2.9 Hz, 4 H), 2.52 - 2.61 (m, 1 H), 2.48 (ddd, *J* = 13.0, 7.0, 1.5 Hz, 1 H), 2.36 (ddd, *J* = 13.6, 8.7, 3.2 Hz, 1 H), 2.14 - 2.23 (m, 1 H), 1.99 (dd, *J* = 13.1, 11.0 Hz, 1 H), 1.85 - 1.94 (m, 1 H), 1.74 (s, 3 H), 1.52 - 1.57 (m, 1 H), 1.25 (td, *J* = 7.1, 2.1 Hz, 6 H). ^{13}C NMR (101MHz, CHLOROFORM-d) δ ppm = 172.7 (C), 172.6 (C), 146.7 (C), 109.3 (CH_2), 61.3 (2 X CH_2), 59.7 (C), 46.4 (CH), 38.9 (CH_2), 33.6 (CH_2), 30.7 (CH_2), 21.1 (CH_3), 14.0 (2 X CH_3). IR (neat, cm^{-1}): 2959 (m) (alkene), 2870 (m), 1724 (s), 1462 (m), 1447 (m), 1366 (s), 1250 (s). HRMS (EI) m/z calculated for $C_{14}H_{22}O_4$ $[M]^+$: 254.1518, found: 254.1495. *(characterized by Terry McCallum)*

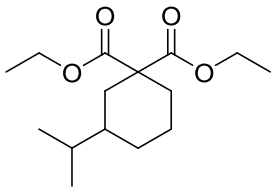

<u>T3.3.2b:</u> 3-isopropyl-cyclohexane-1,1-dicarboxylic acid diethyl ester

Synthesized according to ***GP5.3.3***.

^{1}H NMR (400MHz, CHLOROFORM-d) δ ppm = 4.16 (q, *J* = 7.3 Hz, 3 H), 2.30 - 2.37 (m, 2 H), 1.59 - 1.78 (m, 4 H), 1.50 - 1.56 (m, 1 H), 1.30 - 1.49 (m, 4 H), 1.24 (t, *J* = 7.1 Hz, 6 H), 0.88 (dd, *J* = 6.6, 3.2 Hz, 6 H). ^{13}C NMR (101MHz, CHLOROFORM-d) δ ppm = 172.9 (C), 171.3 (C), 61.2 (CH_2), 60.9 (CH_2), 55.5 (C), 40.0 (CH), 34.5 (CH_2), 32.7 (CH), 31.3 (CH_2), 28.6 (CH_2), 22.9 (CH_2), 19.5 (CH_3), 19.4 (CH_3), 14.1 (CH_3), 14.0 (CH_3). IR (neat,

cm^{-1}): 2839 (m), 1724 (s), 1462 (m), 1447 (m), 1366 (s), 1242 (s). HRMS (EI) m/z calculated for $C_{15}H_{26}O_4$ $[M]^+$: 270.1831, found: 270.1835.

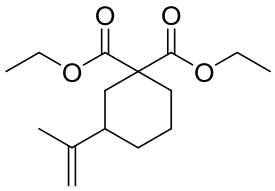

<u>T3.3.2c:</u> 3-isopropenyl-cyclohexane-1,1-dicarboxylic acid diethyl ester

Synthesized according to ***GP5.3.3***.

^{1}H NMR (400MHz, CHLOROFORM-d) δ ppm = 4.69 - 4.74 (m, 2 H), 4.16 (q, *J* = 7.3 Hz, 4 H), 2.58 - 2.68 (m, 1 H), 2.37 - 2.44 (m, 2 H), 1.97 - 2.08 (m, 2 H), 1.76 - 1.82 (m, 2 H), 1.73 (s, 3 H), 1.40 - 1.47 (m, 2 H), 1.24 (t, *J* = 7.0 Hz, 6 H). ^{13}C NMR (101MHz, CHLOROFORM-d) δ ppm = 172.9 (C), 171.3 (C), 149.4 (C), 108.9 (CH_2), 61.3 (CH_2), 61.0 (CH_2), 55.4 (C), 41.1 (CH), 36.2 (CH_2), 31.6 (CH_2), 31.0 (CH_2), 30.5 (CH_2), 20.9 (CH_3), 14.1 (CH_3), 14.0 (CH_3). IR (neat, cm^{-1}): 2932 (m), 2839 (m), 1724 (s), 1462 (m), 1447 (m), 1366 (s), 1242 (s). HRMS (EI) m/z calculated for $C_{15}H_{24}O_4$ $[M]^+$: 268.1675, found: 268.1679. *(characterized by Terry McCallum)*

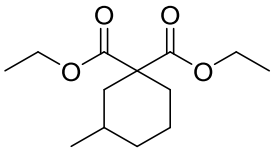

<u>T3.3.3b:</u> 3-methyl-cyclohexane-1,1-dicarboxylic acid diethyl ester

Synthesized according to ***GP5.3.3*** and spectral data was consistent with literature.[118]

^{1}H NMR (400MHz, CHLOROFORM-d) δ ppm = 4.11 - 4.25 (m, 4 H), 2.05 - 2.39 (m, 2 H), 1.61 - 1.74 (m, 2 H), 1.33 - 1.57 (m, 3 H), 1.17 - 1.32 (m, 8 H), 0.91 (d, *J* = 6.6 Hz, 3 H). ^{13}C NMR (101MHz, CHLOROFORM-d) δ ppm = 172.7 (C), 171.3 (C), 61.2 (CH_2), 60.9 (CH_2), 55.4 (C), 39.4 (CH_2), 34.0 (CH_2), 30.9 (CH_2), 28.9 (CH_3), 22.7 (CH_2), 22.5 (CH_3), 14.1 (CH_3), 14.0 (CH_3).

IR (neat, cm^{-1}): 2928 (m), 1724 (s), 1454 (m), 1366 (s), 1246 (s). HRMS (EI) m/z calculated for $C_{13}H_{22}O_4$ $[M]^+$: 242.1518, found: 242.1519.

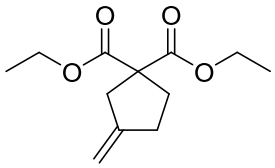

T3.3.4b: 3-methenyl-cyclopentane-1,1-dicarboxylic acid diethyl ester

Synthesized according to ***GP5.3.3*** and spectral data was consistent with literature.[119]

^1H NMR (400MHz, CHLOROFORM-d) δ ppm = 4.90 (dt, *J* = 13.2, 1.8 Hz, 2 H), 4.19 (q, *J* = 7.1 Hz, 4 H), 2.90 - 2.94 (m, 2 H), 2.43 (td, *J* = 7.5, 1.4 Hz, 2 H), 2.27 (t, *J* = 7.4 Hz, 2 H), 1.25 (t, *J* = 7.2 Hz, 6 H). ^{13}C NMR (101MHz, CHLOROFORM-d) δ ppm = 171.7 (2 X C), 148.5 (C), 106.8 (CH_2), 61.4 (2 X CH_2), 60.2 (C), 40.6 (CH_2), 33.7 (CH_2), 31.2 (CH_2), 14.0 (2 X CH_3). IR (neat, cm^{-1}): 2964 (m), 2357 (m), 1724 (s), 1435 (m), 1366 (s), 1265 (s). HRMS (EI) m/z calculated for $C_{12}H_{18}O_4$ $[M]^+$: 226.1205, found: 226.1182.

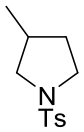

T3.3.5b: 3-methyl-1-tosylpyrrolidine

Synthesized according to ***GP5.3.3*** and spectral data was consistent with literature.[120]

^1H NMR (400MHz, CHLOROFORM-d) δ ppm = 7.72 (dt, *J* = 8.3, 1.7 Hz, 2 H), 7.33 (dd, *J* = 8.5, 0.6 Hz, 2 H), 3.43 (dd, *J* = 9.7, 7.2 Hz, 1 H), 3.32 - 3.39 (m, 1 H), 3.23 (ddd, *J* = 9.8, 8.2, 7.3 Hz, 1 H), 2.76 (dd, *J* = 9.7, 7.8 Hz, 1 H), 2.44 (s, 3 H), 2.05 - 2.18 (m, 1 H), 1.85 - 1.97 (m, 1 H), 1.36 (dd, *J* = 12.3, 8.4 Hz, 1 H), 0.93 (d, *J* = 6.7 Hz, 3 H). ^{13}C NMR (101MHz, CHLOROFORM-d) δ ppm = 143.2 (C), 134.0 (C), 129.6 (2 X CH), 127.5 (2 X CH), 54.7 (CH_2), 47.6 (CH_2), 33.3 (CH), 33.2 (CH_2), 21.5 (CH_3), 17.6 (CH_3). HRMS (EI) m/z calculated for $C_{12}H_{17}NO_2S$ $[M]^+$: 239.0980, found: 239.0954.

HRMS (EI) m/z calculated for $C_{12}H_{16}NO_2SD$ $[M]^+$: 240.1043, found: 240.0995 (4:1 H:D).

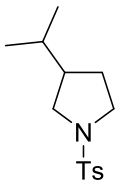

T3.3.6b: 3-isopropyl-1-tosylpyrrolidine

Synthesized according to ***GP5.3.3***.

^{1}H NMR (400MHz, CHLOROFORM-d) δ ppm = 7.72 (d, *J* = 8.2 Hz, 2 H), 7.33 (d, *J* = 8.4 Hz, 2 H), 3.34 - 3.54 (m, 2 H), 3.16 (td, *J* = 9.9, 6.8 Hz, 1 H), 2.79 (t, *J* = 9.7 Hz, 1 H), 2.44 (s, 3 H), 1.86 - 2.00 (m, 1 H), 1.54 - 1.65 (m, 1 H), 1.30 - 1.47 (m, 2 H), 0.85 (d, *J* = 6.7 Hz, 6 H). ^{13}C NMR (101MHz, CHLOROFORM-d) δ ppm = 143.2 (C), 134.0 (C), 129.6 (2 X CH), 127.5 (2 X CH), 52.1 (CH_2), 48.1 (CH_2), 46.4 (CH), 31.8 (CH), 30.0 (CH_2), 21.5 (CH_3), 21.3 (CH_3), 20.9 (CH_3). IR (neat, cm^{-1}): 2860 (br), 1345 (br), 1160 (br), 1070 (br), 1020 (br), 810 (s), 720(s), 660 (s). HRMS (EI) m/z calculated for $C_{14}H_{21}NO_2S$ $[M]^+$: 267.1293, found: 267.1292. *(characterized by Terry McCallum)*

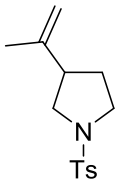

T3.3.6c: 3-isopropenyl-1-tosylpyrrolidine

Synthesized according to ***GP5.3.3.***

^{1}H NMR (400MHZ, CHLOROFORM-d) δ ppm = 7.73 (d, *J* = 8.2 Hz, 2 H), 7.34 (d, *J* = 8.0 Hz, 2 H), 4.74 (d, *J* = 1.0 Hz, 1 H), 4.64 (d, *J* = 1.0 Hz, 1 H), 3.50 (dd, *J* = 9.7, 7.6 Hz, 1 H), 3.35 - 3.47 (m, 1 H), 3.25 (td, *J* = 9.5, 6.8 Hz, 1 H), 3.02 (t, *J* = 9.5 Hz, 1 H), 2.62 (quin, *J* = 8.6 Hz, 1 H), 2.45 (s, 3 H), 1.87 - 2.00 (m, 1 H), 1.67 (s, 3 H), 1.60 - 1.75 (m, 1 H). ^{13}C NMR (101MHz, CHLOROFORM-d) δ ppm = 143.7 (C), 143.3 (C), 134.0 (C), 129.6 (2 X CH), 127.5 (2 X CH), 110.8 (CH_2), 51.5 (CH_2), 47.7 (CH_2), 45.1 (CH), 30.0 (CH_2), 21.5 (CH_3), 21.0 (CH_3). IR (neat, cm^{-1}): 2960 (br) (alkene), 2860 (br), 1345 (br), 1160 (br), 1070 (br), 1020 (br), 810 (s), 720(s), 660 (s). HRMS (EI) m/z calculated for $C_{14}H_{19}NO_2S$ $[M]^+$: 265.1136, found: 265.1140 *(characterized by Terry McCallum)*

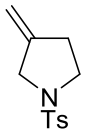

T3.3.7b: 3-methenyl-1-tosylpyrrolidine

Synthesized according to ***GP5.3.3*** and spectral data was consistent with literature.[120]

^{1}H NMR (400MHz, CHLOROFORM-d) δ ppm = 7.68 - 7.77 (m, 2 H), 7.30 - 7.41 (m, *J* = 7.9 Hz, 2 H), 4.85 - 4.97 (m, 2 H), 3.74 - 3.84 (m, 2 H), 3.29 (t, *J* = 7.1 Hz, 2 H), 2.46 - 2.53 (m, 2 H), 2.44 (s, 3 H), ^{13}C NMR (101MHz, CHLOROFORM-d) δ ppm = 144.1 (C), 143.6 (C), 132.7 (C), 129.7(2 X CH), 127.8 (2 X CH), 107.4 (CH_2), 51.9 (CH_2), 48.1 (CH_2), 31.7 (CH_2), 21.5 (CH_3).

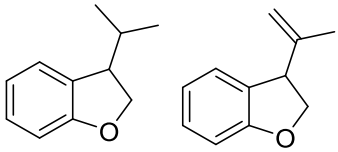

T3.4.1b/c : 2,3-dihydro-3-isopropylbenzofuran/3-(propen-2-yl)-2,3-dihydrobenzofuran

Synthesized according to ***GP5.3.3*** spectral data was consistent with literature.[121]

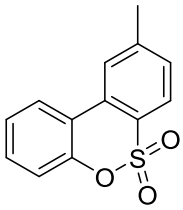

T3.4.2b: 9-methyldibenzo[c,e][1,2]oxathiine 6,6-dioxide

Synthesized according to ***GP5.3.3*** and spectral data was consistent with literature.[122]

^{1}H NMR (400MHz, CHLOROFORM-d) δ ppm = 7.91 (dd, *J* = 7.8, 1.6 Hz, 1 H), 7.86 (d, *J* = 8.0 Hz, 1 H), 7.72 (s, 1 H), 7.45 (dt, *J* = 7.7, 1.7 Hz, 1 H), 7.41 - 7.34 (m, 2 H), 7.31 (td, *J* = 8.1, 0.5 Hz, 1 H), 2.51 (s, 3 H). ^{13}C NMR (101MHz, CHLOROFORM-d) δ ppm = 149.9 (C), 144.7(C), 131.5(C), 131.1 (CH), 129.8 (CH), 129.6 (C), 126.6 (CH), 125.3 (CH), 125.1 (CH), 124.2 (CH), 121.6 (C), 120.0 (CH), 22.0 (CH_3). IR (neat, cm^{-1}): 2920 (br), 1480 (s), 1440 (s), 1360 (s), 1190

(br), 1080 (s), 900 (s), 860 (s), 790 (s), 750 (s), 680 (s). HRMS (EI) m/z calculated for $C_{13}H_{10}O_3S$ $[M]^+$: 246.0351, found: 246.0334.

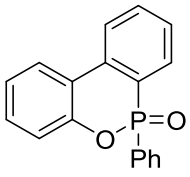

T3.4.3b: 10-phenyl-9-hydro-9-oxa-10-phosphaphenanthrene-10-oxide

Synthesized according to ***GP5.3.3.***

^{1}H NMR (400MHz, CHLOROFORM-d) δ ppm = 8.01 (dd, *J* = 8.1, 4.9 Hz, 6 H), 7.97 (dd, *J* = 7.9, 1.4 Hz, 1 H), 7.86 - 7.76 (m, 2 H), 7.66 (tt, *J* = 7.7, 1.1 Hz, 1 H), 7.62 - 7.51 (m, 2 H), 7.48 - 7.33 (m, 4 H), 7.29 - 7.10 (m, 2 H). ^{13}C NMR (101MHz, CHLOROFORM-d) δ ppm = 149.2 (d, *J* = 8.4Hz, C), 135.8 (d, *J* = 5.5Hz, C), 133.1 (d, *J* = 1.1Hz, CH), 133.1 (d, *J* = 1.8Hz, CH), 132.2 (d, *J* = 11.0Hz, 2 x CH), 131.0 (d, *J* = 12.1Hz, CH), 130.6 (s, CH), 129.6 (d, *J* =144.2Hz, C), 128.6 (d, *J* = 11.4Hz, 2 x CH), 128.3 (d, *J* = 13.9Hz, CH), 125.1 (s, CH), 125.0 (d, *J* =128.4, C), 124.6 (s, CH), 123.6 (d, *J* = 9.9Hz, CH), 122.0 (d, *J* = 11.4Hz, C), 120.7 (d, *J* = 6.2Hz, CH). IR (neat, cm^{-1}): 2350 9 (br), 1510 (s), 1240 (br), 1125 (br), 1125 (s), 910 (br), 750 (br). HRMS (EI) m/z calculated for $C_{18}H_{13}O_2P$ $[M]^+$: 292.0653, found: 292.0666.

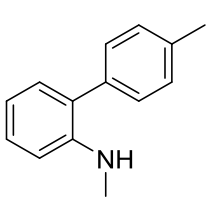

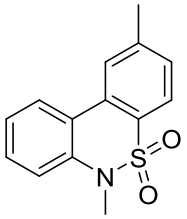

T3.4.4b/c: 2-methylamino-4′-methylbiphenyl / 2,6-dimethyl-6H-dibenzo[c,e][1,2]thiazine-5,5-dioxide

Synthesized according to ***GP5.3.3*** and spectral data was consistent with literature, affording product in comparable ratio (63:37 of **b**:**c**)[123]

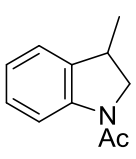

T3.4.5b: 3-methyl-1-(acetyl)indoline

Synthesized according to ***GP5.3.3*** and spectral data was consistent with literature.[124]

^{1}H NMR (400MHz, CHLOROFORM-d) δ ppm = 8.20 (d, *J* = 8.1 Hz, 1 H), 7.21 (t,

J = 7.9 Hz, 1 H), 7.17 (d, *J* = 7.4 Hz, 1 H), 7.05 (td, *J* = 7.4, 0.9 Hz, 1 H), 4.22 (t, *J* = 9.6 Hz, 1 H), 3.55 - 3.63 (m, 1 H), 3.47 - 3.55 (m, 1 H), 2.24 (s, 3 H), 1.37 (d, *J* = 6.9 Hz, 3 H).

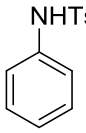

T3.4.6b: N-tosylanilide

Synthesized according to ***GP5.3.3*** and spectral data was consistent with literature.[120] ^{1}H NMR (400MHz, CHLOROFORM-d) δ ppm = 7.67 (d, *J* = 8.3 Hz, 2 H), 7.20 - 7.27 (m, 4 H), 7.12 (d, *J* = 7.4 Hz, 1 H), 7.06 - 7.10 (m, 2 H), 6.81 (br. s., 1 H), 2.38 ppm (s, 3 H), ^{13}C NMR (101MHz, CHLOROFORM-d) δ ppm = 143.9 (C), 136.5 (C), 136.0 (C), 129.6 (2 X CH), 129.3 (2 X CH), 127.2 (2 X CH), 125.3 (CH), 121.6 (2 X CH), 21.5 (CH_3).

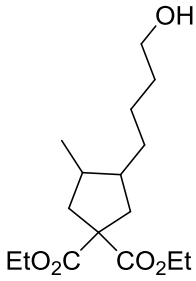

3.2.3: Diethyl 3-(4-hydroxybutyl)-4-methylcyclopentane-1,1-dicarboxylate (5:1 *cis:trans*)

Synthesized according to ***GP5.3.3***, using 3 equivalents of diallyl malonate **3.2.2** and 1 equivalent of 3-bromo-1-propanol **3.2.1**.

^{1}H NMR (400MHz, CHLOROFORM-d) δ ppm = 4.14 (dq, *J* = 7.1, 1.7 Hz, 4 H), 3.62 (t, *J* = 6.6 Hz, 2 H), 2.58 - 1.26 (m, 12 H), 1.21 (dt, *J* = 7.1, 1.0 Hz, 6 H), 0.95 (d, *J* = 6.4 Hz, 1 H[***trans***]), 0.81 (d, *J* = 7.2 Hz, 3 H [***cis***]). ^{13}C NMR (101MHz, CHLOROFORM-d) δ ppm = 173.2 C(), 173.1 (C), 62.9 (CH_2), 61.3 (2 X CH_2), 58.9 (C), 42.7 (CH), 41.4 (CH_2), 38.3 (CH_2), 35.8 (CH), 33.0 (CH_2), 29.3 (CH_2), 24.5 (CH_2) , 14.8 (CH_3), 14.0 (2 X CH_3). IR (neat, cm^{-1}): 2920 (br), 2350 (s), 1720 (s), 1430 (s), 1370 (br), 1250 (br), 1160 9br. HRMS (EI) m/z calculated for $C_{13}H_{23}O_3$ [M – CO_2Et]: 227.1647, found: 227.1649.

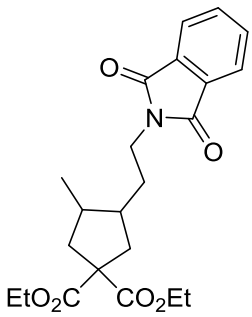

<u>3.2.5:</u> Diethyl-3-(2-(1,3-dioxoisoindolin-2-yl) ethyl)-4-methylcyclopentane -1,1-dicarboxylate (5:1 *cis:trans*)

Synthesized according to ***GP5.3.3***, using 3 equivalents of diallyl malonate **3.2.2** and 1 equivalent of N-chlorophthalimide **3.2.4**.

^{1}H NMR (400MHz, CHLOROFORM-d) δ ppm = 7.81 (dd, *J* = 5.5, 3.0 Hz, 2 H), 7.68 (dd, *J* = 5.4, 3.0 Hz, 2 H), 4.15 (qd, *J* = 8.1, 7.2 Hz, 4 H), 3.66 (t, *J* = 7.5 Hz, 2 H), 2.40 (td, *J* = 13.7, 6.9 Hz, 2 H), 2.22 (td, *J* = 11.5, 6.9 Hz, 1 H), 2.12 - 1.87 (m, 3 H), 1.77 - 1.65 (m, 1 H), 1.64 - 1.51 (m, 1 H), 1.21 (dt, *J* = 3.6, 7.1 Hz, 6 H), 0.95 (d, *J* = 6.3 Hz, 3 H[***trans***]), 0.85 (d, *J* = 7.2 Hz, 3 H[***cis***]). ^{13}C NMR (101MHz, CHLOROFORM-d) δ ppm = 172.9 (C), 172.8 (C), 168.3 (2 X C), 133.9 (2 X CH), 132.2 (2 X C), 123.2 (2 X CH), 61.4 (CH_2), 61.4 (CH_2), 58.9 (C), 41.4 (CH_2), 40.1 (CH), 38.1 (CH_2), 37.0 (CH_2), 35.5 (CH), 28.7 (CH_2), 14.9 (CH_3), 14.0 (CH_3), 14.0 (CH_3). IR (neat, cm^{-1}): 2950 (br), 2375 (br), 1700 (s), 1450 (br), 1400 (s), 1250 (br), 1190 (br), 1040 (br), 860 (s), 710 (s). HRMS (EI) m/z calculated for $C_{22}H_{27}NO_6$ $[M]^+$: 401.1838, found: 401.1878.

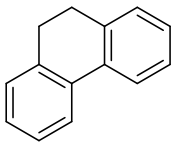

<u>3.3.3 :</u> 9,10-dihydrophenanthrene

Synthesized according to ***GP5.3.3*** and spectral data was consistent with literature.

^{1}H NMR (400MHz, CHLOROFORM-d) δ ppm = 7.77 (d, *J* = 7.6 Hz, 2 H), 7.29 - 7.32 (m, 2 H), 7.23 - 7.26 (m, 4 H), 2.89 (s, 4 H), ^{13}C NMR (101MHz, CHLOROFORM-d) δ ppm = 137.4 (2 X C), 134.5 (2 X C), 128.1 (2 X CH), 127.4 (2 X CH), 126.9 (2 X CH), 123.7 (2 X CH), 29.0 (2 X CH_2).

5.3.1.1 Lighting apparatus for section 3

*Photoreactor is equipped with a fan at the top to keep the reactor at ambient temperature. UVA bulbs and panels are available from Luzchem. A rack can be placed atop the stir plate where reaction vessels can be stirred and exposed to light. (UVA bulbs)

*The concave light capturing disk is mounted upon a box that contains a smaller box within on which to rest magnetic stir-plates upon. The reaction vessels are tied across the concave light capturing disk using string or dental floss. Alternatively, the reactions can be fastened to the disk using duct tape. The light disk is to maximize the amount of light available to the reactions. It should be noted that placing reaction vessels in a beaker on a stir plate in the sun diminishes the amount of light available to the reactions as more Pyrex glass is impeding the

reaction mixtures. This is important because the catalyst is excited at a wavelength that is very close to the cut-off wavelength of Pyrex (~320 nm). (Sunlight)

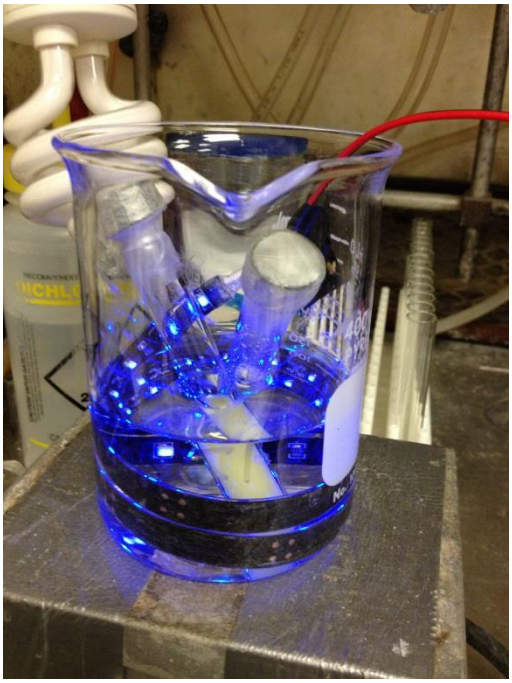

*Blue LED's purchased from superbrightleds.com. Setup similar to those described by Stephenson in photocatalytic publications. (Blue LED)

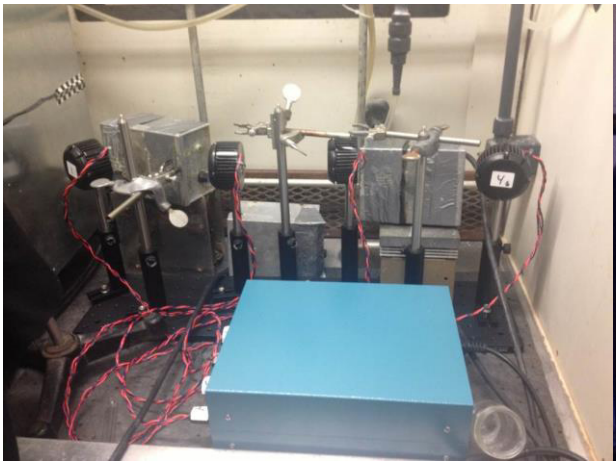

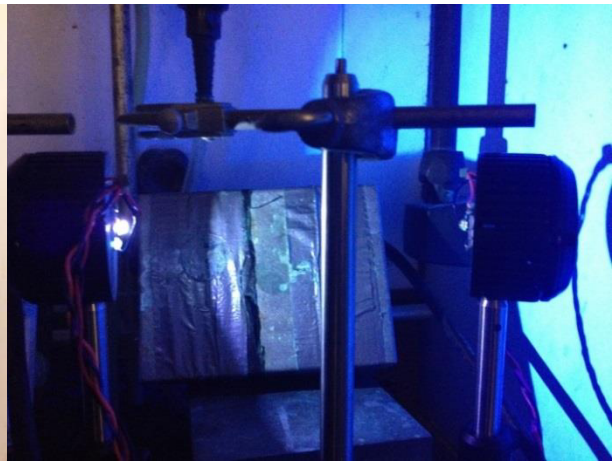

*Shown to the left is the LED setup containing 3 UVA LED (~365 nm) and 1 Violet LED (~400 nm). **UVA LED**- Single Color Ultraviolet (365 nm): LZ4-40U600.**Violet LED**- Single Color Violet (405 nm): LZ4-40UA00

5.3.2 Supplemental results for background and benchmark tests for Chapter 3.2:

Table 5.1 : Blank/control reactions for substrates of varying redox potentials in MeCN.

Entry	Substrate	Cat. mol%	*i*Pr$_2$NEt [eq]	FA [eq]	Light	t [hr]	Product	Yield [%]
1	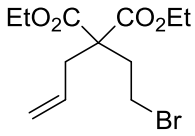	1.0	2.0	---	UVA	2	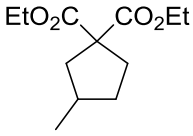	74
2		1.0	2.0	---	Sun	2		86
3		---	2.0	---	UVA	8		0
4[a]		5.0	2.0	---	---	8		0
5		5.0	2.0	---	UVA	16		<5[e]
6	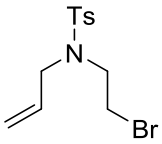	2.5	2.0	---	UVA	36	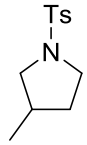	63
7		2.5	2.0	5.0	UVA	2		66
8		---	2.0	---	UVA	36		0
9[a]		5.0	2.0	---	---	36		0
10		---	---	5.0	UVA	36		0
11		---	2.0	5.0	UVA	36		0
12		2.5	---	5.0	UVA	36		4
13[a]		2.5	2.0	5.0	---	36		0
14a	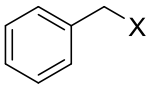	2.5	2.0	---	Sun	2	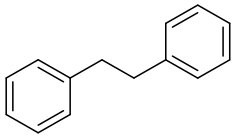	68
15a		---	2.0	---	Sun	8		7[b]
16a[a]		10.0	2.0	---	---	8		0
17a[c]	a: X = Br	2.5	2.0	---	UVA	8		41
18b	b: X = Cl	5.0	2.0	---	Sun	8		60
19b		---	2.0	---	Sun	8		0
20a	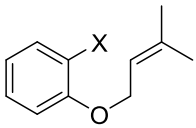	2.5	2.0	---	Sun	8	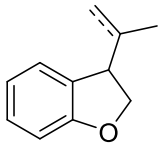	83[d]
21a		---	2.0	---	Sun	8		10[b]
22b		5.0	2.0	---	Sun	16		74[d]
23b	a: X = I b: X = Br	---	2.0	---	Sun	16		0

[a] Reaction was run under same conditions but no light irradiation was provided and was heated to 45°C. [b] Blank reaction (no catalyst) product conversion assigned by disappearance of starting material in percentage as judged by ^{1}H NMR. [c] Reaction run with water as solvent. The implication is that if further reduction of benzyl radicals to benzyl anions forms (which can then displace other BnBr to form bibenzyl) then it will first react with water to form toluene. The formation of bibenzyl suggests that this is not an ionic pathway. [d] The reduced to oxidized product gave a ratio of 2.5:1, which were assigned as judged by ^{1}H NMR. [e] $[Au_2(dppm)]Cl_2$, a dimeric specie with only one dppm ligand ($[1H]^{31}$PNMR: 24.2 ppm), was surveyed because emergence of a peak at 24.2 ppm in phosphine NMR's of reaction mixtures have indicated that possible degradation of the photocatalyst overtime is the loss of a ligand. With this in mind, the reaction did not proceed, as expected.

Table 5.2: Deuteration experiments of photoredox Au(I) reaction (GP5.3.3).

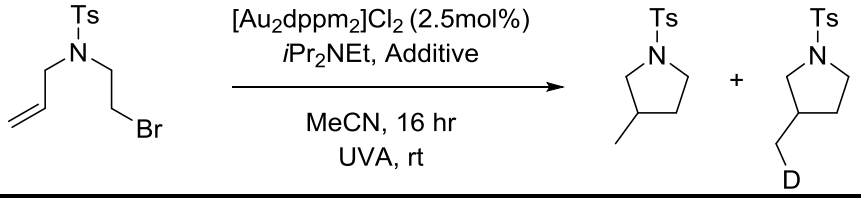

Entry	Eq. *i*Pr$_2$NEt	Additive	Equiv. Additive	Yield [%][b]
1	2	DCOOD	2	60 (20% D)
2	2	HCOOH	5	67 (no D)

[a] Deuterated ACN was used as solvent. [b] See characterization for Deuterated product.

Table 5.3: Benchmark cyclization and reduction reactions using iridium catalysts

Entry	Substrate	Cat[a,b]	Mol [%]	Base/[eq]	FA [eq]	t [hr]	Product	Yield [%][c]
1	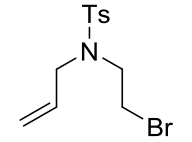	1	2.5	*n*Bu$_3$N/10	10	32	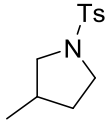	6
		2	3.0	*i*Pr$_2$NEt/10	---	32		17
		Blank	---	*i*Pr$_2$NEt/10	---	32		0
2	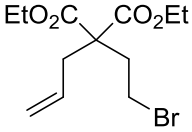	1	2.5	*n*Bu$_3$N/10	10	20	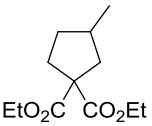	0
		2	3.0	*i*Pr$_2$NEt/10	---	20		<5
3	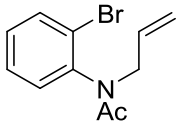	1	2.5	*n*Bu$_3$N/10	10	32	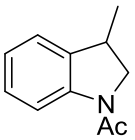	0
		2	3.0	*i*Pr$_2$NEt/10	---	32		0
		Blank	---	*i*Pr$_2$NEt/10	---	32		0
4	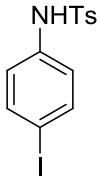	1	2.5	*n*Bu$_3$N/10	10	32	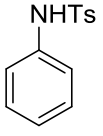	Quant.
		2	3.0	*i*Pr$_2$NEt/10	---	32		70
		Blank	---	*i*Pr$_2$NEt/10	---	32		0

5	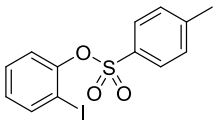	1	2.5	*n*Bu$_3$N/10	10	18	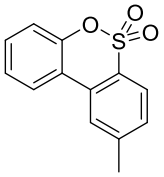	25
6	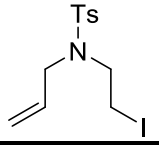	1	2.5	*n*Bu$_3$N/10	10	18	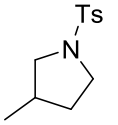	40

Substrate and catalyst were first placed in 8 mL vial and solvated in Acetonitrile. Base and additives were added last and mixtures were degassed using Argon sparging. Reactions were run under a Blue LED strip placed around the inside edge of a beaker filled with water. A 100 W light bulb was also placed beside the beaker, and the reactions ran at 30-35ºC from dissipation of heat by stir plate and light bulb. Mixtures were concentrated in vacuo and placed in 20 mL of Ether, followed by an aqueous extraction using 1N HCl, Saturated Sodium bicarbonate, and Brine. Organic phase was dried further using Magnesium sulfate and concentrated in vacuo. [a] Catalyst 1: fac-Ir(ppy)$_3$ (Stephenson conditions). Catalyst 2: Ir(ppy)$_2$(dtbbpy)PF$_6$ (Lee conditions). [b] Blank reactions were run using Lee conditions in absence of Catalyst 2. [c] Product conversion assigned by disappearance of starting material and formation of product in percentage as judged by ^{1}H NMR.

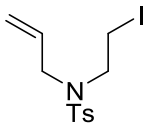

***N*-Allyl-*N*-(2-iodoethyl)-4-methylbenzenesulfonamide** To a flame-dried round-bottom flask equipped with a magnetic stirrer under argon atmosphere was added *N*-Allyl-*N*-(2-bromoethyl)-4-methylbenzenesulfonamide (0.5 mmol, 1.0 eq), Sodium iodide (5.0 mmol, 10 eq), and 3 mL of DMF. The mixture was heated to 90ºC overnight. The mixture was opened after cooling, diluted in ether, and washed with water and brine. The resulting organic phase was evaporated and purified by flash chromatography (1:9 EtOAc:Hex), yielding 130 mg (71%) of pure colourless oil. Spectral data was consistent with literature.[120] ^{1}H NMR (400MHz, CHLOROFORM-d) δ ppm = 7.65 - 7.78 (m, 2 H), 7.30 - 7.39 (m, *J* = 8.0 Hz, 2 H), 5.61 - 5.77 (m, 1 H), 5.13 - 5.26 (m, 2 H), 3.80 (d, *J* = 6.6 Hz, 2 H), 3.35 - 3.49 (m, 2 H), 3.21 - 3.30 (m, 2 H), 2.45 (s, 3 H). ^{13}C NMR (101MHz, CHLOROFORM-d) δ ppm = 143.7 (C), 136.4 (C), 132.9 (CH), 129.9 (2 X CH), 127.1 (CH), 119.6 (CH_2), 51.7 (CH_2), 50.2 (CH_2), 21.5 (CH_3), 1.9 (CH_2).

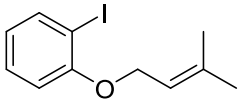

2-iodophenyl 3-methyl-2-propenyl ether (3. i. Table 1. Entries 19-20a)

Synthesized according to ***GP5.3.1*** and spectral data was consistent with literature.[121]

^{1}H NMR (400MHz, CHLOROFORM-d) δ ppm = 7.78 (dd, *J* = 7.8, 1.6 Hz, 1 H), 7.29 (ddd, *J* = 8.2, 7.5, 1.6 Hz, 1 H), 6.83 (dd, *J* = 8.2, 1.2 Hz, 1 H), 6.71 (td, *J* = 7.5, 1.4 Hz, 1 H), 5.52 (tquin, *J* = 6.4, 1.3 Hz, 1 H), 4.59 (d, *J* = 6.7 Hz, 2 H), 1.80 (s, 3 H), 1.76 (s, 3 H). ^{13}C NMR (101MHz, CHLOROFORM-d) δ ppm = 157.5 (C), 139.5 (CH), 137.9 (C), 129.3 (CH), 122.4 (CH), 119.5 (CH), 112.7 (CH), 86.9 (C), 66.3 (CH_2), 25.8 (CH_3), 18.4 (CH_3).

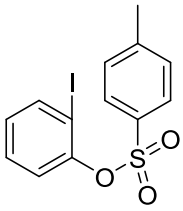

2-bromophenyl 4-methylbenzenesulfonate

Synthesized by standard tosylation procedure using White's method[125] using 2-iodophenol and spectral data was consistent with literature.[126]

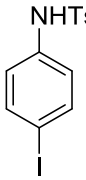

***N*-(4-iodo-phenyl)-4-methyl-benzenesulfonamide (3. iii. Table 3. Entry 4)**

Synthesized using the same procedure as N-(4-bromo-phenyl)-4-methyl-benzenesulfonamide using 4-iodoaniline. Spectral data was consistent with literature.[127]

5.3.3 Compounds and supplemental information for Chapter 3.3

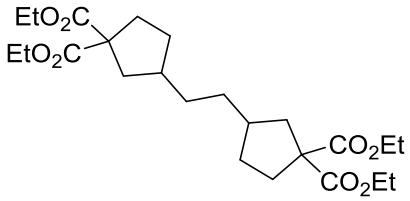

T3.2.1c : tetraethyl 3,3'-(ethane-1,2-diyl)bis(cyclopentane-1,1-dicarboxylate)

^{1}H NMR (400MHz, CHLOROFORM-d) δ ppm = 4.16 (qd, *J* = 7.1, 0.7 Hz, 8 H), 2.42 (dd, *J* = 13.2, 7.1 Hz, 2 H), 2.32 – 2.22 (m, 2 H), 2.16 – 2.06 (m, 2 H), 1.96 – 1.79 (m, 4 H), 1.66 (ddd, *J* = 13.2, 9.9, 1.7 Hz, 2 H), 1.41 – 1.27 (m, 4 H), 1.23 (t, *J* = 7.1 Hz, 14 H, 4 X Ester CH_3's + 2H under t).^{13}C NMR (101MHz, CHLOROFORM-d) δ ppm= 172.7 (2 X C), 172.7 (2 X C), 61.2 (4 X CH_2), 59.9 (2 X C), 40.7 (2 X CH_2), 39.9 (2 X CH), 34.1 (2 X CH_2), 33.7 (2 X CH_2), 32.1 (2 X CH_2), 14.0 (4 X CH_3). IR (neat, cm^{-1}): 2981(m), 2938(m), 1730(vs), 1257(s), 1177(m). HRMS (EI) m/z calculatedd for $C_{24}H_{38}O_8$ $[M]^+$: 454.2567, found: 454.2560.

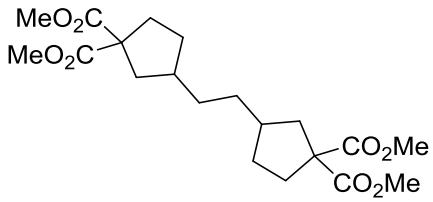

T3.5.1c: tetramethyl 3,3'-(ethane-1,2-diyl)bis(cyclopentane-1,1-dicarboxylate)

^{1}H NMR (400MHz, CHLOROFORM-d) δ ppm = 3.72 (s, 6H), 3.72 (s, 6H), 2.45 (dd, *J* = 13.1, 7.3 Hz, 2 H), 2.35-2.25 (m, 2 H), 2.18-2.09 (m, 2 H), 1.95-1.80 (m, 4 H), 1.68 (ddd, *J* = 13.2, 9.9, 1.2 Hz, 2 H), 1.35-1.19 (m, 6 H). ^{13}C NMR (101MHz, CHLOROFORM-d) δ ppm = 173.2 (4 X C), 59.9 (2 X C), 52.6 (2 X CH_3), 52.6 (2 X CH_3), 40.8 (2 X CH_2), 39.9 (CH), 39.9 (CH), 34.1 (CH_2), 34.1 (CH_2), 33.9 (2 X CH_2), 32.1 (2 X CH_2). IR (neat, cm^{-1}): 2953(m), 2853(m), 1729(vs), 1435(s), 1251(s), 1157(s). HRMS (EI) m/z calculated for $C_{20}H_{30}O_8$ $[M - C_3H_{12}O_3]^+$: 274.1205, found: 274.1240. *(characterized by Huy Tran)*

T3.2.1d: diethyl 3-(bromomethyl)cyclopentane-1,1-dicarboxylate

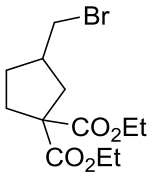

^{1}H NMR (400MHz, CHLOROFORM-d) δ ppm = 4.16 (q, *J* = 7.2 Hz, 4 H), 3.44 - 3.28 (m, 2 H), 2.54 - 2.37 (m, 2 H), 2.37 - 2.26 (m, *J* = 0.2 Hz, 1 H), 2.26 - 2.13 (m, 1 H), 2.00 - 1.86 (m, 2 H), 1.46 (qd, *J* = 12.8, 8.6 Hz, 1 H), 1.23 (t, *J* = 7.1 Hz, 7 H). ^{13}C NMR (101MHz, CHLOROFORM-d) δ ppm = 172.2 (C), 172.2 (C), 61.5 (CH_2), 61.5 (CH_2), 60.2 (C), 41.7 (CH), 39.2 (CH_2), 37.3 (CH_2), 33.7 (CH_2), 30.9 (CH_2), 14.0 (2 X CH_3). HRMS (EI) m/z calculated for $C_{12}H_{19}BrO_4$ $[M]^+$: 306.0467, found: 306.0446.

5.3.4 Compounds and supplemental information for Chapter 3.4

***(GP5.3.5)* General procedure for the UVA LED initiated photocyclization with various Au(I) complexes.**

To an oven-dried 8 mL pyrex screw-top reaction vessel was added the Au_x complex (0.01 mmol, 5 mol%) the corresponding alkyl or aryl bromide (0.20 mmol, 1.00 equiv.), MeCN/MeOH (1:1, 1 mL, 0.2M), *i*Pr_2NEt (1.0 mmol, 5 equiv.) and degassed under argon by sparging. The reaction mixtures were then placed under UVA LED (365 nm) for 1 – 20 h. After few hours of irradiation, the solution becomes dark yellow, red, or brown. . The solutions rapidly became dark yellow, red, or brown. Upon reaction completion, the resulting mixtures were concentrated *in vacuo*, and the crude mixtures were placed in a separatory funnel containing EtOAc, washed with 1 M HCl, sat. $NaHCO_3$, and brine, then dried over sodium sulfate, filtered, and concentrated *in vacuo*. The products were analyzed with ^{1}H and ^{13}C NMR.

***(GP5.3.6)* General procedure for the formation of phosphine based Au_x complexes F3.4.1-3**

Commercially available (chloro(dimethylsulfide)gold(I) (0.2, 1.0 equiv.) was obtained from a glove-box under argon atmosphere and placed in solution with DCM in a round-bottom flask

under argon at room temperature.The appropriate phosphine ligand (2.0 mmol, 1.0 equiv. [*0.66 equiv. for complex F3.4.3*]) was added and the solution was allowed to stir for 1 hours. After this time, the solution was concentrated *in vacuo* and the complex was precipitated out by the addition of ether. The white powder was isolated and washed by filtration using ether, yields ranging from 65-95%. *For NMR analysis, complexes **F3.4.2 [OTf]$_2$** and **F3.4.3 [OTf]$_2$** were obtained from their respective chloride analogues by solvation of the complex (0.20 mmol) in DCM and adding the corresponding silver salt, AgOTf (0.40 mmol, 2 equiv. [*3 equiv. for F3.4.3*]) to the solution. After 1 h the solutions were concentrated *in vacuo* and the complexes were precipitated out by the addition of ether. The white powders were isolated and washed by filtration using ether.

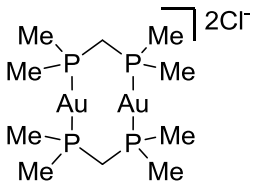

F3.4.1: [Au$_2$(dmpm)$_2$]Cl$_2$ (2)

^{1}H NMR (400MHz, CD_3OD) δ ppm = 3.05 (quin, *J* = 5.3 Hz, 4 H), 1.83 (td, *J* = 3.8, 1.9 Hz, 24 H). ^{13}C NMR (101MHz, CD_3OD) δ ppm = 31.5 (t, *J* = 15.4 Hz, 2 X CH_2), 14.9 (quin, *J* = 10.3 Hz, 8 X CH_3).

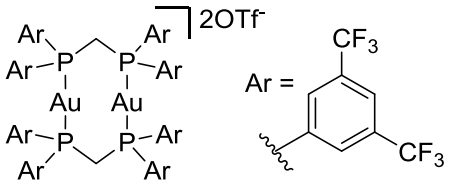

F3.4.2 [OTf]$_2$: [Au$_2$(3,5-CF$_3$-dppm)$_2$](OTf)$_2$

^{1}H NMR (400MHz, CD_3CN) δ ppm = 8.28 - 8.24 (m, 16 H), 8.23 (br. s, 8 H), 5.04 (quin, *J* = 5.7 Hz, 4 H). ^{13}C NMR (101MHz, CD_3CN) δ ppm = 135.31 (br. s., 16 X CH), 133.58 (quinq, *J* = 34.6, 3.3 Hz, 16 X C), 130.57 (quin, *J* = 16.3 Hz, 8 X C), 128.93 (s, 8 X CH), 123.65 (q, *J* = 274.0 Hz, 16 X C), 121.98 (q, *J* = 320.2 Hz, 2 X C), 26.18 (t, *J* = 15.0 Hz, 2 X CH_2). ^{31}P NMR (121MHz, CD_3CN) δ ppm = 40.19 (s, 4 X P).

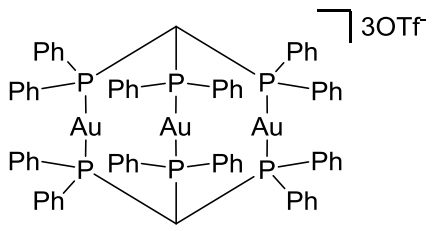

F3.4.3 [OTF]$_2$: [Au$_3$(tppm)$_2$](OTf)$_3$

^{1}H NMR (400MHz, CHLOROFORM-d) δ ppm = 8.14 (br. s., 24 H), 7.34 (t, *J* = 7.2 Hz, 12 H), 7.26 (t, *J* = 7.2 Hz, 24 H), 2.15 (s, 2 H). ^{13}C NMR (101MHz, CHLOROFORM-d) δ ppm = 135.5 (24 X CH), 133.9 (12 X CH), 130.0 (24 X CH), 126.6 (12 X C), 30.9 (2 X CH). ^{31}P NMR (121MHz, CHLOROFORM-d) δ ppm = 45.79 (s, 6 X P).

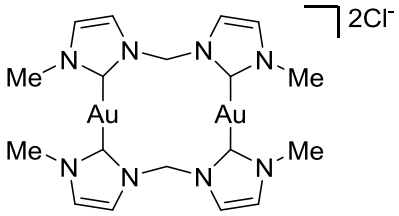

F3.4.4: [Au$_2$(bmimm)$_2$]Cl$_2$

[Au$_2$(bmimm)$_2$]Cl$_2$ was synthesized using a modified procedure reported by Crabtree.[128] To a high pressure reaction flask (oven-dried, under inert atmosphere, equipped with a magnetic stirrer) was added sodium acetate (62 mg, 0.75 mmol, 2.2 equiv.), followed by 1,1'-dimethyl-3,3'-methylene-diimadazolium diiodide (177 mg, 0.41 mmol, 1.2 equiv.) and chloro(dimethylsulfide)gold(I) (100 mg, 0.34 mmol, 1 equiv.). DMF was added and the reaction vessel capped and heated to 160^{o}C for 1.5 hours. The solution was filtered while still hot (Caution: Let cool to below 100^{o}C before opening reaction flask). The filtrate was washed once each with DMF, acetone, and diethyl ether. 131mg (94%) of the desired complex was recovered and used as is for photocatalysis without further purification. ^{1}H NMR (400MHz, CD_3OD) δ ppm = 7.71 (d, *J* = 1.5 Hz, 4 H), 7.45 (d, *J* = 2.0 Hz, 4 H), 7.20 (d, *J* = 14.0 Hz, 2 H), 6.26 (d, *J* = 14.0 Hz, 2 H), 3.94 (12 H). ^{13}C NMR (101MHz, CD_3OD) δ ppm = 185.8 (4 X C), 125.6 (4 X CH), 122.7 (4 X CH), 63.9 (2 X CH_2), 38.9 (4 X CH_3).

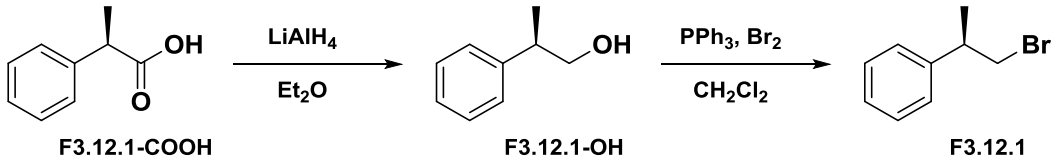

F3.12.1-COOH F3.12.1-OH F3.12.1

F3.12.1: **(*R*)-(1-bromopropan-2-yl)benzene**

To a flame-dried 100 mL round bottom flask under argon equipped with a magnetic stirrer was added 50 mL of diethyl ether which was cooled to 0°C using an ice bath, and to wich was added $LiAlH_4$ (15.0 mmol, 3.0 equiv.). (*R*)-(−)-2-phenylpropionic acid (5.0 mmol, 1.0 equiv.) in a minimum of diethyl ether was then added dropwise to the solution. The reaction mixture was allowed to warm to room temperature and stirred for 1 hour. Upon completion, the reaction was quenched by slow dropwise addition 0.5 mL of water, then dropwise addition of 0.5 mL of a 15% NaOH aqueous solution, and 1.5 mL of water. This solution was allowed to stir for 30 minutes and was then transferred to a seperatory funnel. The ethereal phase was washed 2 times with a saturated sodium bicarbonate solution followed by brine, then dried over sodium sulfate, filtered, concentrated *in vacuo*, and spectral data was consistent with literature.[129]

To a flame-dried 100 mL round bottomed flask under argon equipped with a magnetic stirrer was added PPh_3 (5.5 mmol, 1.1 equiv.) and 50 mL of dichloromethane. The solution was cooled to 0°C using an ice bath and bromine (5.5 mmol, 1.1 equiv.) was added. After stirring for 30 minutes, a white precipitate formed, indicating the presence of a phosphonium bromide intermediate. (*R*)-2-phenylpropan-1-ol (0.5 mmol, 1.0 equiv.) in a minimum of dichloromethane was added dropwise and the solution was allowed to warm to room temperature, and then refluxed overnight. Upon completion, silica was added to the solution, concentrated *in vacuo*, and dry packed upon a chromatography column. The column was eluted (0%-2% EtOAc:Hexane) where relevant fractions were combined and concentrated *in vacuo*. The product

was isolated as an oil (832 mg, 4.2 mmol) with a yield of 84% over both steps and spectral data was consistent with literature.[130]

$[\alpha]_D^{23}$ = +16.6° (c 1.0, $CHCl_3$).

5.3.4.1 Absorption Spectra of Au_x Complexes

(collected by Chris McTiernan)

*Figure 5.1: Absorption spectrum of 3.3 x10-3 mM $Au_2(dppm)_2Cl_2$ (**F3.1.1**) in MeCN.*

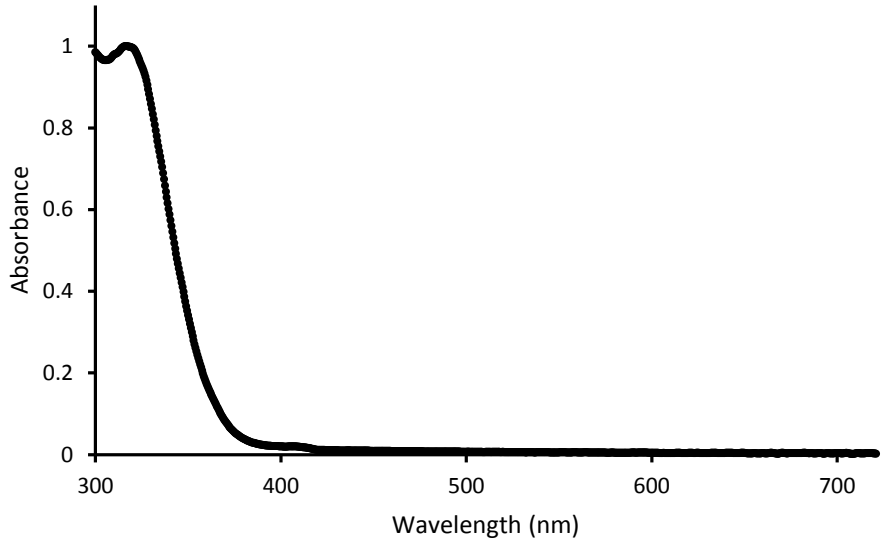

*Figure 5.2 : Absorption spectrum of 0.20 mM $Au_2(dmpm)_2Cl_2$ (**F3.4.1**) in MeCN.*

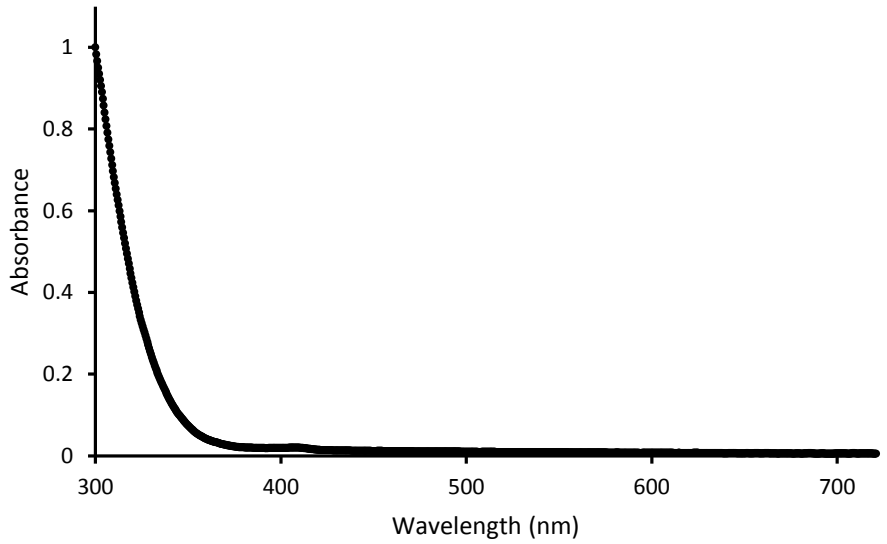

*Figure 5.3: Absorption spectrum of 0.12 mM $Au_2(3,5\text{-}CF_3\text{-}dppm)_2Cl_2$ (**F3.4.2**) in MeCN.*

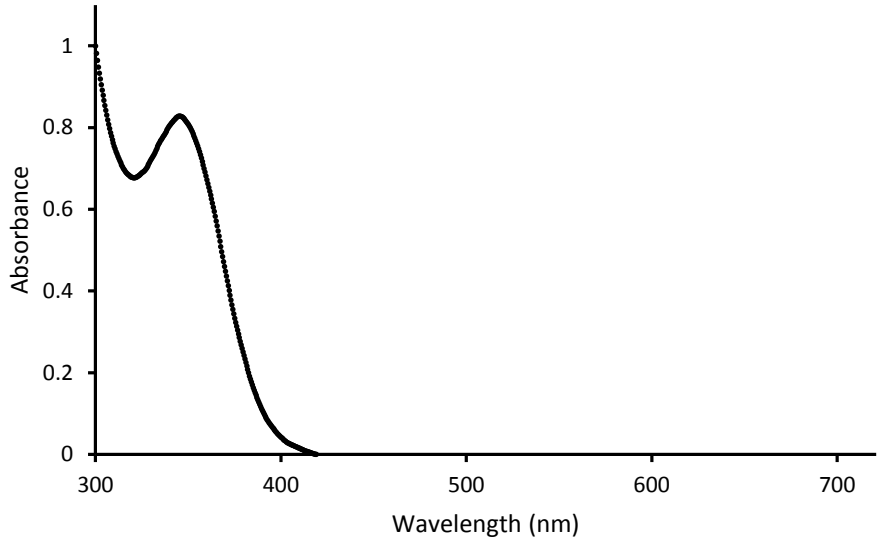

*Figure 5.4: Absorption spectrum of 6.1 x 10^{-2} mM $Au_3(tppm)_2Cl_3$ (**F3.4.3**) in MeCN.*

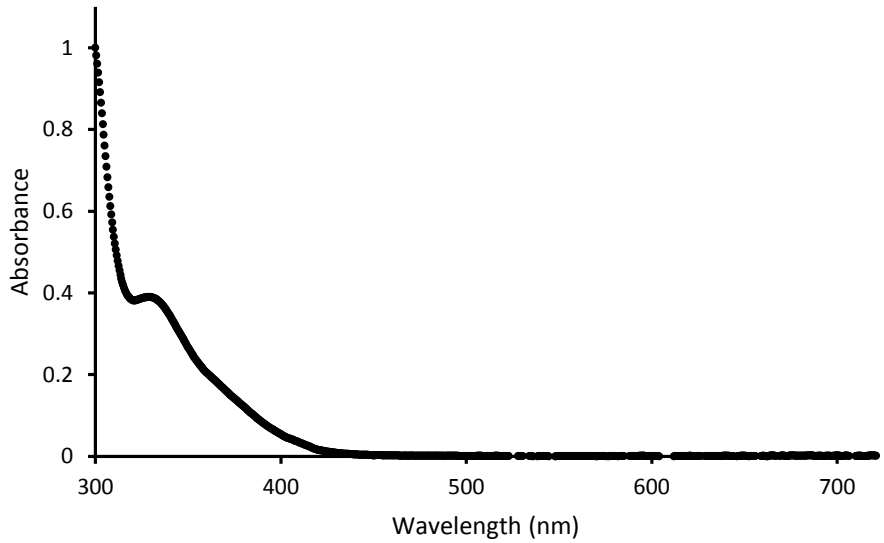

*Figure 5.5: Absorption spectrum of 1.02 mM $Au_2(bmimm)_2Cl_2$ (**F3.4.4**) in MeCN.*

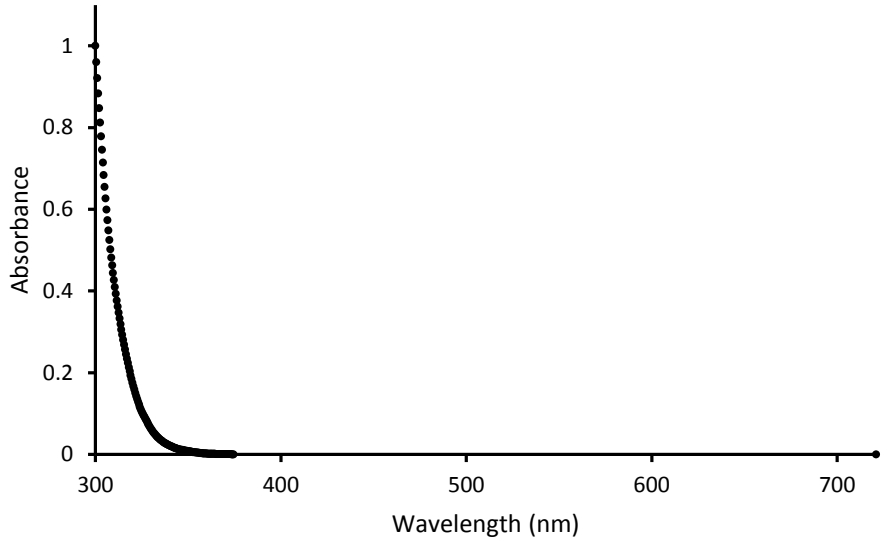

5.3.4.2 77K Phosphorescence spectra of Aux complexes

(collected by Chris McTiernan)

Determination of Triplet Energies (E^*_T)

The low temperature phosphorescence measurements, from which the triplet energy of the Au_x complexes was determined, were carried out in a Photon Technology International (PTI) spectrofluorimeter. Cooling to 77K was accomplished using a quartz cold finger and liquid N_2. Spectra of the Au_x complexes were recorded from ethanol:methanol (1:1) glass in a quartz EPR tube. None of the emission spectra of the Au_x complexes exhibited fine structure. Therefore we have estimated the energy of the $(0\text{-}0)_{T\text{-}S}$ transition from the emission maxima. This most likely results in the triplet energy value being underestimated.

*Figure 5.6: 77 K phosphorescence spectrum of $Au_2(dppm)_2Cl_2$ (**F3.1.1**) in EtOH:MeOH glass.*

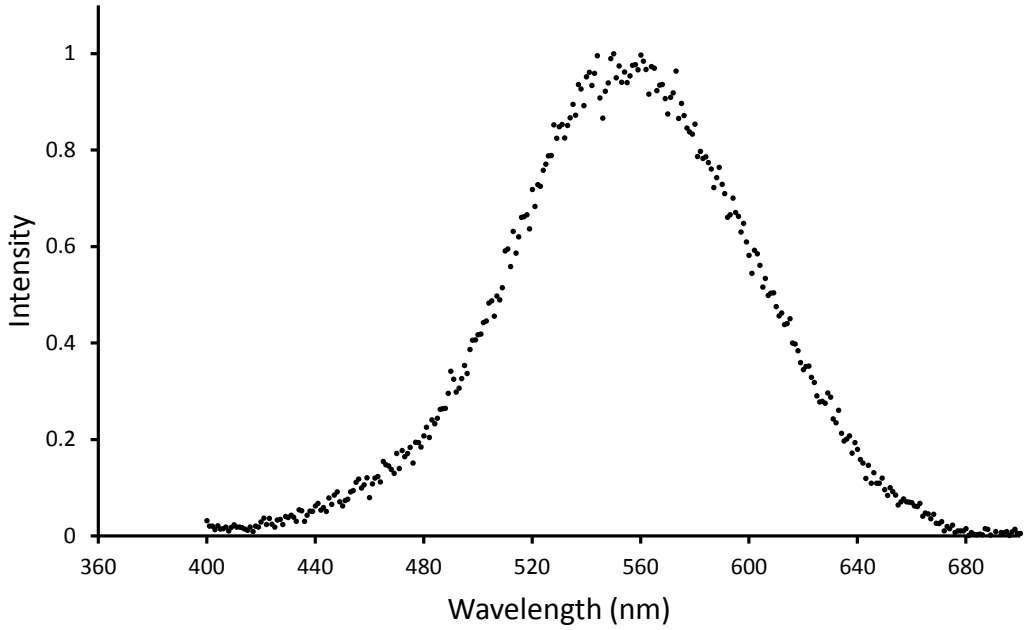

*Figure 5.7: 77 K phosphorescence spectrum of $Au_2(dmpm)_2Cl_2$ (**F3.4.1**) in EtOH:MeOH glass.*

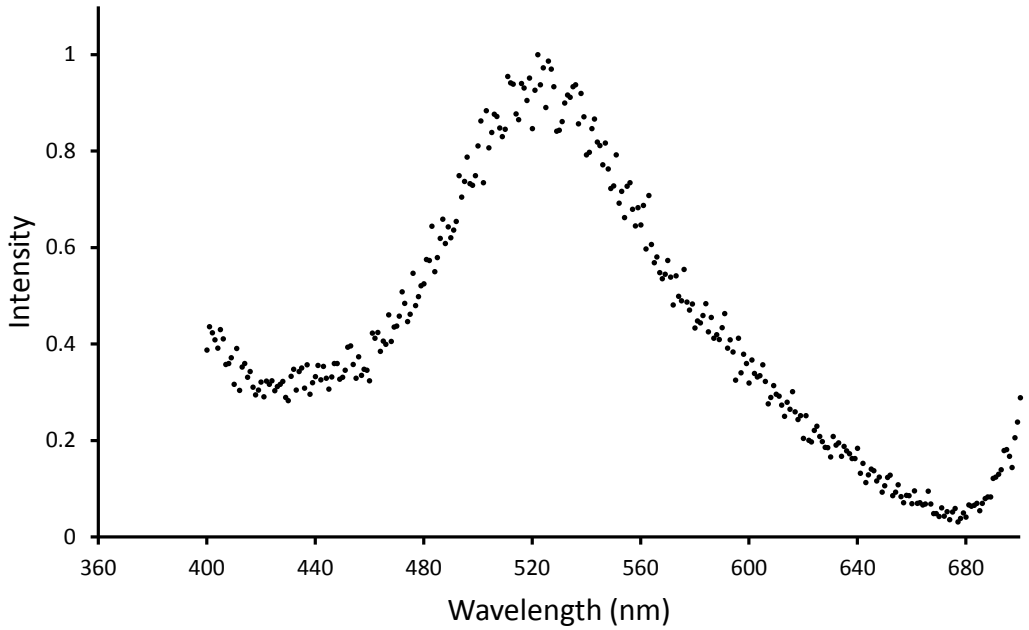

*Figure 5.8 : 77 K phosphorescence spectrum of $Au_2(3,5\text{-}CF_3\text{-}dppm)_2Cl_2$ (**F3.4.2**) in EtOH:MeOH glass.*

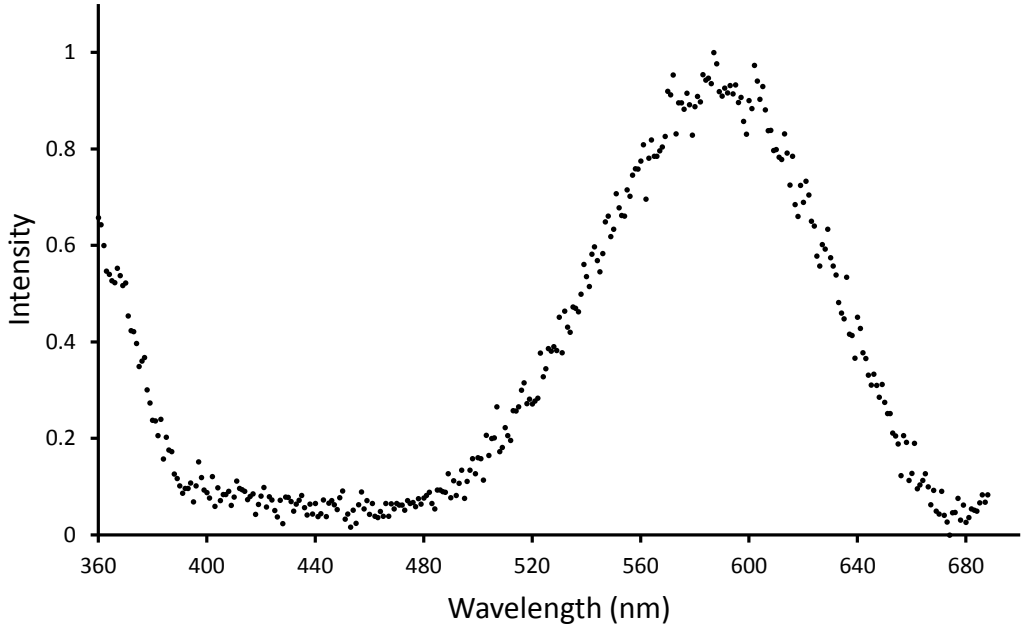

*Figure 5.9: 77 K phosphorescence spectrum of $Au_3(tppm)_2Cl_3$ (**F3.4.3**) in EtOH:MeOH glass.*

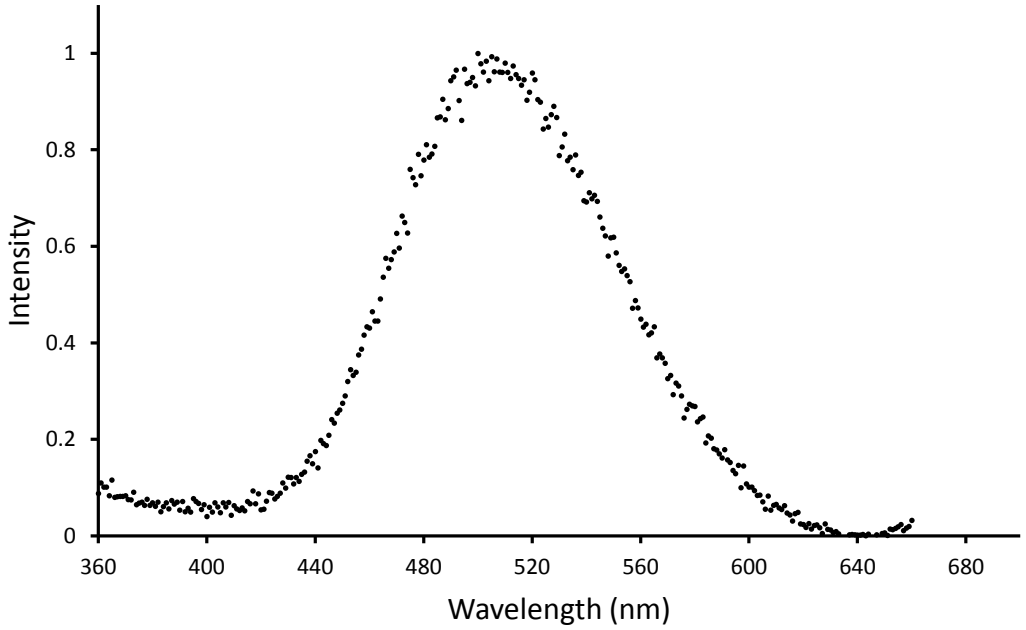

*Figure 5.10 : 77 K phosphorescence spectrum of $Au_2(bmimm)_2Cl_2$ (**F3.4.4**) in EtOH:MeOH glass.*

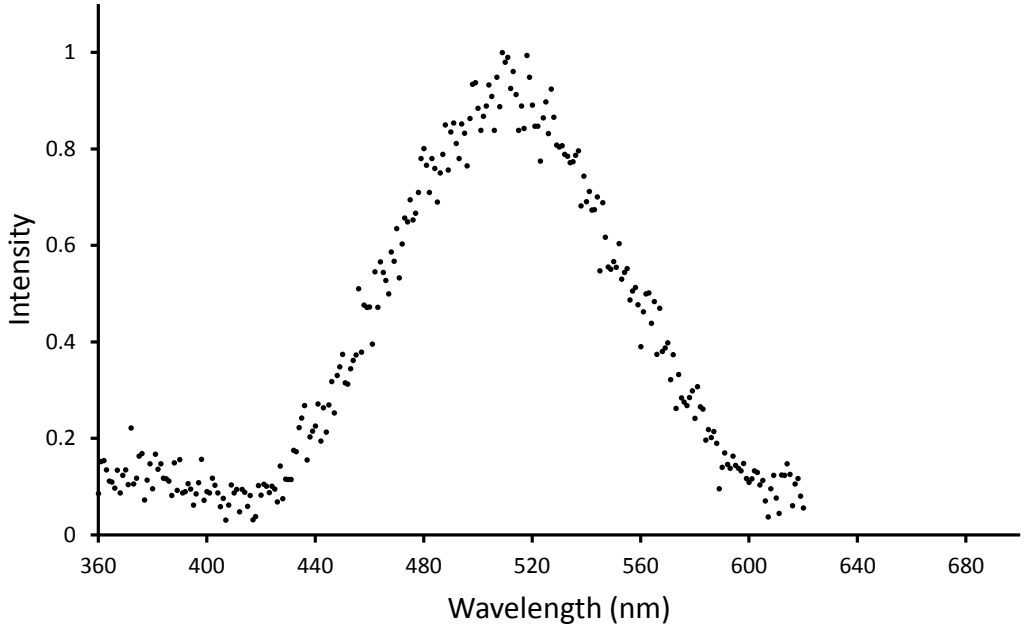

5.3.4.3 Laser flash photolysis data of the Au_x complexes

(collected by Chris McTiernan)

Experiments were performed using either a Q-switched Nd:YAG-laser (355 nm, 10 mJ/pulse) or an excimer laser (308 nm, 10 mJ/pulse) in a LFP-111 laser-flash photolysis (LFP) system (Luzchem Research Inc., Ottawa, Canada) and 1 cm x 1 cm quartz cuvette (Luzchem). Samples of the Au_x complexes were prepared in MeCN with a total volume of 3 mL and an absorbance of ~0.1 at 308 or 355 nm. The samples were degasses with N_2 for 30 minutes prior to use. The substrates used in the quenching studies were also prepared in MeCN and were degassed for the duration of the experiment.

*$Au_2(dppm)_2Cl_2$ (**F3.1.1**)*

Figure 5.11 : Transient emission spectrum showing the $^3Au_2(dppm)_2Cl_2$ signal obtained upon laser pulse excitation (355 nm, 10 mJ) of a $Au_2(dppm)_2Cl_2$ sample which had been purged of oxygen.

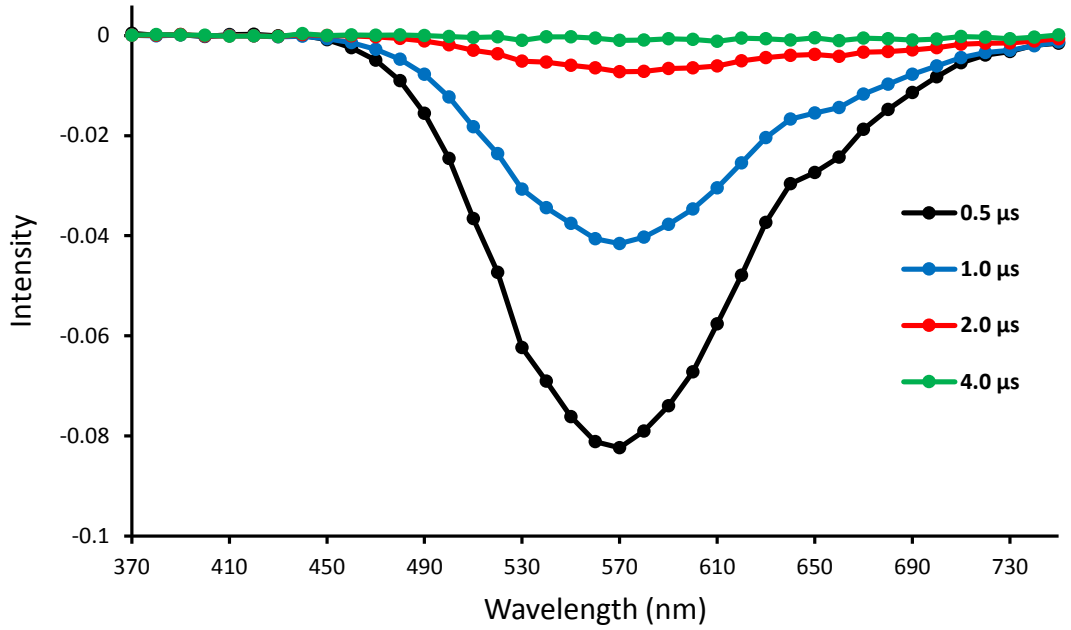

Figure 5.12: Decay trace of $^3Au_2(dppm)_2Cl_2$ at 560 nm obtained upon laser pulse excitation (355 nm, 10 mJ) of a $Au_2(dppm)_2Cl_2$ sample which had been purged of oxygen.

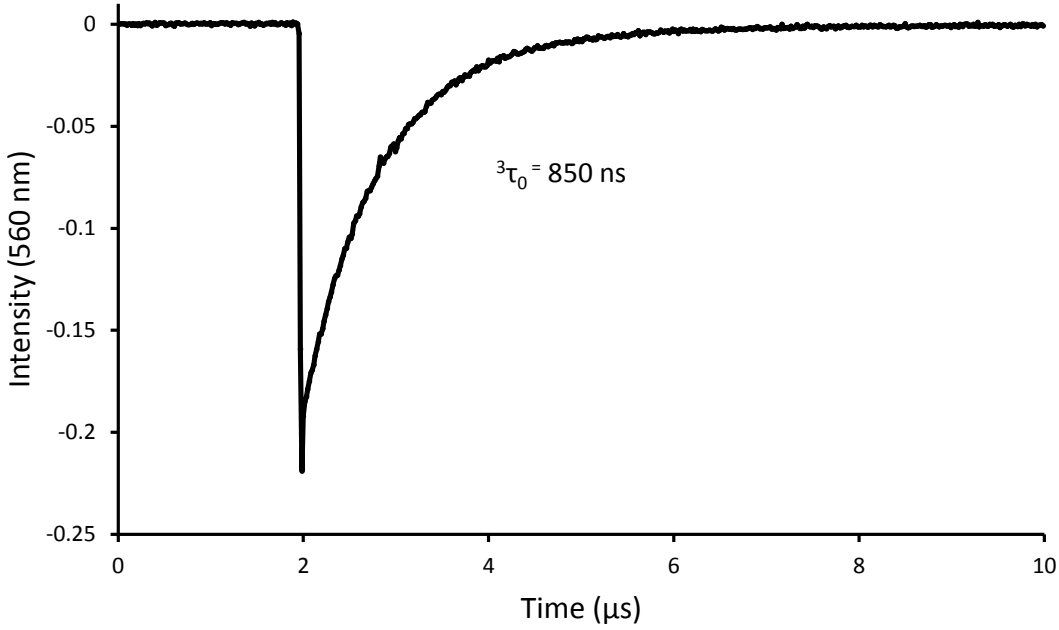

Figure 5.13 : Kinetic quenching plot showing the quenching of $^3Au_2(dppm)_2Cl_2$ by iPr_2NEt. The slope of the plot corresponds to the bimolecular rate constant.

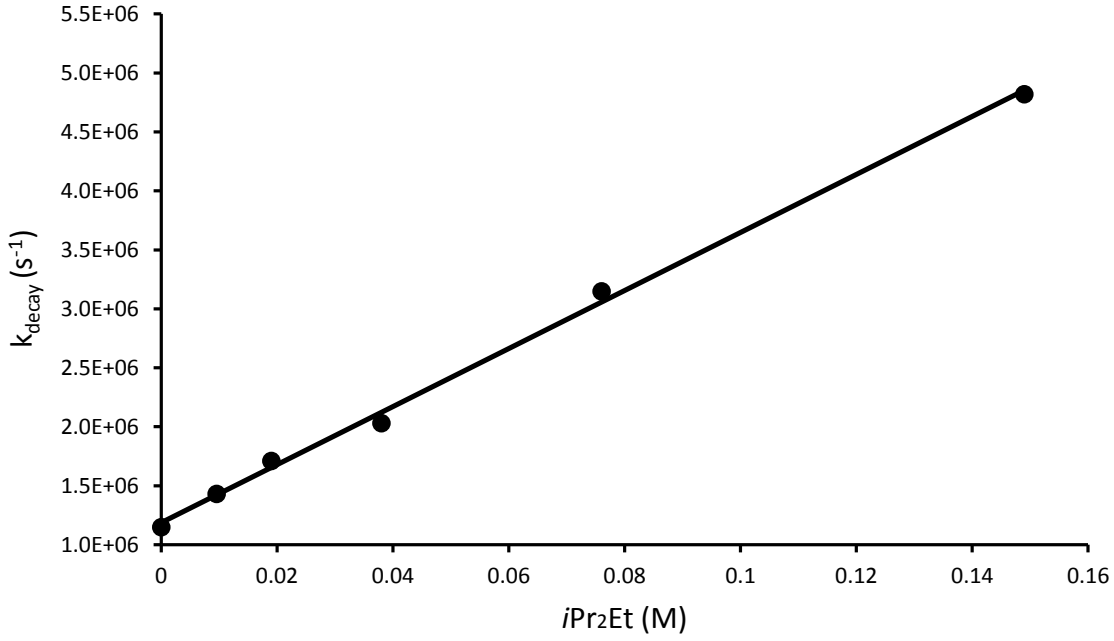

*Figure 5.14: Kinetic quenching plot showing the quenching of $^3Au_2(dppm)_2Cl_2$ by substrate **T3.2.1a**. The slope of the plot corresponds to the bimolecular rate constant.*

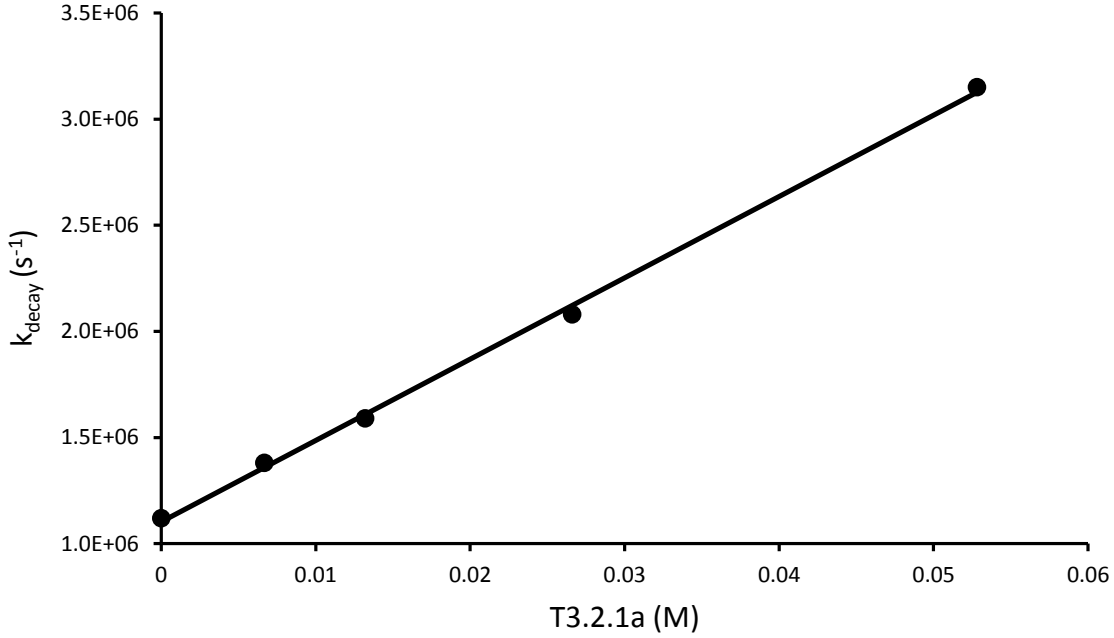

Figure 5.15 : Kinetic quenching plot showing the quenching of $^3Au_2(dppm)_2Cl_2$ by butyl bromide. The slope of the plot corresponds to the bimolecular rate constant.

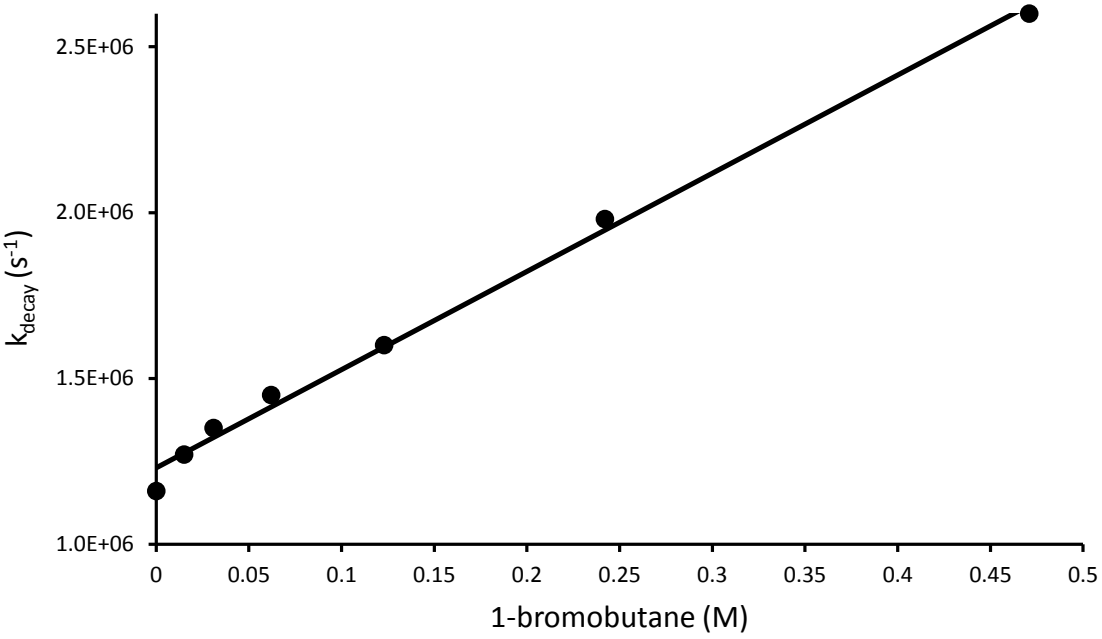

*$Au_2(dmpm)_2Cl_2$ (**F3.4.1**)*

Figure 5.16 : Transient emission spectrum showing the $^3Au_2(dmpm)_2Cl_2$ signal obtained upon laser pulse excitation (308 nm, 10 mJ) of a $Au_2(dmpm)_2Cl_2$ sample which had been purged of oxygen.

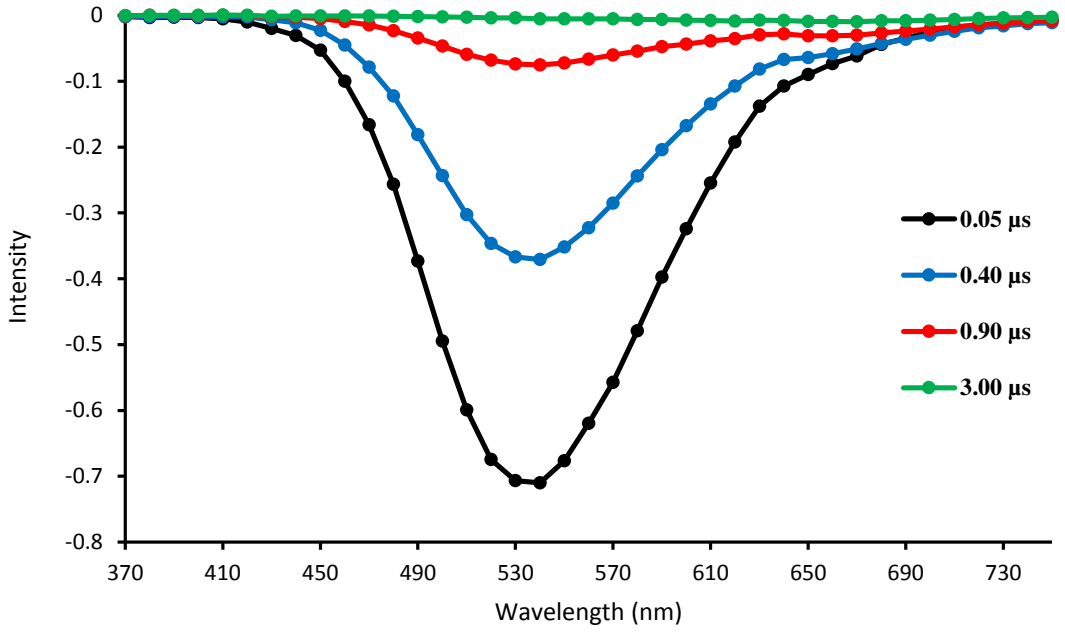

Figure 5.17: Decay trace of $^3Au_2(dmpm)_2Cl_2$ at 525 nm obtained upon laser pulse excitation (308 nm, 10 mJ) of a $Au_2(dmpm)_2Cl_2$ sample which had been purged of oxygen.

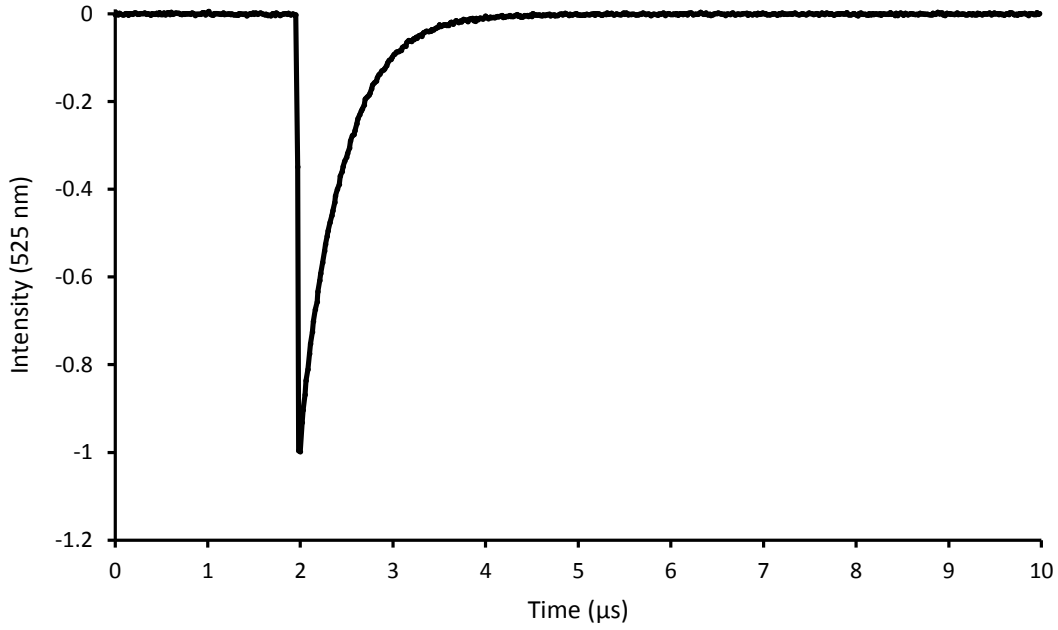

Figure 5.18 : Kinetic quenching plot showing the quenching of $^3Au_2(dmpm)_2Cl_2$ by iPr_2NEt. The slope of the plot corresponds to the bimolecular rate constant

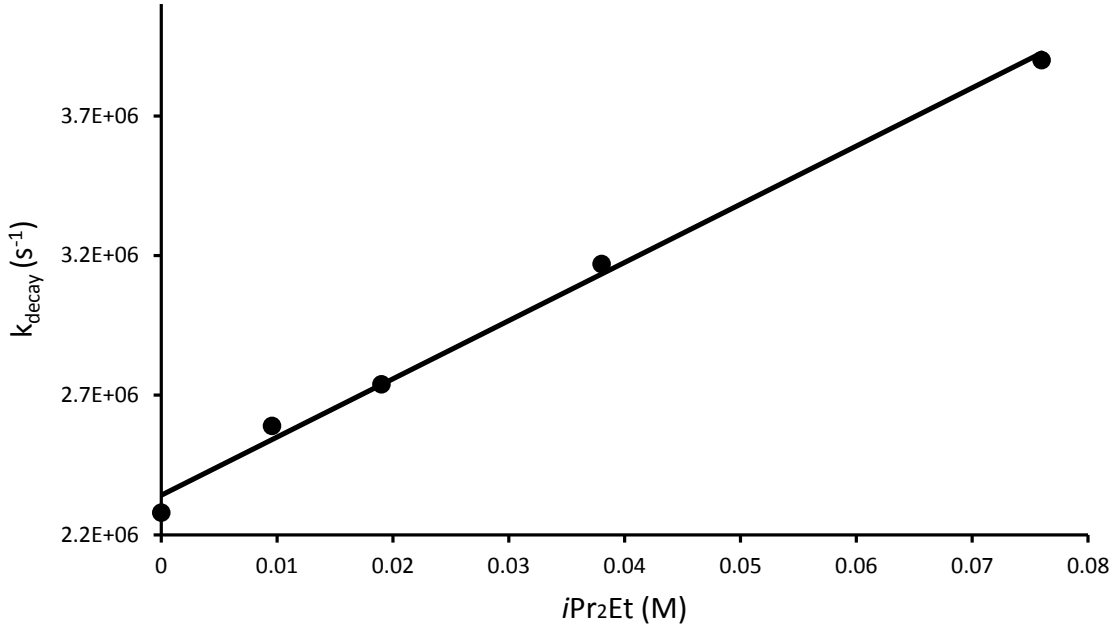

*Figure 5.19 : Kinetic quenching plot showing the quenching of $^3Au_2(dmpm)_2Cl_2$ by substrate **T3.2.1a**. The slope of the plot corresponds to the bimolecular rate constant.*

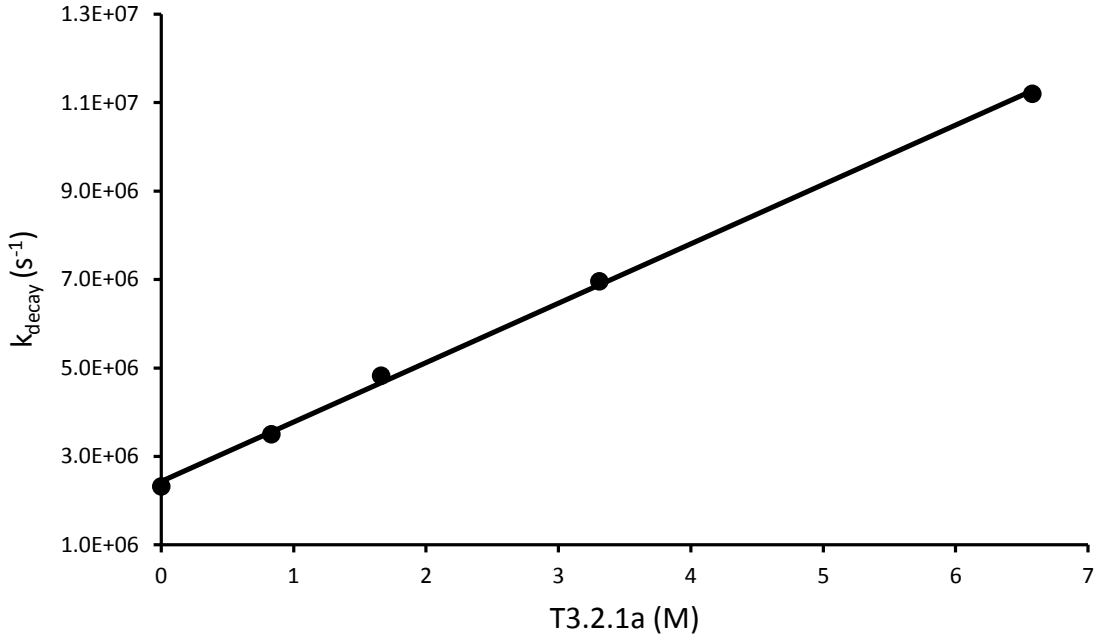

Figure 5.20: Kinetic quenching plot showing the quenching of $^3Au_2(dmpm)_2Cl_2$ by butyl bromide. The slope of the plot corresponds to the bimolecular rate constant.

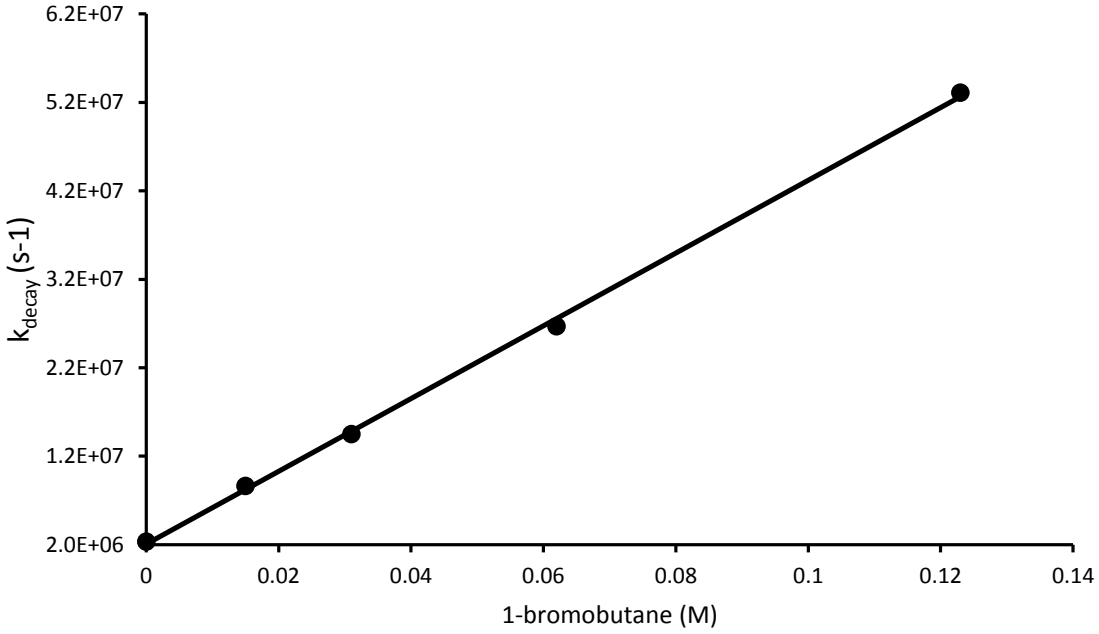

$Au_2(3,5\text{-}CF_3\text{-}dppm)_2Cl_2$ ***(F3.4.2)***

Figure 5.21 : Transient emission spectrum showing the $^3Au_2(3,5\text{-}CF_3\text{-}dppm)_2Cl_2$ signal obtained upon laser pulse excitation (355 nm, 10 mJ) of a $Au_2(3,5\text{-}CF_3\text{-}dppm)_2Cl_2$ sample which had been purged of oxygen.

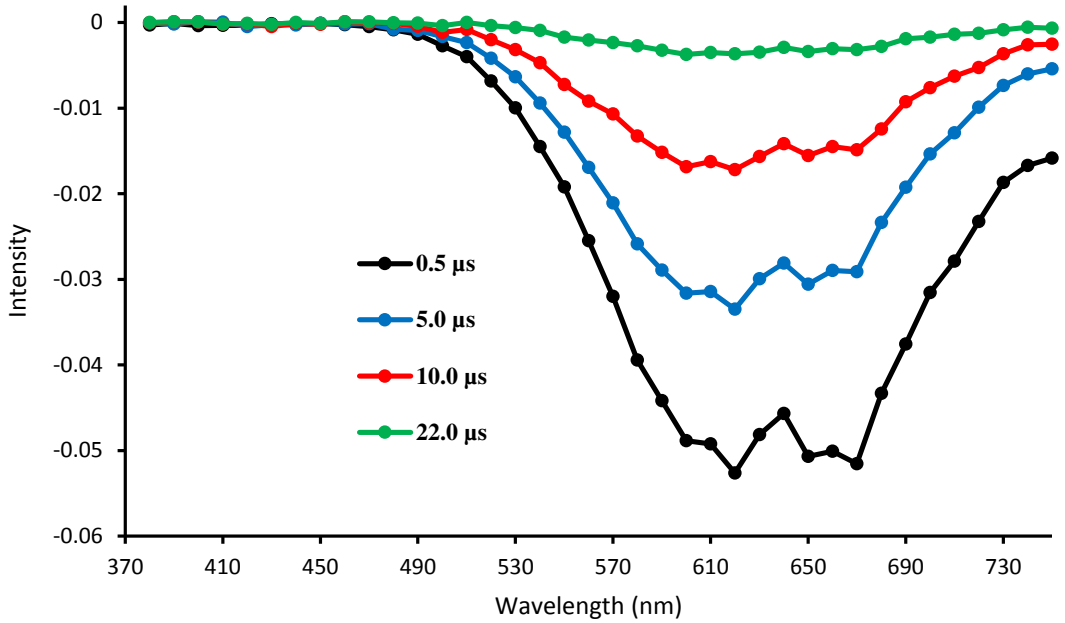

Figure 5.22 : Decay trace of $^3Au_2(3,5\text{-}CF_3\text{-}dppm)_2Cl_2$ at 590 nm obtained upon laser pulse excitation (355 nm, 10 mJ) of a $Au_2(3,5\text{-}CF_3\text{-}dppm)_2Cl_2$ sample which had been purged of oxygen.

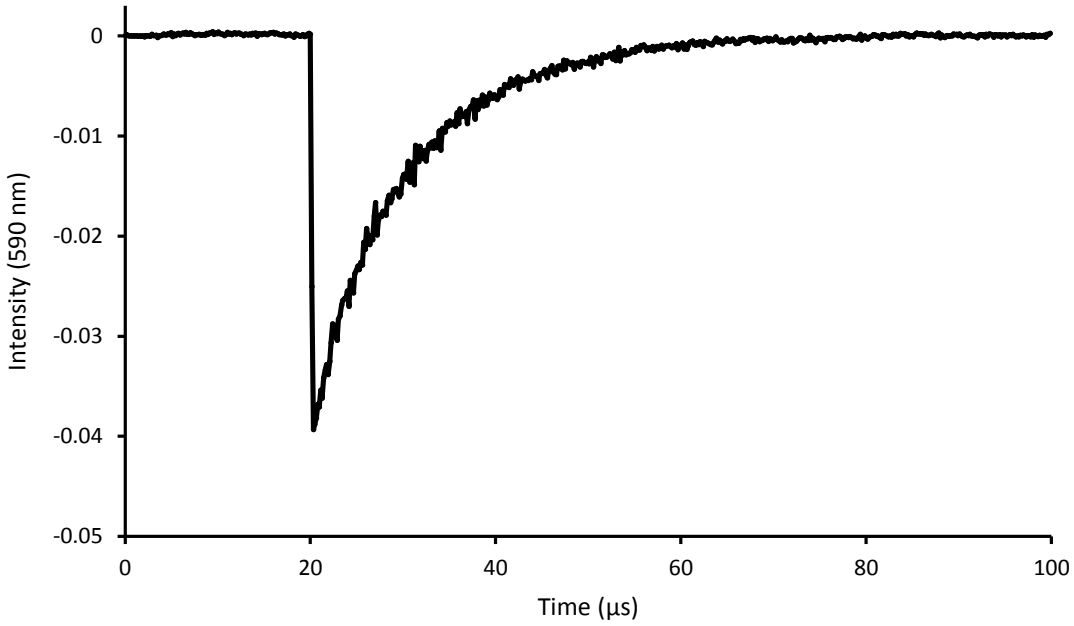

Figure 5.23 : Kinetic quenching plot showing the quenching of $^3Au_2(3,5\text{-}CF_3\text{-}dppm)_2Cl_2$ by iPr_2NEt. The slope of the plot corresponds to the bimolecular rate constant.

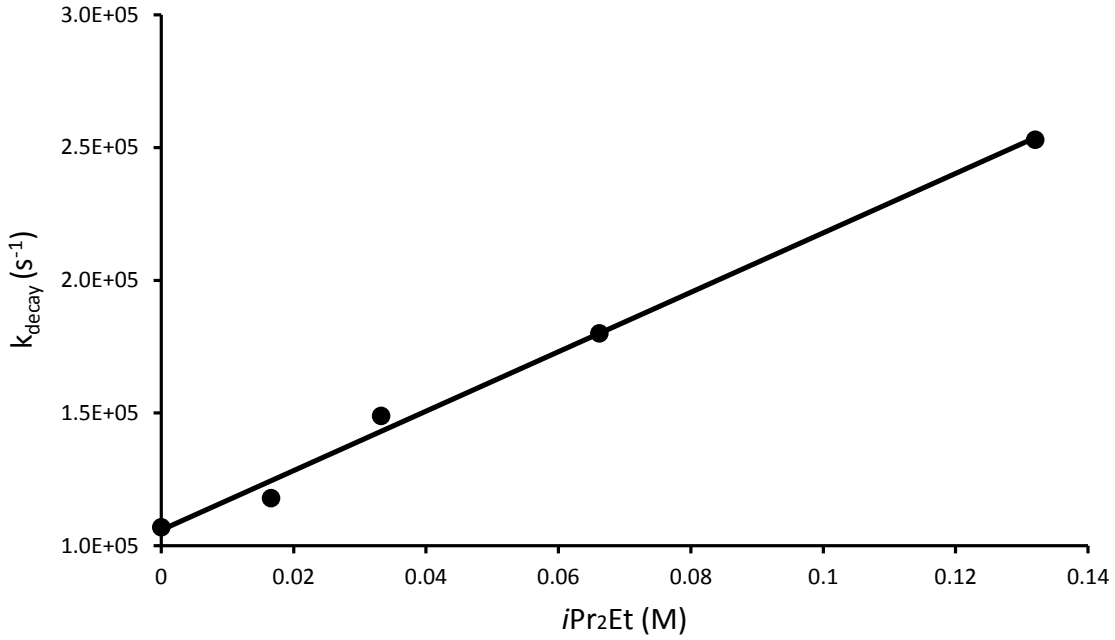

*Figure 5.24 : Kinetic quenching plot showing the quenching of $^3Au_2(3,5\text{-}CF_3\text{-}dppm)_2Cl_2$ by substrate **T3.2.1a**. The slope of the plot corresponds to the bimolecular rate constant.*

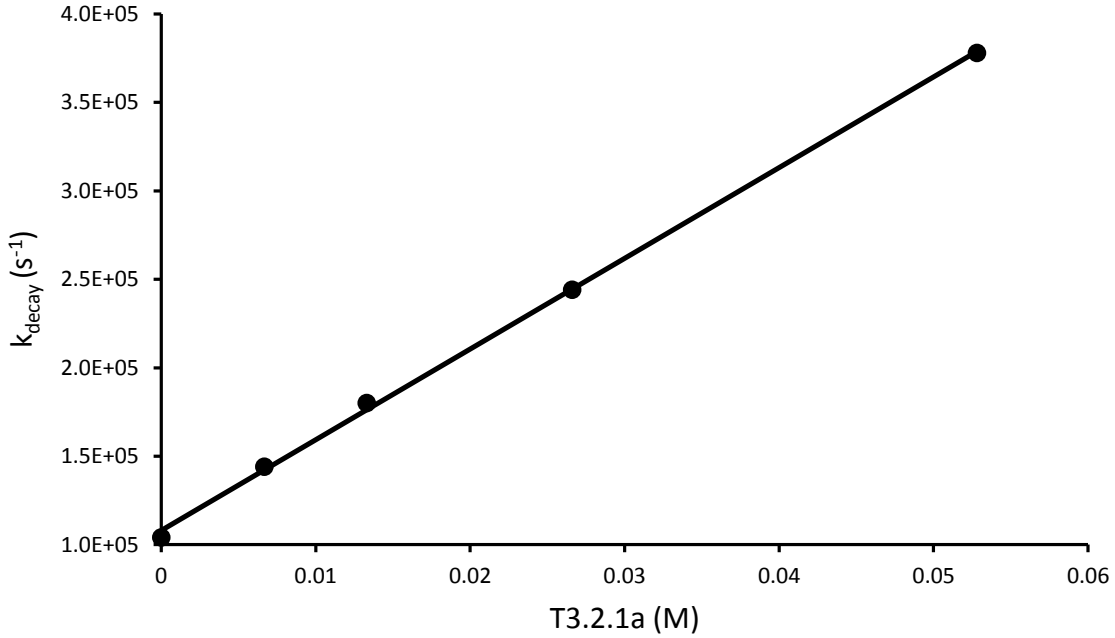

Figure 5.25 : Kinetic quenching plot showing the quenching of $^3Au_2(3,5\text{-}CF_3\text{-}dppm)_2Cl_2$ by butyl bromide. The slope of the plot corresponds to the bimolecular rate constant.

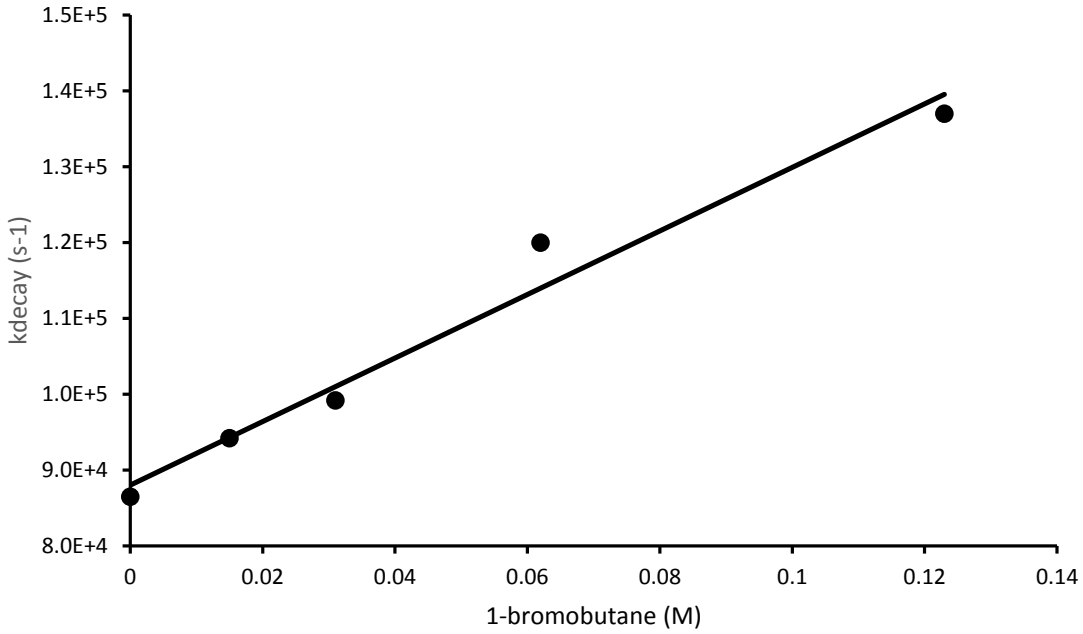

*$Au_3(tppm)_2Cl_3$ **(F3.4.3)***

Figure 5.26 : Transient emission spectrum showing the $^3Au_3(tppm)_2Cl_3$ signal obtained upon laser pulse excitation (355 nm, 10 mJ) of a $Au_3(tppm)_2Cl_3$ sample which had been purged of oxygen.

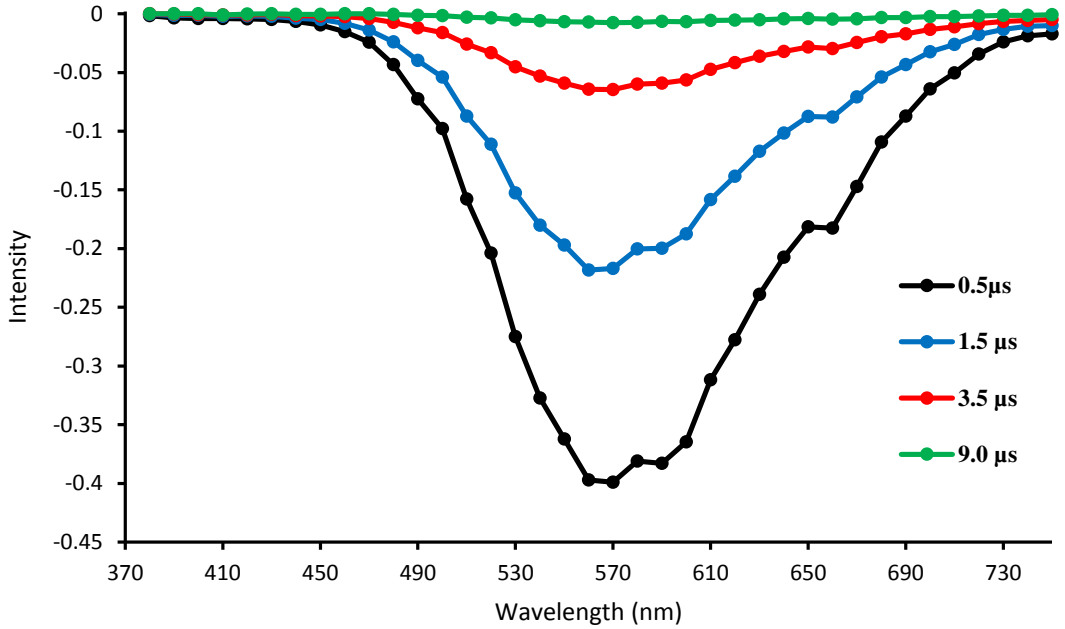

Figure 5.27 : Decay trace of $^3Au_3(tppm)_2Cl_3$ at 560 nm obtained upon laser pulse excitation (355 nm, 10 mJ) of a $Au_3(tppm)_2Cl_3$ sample which had been purged of oxygen.

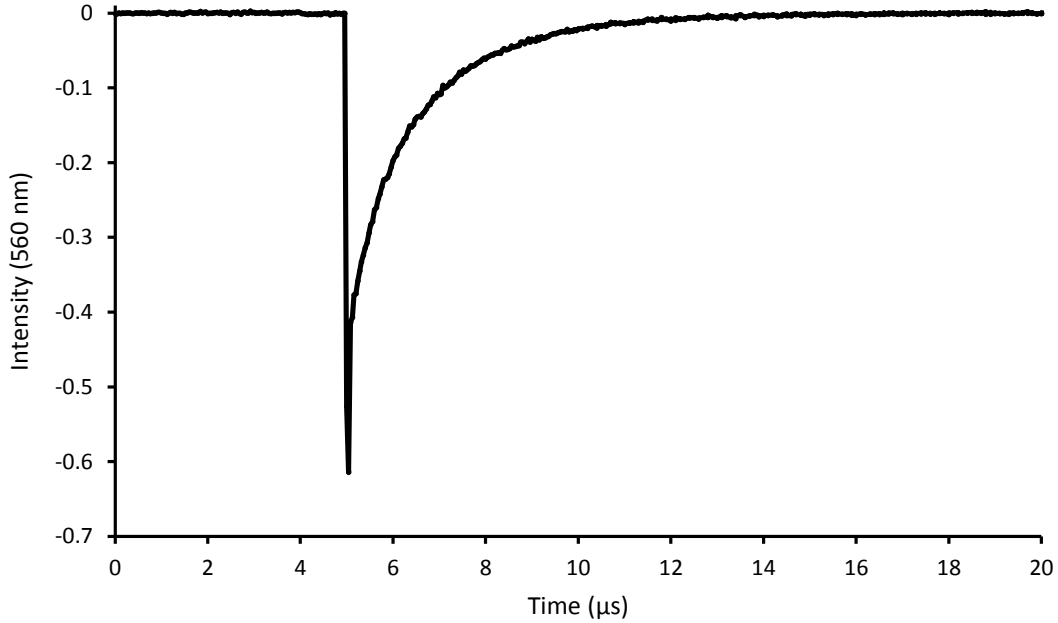

Figure 5.28 : Kinetic quenching plot showing the quenching of $^3Au_3(tppm)_2Cl_3$ by iPr_2NEt. The slope of the plot corresponds to the bimolecular rate constant.

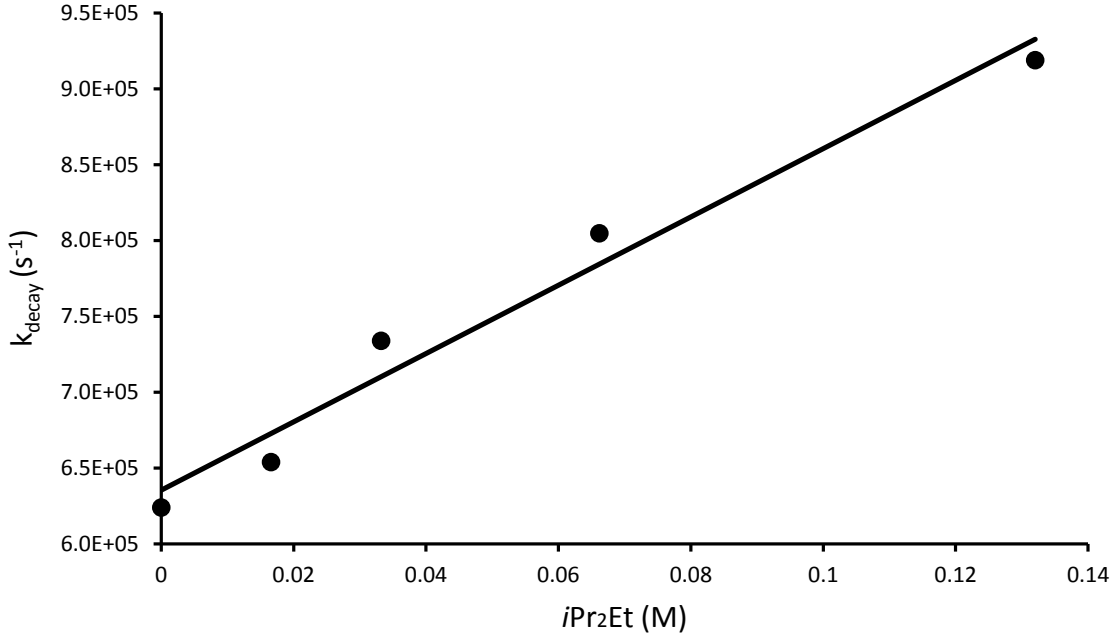

*Figure 5.29 : Kinetic quenching plot showing the quenching of $^3Au_3(tppm)_2Cl_3$ by substrate **T3.2.1a**. The slope of the plot corresponds to the bimolecular rate constant.*

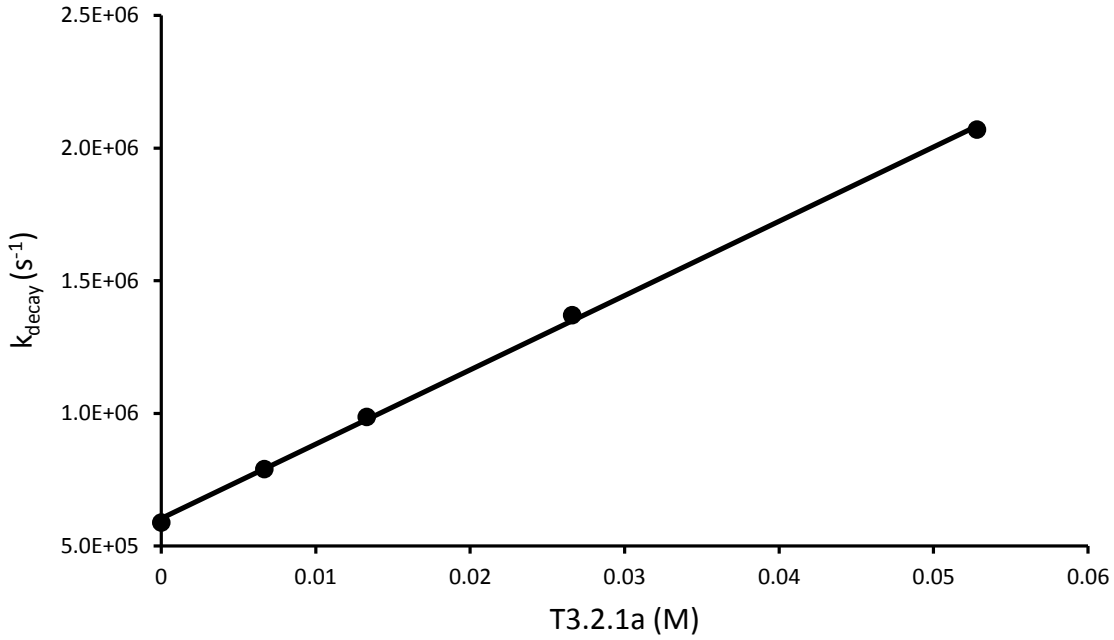

Figure 5.30 : Kinetic quenching plot showing the quenching of $^3Au_3(tppm)_2Cl_3$ by butyl bromide. The slope of the plot corresponds to the bimolecular rate constant.

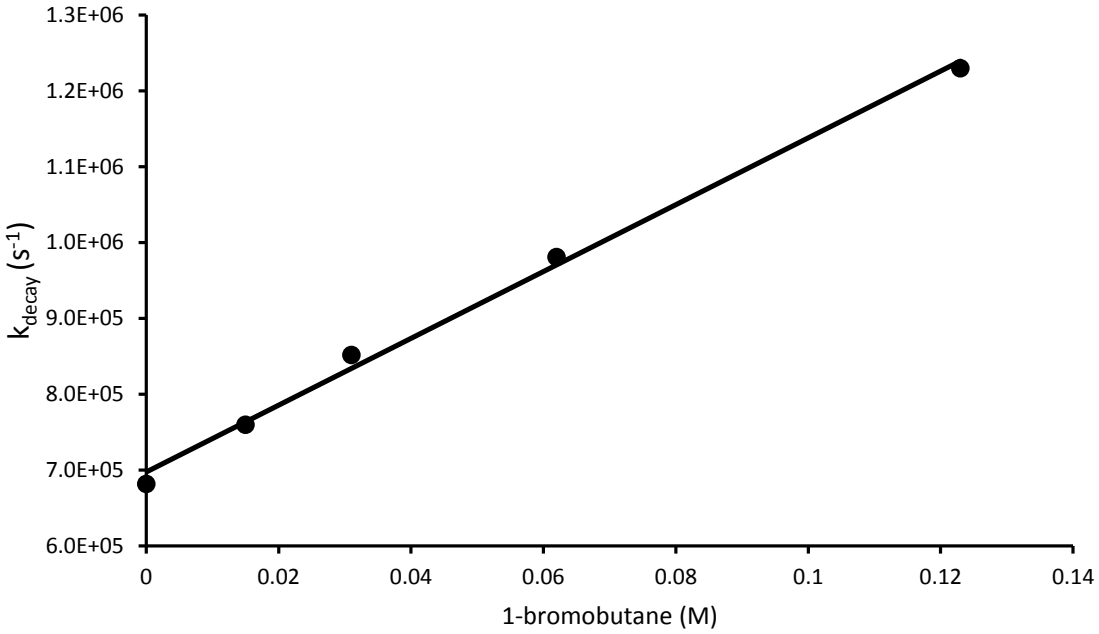

$Au_2(bmimm)_2Cl_2$ ***(F3.4.4)***

Figure 5.31 : Transient emission spectrum showing the $^3Au_2(bmimm)_2Cl_2$ signal obtained upon laser pulse excitation (308 nm, 10 mJ) of a $Au_2(bmimm)_2Cl_2$ sample which had been purged of oxygen.

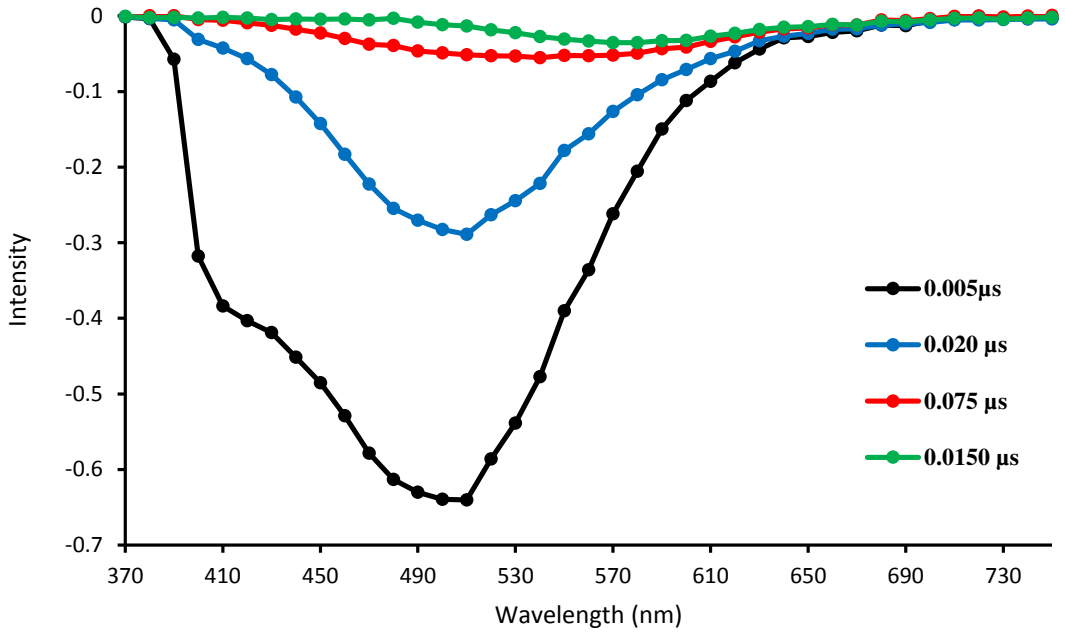

Figure 5.32 : Decay trace of $^3Au_2(bmimm)_2Cl_2$ at 510 nm obtained upon laser pulse excitation (308 nm, 10 mJ) of a $Au_2(bmimm)_2Cl_2$ sample which had been purged of oxygen.

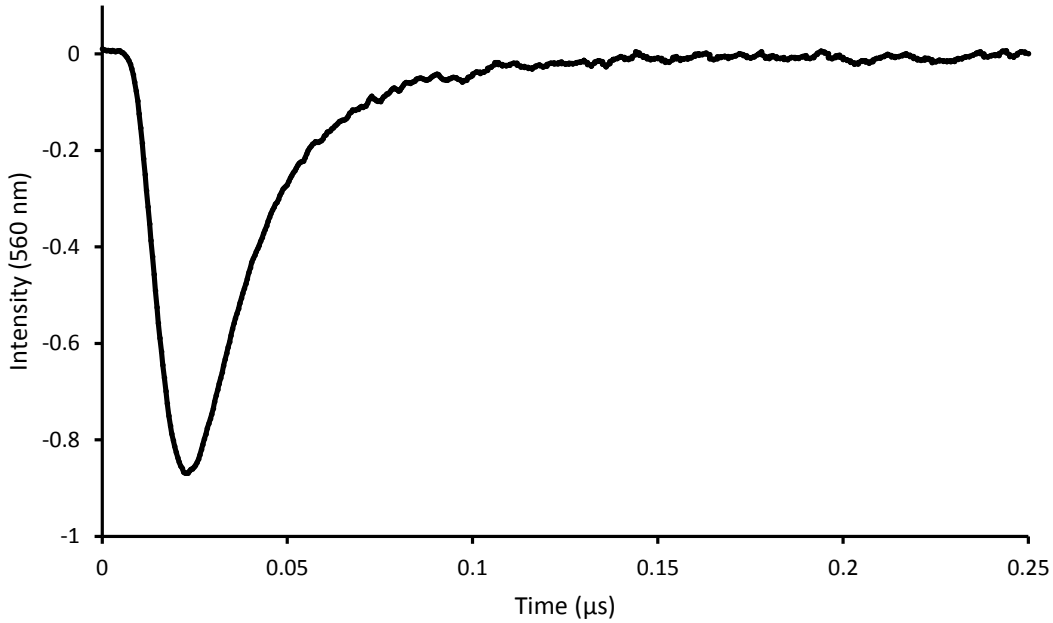

Figure 5.33 : Kinetic quenching plot showing the quenching of $^3Au_2(bmimm)_2Cl_2$ by iPr_2NEt. The slope of the plot corresponds to bimolecular rate constant.

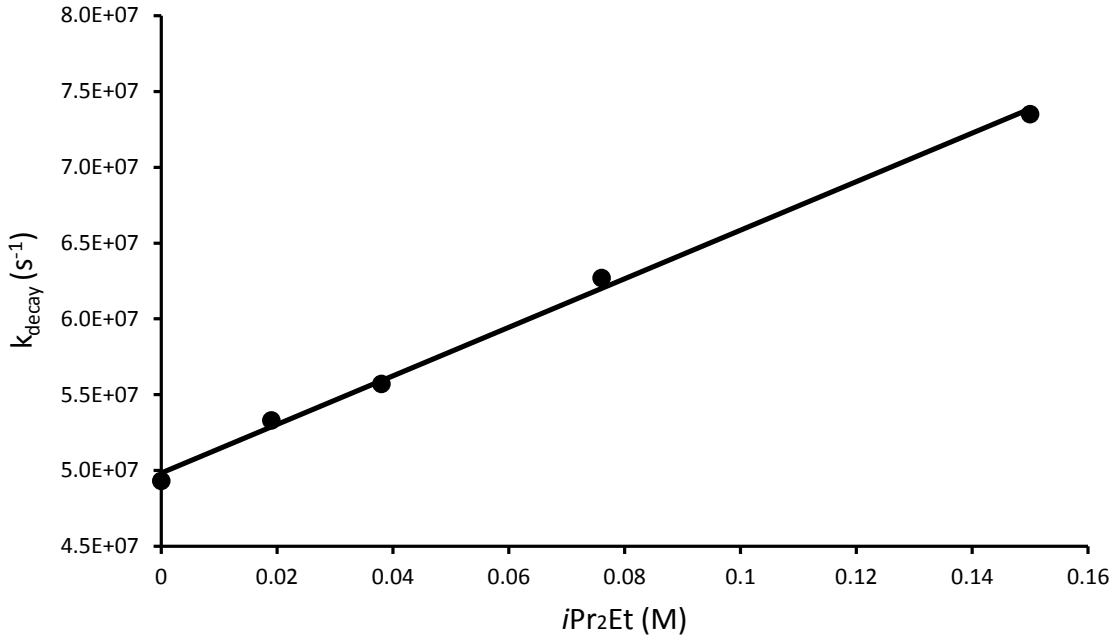

*Figure 5.34 : Kinetic quenching plot showing the quenching of $^3Au_2(bmimm)_2Cl_2$ by substrate **T3.2.1a**. The slope of the plot corresponds to bimolecular rate constant.*

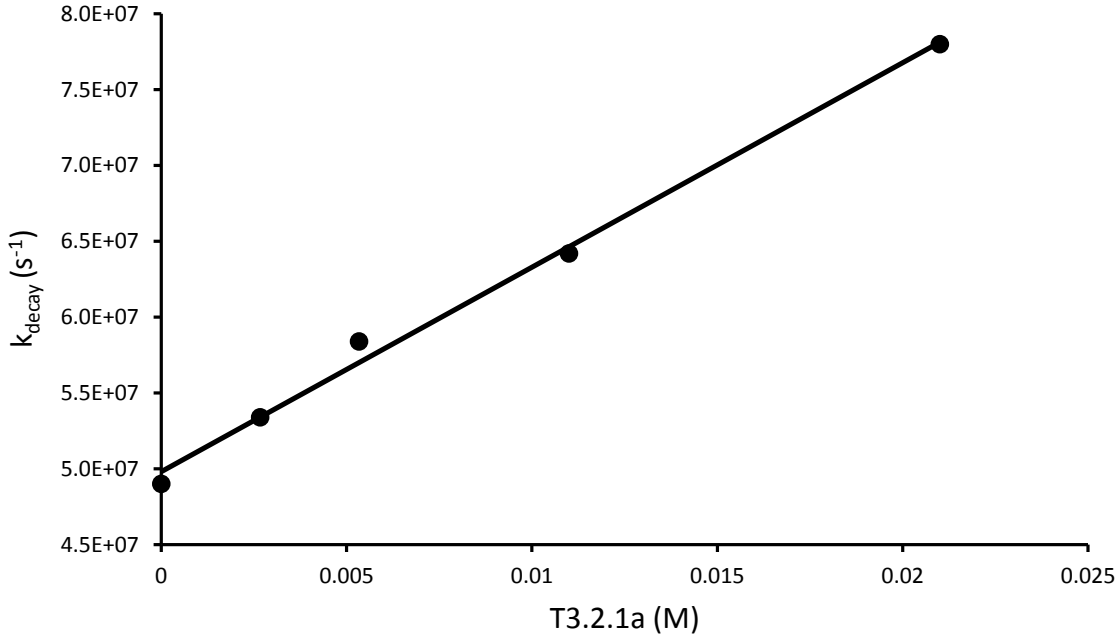

Figure 5.35: Kinetic quenching plot showing the quenching of $^3Au_2(bmimm)_2Cl_2$ by butyl bromide. The slope of the plot corresponds to bimolecular rate constant.

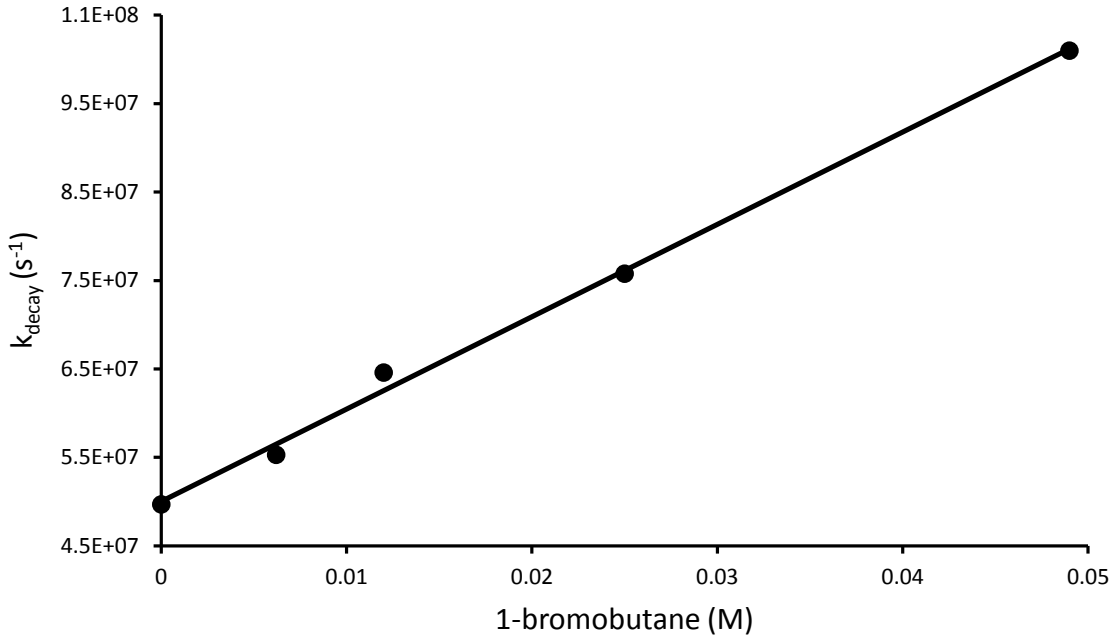

5.3.4.4 Cyclic voltametry measurements of the Au_x complexes

(collected by Chris McTiernan)

Conditions for cyclic voltammetry measurements: scan rate = 100 mV s^{-1}; 0.5-2.0 mM Au (I) complex in Ar degassed MeCN containing 100 mM Bu_4NClO_4 supporting electrolyte; Pt wire working electrode; Pt wire counter electrode; Ag wire pseudo-reference electrode; Fc/Fc^+ redox couple as internal reference (0.41 V vs. SCE); oxidation and reduction potential reported as peak anodic (E_{pa}) and peak cathodic (E_{pc}) potentials due to their irreversible nature.

*$Au_2(dppm)_2Cl_2$ (**F3.1.1**)*

Figure 5.36 : Cyclic voltammogram of $Au_2(dppm)_2Cl_2$ [Anodic Scan].

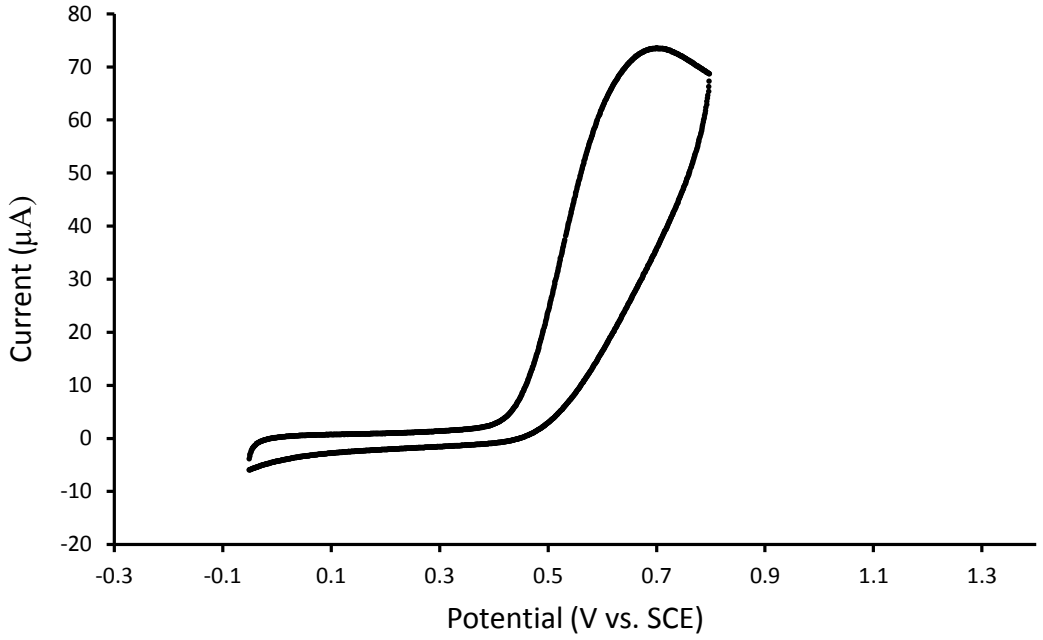

Figure 5.37 : Cyclic voltammogram of $Au_2(dppm)_2Cl_2$ [Cathodic Scan].

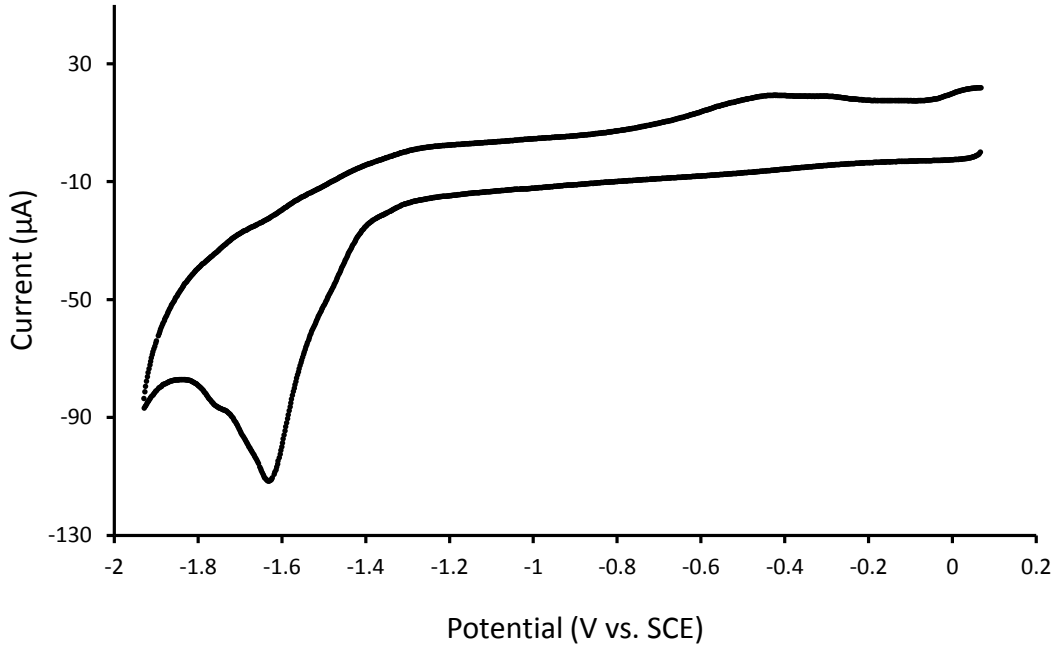

*$Au_2(dppm)_2Cl_2$ (**F3.1.1**)*

Figure 5.38 : Cyclic voltammogram of $Au_2(dmpm)_2Cl_2$ [Anodic Scan].

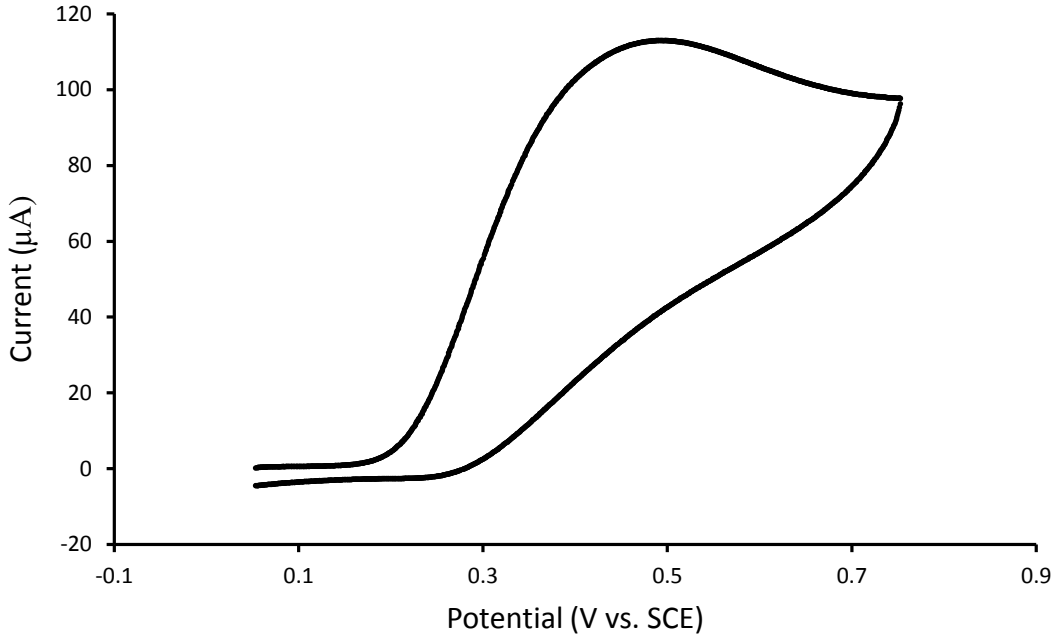

Figure 5.39 : Cyclic voltammogram of $Au_2(dmpm)_2Cl_2$ [Cathodic Scan].

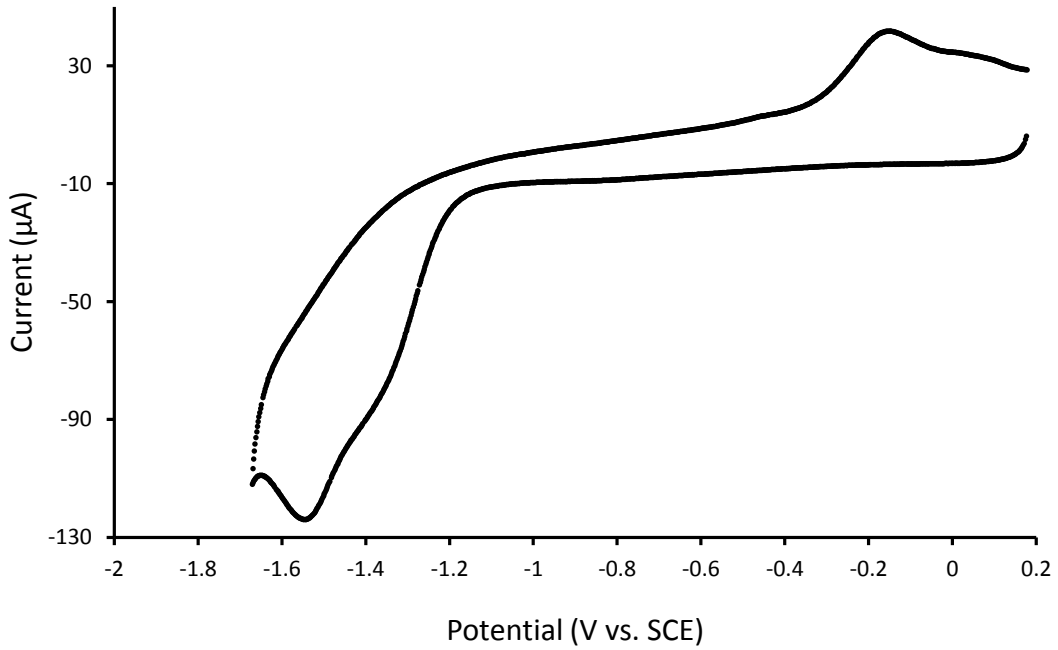

$Au_2(3,5\text{-}CF_3\text{-}dppm)_2Cl_2$ ***(F3.4.2)***

Figure 5.40 : Cyclic voltammogram of $Au_2(3,5\text{-}CF_3\text{-}dppm)_2Cl_2$ [Anodic Scan].

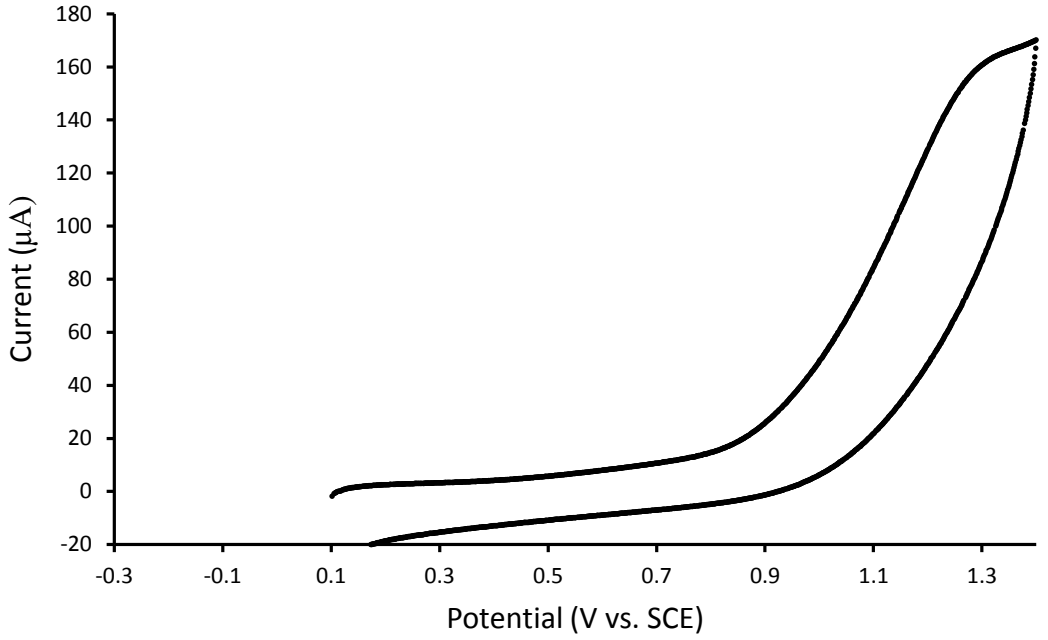

Figure 5.41 : Cyclic voltammogram of $Au_2(3,5\text{-}CF_3\text{-}dppm)_2Cl_2$ [Cathodic Scan].

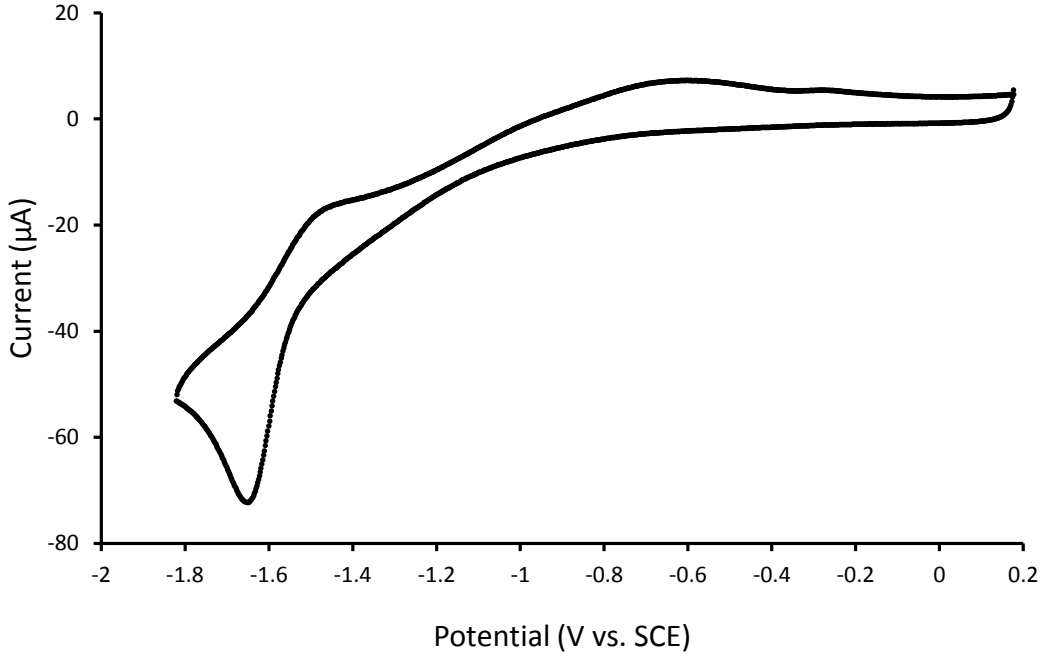

$Au_3(tppm)_2Cl_3$ ***(F3.4.3)***

Figure 5.42 : Cyclic voltammogram of $Au_3(tppm)_2Cl_3$ [Anodic Scan].

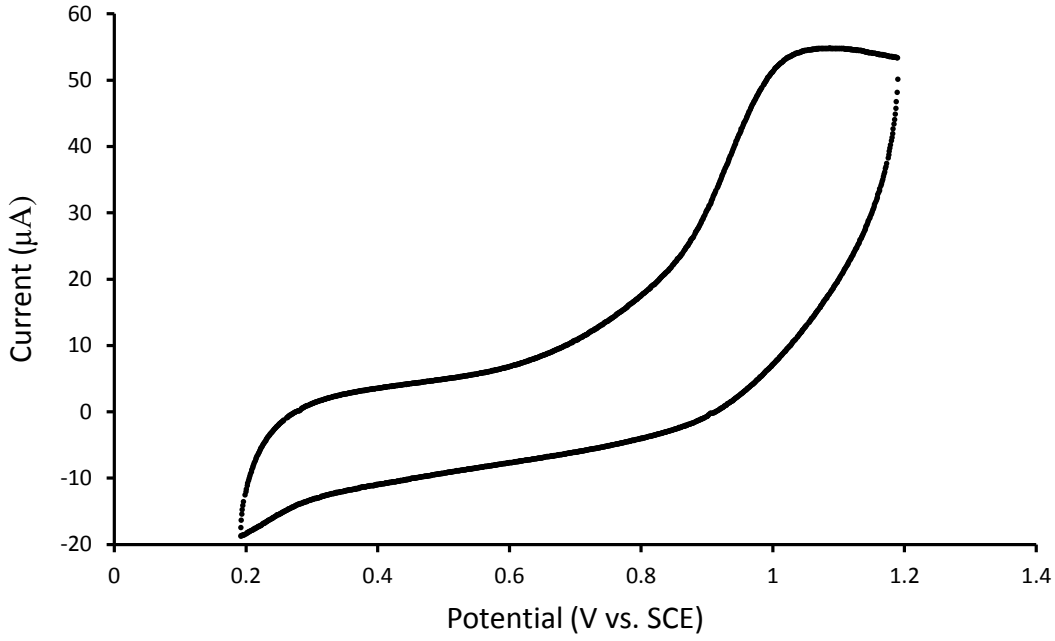

Figure 5.43 : Cyclic voltammogram of $Au_3(tppm)_2Cl_3$ [Cathodic Scan].

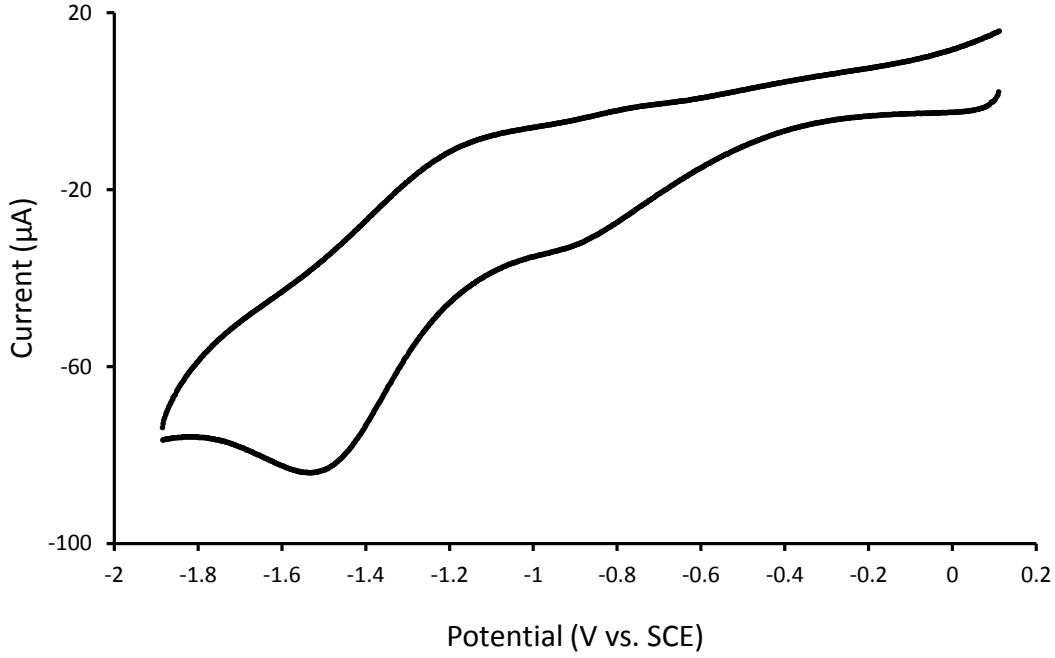

$Au_2(bmimm)_2Cl_2$ ***(F3.4.4)***

Figure 5.44 : Cyclic voltammogram of $Au_2(bmimm)_2Cl_2$ [Anodic Scan].

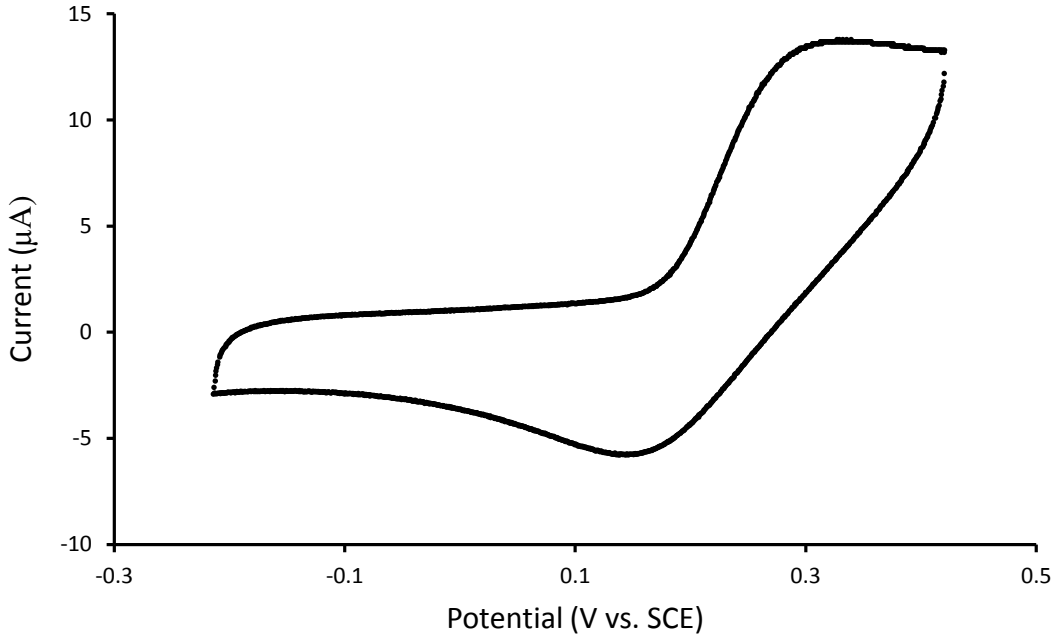

5.3.5 Compounds and supplemental information for Chapter 3.5

(***GP5.3.7***) **General procedure for the formation of biarenes from iodoarenes**

To an oven dried 8 mL Pyrex screw-top reaction vessel was added the iodoarene (0.2 mmol, 1.0 equiv.), $[Au_2(dppm)_2]Cl_2$ (0.01 mmol, 0.05 equiv.), K_2HPO_4 (0.2 mmol, 1.0 equiv.), degassed MeCN and degassed MeOH (1:1, 400 μL total, 0.5 M). Triethylamine (0.2 mmol, 1.0 equiv.) was then added to the solution. The reaction vessel was capped and back-filled with argon for 30 seconds, then irradiated with a UVA (365 nm) LED at an approximate distance of 5 mm for 16 hours. The resulting mixture was concentrated and the crude residue was further purified by flash chromatography (0-100% EtOAc:Hexanes), where the product was isolated from the relevant fractions.

(***GP5.3.8***) **General procedure for the formation of of homocoupled bromoalkanes**

To an oven dried 8 mL Pyrex screw-top reaction vessel was added the bromoalkane (0.4 mmol, 1.0 equiv.), $[Au_2(dppm)_2]Cl_2$ (0.02 mmol, 0.05 equiv.), CD_3CN and CD_3OD (1:1, 0.8 mL total, 0.5 M), and d_{15}-Triethylamine (0.4 mmol, 1.0 equiv., added after sparging). The reaction vessel was capped, degassed with argon by sparging for 5 minutes, then irradiated with a UVA (365 nm) LED at an approximate distance of 5 mm for 16 hours. The resulting mixture was concentrated and the crude residue was further purified by flash chromatography (0-100% EtOAc:Hexanes), where the product was isolated from the relevant fractions.

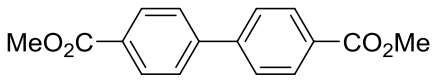

T3.11.2: dimethyl [1,1'-biphenyl]-4,4'-dicarboxylate

Synthesized according to ***GP5.3.7*** affording 25 mg (91%) of an amorphous solid, spectral data was consistent with literature.[131]

^{1}H NMR (400MHz, CHLOROFORM-d) δ ppm = 8.14 (dt, *J* = 8.4, 1.9 Hz, 4 H), 7.70 (dt, *J* = 8.4, 1.8 Hz, 4 H), 3.96 (s, 6 H). ^{13}C NMR (101MHz, CHLOROFORM-d) δ ppm = 166.8 (2 X C), 144.3 (2 X C), 130.2 (4 X CH), 129.7 (2 X C), 127.2 (4 X CH), 52.2 (2 X CH_3).

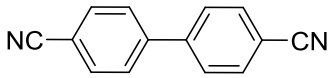

F3.13.2a: [1,1'-biphenyl]-4,4'-dicarbonitrile

Synthesized according to ***GP5.3.7***, affording 12 mg (60%) of an amorphous solid, spectral data was consistent with literature.[132]

^{1}H NMR (400MHz, CHLOROFORM-d) δ ppm = 7.79-7.73 (m, 4 H), 7.71-7.64 (m, 4 H). ^{13}C NMR (101MHz, CHLOROFORM-d) δ ppm = 143.5 (2 X C), 132.9 (4 X CH), 128.0 (4 X CH), 118.4 (2 X C), 112.5 (2 X C).

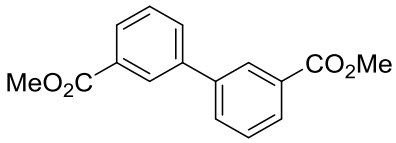

F3.13.2b: dimethyl [1,1'-biphenyl]-3,3'-dicarboxylate

Synthesized according to ***GP5.3.7***, affording 18 mg (66%) of an amorphous solid, spectral data was consistent with literature.[1]

^{1}H NMR (400MHz, CHLOROFORM-d) δ ppm = 8.31 (t, *J* = 1.7 Hz, 2 H), 8.06 (dt, *J* = 7.8, 1.3 Hz, 2 H), 7.85-7.80 (m, 2 H), 7.55 (t, *J* = 7.7 Hz, 2 H), 3.97 (s, 6 H). ^{13}C NMR (101MHz, CHLOROFORM-d) δ ppm = 166.9 (2 X C), 140.4 (2 X C), 131.5 (2 X CH), 130.9 (2 X C), 129.0 (2 X CH), 128.8 (2 X CH), 128.3 (2 X CH), 52.3 (2 X CH_3).

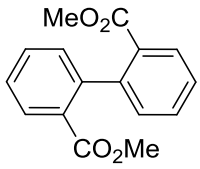

F3.13.2c: dimethyl [1,1'-biphenyl]-2,2'-dicarboxylate

Synthesized according to ***GP5.3.7***, affording 4 mg (14%) of an amorphous solid, spectral data was consistent with literature.[131]

^{1}H NMR (400MHz, CHLOROFORM-d) δ ppm = 8.02 (dd, *J* = 7.8, 1.4 Hz, 2 H), 7.55 (td, *J* = 7.5, 1.5 Hz, 2 H), 7.44 (td, *J* = 7.6, 1.3 Hz, 2 H), 7.22 (dd, *J* = 7.5, 1.2 Hz, 2 H), 3.63 (s, 6 H).^{13}C NMR (101MHz, CHLOROFORM-d) δ ppm = 167.4 (2 X C), 143.3 (2 X C), 131.4 (2 X CH), 130.2 (2 X CH), 129.8 (2 X CH), 129.4 (2 X C), 127.2 (2 X CH), 51.8 (2 X CH_3).

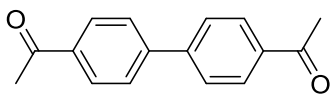

<u>F3.13.2d:</u> 1,1'-([1,1'-biphenyl]-4,4'-diyl)bis(ethan-1-one)

Synthesized according to ***GP5.3.7***, affording 15 mg (63%) of an amorphous solid, spectral data was consistent with literature.[131]

^{1}H NMR (400MHz, CHLOROFORM-d) δ ppm = 8.08-8.00 (m, 4 H), 7.74-7.67 (m, 4 H), 2.63 (s, 6 H). ^{13}C NMR (101MHz, CHLOROFORM-d) δ ppm = 197.6 (2 X C), 144.3 (2 X C), 136.6 (2 X C), 129.0 (4 X CH), 127.5 (4 X CH), 26.7 (2 X CH_3).

<u>F3.13.2e:</u> [1,1'-biphenyl]-4,4'-dicarbaldehyde

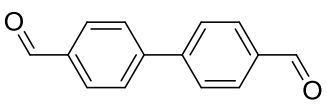

Synthesized according to ***GP5.3.7***, affording 12 mg (59%) of an amorphous solid, spectral data was consistent with literature.[131]

^{1}H NMR (400MHz, CHLOROFORM-d) δ ppm = 10.10 (s, 2 H), 8.04-7.97 (m, 4 H), 7.85-7.78 (m, 4 H). ^{13}C NMR (101MHz, CHLOROFORM-d) δ ppm = 191.7 (2 X CH), 145.6 (2 X C), 136.0 (2 X C), 130.4 (4 X CH), 128.0 (4 X CH).

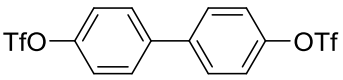

<u>F3.13.2f:</u> [1,1'-biphenyl]-4,4'-diyl bis(trifluoromethanesulfonate)

Synthesized according to ***GP5.3.7***, affording 26 mg (57%) of an amorphous solid. *(characterized by Huy Tran)*

^{1}H NMR (400MHz, CHLOROFORM-d) δ ppm = 7.63 (s, 4 H), 7.41-7.37 (m, 4 H). ^{13}C NMR (101MHz, CHLOROFORM-d) δ ppm = 149.4 (2 X C), 139.7 (2 X C), 129.0 (4 X CH), 122.0 (4 X CH), 118.8 (q, *J* = 321.3 Hz, 2 X C). IR (neat, cm^{-1}): 1421(s), 1204(vs), 1134(vs), 878(s), 829(s), 743(s). HRMS (EI) m/z calculatedd for $C_{14}H_8F_6O_6S_2$ $[M]^+$: 449.9666 found: 449.9700.

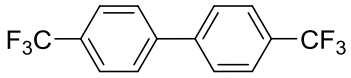

F3.13.2g: 4,4'-bis(trifluoromethyl)-1,1'-biphenyl

Synthesized according to ***GP5.3.7***, affording 18 mg (61%) of an amorphous solid, spectral data was consistent with literature.[131]

^{1}H NMR (400MHz, CHLOROFORM-d) δ ppm = 7.78-7.69 (m, 8 H). ^{13}C NMR (101MHz, CHLOROFORM-d) δ ppm = 143.2 (2 X C), 130.3 (q, *J* = 32.6 Hz, 2 X C), 127.6 (4 X CH), 125.9 (q, *J* = 3.8 Hz, 4 X CH), 124.1 (q, *J* = 272.2 Hz, 2 X C).

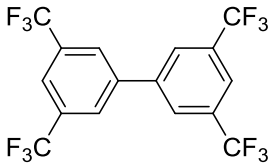

F3.13.2h: 3,3',5,5'-tetrakis(trifluoromethyl)-1,1'-biphenyl

Synthesized according to ***GP5.3.7***, affording 15 mg (35%) of an amorphous solid, spectral data was consistent with literature.[133]

^{1}H NMR (400MHz, CHLOROFORM-d) δ ppm = 8.01 (s, 4 H), 7.97 (s, 2 H). ^{13}C NMR (101MHz, CHLOROFORM-d) δ ppm = 140.4 (2 X C), 132.9 (q, *J* = 34.5 Hz, 4 X C), 127.5 (d, *J* = 2.9 Hz, 4 X CH), 122.6 (spt, *J* = 3.7 Hz, 2 X CH), 123.0 (q, *J* = 272.2 Hz, 4 X C).

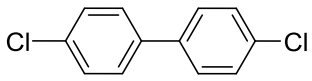

F3.13.2i: 4,4'-dichloro-1,1'-biphenyl

Synthesized according to ***GP5.3.7***, affording 12 mg (52%) of an amorphous solid, spectral data was consistent with literature.[134]

^{1}H NMR (400MHz, CHLOROFORM-d) δ ppm = 7.52-7.46 (m, 4 H), 7.45-7.39 (m, 4 H). ^{13}C NMR (101MHz, CHLOROFORM-d) δ ppm = 138.4 (2 X C), 133.8 (2 X C), 129.1 (4 X CH), 128.2 (4 X CH).

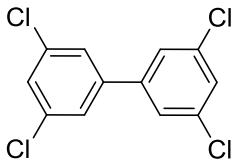

F3.13.2j: 3,3',5,5'-tetrachloro-1,1'-biphenyl

Synthesized according to ***GP5.3.7***, affording 15 mg (52%) of an amorphous solid, spectral data was consistent with literature.[135]

^{1}H NMR (400MHz, CHLOROFORM-d) δ ppm = 7.44-7.38 (m, 6 H). ^{13}C NMR (101MHz, CHLOROFORM-d) δ ppm = 141.4 (2 X C), 135.7 (4 X C), 128.4 (2 X CH), 125.6 (4 X CH).

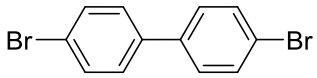

F3.13.2k: 4,4'-dibromo-1,1'-biphenyl

Synthesized according to ***GP5.3.7***, affording 10 mg (31%) of an amorphous solid, spectral data was consistent with literature.[131]

^{1}H NMR (400MHz, CHLOROFORM-d) δ ppm = 7.60-7.54 (m, 4 H), 7.46-7.39 (m, 4 H). ^{13}C NMR (101MHz, CHLOROFORM-d) δ ppm = 138.9 (2 X C), 132.0 (4 X CH), 128.5 (4 X CH), 122.0 (2 X C).

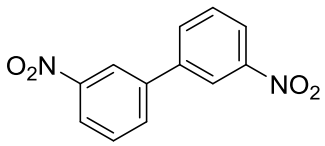

F3.13.2l: 3,3'-dinitro-1,1'-biphenyl

Synthesized according to ***GP5.3.7***, affording 10 mg (39%) of an amorphous solid, spectral data was consistent with literature.[136]

^{1}H NMR (400MHz, CHLOROFORM-d) δ ppm = 8.48 (t, *J* = 2.0 Hz, 2 H), 8.31-8.25 (m, 2 H), 7.99-7.92 (m, 2 H), 7.69 (t, *J* = 8.0 Hz, 2 H). ^{13}C NMR (101MHz, CHLOROFORM-d) δ ppm = 148.9 (2 X C), 140.3 (2 X C), 133.0 (2 X CH), 130.3 (2 X CH), 123.3 (2 X CH), 122.1 (2 X CH).

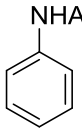

F3.13.2m: N-phenylacetamide

Synthesized according to ***GP5.3.7***, affording 23 mg (85%) of an amorphous solid, spectral data was consistent with literature.[137]

^{1}H NMR (400MHz, $(CD_3)_2CO$) δ ppm = 9.13 (br. s., 1 H), 7.63 (d, *J* = 7.8 Hz, 2 H), 7.27 (t, *J* = 7.9 Hz, 2 H), 7.02 (t, *J* = 7.4 Hz, 1 H), 2.07 (s, 3 H). ^{13}C NMR (101MHz, $(CD_3)_2CO$) δ ppm = 168.8 (C), 140.7 (C), 129.5 (2 X CH), 124.0 (CH, rotamers), 120.0-119.9 (2 X CH, rotamers), 24.3 (CH_3).

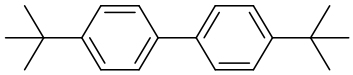

F3.13.2n: 4,4'-di-tert-butyl-1,1'-biphenyl

Synthesized according to ***GP5.3.7***, affording 14 mg (53%) of an amorphous solid, spectral data was consistent with literature.[138]

^{1}H NMR (400MHz, CHLOROFORM-d) δ ppm = 7.55 (dt, *J* = 8.4, 2.0 Hz, 4 H), 7.47 (dt, *J* = 8.3, 1.7 Hz, 4 H), 1.38 (s, 18 H). ^{13}C NMR (101MHz, CHLOROFORM-d) δ ppm = 149.9 (2 X C), 138.2 (2 X C), 126.6 (4 X CH), 125.6 (4 X CH), 34.5 (2 X C), 31.4 (6 X CH_3).

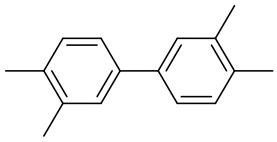

F3.13.2o: 3,3',4,4'-tetramethyl-1,1'-biphenyl

Synthesized according to ***GP5.3.7***, affording 10 mg (47%) of an amorphous solid, spectral data was consistent with literature.[136]

^{1}H NMR (400MHz, CHLOROFORM-d) δ ppm = 7.37-7.33 (m, 2 H), 7.31 (dd, *J* = 7.6, 1.8 Hz, 2 H), 7.17 (d, *J* = 7.8 Hz, 2 H), 2.32 (s, 6 H), 2.29 (s, 6 H). ^{13}C NMR (101MHz, CHLOROFORM-d) δ ppm = 138.9 (2 X C), 136.8 (2 X C), 135.3 (2 X C), 130.0 (2 X CH), 128.3 (2 X CH), 124.4 (2 X CH), 19.9 (2 X CH_3), 19.4 (2 X CH_3).

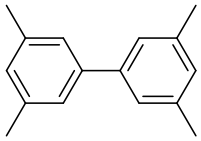

F3.13.2p: 3,3',5,5'-tetramethyl-1,1'-biphenyl

Synthesized according to ***GP5.3.7***, affording 7 mg (34%) of an amorphous solid, spectral data was consistent with literature.[139]

^{1}H NMR (400MHz, CHLOROFORM-d) δ ppm = 7.18 (s, 4 H), 6.96 (s, 2 H), 2.36 (s, 6 H), 2.36 (s, 6 H). ^{13}C NMR (101MHz, CHLOROFORM-d) δ ppm = 141.5 (2 X C), 138.1 (4 X C), 128.7 (2 X CH), 125.1 (4 X CH), 21.4 (4 X CH_3).

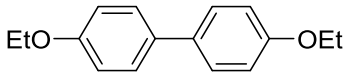

F3.13.2q: 4,4'-diethoxy-1,1'-biphenyl

Synthesized according to ***GP5.3.7***, affording 7 mg (29%) of an amorphous solid, spectral data was consistent with literature.[140]

^{1}H NMR (400MHz, CHLOROFORM-d) δ ppm = 7.50-7.45 (m, 4 H), 6.99-6.92 (m, 4 H), 4.08 (q, *J* = 7.0 Hz, 4 H), 1.45 (t, *J* = 7.0 Hz, 6 H). ^{13}C NMR (101MHz, CHLOROFORM-d) δ ppm = 158.0 (2 X C), 133.4 (2 X C), 127.7 (4 X CH), 114.7 (4 X CH), 63.5 (2 X CH_2), 14.9 (2 X CH_3).

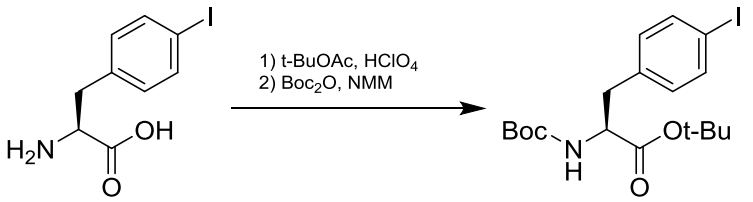

F3.13.1r: tert-butyl (S)-2-((tert-butoxycarbonyl)amino)-3-(4-iodophenyl)propanoate

Synthesized according to literature procedure and spectral data was consistent with literature.[141]

^{1}H NMR (400MHz, CHLOROFORM-d) δ ppm = 7.60-7.58 (m, 2H), 6.91-6.89 (m, 2H), 4.96 (d, *J* = 7.5 Hz, 1H), 4.40 (q, *J* = 6.8 Hz, 1H), 3.03-2.92 (m, 2H), 1.40 (s, 9H), 1.39 (s, 9H). ^{13}C NMR (101MHz, CHLOROFORM-d) δ ppm = 170.6 (C), 155.0 (C), 137.4 (2 X CH), 136.1 (C), 131.6 (2 X CH), 92.2 (C), 82.3 (C), 79.8 (C), 54.6 (CH), 38.0 (CH_2), 28.3 (3 X CH_3), 28.0 (3 X CH_3).

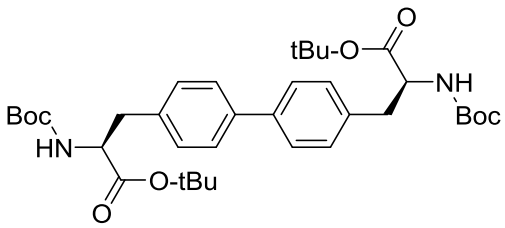

<u>F3.13.2r:</u> di-tert-butyl 3,3'-([1,1'-biphenyl]-4,4'-diyl)(2S,2'S)-bis(2-((tert-butoxycarbonyl)amino)propanoate)

Synthesized according to ***GP5.3.7*** on a 0.181 mmol scale, affording 38 mg (66%) of an amorphous solid.

^{1}H NMR (400MHz, CHLOROFORM-d) δ ppm = 7.47 (d, *J* = 8.0 Hz, 2 H), 7.28-7.14 (m, 6 H), 5.02-4.73 (m, 2 H), 4.48-4.27 (m, 2 H), 3.05 (dd, *J* = 16.1, 5.9 Hz, 4 H), 1.40 (s, 9 H), 1.40 (s, 9 H), 1.39 (s, 9 H), 1.37 (s, 9 H). ^{13}C NMR (101MHz, CHLOROFORM-d) δ ppm = 171.9 (2 X C), 155.1 (2 X C), 139.3 (2 X C), 136.4 (C), 135.4 (C), 129.9 (2 X CH), 129.5 (2 X CH), 128.3 (2 X CH), 126.8 (CH), 126.8 (CH), 82.1 (C), 82.0 (C), 79.6 (C), 79.6 (C), 54.8 (2 X CH), 38.5 (CH_2), 38.2 (CH_2), 28.3 (6 X CH_3), 27.9 (3 X CH_3), 27.9 (3 X CH_3). IR (neat, cm^{-1}): 3441(br), 2977(m), 2932(m), 1712(vs), 1709(vs), 1702(vs), 1698(vs), 1497(m), 1366(s), 701 (vs). HRMS (ESI) m/z calculated for $C_{36}H_{52}N_2NaO_8$ [M + Na^+] 663.3616, found: 663.3621. *(characterized by Huy Tran)*

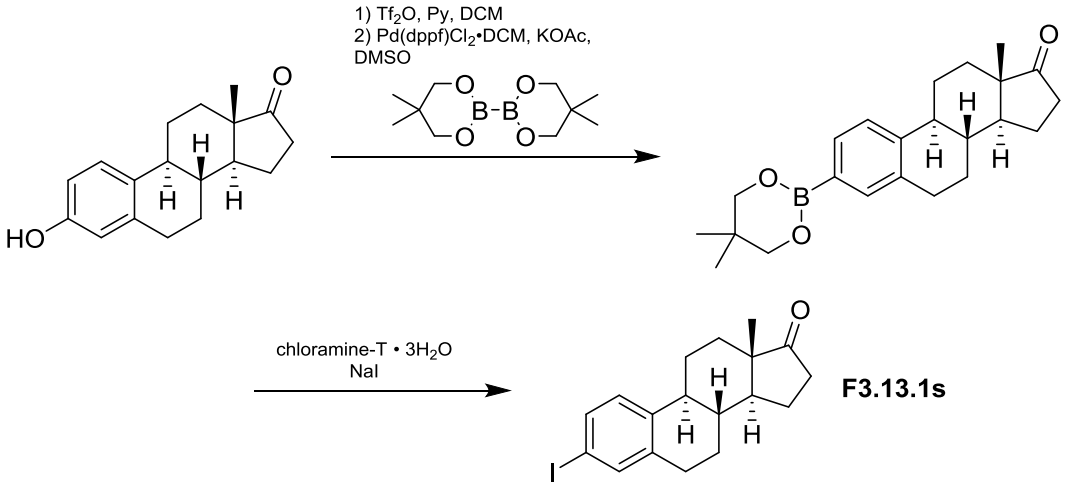

F3.13.1s: (8R,9S,13S,14S)-3-iodo-13-methyl-6,7,8,9,11,12,13,14,15,16-decahydro-17H-cyclopenta[a]phenanthren-17-one

Synthesized according to literature procedure and spectral data was consistent with literature.[142] ^{1}H NMR (400MHz, CHLOROFORM-d) δ ppm = 7.50-7.43 (m, 2 H), 7.03 (d, *J* = 8.0 Hz, 1 H), 2.88 (dd, *J* = 8.7, 4.1 Hz, 2 H), 2.52 (dd, *J* = 18.8, 8.5 Hz, 1 H), 2.42-2.34 (m, 1 H), 2.30-2.21 (m, 1 H), 2.21-1.94 (m, 4 H), 1.70-1.36 (m, 6 H), 0.91 (s, 3 H). ^{13}C NMR (101MHz, CHLOROFORM-d) δ ppm = 220.5 (C), 139.4 (C), 139.1 (C), 137.6 (CH), 134.6 (CH), 127.3 (CH), 91.1 (CH), 50.3 (CH), 47.8 (C), 44.1 (CH), 37.7 (CH), 35.7 (CH_2), 31.4 (CH_2), 28.9 (CH_2), 26.1 (CH_2), 25.4 (CH_2), 21.5 (CH_2), 13.7 (CH_3).

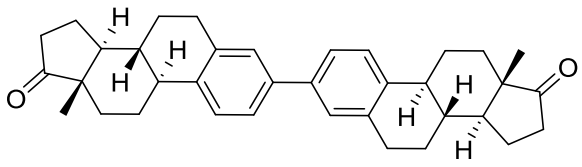

F3.13.2s: estrone dimer

Synthesized according to ***GP5.3.7***, affording 14 mg (28%) of an amorphous solid.

^{1}H NMR (400MHz, CHLOROFORM-d) δ ppm = 7.41-7.35 (m, 4 H), 7.33 (s, 2 H), 3.00 (dd, *J* = 8.8, 4.0 Hz, 4 H), 2.56-2.46 (m, 4 H), 2.37 (td, *J* = 10.7, 3.6 Hz, 2 H), 2.21-1.98 (m, 8 H), 1.71-1.47 (m, 12 H), 0.94 (s, 6 H). ^{13}C NMR (101MHz, CHLOROFORM-d) δ ppm = 220.89 (2 X C), 138.7 (2 X C), 138.6 (2 X C), 136.8 (2 X C), 127.5 (2 X CH), 125.7 (2 X CH), 124.4 (2 X CH), 50.5 (2 X CH), 48.0 (2 X C), 44.4 (2 X CH), 38.2 (2 X CH), 35.8 (2 X CH_2), 31.6 (2 X CH_2), 29.5 (2 X CH_2), 26.5 (2 X CH_2), 25.7 (2 X CH_2), 21.6 (2 X CH_2), 13.8 (2 X CH_3). IR (neat, cm^{-1}): 2928(m), 2863(m), 1737(vs). HRMS (EI) m/z calculated for $C_{36}H_{42}O_2$ $[M]^+$ 506.3185, found 506.3205.

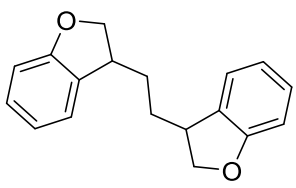

3.9.2: 1,2-bis(2,3-dihydrobenzofuran-3-yl)ethane

Synthesized according to ***GP5.3.7*** affording 5 mg (20%) of an amorphous solid, isolated as a diasteromeric mixture, spectral data was consistent with literature.[143]

^{1}H NMR (400MHz, CHLOROFORM-d) δ ppm = 7.22-7.09 (m, 4 H), 6.87 (tdd, *J* = 7.4, 1.6, 1.0 Hz, 2 H), 6.83-6.75 (m, 2 H), 4.63 (t, *J* = 8.8 Hz, 2 H), 4.22 (ddd, *J* = 8.8, 6.2, 1.5 Hz, 2 H), 3.52-3.36 (m, 2 H), 1.98-1.85 (m, 1 H), 1.85-1.68 (m, 2 H), 1.66-1.56 (m, 1 H). ^{13}C NMR (101MHz, CHLOROFORM-d) δ ppm = 159.9 (2 X C), 130.4 (C), 130.3 (C), 128.3 (2 X CH), 124.3 (CH), 124.2 (CH), 120.4 (CH), 120.4 (CH), 109.6 (2 X CH), 76.6 (CH_2), 76.5 (CH_2), 41.9 (CH), 41.9 (CH), 32.3 (CH_2), 32.2 (CH_2).

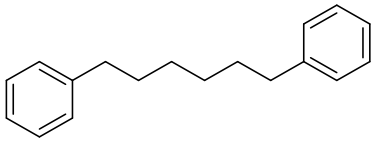

<u>F3.14.2a:</u> 1,6-diphenylhexane

Synthesized according to ***GP5.3.8***, affording 23 mg (50%) of an off yellow oil, spectral data was consistent with literature.[144]

^{1}H NMR (400MHz, CHLOROFORM-d) δ ppm = 7.32-7.27 (m, 4 H), 7.22-7.16 (m, 6 H), 2.65-2.58 (m, 4 H), 1.69-1.59 (m, 4 H), 1.44-1.35 (m, 4 H). ^{13}C NMR (101MHz, CHLOROFORM-d) δ ppm = 142.8 (2 X C), 128.4 (4 X CH), 128.2 (4 X CH), 125.6 (2 X CH), 35.9 (2 X CH_2), 31.4 (2 X CH_2), 29.1 (2 X CH_2).

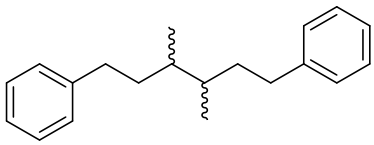

<u>F3.14.2b:</u> (3,4-dimethylhexane-1,6-diyl)dibenzene

Synthesized according to ***GP5.3.8*** 0.258 mmol scale, affording 18 mg (51%) of an off yellow oil as a statistical diastereomeric mixture, spectral data was consistent with literature.[145]

^{1}H NMR (400MHz, CHLOROFORM-d) δ ppm = 7.32-7.27 (m, 4 H), 7.22-7.15 (m, 6 H), 2.72-2.43 (m, 4 H), 1.71-1.60 (m, 2 H), 1.54-1.32 (m, 4 H), 0.93 (d, *J* = 6.7 Hz, 3 H), 0.87 (d, *J* = 6.5

Hz, 3 H). ^{13}C NMR (101MHz, CHLOROFORM-d) δ ppm = 143.1 (2 X C), 143.1 (2 X C), 128.4 (4 X CH), 128.3 (4 X CH), 128.3 (4 X CH), 128.3 (4 X CH), 125.6 (2 X CH), 125.6 (2 X CH), 37.1 (2 X CH), 36.9 (2 X CH_2), 36.2 (2 X CH), 35.0 (2 X CH_2), 34.1 (2 X CH_2), 34.0 (2 X CH_2), 16.3 (2 X CH_3), 14.3 (2 X CH_3).

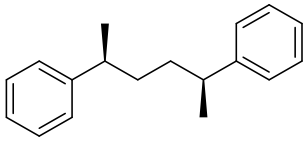

F3.14.2c ((2S,5S)-hexane-2,5-diyl)dibenzene

Synthesized according to ***GP5.3.8*** (51%) using **(*R*)-(1-bromopropan-2-yl)benzene** that was synthesized according to Barriault`s method[146] affording 24 mg (51%) of an off yellow oil, spectral data was consistent with literature.[147,148]

^{1}H NMR (400MHz, CHLOROFORM-d) δ ppm = 7.31-7.26 (m, 4 H), 7.21-7.11 (m, 6 H), 2.72-2.60 (m, 2 H), 1.54-1.44 (m, 4 H), 1.21 (d, *J* = 6.9 Hz, 6 H). ^{13}C NMR (101MHz, CHLOROFORM-d) δ ppm = 147.6 (2 X C), 128.2 (4 X CH), 127.0 (4 X CH), 125.8 (2 X CH), 40.0 (2 X CH), 36.1 (2 X CH_2), 22.5 (2 X CH_3). **$[\alpha]_D^{23}$** = +13.0° (c 1.0, $CHCl_3$).

Corresponding racemic analog provided a statistical mixture of diastereomers under ***GP5.3.8*** in similar yield and appearance, spectral data was consistent with literature.

^{1}H NMR (400MHz, CHLOROFORM-d) δ ppm = 7.32-7.24 (m, 4 H), 7.21-7.09 (m, 6 H), 2.70-2.57 (m, 2 H), 1.61-1.39 (m, 4 H), 1.20 (d, *J* = 7.0 Hz, 6 H). ^{13}C NMR (101MHz, CHLOROFORM-d) δ ppm = 147.7 (2 X C), 147.6 (2 X C), 128.3 (4 X CH), 128.2 (4 X CH), 127.0 (4 X CH), 127.0 (4 X CH), 125.8 (2 X CH, both diastereomers), 40.1 (2 X CH), 40.0 (2 X CH), 36.5 (2 X CH_2), 36.1 (2 X CH_2), 22.5 (2 X CH_3), 22.3 (2 X CH_3).

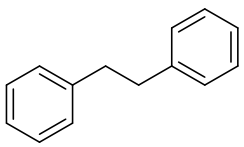

F3.14.2d: bibenzyl

Synthesized according to ***GP5.3.8***, affording 28 mg (77%) of an off yellow

oil, spectral data was consistent with literature.[149]

^{1}H NMR (400MHz, CHLOROFORM-d) δ ppm = 7.35-7.28 (m, 4 H), 7.26-7.19 (m, 6 H), 2.96 (s, 4 H). ^{13}C NMR (101MHz, CHLOROFORM-d) δ ppm = 141.8 (2 X C), 128.4 (4 X CH), 128.3 (4 X CH), 125.9 (2 X CH), 37.9 (2 X CH_2).

5.4 Supplemental Information Chapter 4

5.4.1 Compounds and supplemental information for Chapter 4.1

(GP5.4.1) **General procedure for preparation of brominated substrates from alcohols**

To an oven-dried 8 mL Pyrex screw-top reaction vessel was added the alcohol substrate (0.30 mmol, 1.0 equiv.), dimethylformamide (3 mL, 0.1M), and carbontetrabromide (0.30 mmol, 1.0 equiv.). The reaction mixture was capped and irradiated with a UVA LED at a distance of 1 cm for 15 minutes to 1 hour until all starting material was judged consumed by TLC. If the formyl ester spot was present on TLC after 1 hr of stirring (indicating presence of intermediate that has not reacted with bromide), 2-3 equivalents of NaBr was added and allowed to stir until judged completed by TLC analysis (1-16 hr at 23-35^{o}C). The resulting mixture was then poured into a seperatory funnel containing a 1:1 mixture of diethyl ether and hexanes (ethyl acetate added for compounds which needed further solubility). This was washed with saturated sodium bicarbonate and water, and the combined aqueous fractions were re-extracted with 1:1 diethyl ether and hexanes. The combined organic portions were washed with saturated sodium thiosulfate, brine, and dried over magnesium sulfate. The solution was concentrated *in vacuo* and crude products were further purified by column chromatography and isolated from relevant fractions.

*In many cases products were added an internal standard (mesitylene) to confirm that yields were not overestimated in case of residual CBr_4 remaining.

Method is also compatible with adding 3 equivalents of 2,6-lutidine for compounds with acid sensitive functional groups to attenuate the formation of HBr.

(GP5.4.2) **General procedure for preparation of iodinated substrates from alcohols**

To an oven-dried 8 mL Pyrex screw-top reaction vessel was added alcohol substrate (0.30 mmol, 1.0 equiv.), dimethylformamide (3 mL, 0.1M), and iodoform (0.30 mmol, 1.0 equiv.). The

reaction mixture was capped and irradiated with a 410 nm LED at a distance of 1 cm for 1-2 hours until all starting material was judged consumed by TLC. If the formyl ester spot was present on TLC after 1 hr of stirring (indicating presence of intermediate that has not reacted with bromide), 2-3 equivalents of NaI was added and allowed to stir until judged completed by TLC analysis (1-16 hr at rt). The resulting mixture was poured into a seperatory funnel containing a 1:1 mixture of diethyl ether and hexanes (ethyl acetate added for compounds which needed further solubility). This was washed with saturated sodium bicarbonate and water, and the combined aqueous fractions were re-extracted with 1:1 diethyl ether and hexanes. The combined organic portions were washed with saturated sodium thiosulfate, brine, and dried over magnesium sulfate. The solution was concentrated *in vacuo* and crude products were further purified by column chromatography and isolated from relevant fractions.

(GP5.4.3) **General procedure for preparation of deoxygenated compounds from alcohols**

To an obven-dried 8 mL Pyrex screw-top reaction vessel was added alcohol substrate (0.10-0.30 mmol, 1.0 equiv.), dimethylformamide (1-3 mL, 0.1M), and carbontetrabromide (0.10-0.30 mmol, 1.0 equiv.). The reaction mixture was capped and irradiated with a 365 nm LED at a distance of 1 cm for 1 hour until all starting material was judged consumed by TLC. If the formyl ester spot was present on TLC after 1 hr of stirring (indicating presence of intermediate that has not reacted with bromide), 2-3 equivalents of NaBr was added and allowed to stir until judged completed by TLC analysis (1-16 hr at 23-35^{o}C). To the resulting mixture was then added an equal amount iPrOH as compared to DMF and diisopropylethylamine (1.0-3.0 mmol, 10 equiv.). After 10 min of stirring, $[Au_2(dppm)_2]Cl_2$ (0.005-0.0150 mmol, 0.05 equiv.) was added and the solution was degassed by argon sparging. The resulting mixture was then irradiated with a UVA (365 nm) LED at a distance of 1 cm for 2-3 hrs. The resulting mixture was poured into a

seperatory funnel containing 25 mL of a 1:1 mixture of diethyl ether and hexanes (ethyl acetate added for compounds which needed further solubility). This was washed with saturated sodium bicarbonate and water, and the combined aqueous fractions were re-extracted with 25 mL of 1:1 diethyl ether and hexanes. The combined organic portions were washed with saturated sodium thiosulfate, brine, and dried over magnesium sulfate. The solution was concentrated *in vacuo* and crude products were further purified by column chromatography and isolated from relevant fractions.

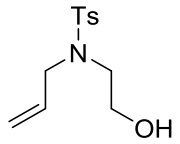

F4.1.1e: N-allyl-N-(2-hydroxyethyl)-4-methylbenzenesulfonamide

Spectral data was consistent with literature..[150]

^{1}H NMR (400MHz, CHLOROFORM-d): δ ppm = 7.75 - 7.67 (m, 2 H), 7.36 - 7.29 (m, 2 H), 5.69 (ddt, *J* = 16.9, 10.3, 6.4 Hz, 1 H), 5.29 - 5.07 (m, 2 H), 3.86 (d, *J* = 6.4 Hz, 2 H), 3.75 (t, *J* = 5.3 Hz, 2 H), 3.25 (t, *J* = 5.4 Hz, 2 H), 2.45 (s, 3 H), 1.86 (br s, 1 H).

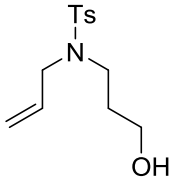

F4.1.1f: N-allyl-N-(3-hydroxypropyl)-4-methylbenzenesulfonamide

^{1}H NMR (400MHz, CHLOROFORM-d): δ ppm = 7.75 - 7.67 (m, *J* = 8.2 Hz, 2 H), 7.36 - 7.29 (m, *J* = 8.0 Hz, 2 H), 5.63 (ddt, *J* = 16.9, 10.2, 6.6 Hz, 1 H), 5.22 - 5.10 (m, 2 H), 3.82 (d, *J* = 6.6 Hz, 2 H), 3.75 (t, *J* = 5.7 Hz, 2 H), 3.26 (t, *J* = 6.5 Hz, 2 H), 2.44 (s, 3 H), 2.16 (br s, 1 H), 1.73 (quin, *J* = 6.1 Hz, 2 H). ^{13}C NMR (101MHz, CHLOROFORM-d): δ ppm = 143.4 (C), 136.6 (C), 133.0 (CH), 129.8 (2 X CH), 127.1 (2 X CH), 119.1 (CH_2), 58.7 (CH_2), 51.2 (CH_2), 43.8 (CH_2), 30.7 (CH_2), 21.5 (CH_3). IR (neat, cm^{-1}): 3536(br), 2923(m), 2878(m), 1331(s), 1154(vs), 1090(s). HRMS (EI) m/z calculated for $C_{13}H_{19}NO_3S$ $[M]^+$ 269.1086, found: 269.1042.

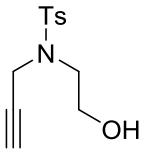

F4.1.1g: N-(2-hydroxyethyl)-4-methyl-N-(prop-2-yn-1-yl)benzenesulfonamide (5g)

Spectral data was consistent with literature.[151]

^{1}H NMR (400MHz, CHLOROFORM-d): δ ppm = 7.80 - 7.71 (m, *J* = 8.3 Hz, 2 H), 7.36 - 7.29 (m, *J* = 8.1 Hz, 2 H), 4.22 (d, *J* = 2.4 Hz, 2 H), 3.82 (t, *J* = 5.1 Hz, 2 H), 3.37 (t, *J* = 5.2 Hz, 2 H), 2.44 (s, 3 H), 2.10 (t, *J* = 2.5 Hz, 1 H), 1.76 (br s, 1 H). ^{13}C NMR (101MHz, CHLOROFORM-d): δ ppm = 143.9 (C), 135.5 (C), 129.6 (2 X CH), 127.8 (2 X CH), 77.2 (C), 73.9 (CH), 60.6 (CH_2), 49.1 (CH_2), 38.0 (CH_2), 21.6 (CH_3).

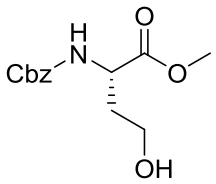

F4.3.1d: methyl ((benzyloxy)carbonyl)-L-homoserinate

Synthesized as described by patent procedure WO2009069100 (A1) – Phosphonic acid derivates and their use as P2Y12 receptor antagonists (US2010261678A1) and spectral data was consistent with literature.[152]

$[\alpha]^{23}_D$ = -3.9^o (c 0.5, 1:1 DMF:H_2O) (L-homoserine).

$[\alpha]^{23}_D$ = -32.5^o (c 1.0, DMF) (methyl ((benzyloxy)carbonyl)-L-homoserinate).

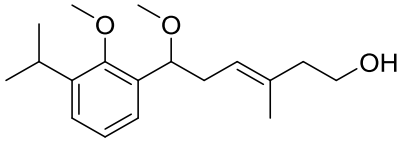

F4.3.1h: (±)-(3*E*)-6-methoxy-6-[2-methoxy-3-isopropylphenyl]-3-methylhex-3-en-1-ol

^{1}H NMR (400MHz, CHLOROFORM-d): δ ppm = 7.25 (dd, *J* = 7.3, 2.0 Hz, 1 H), 7.22 - 7.18 (m, 1 H), 7.18 - 7.12 (m, 1 H), 5.26 (td, *J* = 7.5, 1.2 Hz, 1 H), 4.54 (t, *J* = 6.8 Hz, 1 H), 3.75 (s, 3 H), 3.65 - 3.51 (m, 2 H), 3.31 (spt, *J* = 6.9 Hz, 1 H), 3.27 (s, 3 H), 2.58 (dt, *J* = 13.9, 6.8 Hz, 1 H), 2.40 (dt, *J* = 14.1, 7.3 Hz, 1 H), 2.26 - 2.09 (m, 2 H), 1.98 (br s, 1 H), 1.39 (s, 3 H), 1.27 (d, *J*

= 7.0 Hz, 3 H), 1.22 (d, *J* = 6.9 Hz, 3 H). ^{13}C NMR (101MHz, CHLOROFORM-d): δ ppm = 155.1 (C), 141.7 (C), 134.7 (C), 133.6 (C), 126.0 (CH), 125.0 (CH), 124.5 (CH), 123.2 (CH), 77.6 (CH), 62.1 (CH_3), 59.7 (CH_2), 56.7 (CH_3), 42.7 (CH_2), 36.6 (CH_2), 26.1 (CH), 24.3 (CH_3), 23.8 (CH_3), 15.5 (CH_3). IR (neat, cm^{-1}): 3423 (br), 2963 (m), 2931 (m), 2871 (m), 1459 (s), 1096 (s), 1050 (s), 1009(s). HRMS (ESI) m/z calculated for $C_{18}H_{28}O_3Na$ $[M]^+$ 315.1936, found 315.1951. *(characterized by Alex Cannillo)*

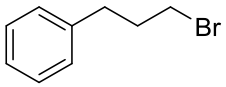

4.3.3 : (3-bromopropyl)benzene

Synthesized according to ***GP5.4.1*** and spectral data was consistent with literature.[153]

F4.1.1a: 1-bromoheptadecane

Synthesized according to ***GP5.4.1*** and spectral data was consistent with literature.[154]

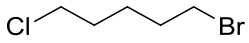

F4.1.1b: 1-bromo-5-chloropentane

Synthesized according to ***GP5.4.1*** and spectral data was consistent with literature.[155]

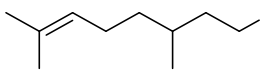

F4.1.1c 3,7-dimethyloctyl-6-enyl bromide ((±)-citronellyl bromide)

Synthesized according to ***GP5.4.1*** and spectral data was consistent with literature.[156]

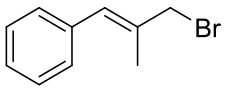

F4.1.1d: (E)-(3-bromo-2-methylprop-1-en-1-yl)benzene

Synthesized according to ***GP5.4.1*** and spectral data was consistent with literature.[157]

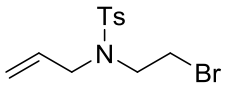

F4.1.1e: ***N*-allyl-*N*-(2-bromoethyl)-4-methylbenzenesulfonamide**

Synthesized according to ***GP5.4.1*** and spectral data was consistent with literature.[158]

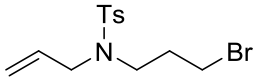

F4.1.1f: ***N*-allyl-*N*-(3-bromopropyl)-4-methylbenzenesulfonamide**

Synthesized according to ***GP5.4.1*** and spectral data was consistent with literature.[159]

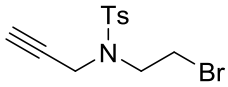

F4.1.1g: ***N*-propargyl-*N*-(2-bromoethyl)-4-methylbenzenesulfonamide**

Synthesized according to ***GP5.4.1*** spectral data was consistent with literature.[158]

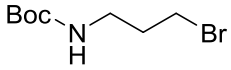

F4.1.1h: **tert-butyl (3-bromopropyl)carbamate**

Synthesized according to ***GP5.4.1*** and spectral data was consistent with literature.[109]

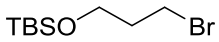

F4.1.1i: **(3-bromopropoxy)(*tert*-butyl)dimethylsilane**

Synthesized according to ***GP5.4.1*** and spectral data was consistent with literature.[160]

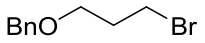

F4.1.1j: **1-(benzyloxy)-3-bromopropane**

Synthesized according to ***GP5.4.1*** and spectral data was consistent with literature.[161]

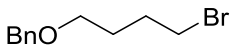

F4.1.1k: **1-(benzyloxy)-4-bromobutane**

Synthesized according to ***GP5.4.1*** and spectral data was consistent with literature.[162]

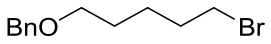

F4.1.1l: 1-(benzyloxy)-5-bromopentane

Synthesized according to ***GP5.4.1*** and spectral data was consistent with literature.[159]

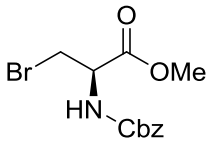

F4.1.1m: methyl (R)-2-(((benzyloxy)carbonyl)amino)-3-bromopropanoate

Synthesized according to ***GP5.4.1*** and spectral data was consistent with literature.[109]

$[\alpha]^{23}_{D}$ = -12.2° (c 1.0, DMF) (N-Cbz-L-serine methyl-ester).

$[\alpha]^{23}_{D}$ = -22.0° (c 1.0, DMF).

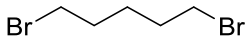

F4.1.1n: 1,5-dibromopentane

Synthesized according to ***GP5.4.1*** and spectral data was consistent with literature.[163]

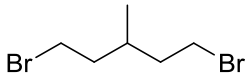

F4.1.1o: 3-methyl-1,5-dibromopentane

Synthesized according to ***GP5.4.1*** and spectral data was consistent with literature.[164]

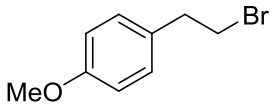

F4.1.1p: 1-(2-bromoethyl)-4-methoxybenzene

Synthesized according to ***GP5.4.1*** and spectral data was consistent with literature.[165]

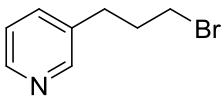

F4.1.1q: 3-(pyridin-3-yl)-1-bromopropane

Synthesized according to ***GP5.4.1*** and spectral data was consistent with

literature.[166]

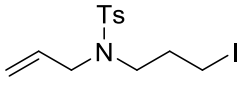

F4.2.2a: ***N*-allyl-*N*-(3-iodopropyl)-4-methylbenzenesulfonamide**

Synthesized according to ***GP5.4.2***.

^{1}H NMR ($CDCl_3$, 300 MHz): δ ppm = 7.79 - 7.62 (m, *J* = 8.3 Hz, 2 H), 7.37 - 7.28 (m, *J* = 8.1 Hz, 2 H), 5.63 (ddt, *J* = 16.9, 10.2, 6.5 Hz, 1 H), 5.29 - 5.05 (m, 2 H), 3.79 (d, *J* = 6.5 Hz, 2 H), 3.17 (t, *J* = 6.9 Hz, 2 H), 3.16 (t, *J* = 6.4 Hz, 2 H), 2.43 (s, 3 H), 2.08 (quin, *J* = 6.9 Hz, 2 H).

^{13}C NMR ($CDCl_3$, 75 MHz): δ ppm = 143.4 (C), 136.5 (C), 132.9 (CH), 129.7 (2 X CH), 127.1(2 X CH), 119.4 (CH_2), 51.5 (CH_2), 48.0 (CH_2), 32.4 (CH_2), 21.5 (CH_3), 2.4 (CH_2). IR (neat, cm^{-1}): 2923(m), 1551(m), 1334(s), 1155(vs), 1091(s). HRMS (EI) m/z calculated for $C_{13}H_{18}INO_2S$ $[M]^{+:}$ 379.0103, found 379.0099. *(characterized by Terry McCallum)*

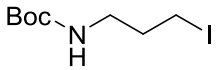

F4.2.2b: tert-butyl (3-iodopropyl)carbamate

Synthesized according to ***GP5.4.2*** and spectral data was consistent with literature.[167]

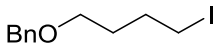

F4.2.2c: 1-(benzyloxy)-4-iodobutane

Synthesized according to ***GP5.4.2*** and spectral data was consistent with literature.[168]

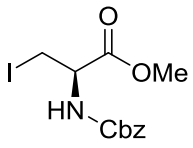

F4.2.2d: methyl (R)-2-(((benzyloxy)carbonyl)amino)-3-iodopropanoate

Synthesized according to ***GP5.4.2*** and spectral data was consistent with literature.[169]

$[\alpha]^{23}_D$ = -12.2° (c 1.0, DMF) (N-Cbz-L-serine methyl-ester).

$[\alpha]^{23}_D$ = -28.9° (c 1.0, DMF).

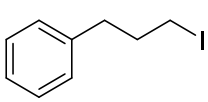

F4.2.1e: (3-iodopropyl)benzene

Synthesized according to ***GP5.4.2*** and spectral data was consistent with literature.[170]

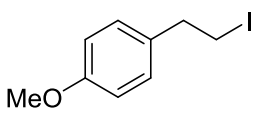

F4.2.1f: 1-(2-iodoethyl)-4-methoxybenzene

Synthesized according to ***GP5.4.2*** and spectral data was consistent with literature.[171]

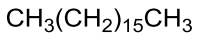

F4.3.3a: heptadecane

Synthesized according to ***GP5.4.3*** and spectral data was consistent with literature.[172]

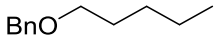

F4.3.3b: ((Pentyloxy)methyl)benzene

Synthesized according to ***GP5.4.3*** and spectral data was consistent with literature.[173]

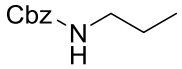

F4.3.3c: Benzyl propylcarbamate

Synthesized according to ***GP5.4.3*** and spectral data was consistent with literature.[174]

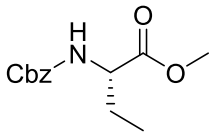

F4.3.3d: methyl (S)-2-(((benzyloxy)carbonyl)amino)butanoate

Synthesized according to ***GP5.4.3***.

^{1}H NMR (400MHz, CHLOROFORM-d): δ ppm = 7.45 - 7.29 (m, 5 H), 5.30 (d, *J* = 6.9 Hz, 1 H), 5.12 (s, 2 H), 4.41 - 4.31 (m, 1 H), 3.76 (s, 3 H), 1.90 (dquin, *J* = 14.3, 7.3 Hz, 1 H), 1.73 (dquin, *J* = 14.3, 7.3 Hz, 1 H), 0.93 (t, *J* = 7.5 Hz, 3 H). ^{13}C NMR (101MHz, CHLOROFORM-

d): δ ppm = 172.8 (C), 155.8 (C), 136.2 (C), 128.5 (2 X CH), 128.2(CH), 128.1 (2 X CH), 67.0 (CH_2), 54.9 (CH), 52.3 (CH_3), 25.8 (CH_2), 9.4 (CH_3). IR (neat, cm^{-1}): 3341(br), 2955(m), 1720(vs), 1693(s), 1523(s), 1208(vs). HRMS (EI) m/z calculated for $C_{13}H_{17}NO_4$ $[M]^+$: 251.1158, found: 251.1139. $[\alpha]^{23}_D$ = -2.8° (c 0.5, DMF). *(characterized by Terry McCallum)*

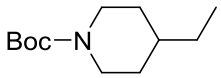

F4.3.3e: tert-butyl 4-ethylpiperidine-1-carboxylate

Synthesized according to ***GP5.4.3***.

^{1}H NMR (400MHz, CHLOROFORM-d): δ ppm = 4.07 (m, 2 H), 2.67 (m, 2 H), 1.72 - 1.59 (m, 2 H), 1.45 (s, 9 H), 1.34 - 1.21 (m, 3 H), 1.15 - 0.98 (m, 2 H), 0.89 (t, *J* = 7.3 Hz, 3 H). ^{13}C NMR (101MHz, CHLOROFORM-d): δ ppm = 154.9 (C), 79.1 (C), 44.0 (2 X CH_2), 37.7 (CH), 31.8 (2 X CH_2), 29.2 (CH_2), 28.5 (3 X CH_3), 11.2 (CH_3). IR (neat, cm^{-1}): 2965(m), 2924(m), 2852(m), 1690v(s), 1418(s), 1149(s). HRMS (EI) m/z calculated for $C_{12}H_{23}NO_2$ $[M]^+$: 213.1729, found: 213.1710. *(characterized by Terry McCallum)*

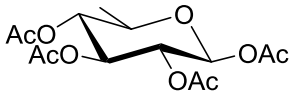

F4.3.3f: 1,2,3,4-Tetra-*O*-acetyl-6-deoxy-β-D-glucopyranose

Synthesized according to ***GP5.4.3*** and spectral data was consistent with literature.[175]

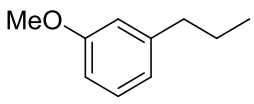

F4.3.3g : 3-*n*-Propylanisole

Synthesized according to ***GP5.4.3*** and spectral data was consistent with literature.[176]

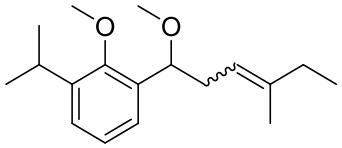

F4.3.3h: 1-isopropyl-2-methoxy-3-(1-methoxy-4-methylhex-3-en-1-yl)benzene (77:23 E/Z)

Synthesized according to ***GP5.4.3***. Peaks presented are for E compound where differentiable peaks for the Z compound are given.

^{1}H NMR (400MHz, CHLOROFORM-d): δ ppm = 7.24 (dd, *J* = 7.3, 2.0 Hz, 1 H), 7.22 - 7.17 (m, 1 H), 7.16 - 7.11 (m, 1 H), 5.21 (tq, *J* = 6.9, 1.3 Hz, 1 H), 4.57 (dd, *J* = 7.7, 5.5 Hz, 1 H), 3.75 (s, 3 H) *(Z = 3.74 (s, 3H))*, 3.33 (spt, *J* = 6.9 Hz, 1 H), 3.25 (s, 3 H) *(Z = 3.24 (s, 3H))*, 2.55 - 2.35 (m, 2 H), 1.98 (q, *J* = 7.3 Hz, 2 H), 1.52 (s, 3 H) *(Z = 1.68 (q, J = 1.3 Hz, 3 H))*, 1.26 (d, *J* = 6.9 Hz, 3 H), 1.23 (d, *J* = 7.0 Hz, 3 H), 0.96 (t, *J* = 7.4 Hz, 3 H) *(Z = 0.88 (t, J = 7.6 Hz, 3 H))*. ^{13}C NMR (101MHz, CHLOROFORM-d): δ ppm = 155.5 (C), 141.6 (C), 138.8 (C), 135.0 (C), 125.7 (CH), 124.7 (CH), 124.6 (CH), 119.1 (CH) *(Z = 120.3 (CH))*, 77.9 (CH), 62.2 (CH_3), 56.7 (CH_3), 36.1 (CH_2) *(Z = 35.9 (CH_2))*, 32.4 (CH_2) *(Z = 24.2 (CH_2))*, 26.2 (CH), 24.9, 24.2 (CH_3), 23.8 (CH_3), 16.0 (CH_3) *(Z = 22.9 (CH_3))*, 12.6 (CH_3). IR (neat, cm^{-1}): 2963(m), 2929(m), 2875(m), 1459(s), 1100 (s), 1051(s), 1012(s). HRMS (EI) m/z calculated for $C_{12}H_{17}O_2^{\cdot}$ [M^+ - $C_6H_{11}^{\cdot}$]: 193.1229, found 193.1227. *(characterized by Terry McCallum)*

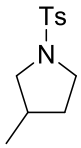

4.4.1: 3-methyl-1-tosylpyrrolidine (8)

Synthesized according to ***GP5.4.3*** and spectral data was consistent with literature.[158] [9].

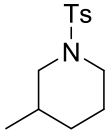

4.4.2: **3-methyl-1-tosylpiperidine**

Synthesized according to ***GP5.4.3*** and spectral data was consistent with literature.[177]

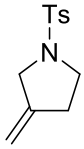

4.4.3: 3-methenyl-1-tosylpyrrolidine

Synthesized according to ***GP5.4.3*** and spectral data was consistent with literature.[158]

5.4.2 Compounds for Chapter 4.2

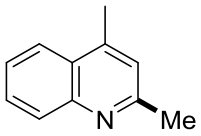

2,4-dimethylquinoline

Synthesized according to ***GP5.4.3*** and spectral data was consistent with literature. [178]

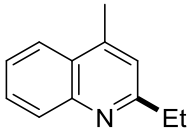

2-ethyl-4-methylquinoline

Synthesized according to ***GP5.4.3*** and spectral data was consistent with literature.[178]

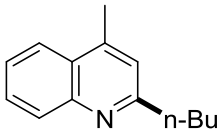

2-butyl-4-methylquinoline

Synthesized according to ***GP5.4.3*** and spectral data was consistent with literature.[179]

---

[107] Lokanatha, R. K. M.; Hassner, A. *Heterocycles* **1990**, *30*, 817 – 830
[108] Pandey, G.; Rao K. S. S. P.; Palit, D. K.; Mittal, J. P. *J. Org. Chem.* **1998**, *63*, 3968 – 3978
[109] Dai, C.; Narayanam, J. M. R.; Stephenson, C. R. J. *Nature Chem.* **2011**, *3*, 140 – 145
[110] Braun, M.; Veith, R.; Moll, G. *Chem. Ber*. **1985**, *118*, 1058 – 1070
[111] Baker, R. W.; Nicoletti, R. M.; Birkbeck, A. A.; Giles, R. B. F.; Sargent, M. V.; Skelton, B. W.; White, A. H. *J. Chem. Soc., Perkin Trans. 1.* **1991**, *6*, 1589 – 1600
[112] Sharghi, H.; Shahsavari-Fard, Z. *Helvetica Chimica Acta,*. **2005**, *88*, 42 – 52

[113] Heller, B.; Gutnov, A.; Fischer, C.; Drexler, H.; Spannenberg, A.; Redkin, D.; Sundermann, C.; Sundermann, B. *Chem. Eur. J.* **2006**, *13*, 1117 – 1128
[114] Hiroi, K.; Suzuki, Y.; Abe, I.; Hasegawa, Y.; Suzuki, K. *Tetrahedron: Asymmetry* **1998**, *9*, 3797 – 3817
[115] Togo, H.; Kikuchi, O. *Heterocycles*, **1989**, *28*, 373 – 381
[116] Ball, L. T.; Lloyd-Jones, G. C.; Russell, C. A. *Chem. Euro. J.* **2012**, *18*, 2931 – 2937
[117] Kadyrov, R. *Chem. Euro. J*. **2013**, *19*, 1002 – 1012
[118] Krapcho, P.; Weimaster, J. F. *J. Org. Chem.* **1980**, *45*, 4105 – 4111
[119] Firmansjah, L.; Fu, G. *J. Am. Chem. Soc.* **2007**, *129*, 11340 – 11341
[120] Nguyen, J. D.; D'Amato E. M.; Narayanam, J. M. R.; Stephenson, C. R. J. *Nature Chem*. **2012**, *4*, 854 – 859
[121] Curran, D. P.; Totleben, M. J. *J. Am. Chem. SOL,* **1992**, *114*, 6050 - 6058
[122] Li, F.; Jiang, T.; Cai, H.; Wang G. *Chin. J. Chem.* **2012**, *30*, 2041 – 2046
[123] Ryokawa, A.; Togo, H. Tetrahedron, **2001**, *57*, 5915 – 5921
[124] Kim, H.; Lee, C. *Angew. Chem. Int. Ed*. **2012**, *51*, 12303 – 12306
[125] Baker, R. W.; Nicoletti, R. M.; Birkbeck, A. A.; Giles, R. B. F.; Sargent, M. V.; Skelton, B. W.; White, A. H. *J. Chem. Soc., Perkin Trans. 1.* **1991**, *6*, 1589 – 1600
[126] Sharghi, H.; Shahsavari-Fard, Z. *Helvetica Chimica Acta,*. **2005**, *88*, 42 – 52
[127] Bapna, A.; Vickerstaffe, E.; Warrington, B. H.; Ladlow, M.; Fan, T. P.; Ley, S. V. *Org. Biomol. Chem.* **2004**, *2*, 611 – 620
[128] Poyatos, M.; McNamara, W.; Incarvito, C.; Peris, E.; Crabtree, R. H. *Chem. Commun.* **2007**, *22,* 2267 – 2269
[129] Szostak, M.; Spain, M.; Eberhart, A. J.; Procter, D. J. *J. Org. Chem.* **2014**, *79*, 11988 – 12003
[130] Prins, L. J.; Hulst, R.; Timmerman, P.; Reinhoudt, D. N. *Chem. Eur. J*. **2002**, *8*, 2288 – 2301
[131] Chen, Y.-A.; Liu, C.-Y. *RSC Adv.* **2015**, *5*, 74180 – 74188
[132] Xu, Z.; Xiao, Y.; Ding, H.; Cao, C.; Li, H.; Pang, G.; Shi, Y. *Synthesis* **2015**, *47*, 1560 – 1566
[133] Vogler, T.; Studer, A. *Adv. Synth. Catal.* **2008**, *350*, 1963 – 1967
[134] Buter, J.; Heijnen, D.; Vila, C.; Hornillos, V.; Otten, E.; Giannerini, M.; Minnaard, A. J.; Feringa, B. L. *Angew. Chem. Int. Ed.* **2016**, *55*, 3620 – 3624
[135] Kirai, N.; Yamamoto, Y. *Eur. J. Org. Chem.* **2009**, *12*, 1864 – 1867
[136] Puthiaraj, P.; Suresh, P.; Pitchumani, K. *Green Chem.* **2014**, *16*, 2865 – 2875
[137] Camilleri, P.; Kirby, A. J.; Lewis, R. J.; Sanders, J. K. M. *J. Chem. Soc. Chem. Commun.* **1988**, 1537 – 1538
[138] Zhou, Q.; Wang, Y.-N.; Guo, X.-Q.; Zhu, X.-H.; Li, Z.-M.; Hou, X.-F. *Organometallics* **2015**, *34*, 1021 – 1028
[139] Xiong, Q.; Fu, Z.; Li, Z.; Cai, H. *Synlett* **2015**, *26*, 975 – 979
[140] Nishimura, N.; Yoza, K.; Kobayashi, K. *J. Am. Chem. Soc.* **2010**, *132*, 777 – 790
[141] Wang, L.; Murai, Y.; Yoshida, T.; Ishida, A.; Masuda, K.; Sakihama, Y.; Hashidoko, Y.; Hatanaka, Y.; Hashimoto, M. *Org. Lett.* **2015**, *17*, 616 – 619
[142] van der Born, D.; Sewing, C.; Herscheid, J. D. M.; Windhorst, A. D.; Orru, R. V. A.; Vugts, D. J. *Angew. Chem. Int. Ed.* **2014**, *53*, 11046 – 11050
[143] Lhermet, R.; Durandetti, M.; Maddaluno, J. *Beilstein J. Org. Chem.* **2013**, *9*, 710 – 716
[144] Horino, Y.; Takahashi, Y.; Koketsu, K.; Abe, H.; Tsuge, K. *Org. Lett.* **2014**, *16*, 3184 – 3187
[145] Ozaki, S.; Matsushita, H.; Ohmori, H. *J. Chem. Soc. Perkin Trans. 1.* **1993**, 649 – 651
[146] McTiernan, C. D.; Morin, M.; McCallum, T.; Scaiano, J. C.; Barriault, L. *Catal. Sci. Technol.* **2016**, *6*, 201 – 207
[147] Bywater, S.; Lachance, P.; Worsfold, D. J. *J. Phys. Chem.* **1975**, *79*, 2148 – 2153

[148] Dulog, L.; David, K.-H. *Makromol. Chem.* **1976**, *177*, 1717 – 1724
[149] Zhu, J.; Pérez, M.; Caputo, C. B.; Stephan, D. W. *Angew. Chem. Int. Ed.* **2016**, *55*, 1417 – 1421
[150] Poornachandran, M.; Raghunathan, R. *Tetrahedron* **2008**, *64*, 6461 – 6474
[151] Ishizaki, M.; Hoshino, O. *Tetrahedron* **2000**, *56*, 8813 – 8819
[152] Garrard, E.; Borman, E.; Cook, B.; Pike, E.; Alberg, D. *Org. Lett*. **2000**, *2*, 3639 – 3642
[153] Liu, Y.; Xu, Y.; Jung, S. H.; Chae, J. *Synlett.* **2012**, *23*, 2692 – 2698
[154] Kulkarni, B. A.; Sankaranarayanan, S.; Subbaraman, A. S.; Chattopadhyay, S. *Tetrahedron: Asymmetry* **1999**, *10*, 1571 – 1577
[155] Zhang, Y.; Dong, M.; Jiang, X.; Chow, Y. L. *Can. J. Chem*. **1990**, *68*, 1668 – 1675
[156] Flachsbarth, B.; Fritzsche, M.; Weldon, P. J.; Schulz, S. *Chemistry & Biodiversity* **2009**, *6*, 1 – 37
[157] Kern, N.; Blanc, A.; Weibel, J.; Pale, P. *Chem. Commun.* **2011**, *47*, 6665 – 6667
[158] Revol, G.; McCallum, T.; Morin, M.; Gagosz, F.; Barriault, L. *Angew. Chem. Int. Ed*. **2013**, *52*, 13342 – 13345
[159] Chowdhury, R.; Ghosh, S. K. *Org. Lett.* **2009**, *11*, 3270 – 3273
[160] Christiansen, M. A.; Andrus, M. B. *Tetrahedron Lett.* **2012**, *53*, 4805 – 4808
[161] Frankowski, K. J.; Golden, J. E.; Zeng, Y.; Lei, Y.; Aubé, J. *J. Am. Chem. Soc*. **2008**, *130*, 6018 – 6024
[162] Kushner, A. M.; Gabuchian, V.; Johnson, E. G.; Guan, Z. *J. Am. Chem. Soc*. **2007**, *129*, 14110 – 14111
[163] Nguyen, B. T.; Cartledge, F. K. *J. Org. Chem.* **1986**, *51*, 2206 – 2210
[164] Geny, A.; Agenet, N.; Iannazzo, L.; Malacria, M.; Aubert, C.; Gandon, V. *Angew. Chem. Int. Ed*. **2009**, *48*, 1810 – 1813
[165] Okano, K.; Fujiwara, H.; Noji, T.; Fukuyama, T.; Tokuyama, H. *Angew. Chem. Int. Ed*. **2010**, *49*, 5925 – 5929
[166] Solladie, G.; Somny, F.; Colobert, F. *Tetrahedron: Asymmetry* **1997**, *8*, 801 – 810
[167] Ellwood, A.; Porter, M. *J. Org. Chem*. **2009**, *74*, 7982 – 7985
[168] Bull, J. A.; Charette, A. B. *J. Org. Chem.* **2008**, *73*, 8097 – 8100
[169] Hattori, Y.; Asano, T.; Kirihata, M.; Yamaguchi, Y.; Wakamiya, T. *Tetrahedron Lett.* **2008**, *49*, 4977 – 4980
[170] Guisan-Ceinos, M.; Soler-Yanes, R.; Collado-Sanz, D.; Phapale, V. B.; Bunuel, E.; Cardenas, D. J. *Chem. Eur. J*. **2013**, *19*, 8405 – 8410
[171] Guziec Jr., F. S.; Wei, D. *J. Org. Chem.* **1992***, 57,* 3772 – 3776
[172] Zhao, F.; Rutherford, M.; Grisham, S. Y.; Peng, X. *J. Am. Chem. Soc*. **2009**, *131*, 5350 – 5358
[173] Kleinke, A. S.; Jamison, T. F. *Org. Lett*. **2013**, *15*, 710 – 713
[174] Nguyen, J. D.; ReiB, B.; Dai, C.; Stephenson, C. R. J. *Chem. Commun.* **2013**, *49*, 4352 – 4554
[175] Ueng, S.; Fensterbank, L.; Lacote, E.; Malacria, M.; Curran, D. P. *Org. Biomol. Chem*. **2011***, 9*, 3415 – 3420
[176] Tietze, L. F.; Vock, C. A.; Krimmelbein, I. K.; Nacke, L. *Synthesis* **2009**, *12*, 2040 – 2060
[177] Verendel, J. J.; Zhou, T.; Li, J.; Paptchikhine, A.; Lebedev, O.; Andersson, P. G. *J. Am. Chem. Soc.* **2010**, *132*, 8880 – 8881
[178] Bellan, A. B.; Kuzmina, O. M.; Vetsova, V. A.; Knochel, P. *Synthesis* **2017**, *49*, 188 – 194
[179] Stopka, T.; Niggerman, M. *Chem. Commun.* **2016**, *52*, 5761 – 5764

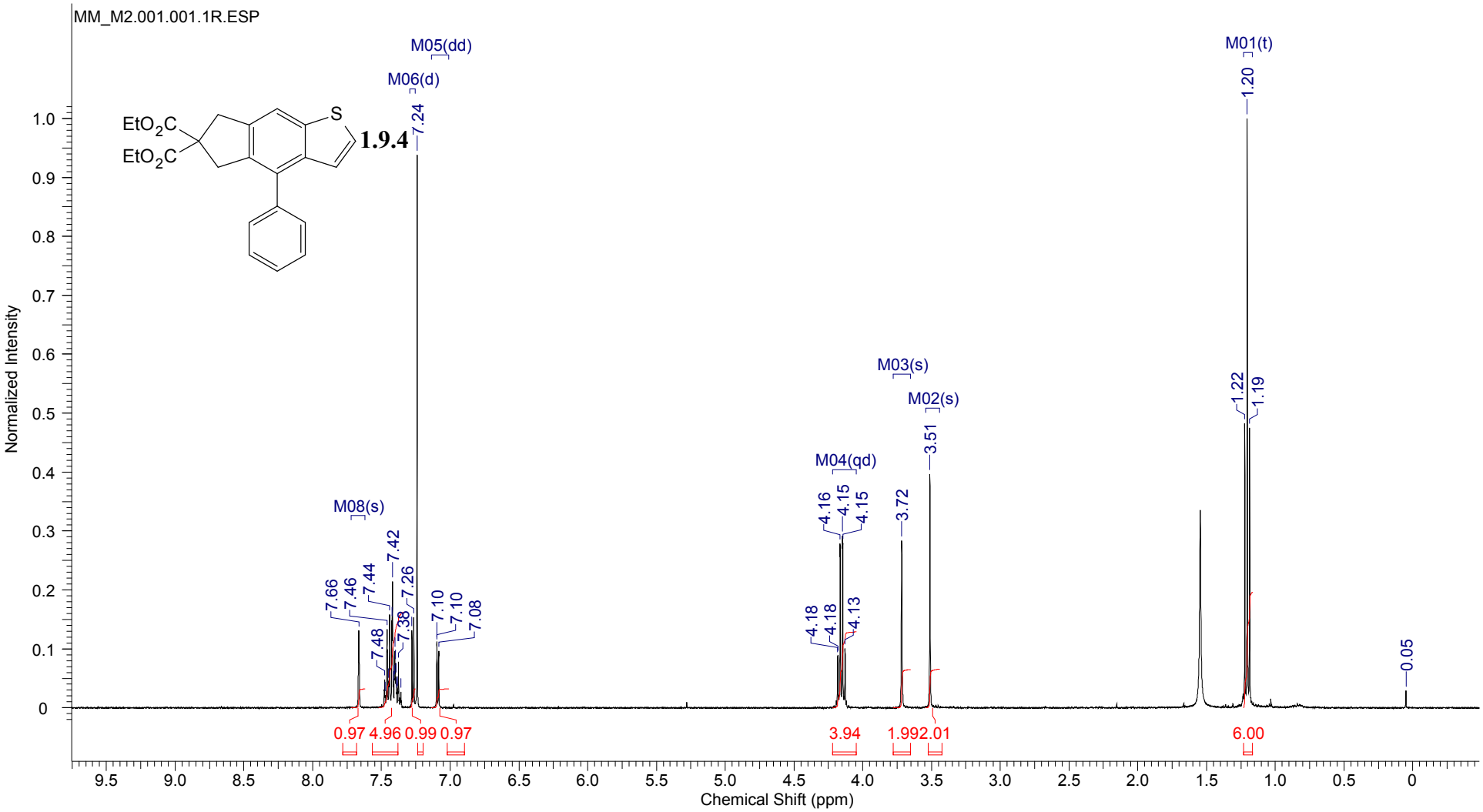
MM_M2.001.001.1R.ESP
M05(dd)
M06(d)
M01(t)
M03(s)
M02(s)
M04(qd)
M08(s)
1.9.4
EtO2C
EtO2C
S
7.24
1.20
1.22
1.19
3.51
3.72
4.16
4.15
4.15
4.18
4.18
4.13
7.66
7.46
7.44
7.42
7.26
7.48
7.38
7.10
7.10
7.08
0.05
0.97
4.96
0.99
0.97
3.94
1.99
2.01
6.00
Normalized Intensity
Chemical Shift (ppm)

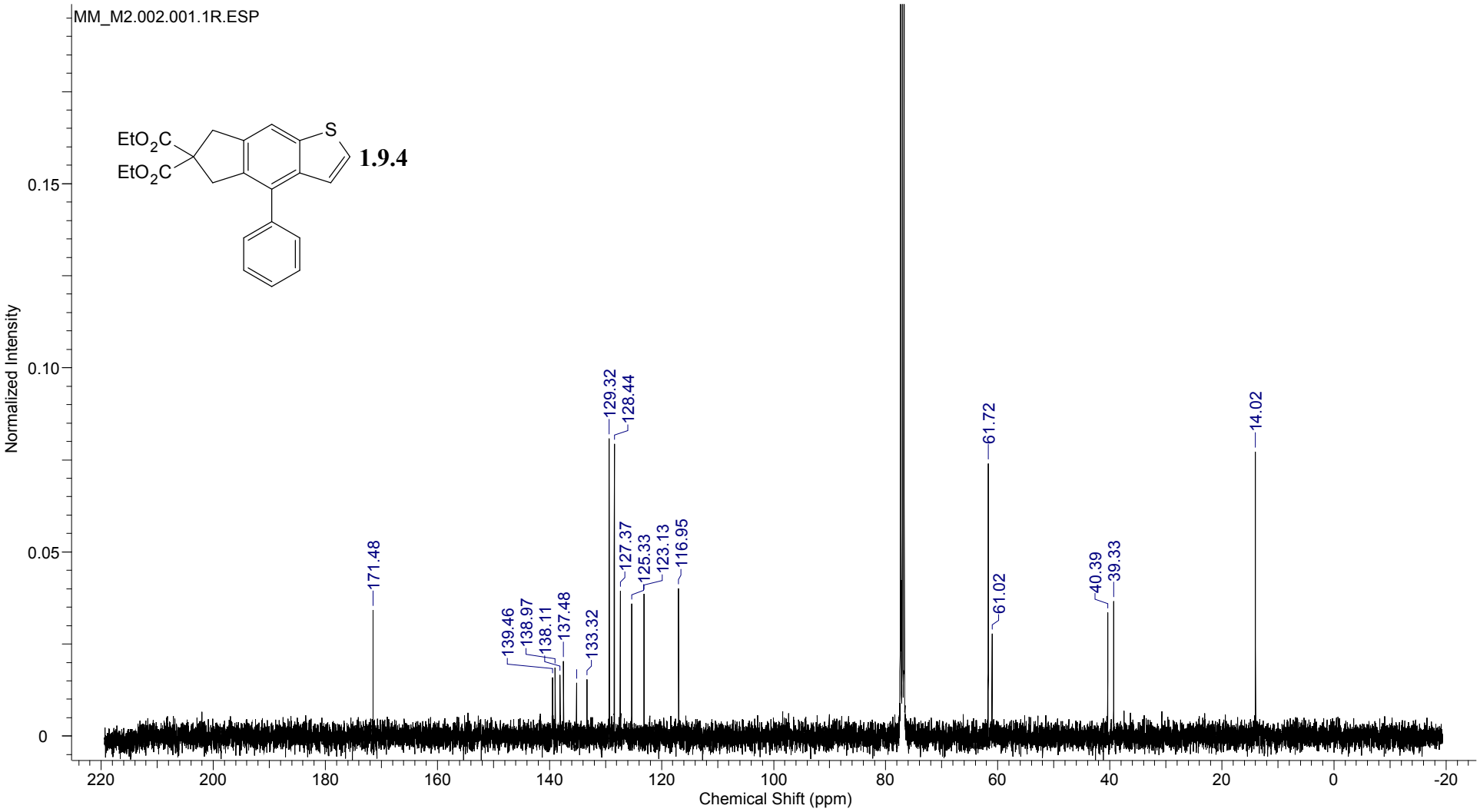
MM_M2.002.001.1R.ESP
EtO2C
EtO2C
S
1.9.4
Normalized Intensity
0.15
0.10
0.05
0
171.48
139.46
138.97
138.11
137.48
133.32
129.32
128.44
127.37
125.33
123.13
116.95
61.72
61.02
40.39
39.33
14.02
220
200
180
160
140
120
100
80
60
40
20
0
-20
Chemical Shift (ppm)

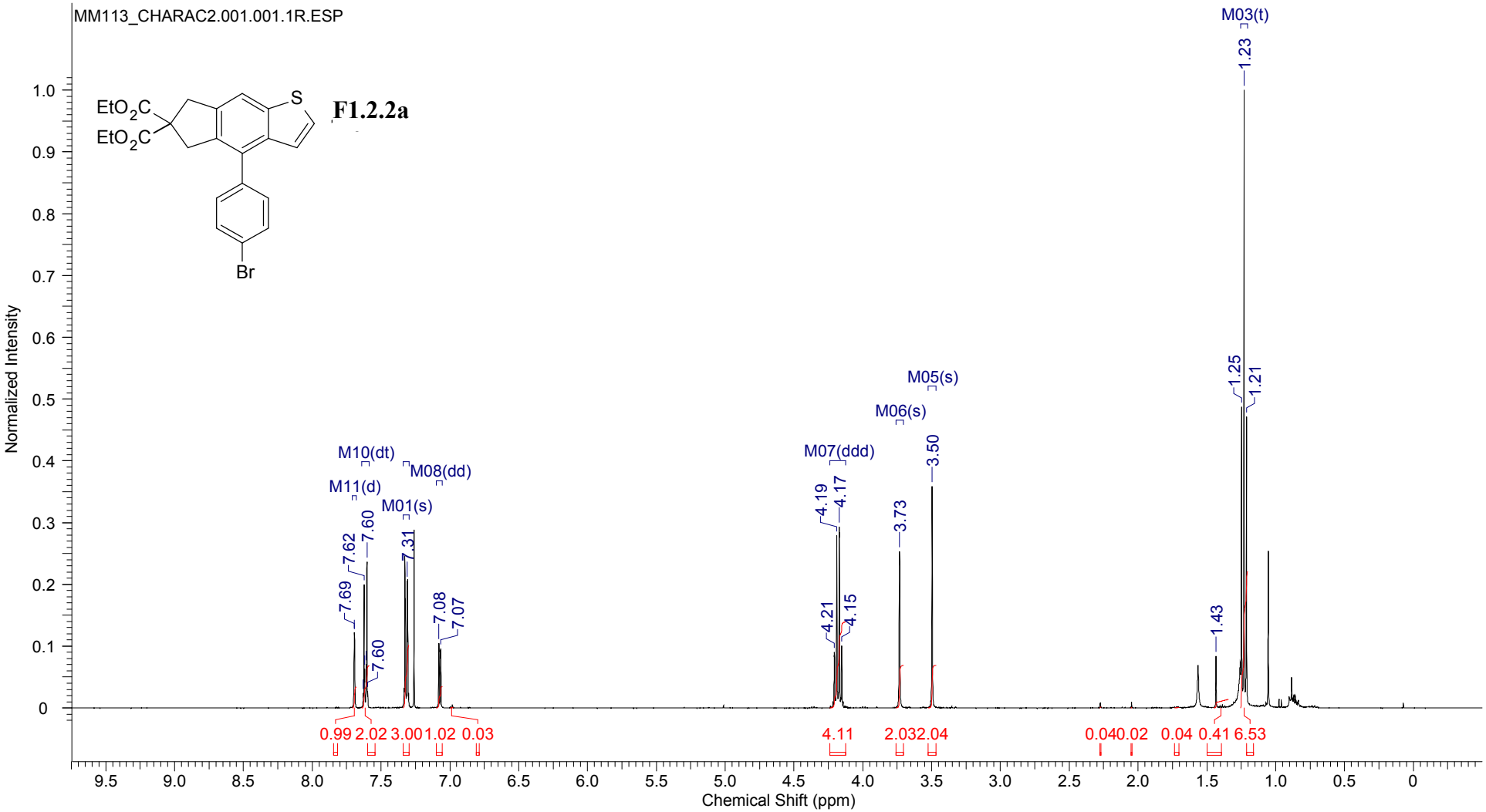
MM113_CHARAC2.001.001.1R.ESP
EtO2C
EtO2C
S
Br
F1.2.2a
Normalized Intensity
Chemical Shift (ppm)
M03(t)
1.23
M05(s)
M06(s)
M07(ddd)
M10(dt)
M08(dd)
M11(d)
M01(s)
1.25
1.21
3.50
3.73
4.19
4.17
7.62
7.60
7.31
7.69
7.08
7.07
4.21
4.15
7.60
1.43
0.99 2.02 3.00 1.02 0.03
4.11
2.03 2.04
0.04 0.02
0.04
0.41
6.53

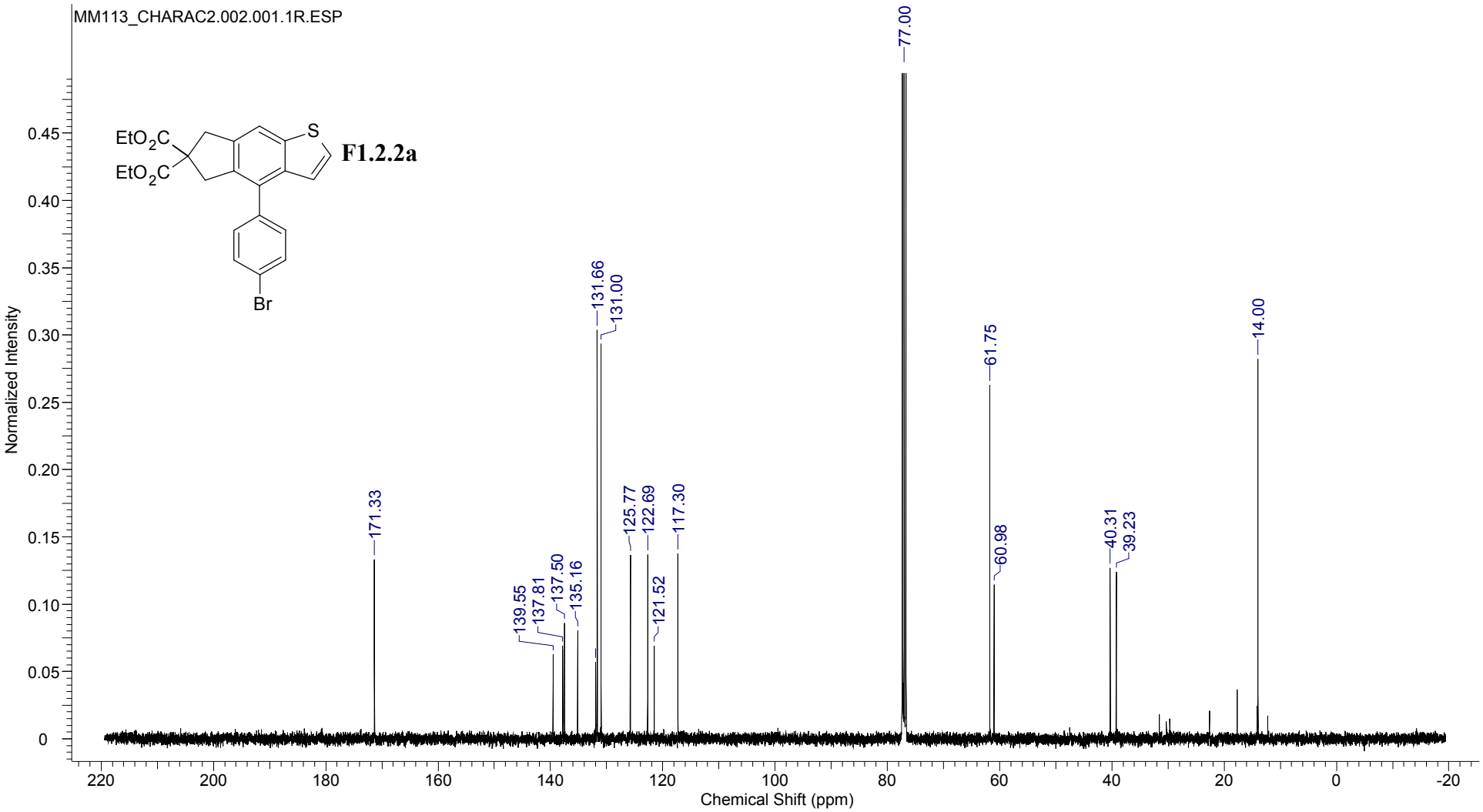
MM113_CHARAC2.002.001.1R.ESP
EtO2C
EtO2C
S
Br
F1.2.2a
Normalized Intensity
Chemical Shift (ppm)
171.33
139.55
137.81
137.50
135.16
131.66
131.00
125.77
122.69
121.52
117.30
77.00
61.75
60.98
40.31
39.23
14.00

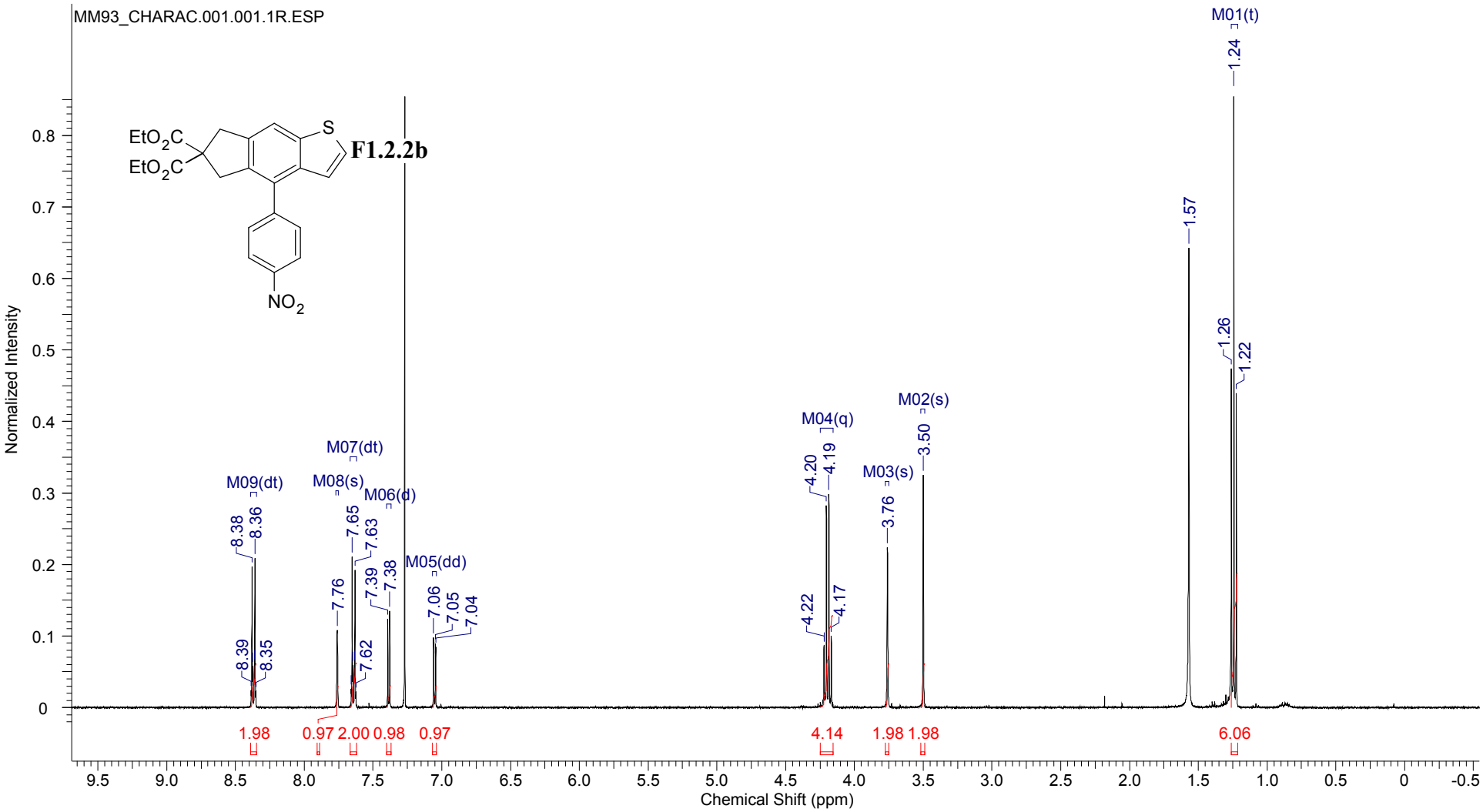
MM93_CHARAC.001.001.1R.ESP
F1.2.2b
Normalized Intensity
Chemical Shift (ppm)
M01(t)
M02(s)
M03(s)
M04(q)
M05(dd)
M06(d)
M07(dt)
M08(s)
M09(dt)
1.98
0.97
2.00
0.98
0.97
4.14
1.98
1.98
6.06

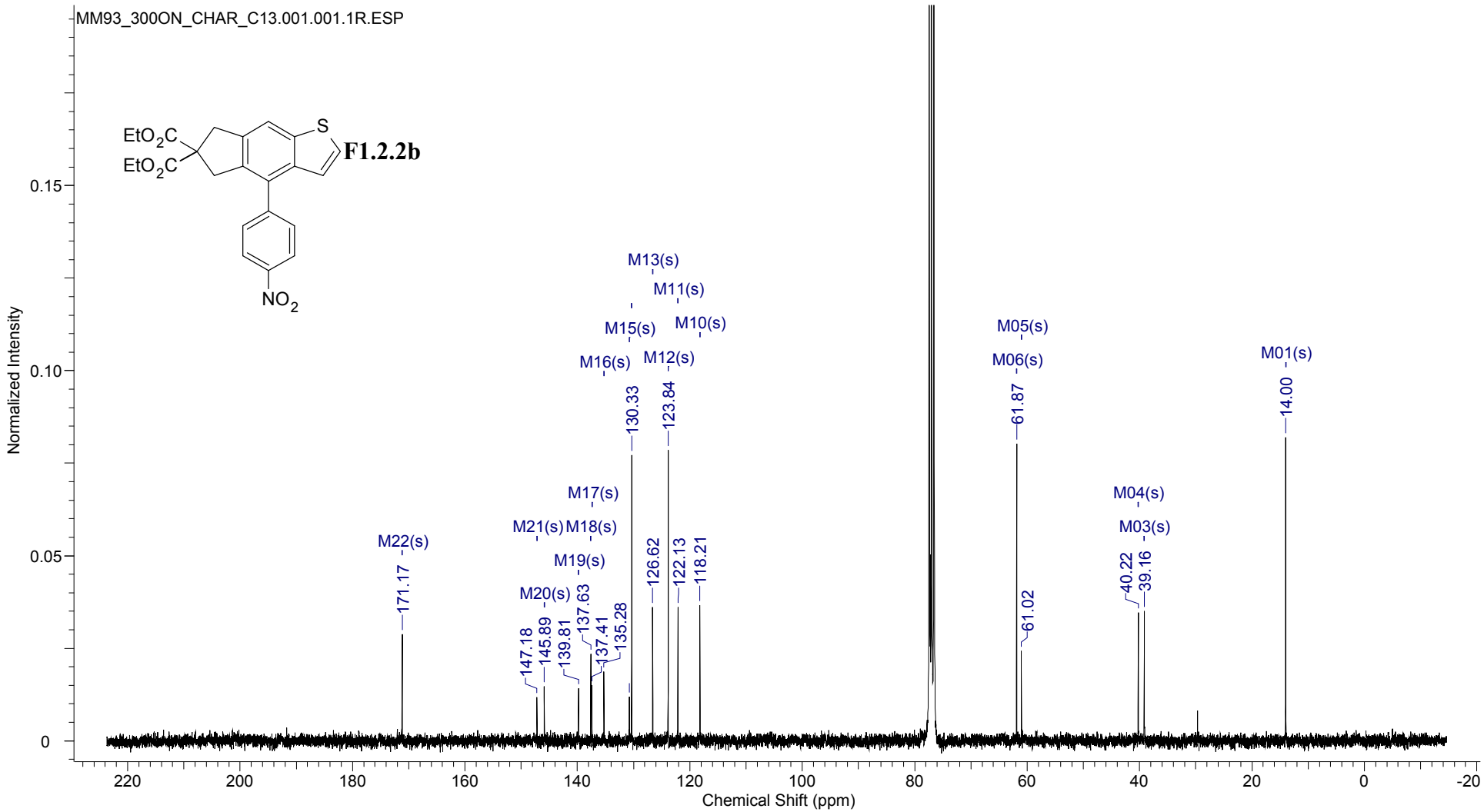
MM93_300ON_CHAR_C13.001.001.1R.ESP
EtO2C
EtO2C
S
NO2
F1.2.2b
Normalized Intensity
0.15
0.10
0.05
0
M13(s)
M11(s)
M15(s)
M10(s)
M16(s)
M12(s)
M05(s)
M06(s)
M01(s)
130.33
123.84
61.87
14.00
M17(s)
M04(s)
M21(s)
M18(s)
M03(s)
M22(s)
M19(s)
126.62
122.13
118.21
M20(s)
171.17
137.63
147.18
145.89
139.81
137.41
135.28
61.02
40.22
39.16
220
200
180
160
140
120
100
80
60
40
20
0
-20
Chemical Shift (ppm)

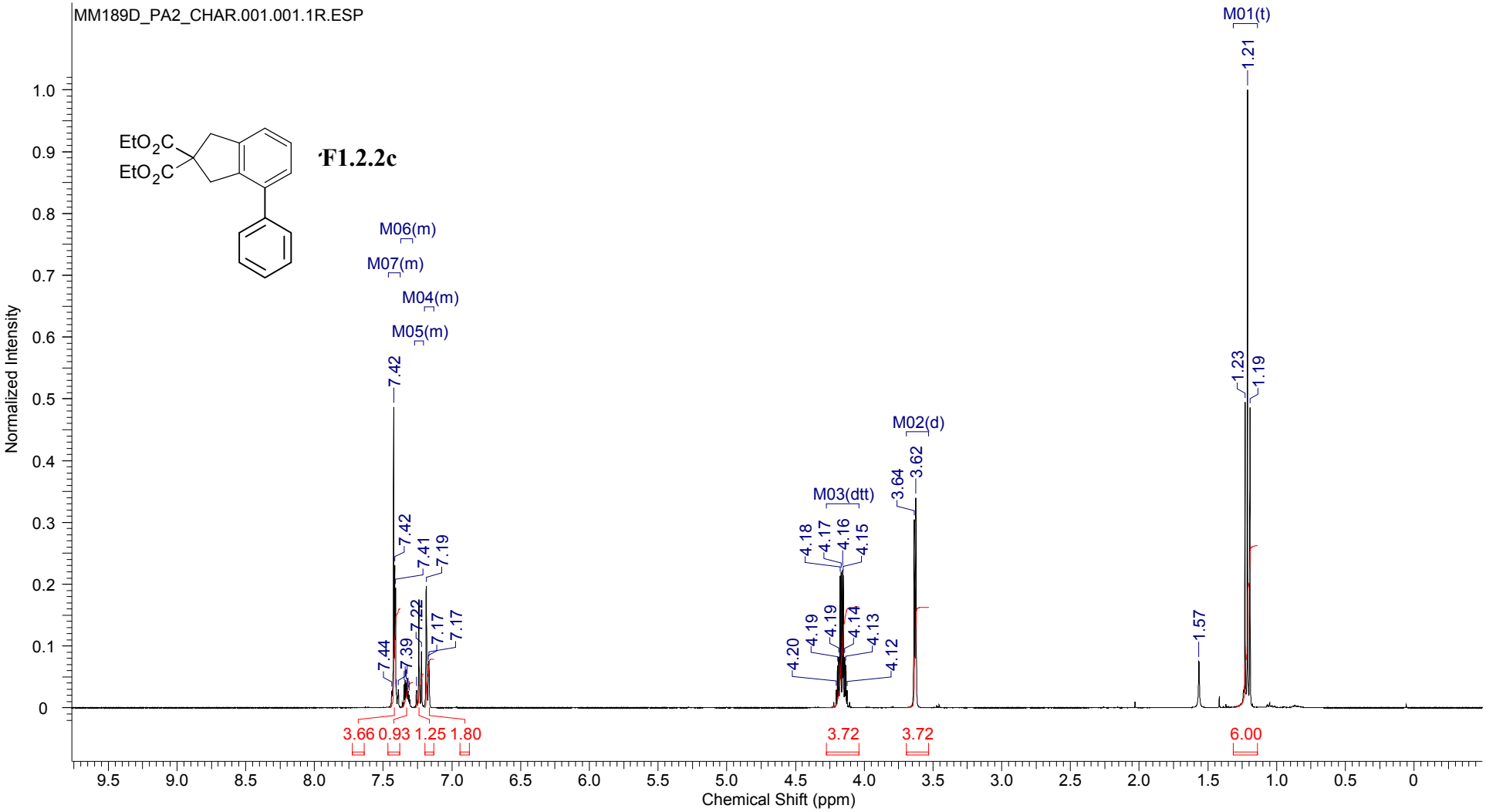
MM189D_PA2_CHAR.001.001.1R.ESP
EtO2C
EtO2C
F1.2.2c
M01(t)
M02(d)
M03(dtt)
M04(m)
M05(m)
M06(m)
M07(m)
1.21
1.23
1.19
3.64
3.62
1.57
4.18
4.17
4.16
4.15
4.20
4.19
4.19
4.14
4.13
4.12
7.42
7.42
7.41
7.19
7.44
7.39
7.22
7.17
7.17
3.66
0.93
1.25
1.80
3.72
3.72
6.00
Normalized Intensity
Chemical Shift (ppm)

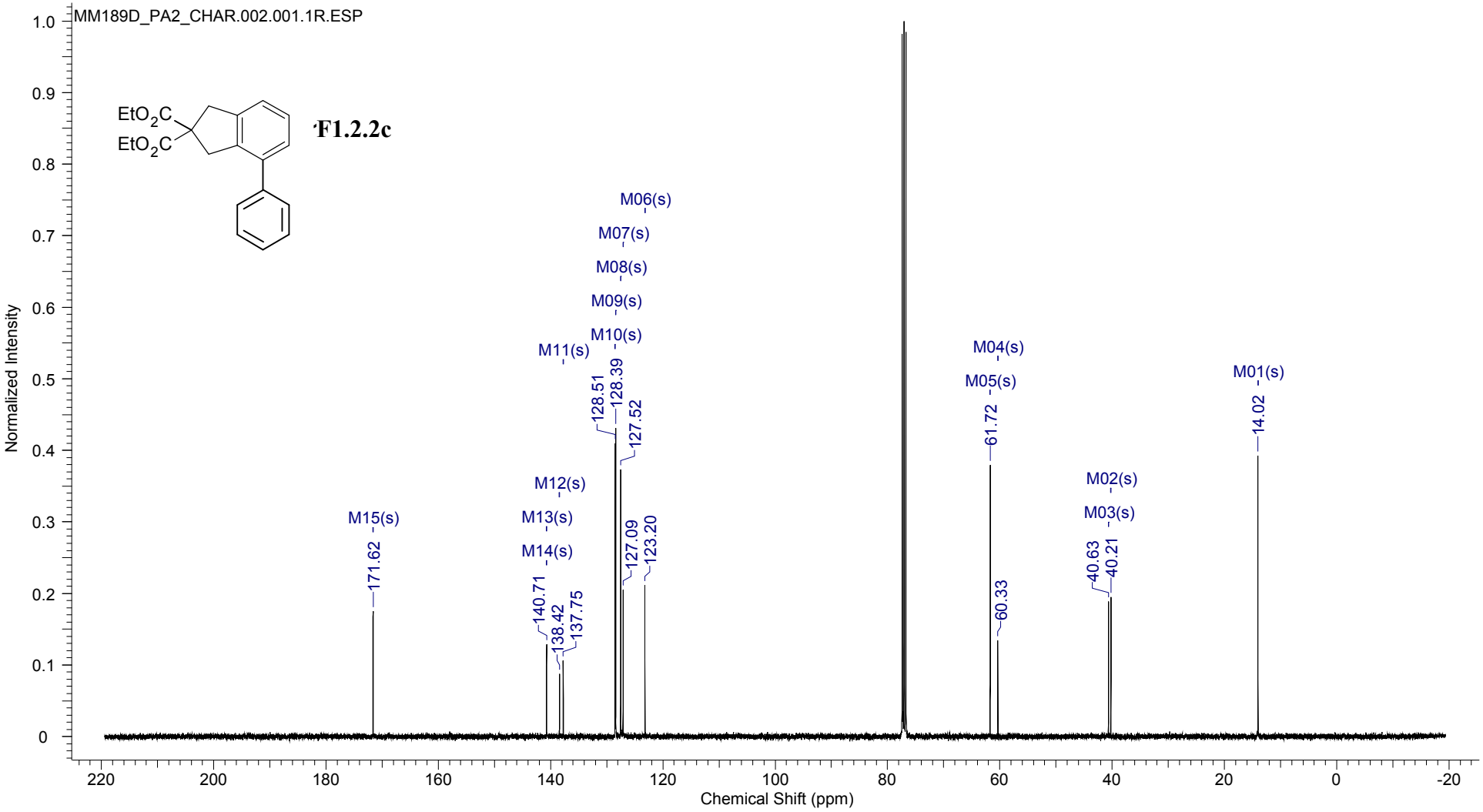
MM189D_PA2_CHAR.002.001.1R.ESP
EtO2C
EtO2C
F1.2.2c
M06(s)
M07(s)
M08(s)
M09(s)
M10(s)
M11(s)
M04(s)
M05(s)
M01(s)
M12(s)
M02(s)
M03(s)
M15(s)
M13(s)
M14(s)
171.62
140.71
138.42
137.75
128.51
128.39
127.52
127.09
123.20
61.72
60.33
40.63
40.21
14.02
Normalized Intensity
Chemical Shift (ppm)

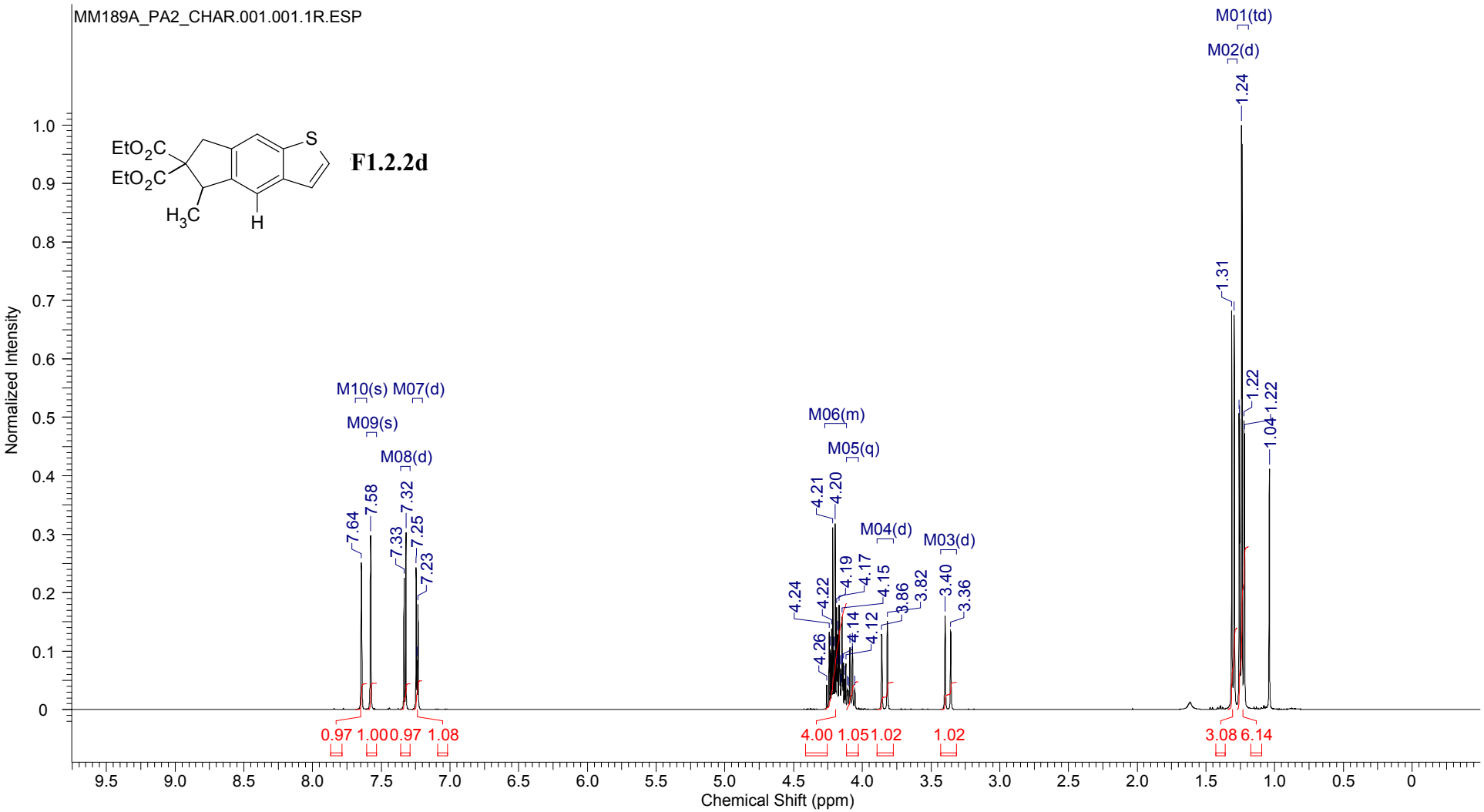
MM189A_PA2_CHAR.001.001.1R.ESP
F1.2.2d
M01(td)
M02(d)
M10(s) M07(d)
M09(s)
M08(d)
M06(m)
M05(q)
M04(d)
M03(d)
Normalized Intensity
Chemical Shift (ppm)
0.97 1.00 0.97 1.08
4.00 1.05 1.02
1.02
3.08 6.14

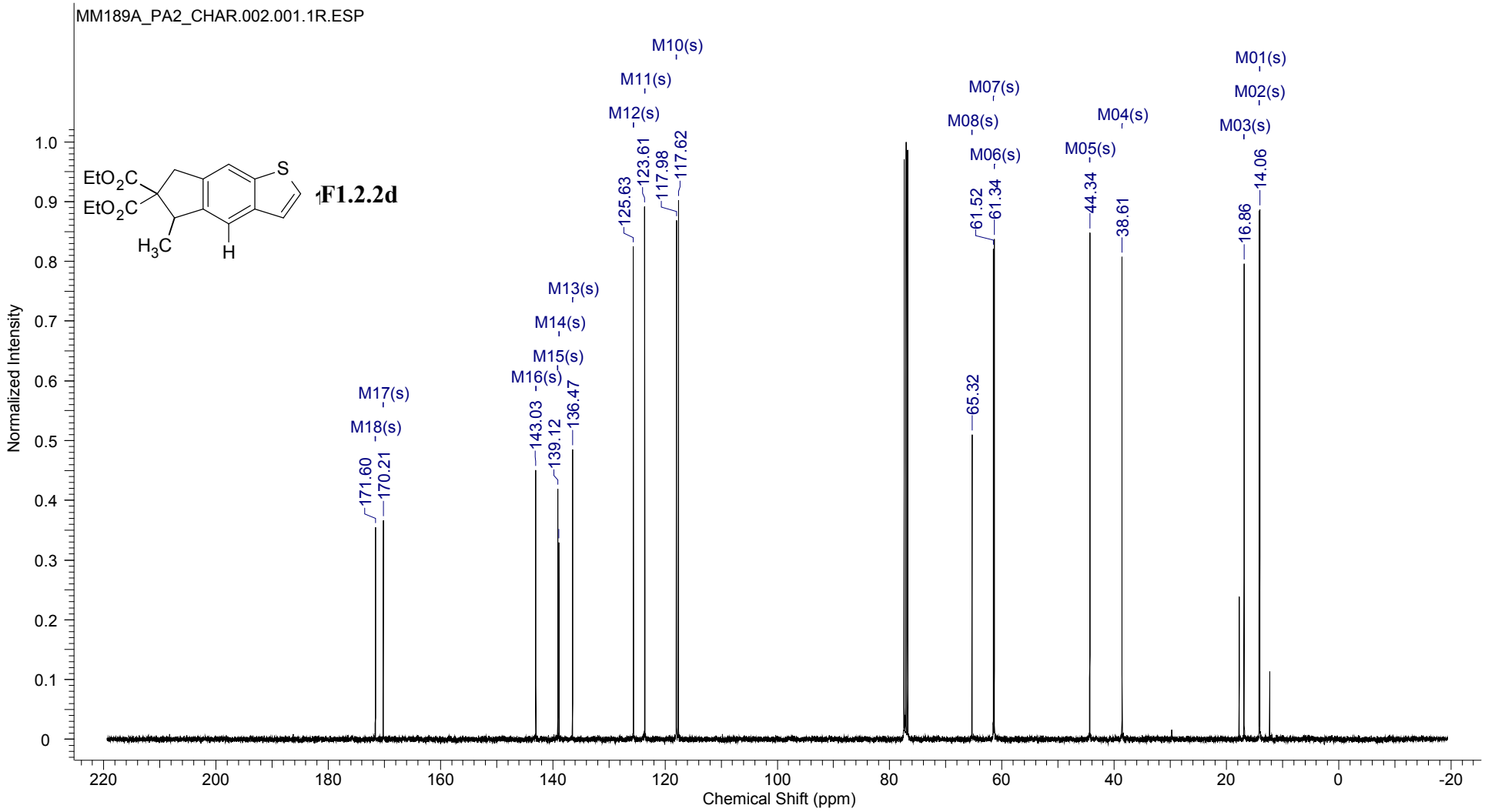
MM189A_PA2_CHAR.002.001.1R.ESP
EtO2C
EtO2C
H3C
S
H
F1.2.2d
M10(s)
M11(s)
M12(s)
M13(s)
M14(s)
M15(s)
M16(s)
M17(s)
M18(s)
M07(s)
M08(s)
M06(s)
M04(s)
M05(s)
M01(s)
M02(s)
M03(s)
125.63
123.61
117.98
117.62
171.60
170.21
143.03
139.12
136.47
65.32
61.52
61.34
44.34
38.61
16.86
14.06
Normalized Intensity
Chemical Shift (ppm)

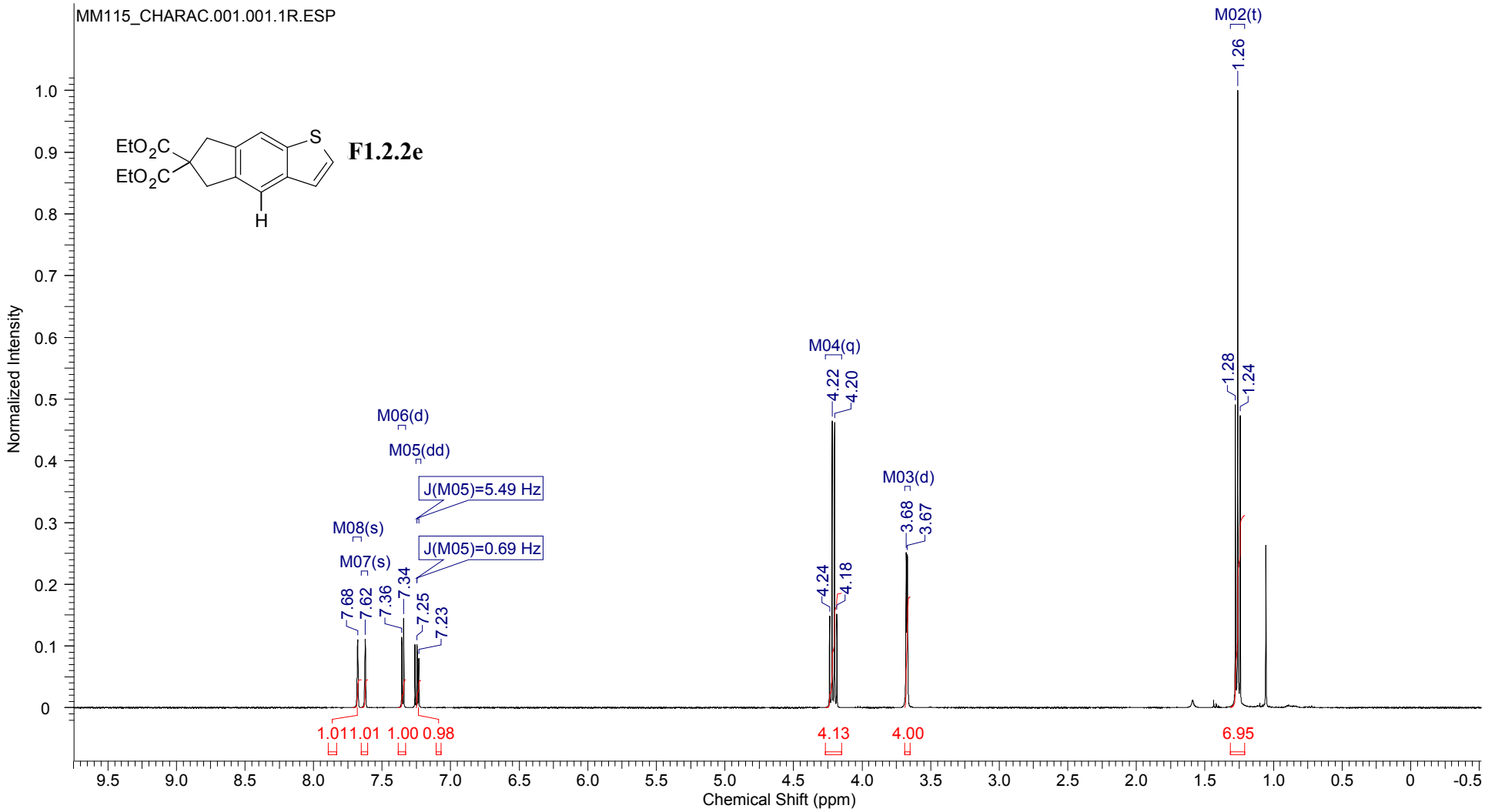
MM115_CHARAC.001.001.1R.ESP
F1.2.2e
M02(t)
1.26
M04(q)
4.22
4.20
M06(d)
M05(dd)
J(M05)=5.49 Hz
M08(s)
J(M05)=0.69 Hz
M07(s)
7.68
7.62
7.36
7.34
7.25
7.23
4.24
4.18
M03(d)
3.68
3.67
1.28
1.24
1.01
1.01
1.00
0.98
4.13
4.00
6.95
Normalized Intensity
Chemical Shift (ppm)

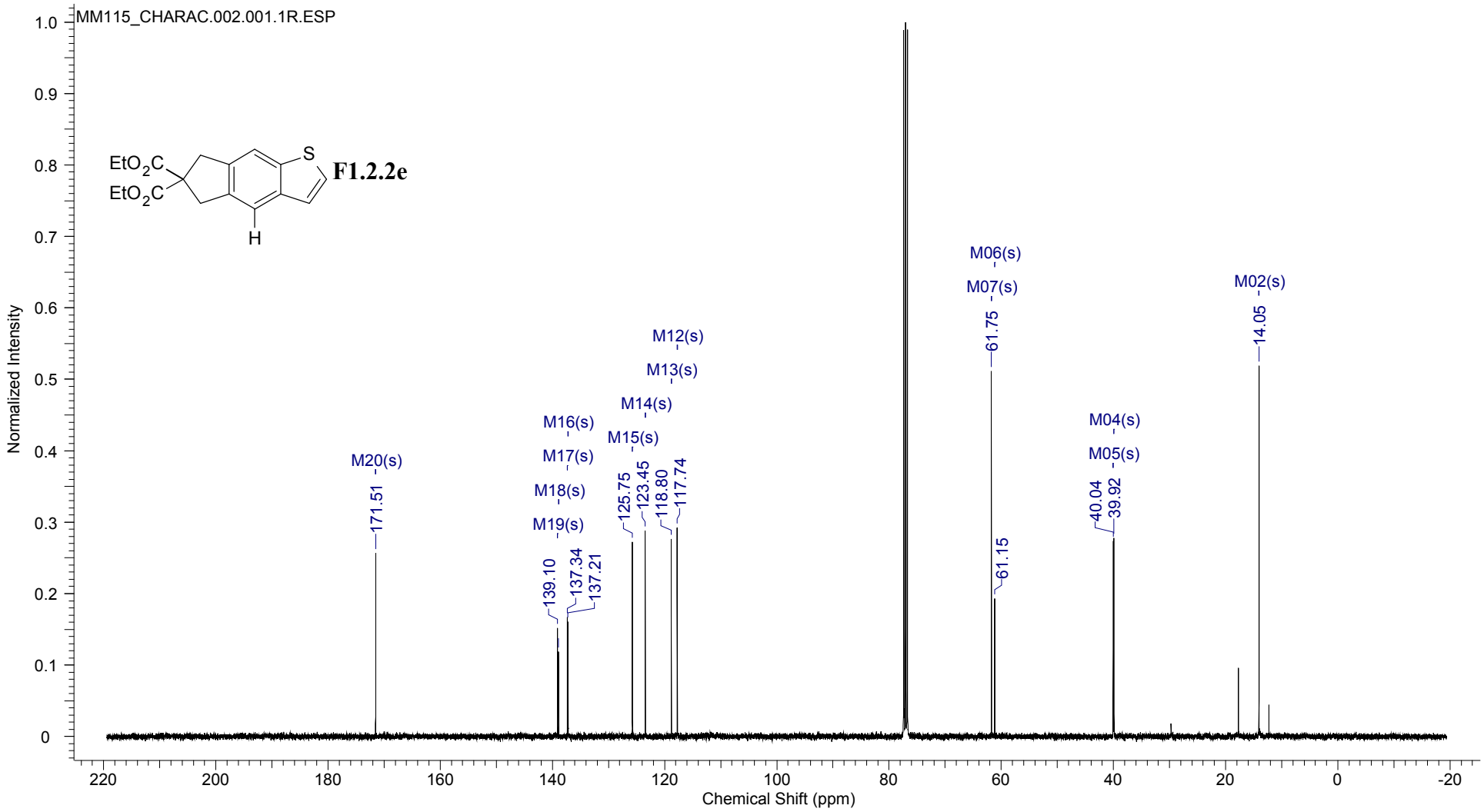
MM115_CHARAC.002.001.1R.ESP
EtO2C
EtO2C
S
H
F1.2.2e
Normalized Intensity
Chemical Shift (ppm)
M20(s)
171.51
M16(s)
M17(s)
M18(s)
M19(s)
139.10
137.34
137.21
M15(s)
125.75
123.45
M14(s)
118.80
117.74
M12(s)
M13(s)
M06(s)
M07(s)
61.75
61.15
M04(s)
M05(s)
40.04
39.92
M02(s)
14.05

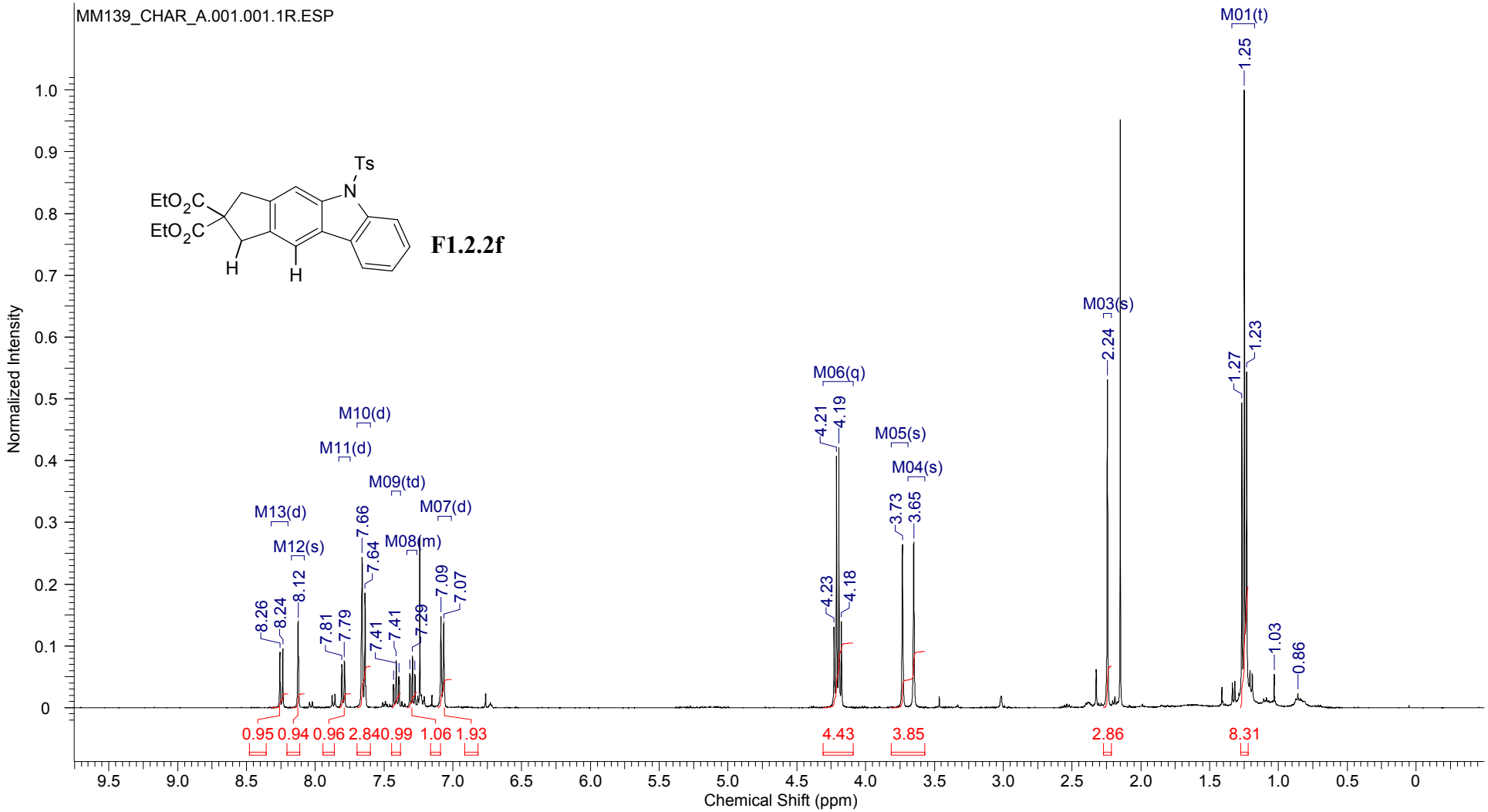
MM139_CHAR_A.001.001.1R.ESP
Ts
N
EtO2C
EtO2C
H
H
F1.2.2f
M01(t)
1.25
M03(s)
2.24
1.27
1.23
M06(q)
4.21
4.19
M05(s)
M04(s)
3.73
3.65
M10(d)
M11(d)
M09(td)
M07(d)
M13(d)
M12(s)
M08(m)
7.66
7.64
7.09
7.07
8.26
8.24
8.12
7.81
7.79
7.41
7.41
7.29
4.23
4.18
1.03
0.86
0.95 0.94 0.96 2.84 0.99 1.06 1.93
4.43
3.85
2.86
8.31
Normalized Intensity
Chemical Shift (ppm)

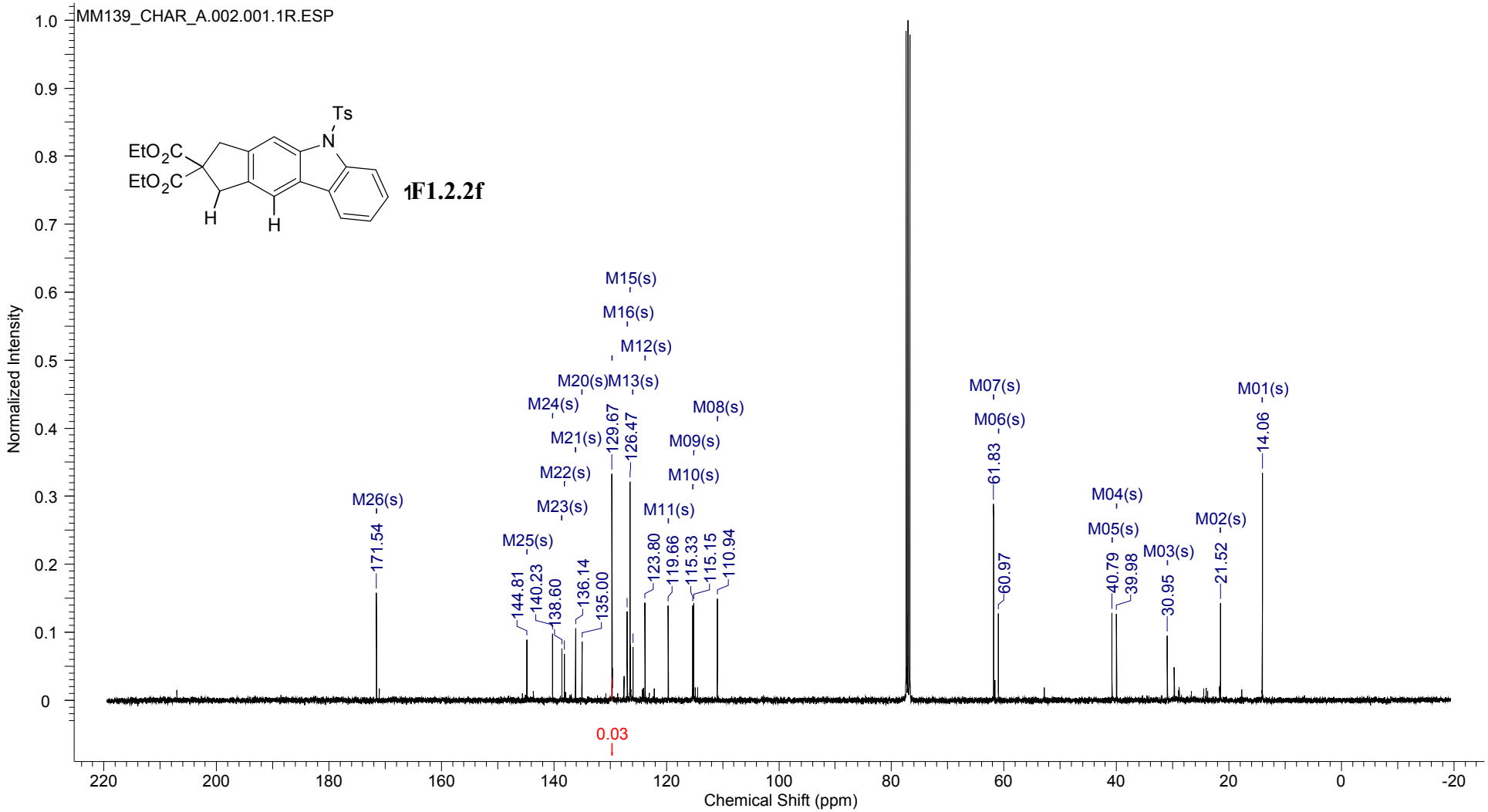
MM139_CHAR_A.002.001.1R.ESP
Ts
N
EtO2C
EtO2C
H
H
1F1.2.2f
Normalized Intensity
Chemical Shift (ppm)
M15(s)
M16(s)
M12(s)
M20(s)
M13(s)
M24(s)
M08(s)
M21(s)
M09(s)
M22(s)
M10(s)
M23(s)
M11(s)
M26(s)
M25(s)
M07(s)
M06(s)
M04(s)
M05(s)
M02(s)
M03(s)
M01(s)
171.54
144.81
140.23
138.60
136.14
135.00
129.67
126.47
123.80
119.66
115.33
115.15
110.94
61.83
60.97
40.79
39.98
30.95
21.52
14.06
0.03

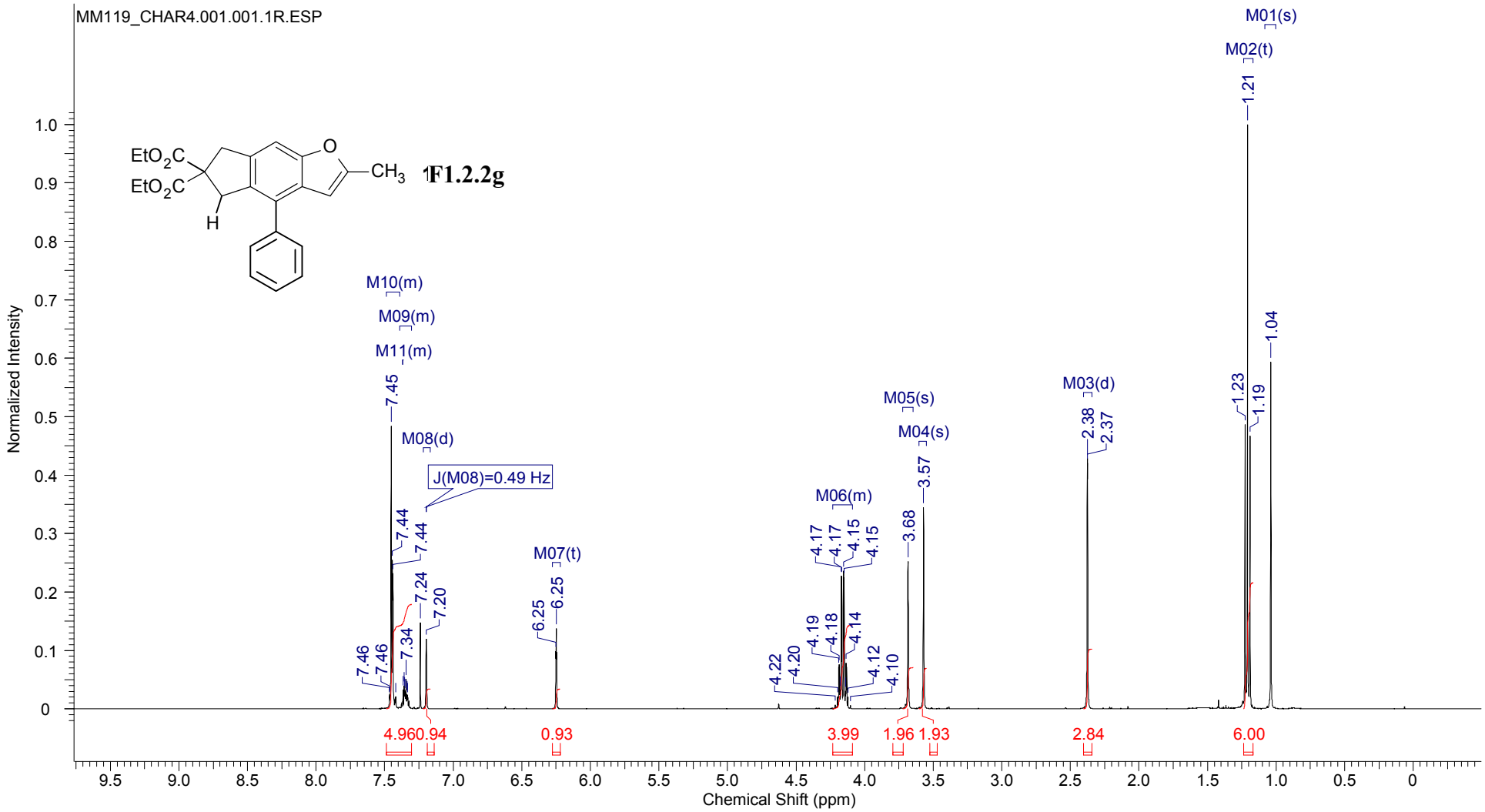
MM119_CHAR4.001.001.1R.ESP
EtO2C
EtO2C
H
O
CH3
1F1.2.2g
M01(s)
M02(t)
M03(d)
M04(s)
M05(s)
M06(m)
M07(t)
M08(d)
M09(m)
M10(m)
M11(m)
J(M08)=0.49 Hz
1.21
1.04
1.23
1.19
2.38
2.37
3.57
3.68
4.17
4.17
4.15
4.15
4.19
4.18
4.14
4.22
4.20
4.12
4.10
6.25
6.25
7.45
7.44
7.44
7.24
7.20
7.46
7.46
7.34
4.96
0.94
0.93
3.99
1.96
1.93
2.84
6.00
Normalized Intensity
Chemical Shift (ppm)

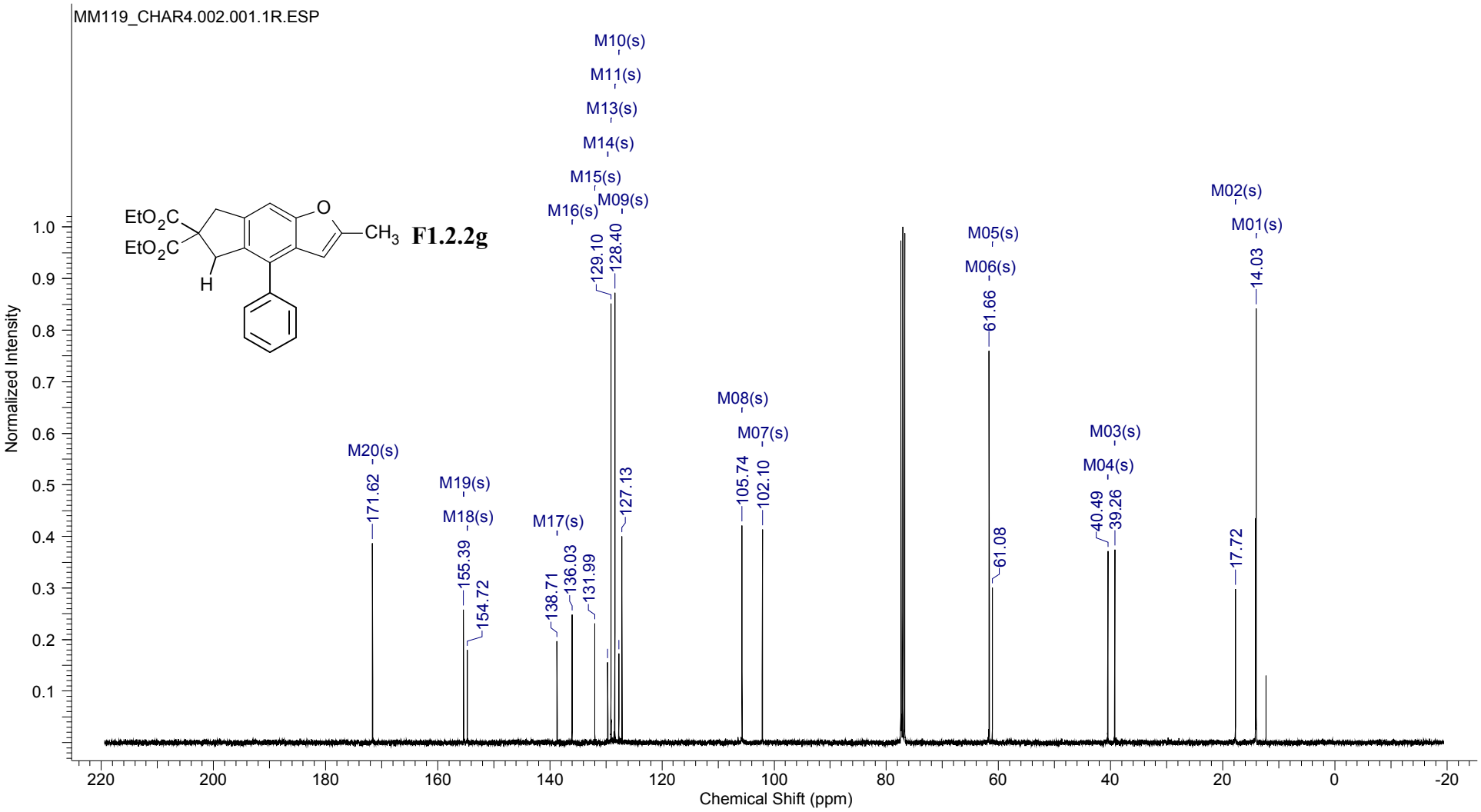
MM119_CHAR4.002.001.1R.ESP
EtO2C
EtO2C
H
O
CH3
F1.2.2g
M10(s)
M11(s)
M13(s)
M14(s)
M15(s)
M16(s)
M09(s)
M02(s)
M01(s)
M05(s)
M06(s)
M08(s)
M07(s)
M03(s)
M04(s)
M20(s)
M19(s)
M18(s)
M17(s)
129.10
128.40
14.03
61.66
171.62
155.39
154.72
138.71
136.03
131.99
127.13
105.74
102.10
61.08
40.49
39.26
17.72
Normalized Intensity
Chemical Shift (ppm)

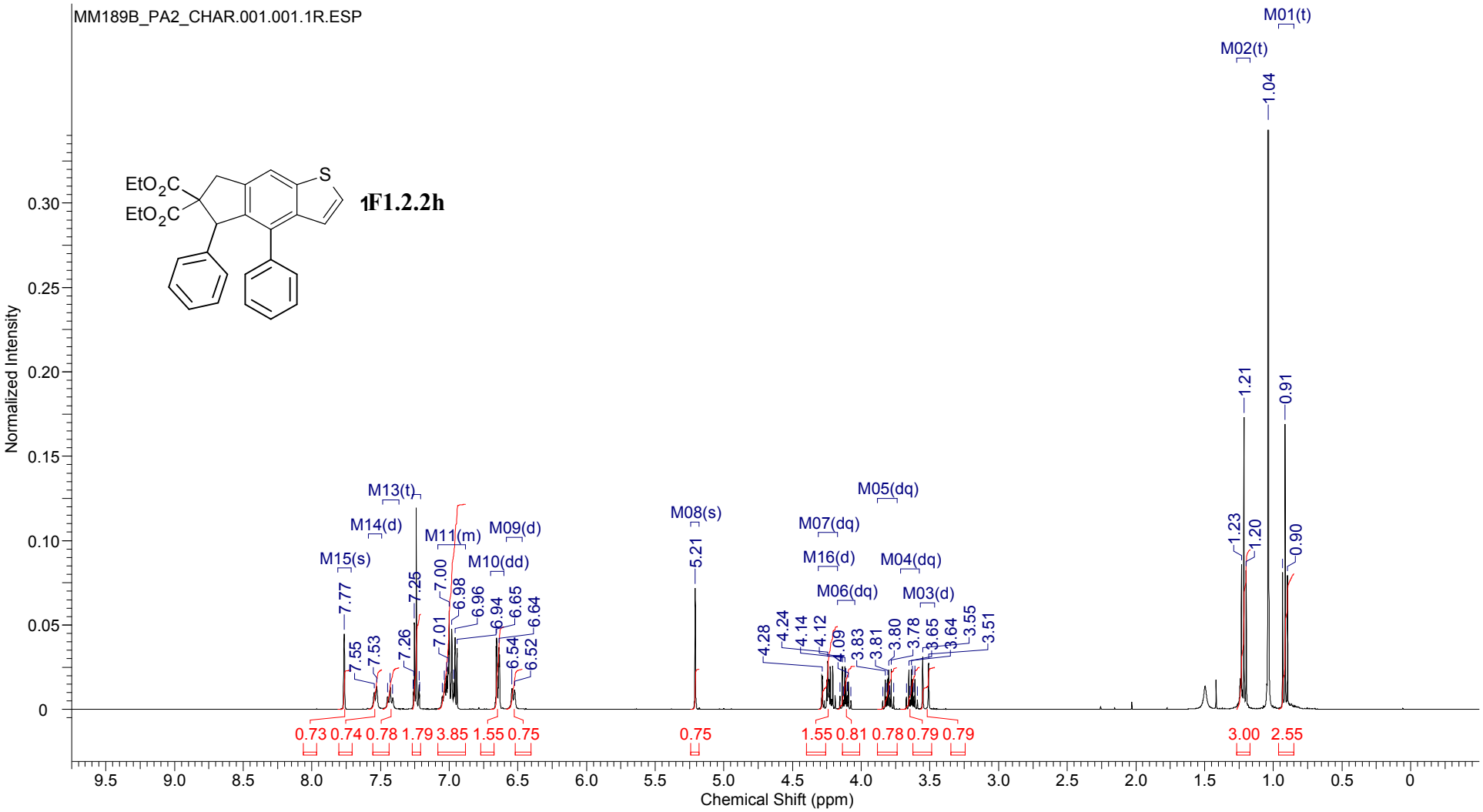
MM189B_PA2_CHAR.001.001.1R.ESP
EtO2C
EtO2C
S
1F1.2.2h
M01(t)
M02(t)
1.04
1.21
0.91
1.23
1.20
0.90
M13(t)
M14(d)
M15(s)
M11(m)
M09(d)
M10(dd)
M08(s)
5.21
M05(dq)
M07(dq)
M16(d)
M04(dq)
M06(dq)
M03(d)
7.77
7.55
7.53
7.26
7.25
7.01
7.00
6.98
6.96
6.94
6.65
6.64
6.54
6.52
4.28
4.24
4.14
4.12
4.09
3.83
3.81
3.80
3.78
3.65
3.64
3.55
3.51
0.73 0.74 0.78 1.79 3.85 1.55 0.75
0.75
1.55 0.81 0.78 0.79 0.79
3.00 2.55
Normalized Intensity
Chemical Shift (ppm)

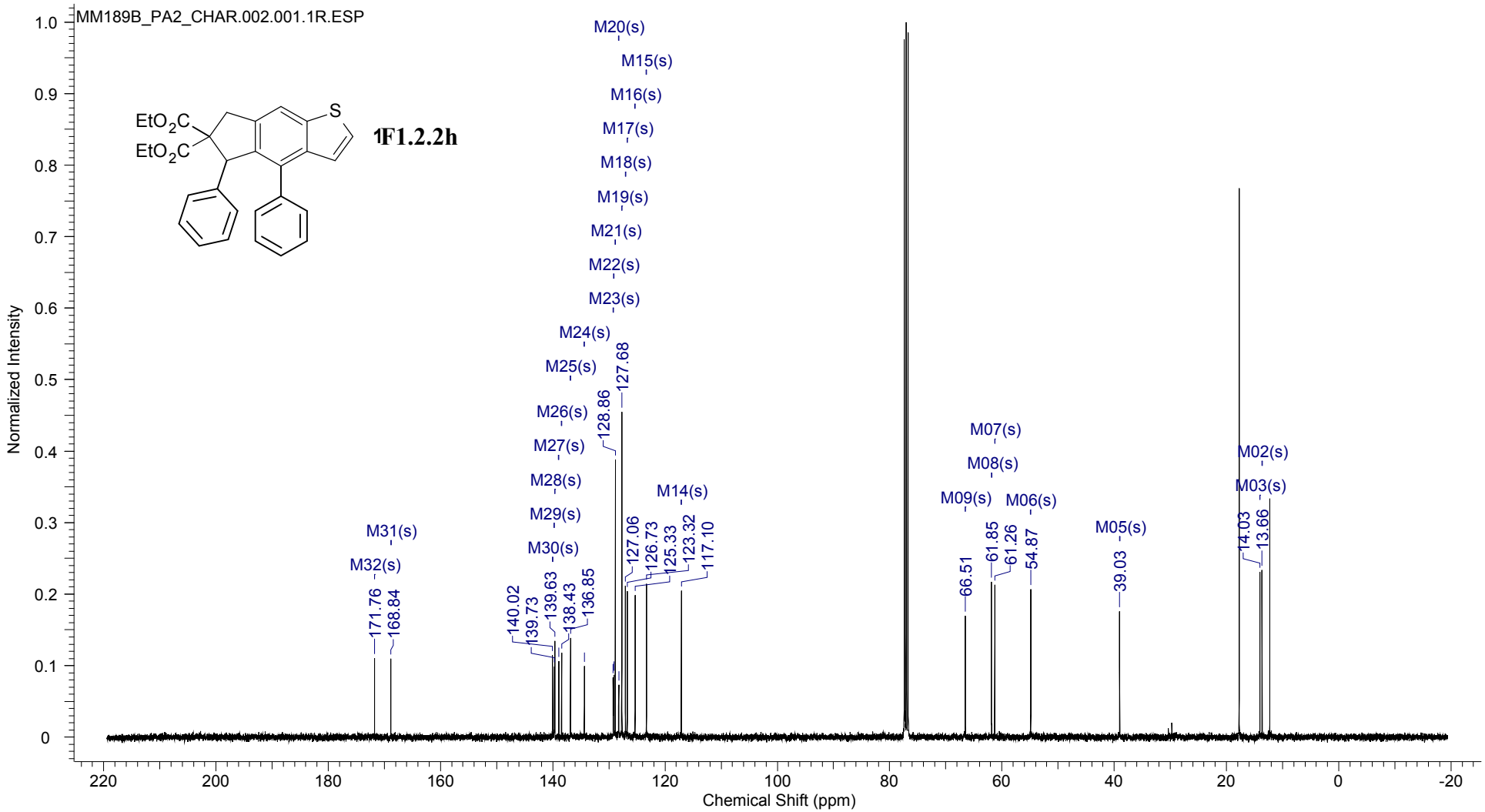
MM189B_PA2_CHAR.002.001.1R.ESP
EtO2C
EtO2C
S
1F1.2.2h
M20(s)
M15(s)
M16(s)
M17(s)
M18(s)
M19(s)
M21(s)
M22(s)
M23(s)
M24(s)
M25(s)
M26(s)
M27(s)
M28(s)
M29(s)
M30(s)
M31(s)
M32(s)
M14(s)
M07(s)
M08(s)
M09(s)
M06(s)
M05(s)
M02(s)
M03(s)
127.68
128.86
127.06
126.73
125.33
123.32
117.10
171.76
168.84
140.02
139.73
139.63
138.43
136.85
66.51
61.85
61.26
54.87
39.03
14.03
13.66
Normalized Intensity
Chemical Shift (ppm)

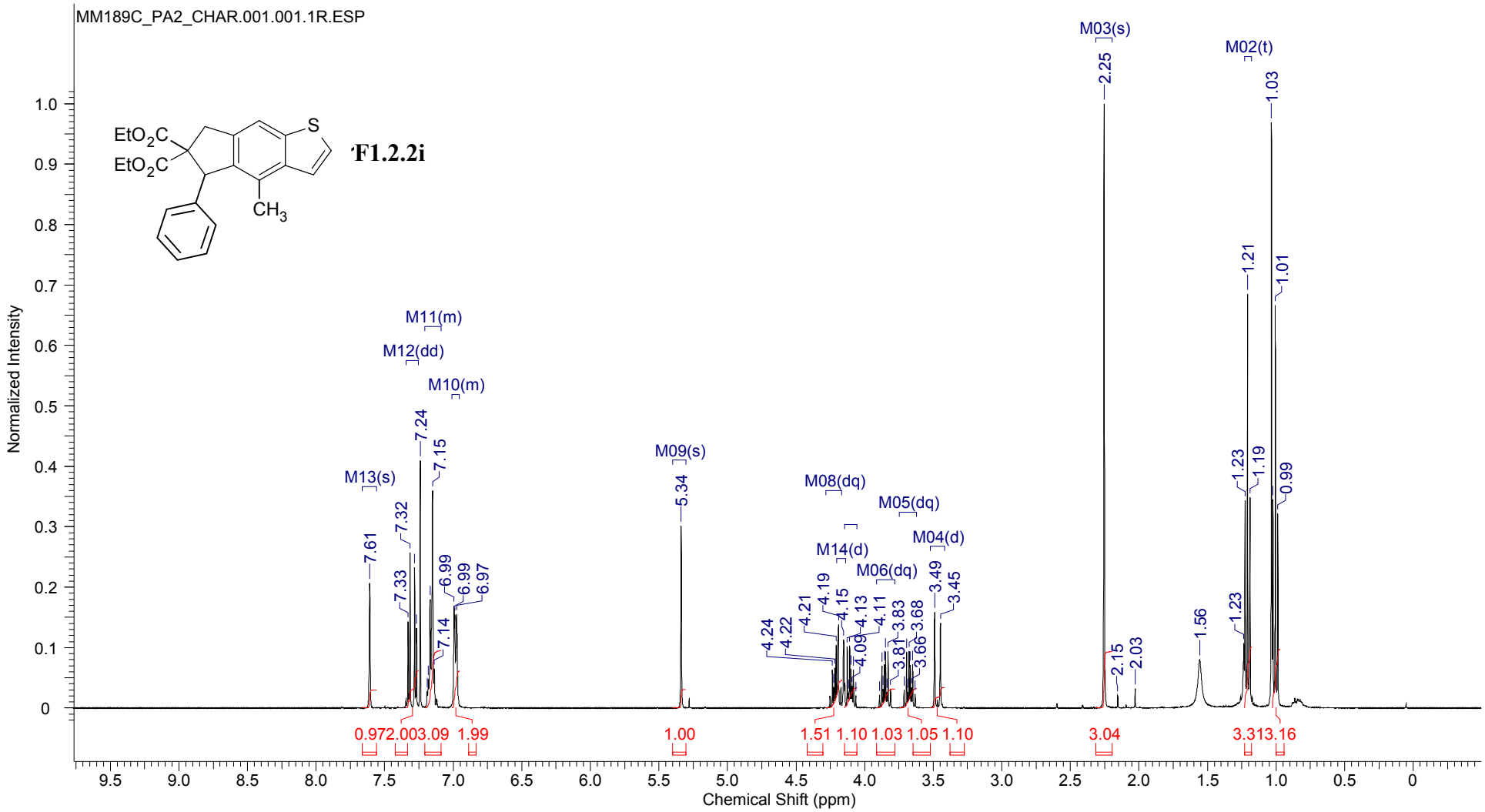
MM189C_PA2_CHAR.001.001.1R.ESP
EtO2C
EtO2C
S
CH3
F1.2.2i
M03(s)
M02(t)
M11(m)
M12(dd)
M10(m)
M13(s)
M09(s)
M08(dq)
M05(dq)
M04(d)
M14(d)
M06(dq)
7.61
7.33
7.32
7.24
7.15
7.14
6.99
6.99
6.97
5.34
4.24
4.22
4.21
4.19
4.15
4.13
4.11
4.09
3.83
3.81
3.68
3.66
3.49
3.45
2.25
2.15
2.03
1.56
1.23
1.23
1.21
1.19
1.03
1.01
0.99
0.97 2.00 3.09 1.99
1.00
1.51 1.10 1.03 1.05 1.10
3.04
3.31 3.16
Normalized Intensity
Chemical Shift (ppm)

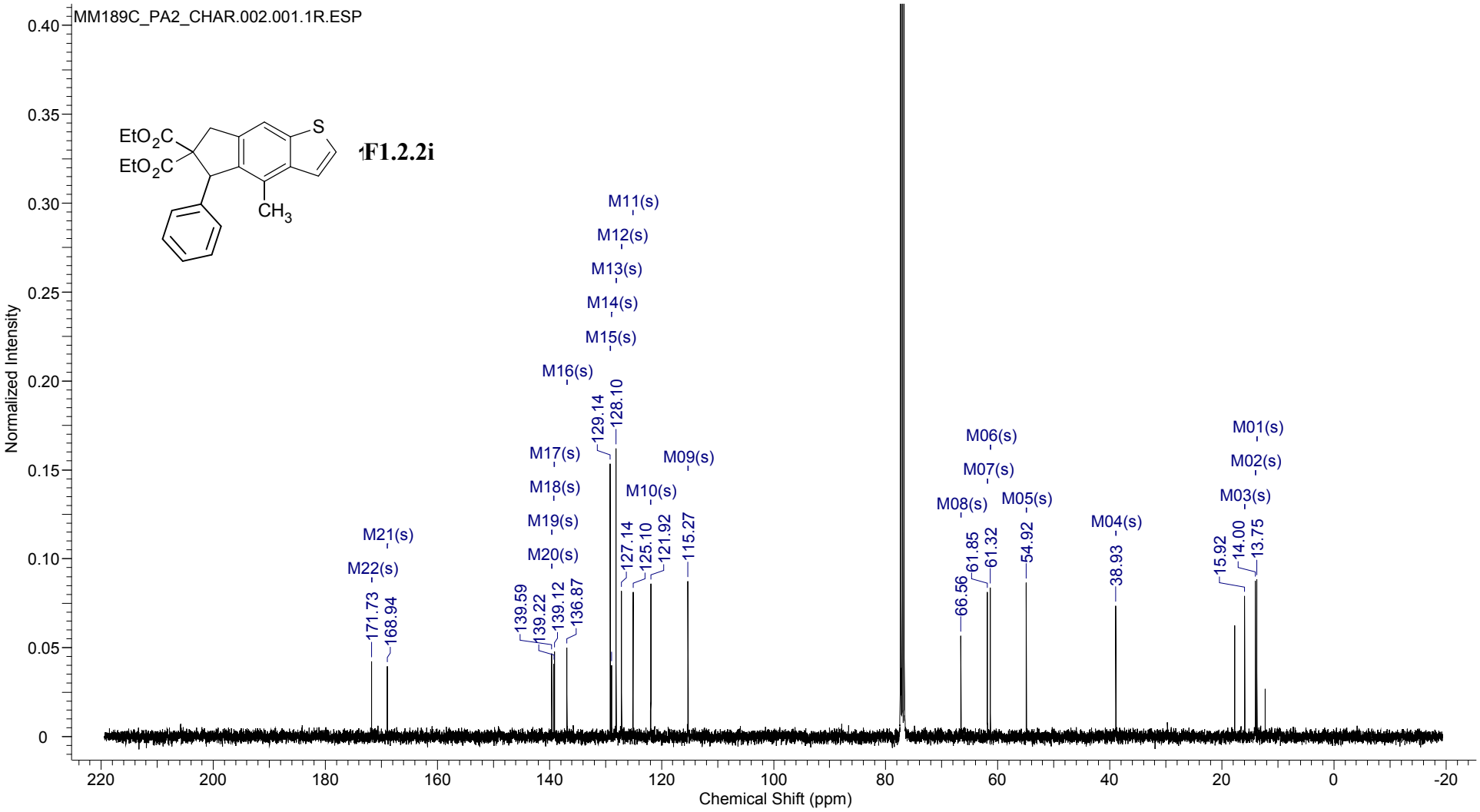
MM189C_PA2_CHAR.002.001.1R.ESP
EtO2C
EtO2C
S
CH3
1F1.2.2i
Normalized Intensity
Chemical Shift (ppm)
M01(s)
M02(s)
M03(s)
M04(s)
M05(s)
M06(s)
M07(s)
M08(s)
M09(s)
M10(s)
M11(s)
M12(s)
M13(s)
M14(s)
M15(s)
M16(s)
M17(s)
M18(s)
M19(s)
M20(s)
M21(s)
M22(s)
171.73
168.94
139.59
139.22
139.12
136.87
129.14
128.10
127.14
125.10
121.92
115.27
66.56
61.85
61.32
54.92
38.93
15.92
14.00
13.75

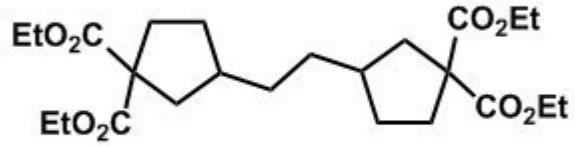
EtO2C
CO2Et
EtO2C
CO2Et

T3.2.1c

4.18
4.17
4.16
4.15
4.13
2.42
2.41
2.39
2.27
2.12
2.12
1.87
1.86
1.85
1.66
1.65
1.33
1.32
1.32
1.24
1.23
1.21
8.00
1.97 2.06 2.08 3.96 1.98 3.99 14.07
Chemical Shift (ppm)
mali e te it

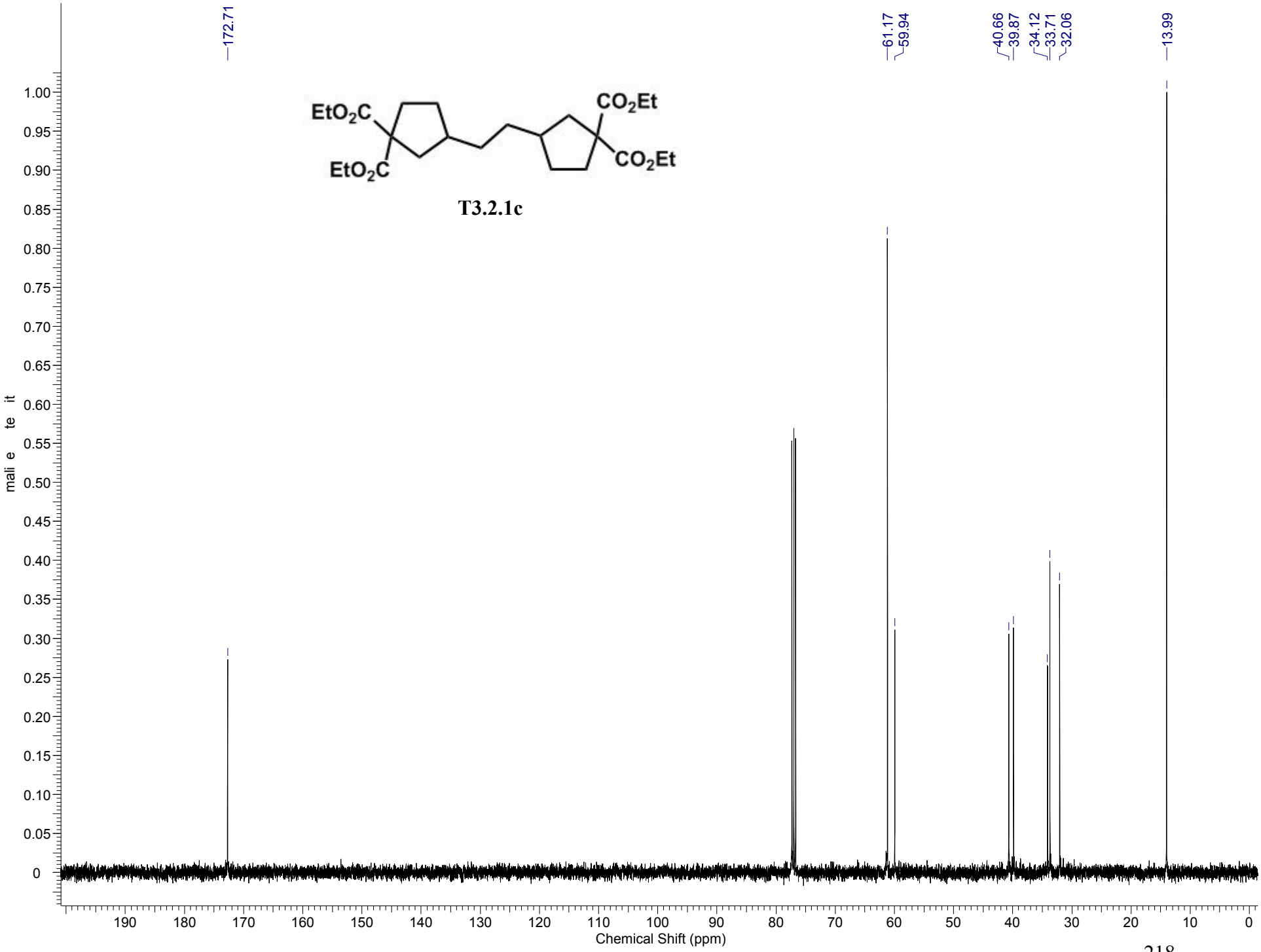
172.71
61.17
59.94
40.66
39.87
34.12
33.71
32.06
13.99
EtO2C
EtO2C
CO2Et
CO2Et
T3.2.1c
mali e te it
Chemical Shift (ppm)

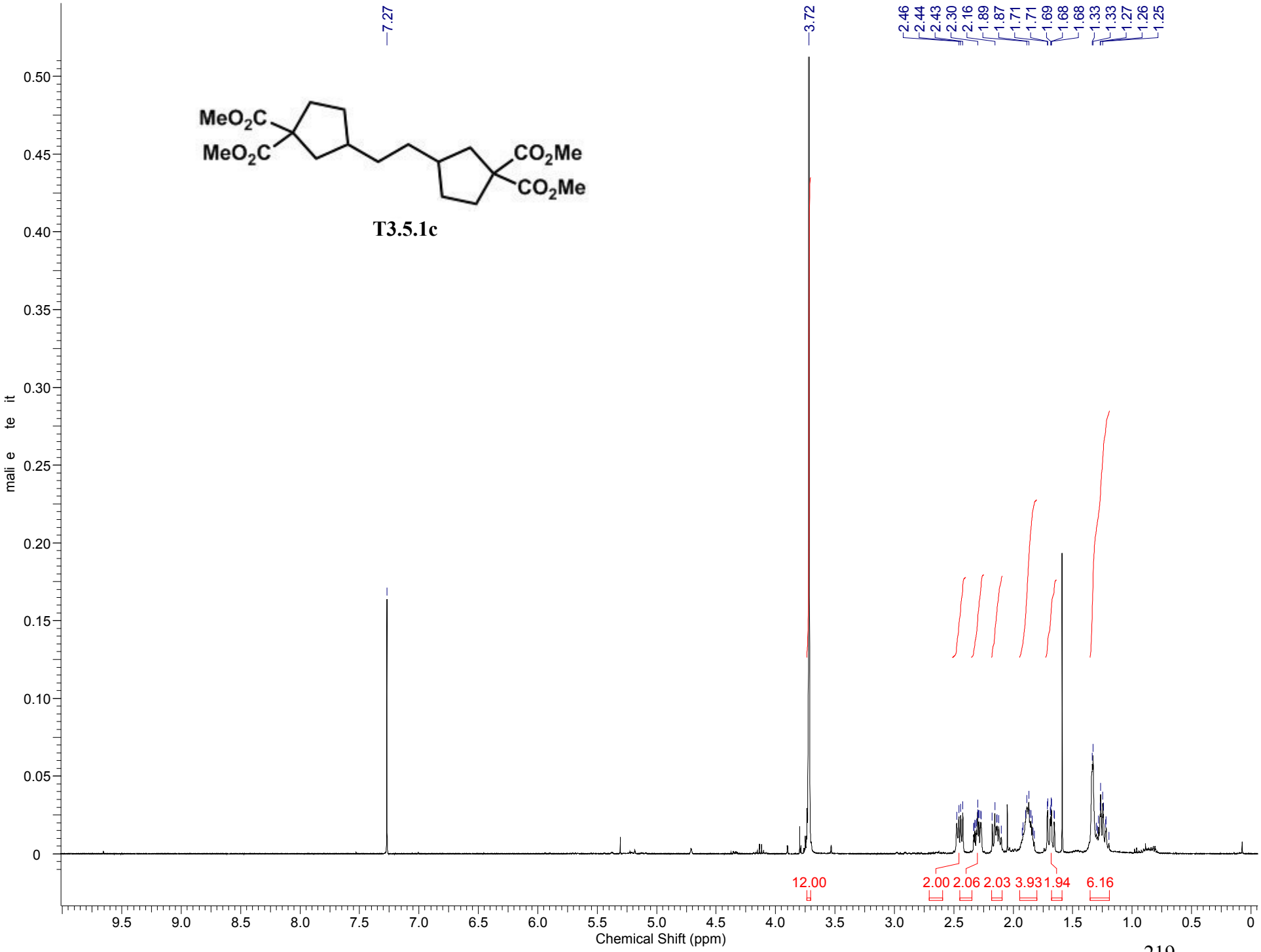
7.27
3.72
2.46
2.44
2.43
2.30
2.16
1.89
1.87
1.71
1.71
1.69
1.68
1.68
1.33
1.33
1.27
1.26
1.25
MeO2C
MeO2C
CO2Me
CO2Me
T3.5.1c
12.00
2.00
2.06
2.03
3.93
1.94
6.16
Chemical Shift (ppm)

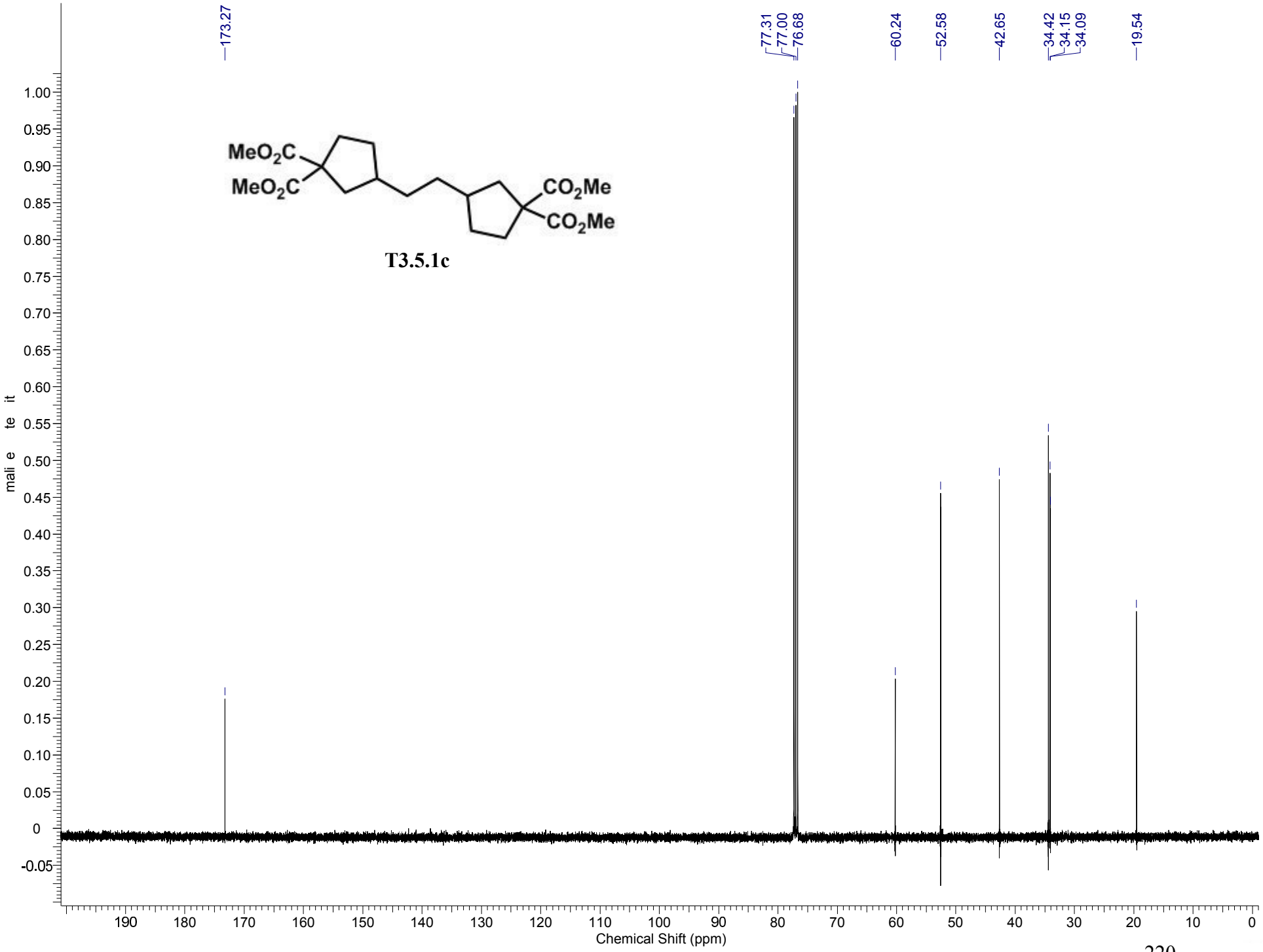
173.27
77.31
77.00
76.68
60.24
52.58
42.65
34.42
34.15
34.09
19.54
MeO2C
MeO2C
CO2Me
CO2Me
T3.5.1c
mali e te it
Chemical Shift (ppm)

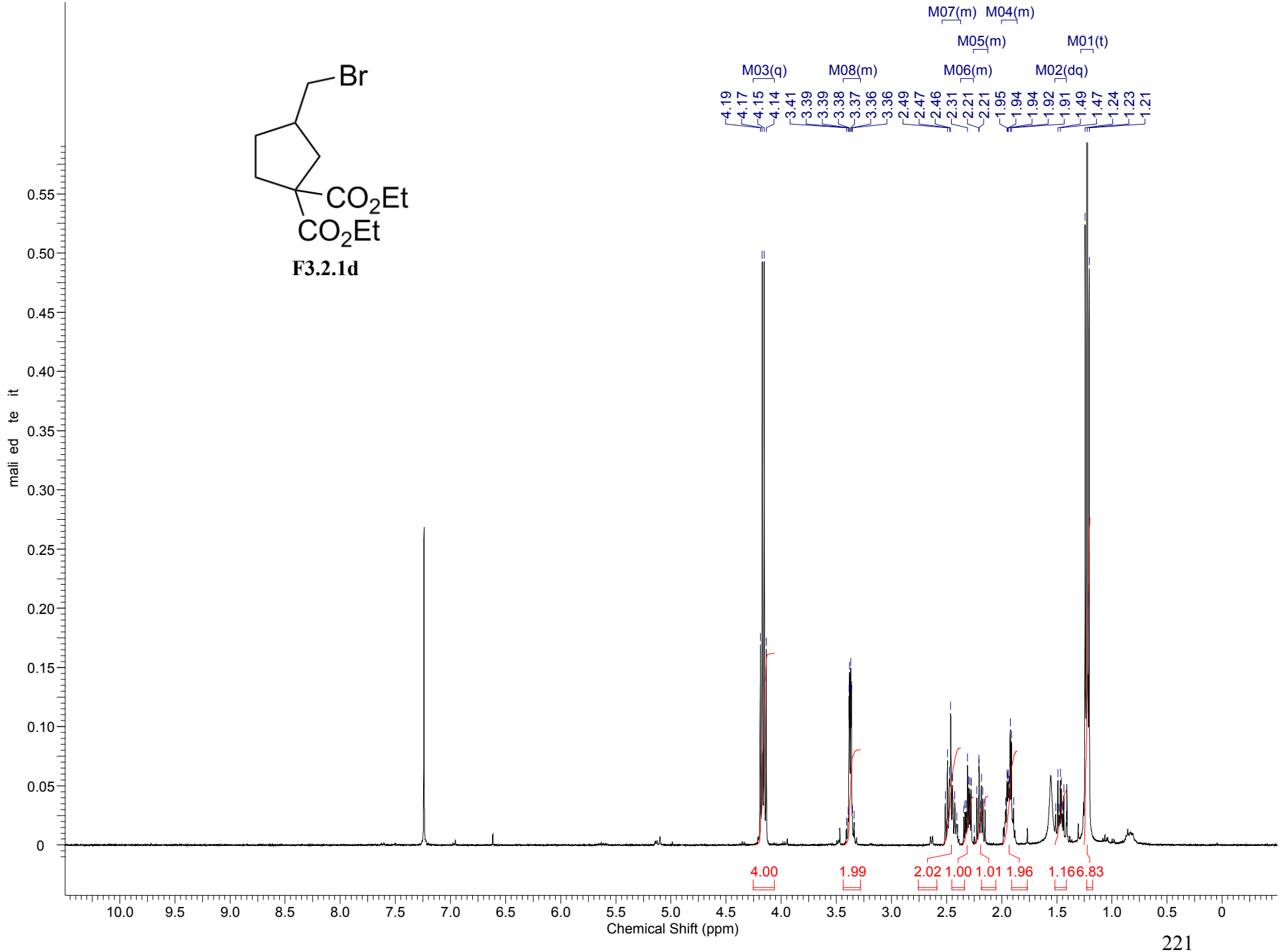
Br
CO2Et
CO2Et
F3.2.1d
M07(m) M04(m)
M05(m)
M01(t)
M03(q)
M08(m)
M06(m)
M02(dq)
4.19 4.17 4.15 4.14 3.41 3.39 3.39 3.38 3.37 3.36 3.36 2.49 2.47 2.46 2.31 2.21 2.21 1.95 1.94 1.94 1.92 1.91 1.49 1.47 1.24 1.23 1.21
4.00 1.99 2.02 1.00 1.01 1.96 1.16 6.83
mali ed te it
Chemical Shift (ppm)

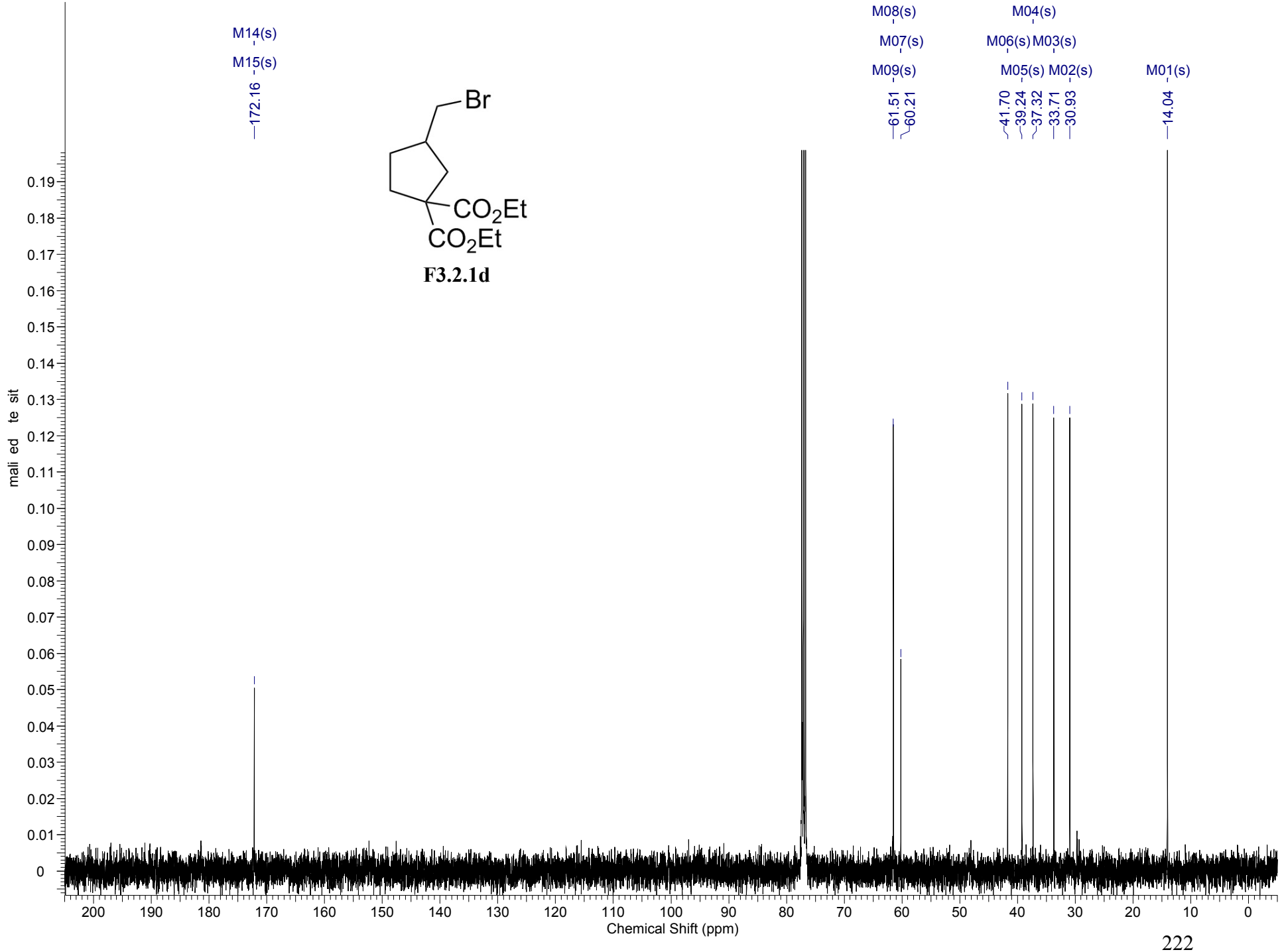
M14(s)
M15(s)
172.16
M08(s)
M07(s)
M09(s)
61.51
60.21
M04(s)
M06(s)
M03(s)
M05(s)
M02(s)
41.70
39.24
37.32
33.71
30.93
M01(s)
14.04
Br
CO2Et
CO2Et
mali ed te sit
Chemical Shift (ppm)

F3.2.1d

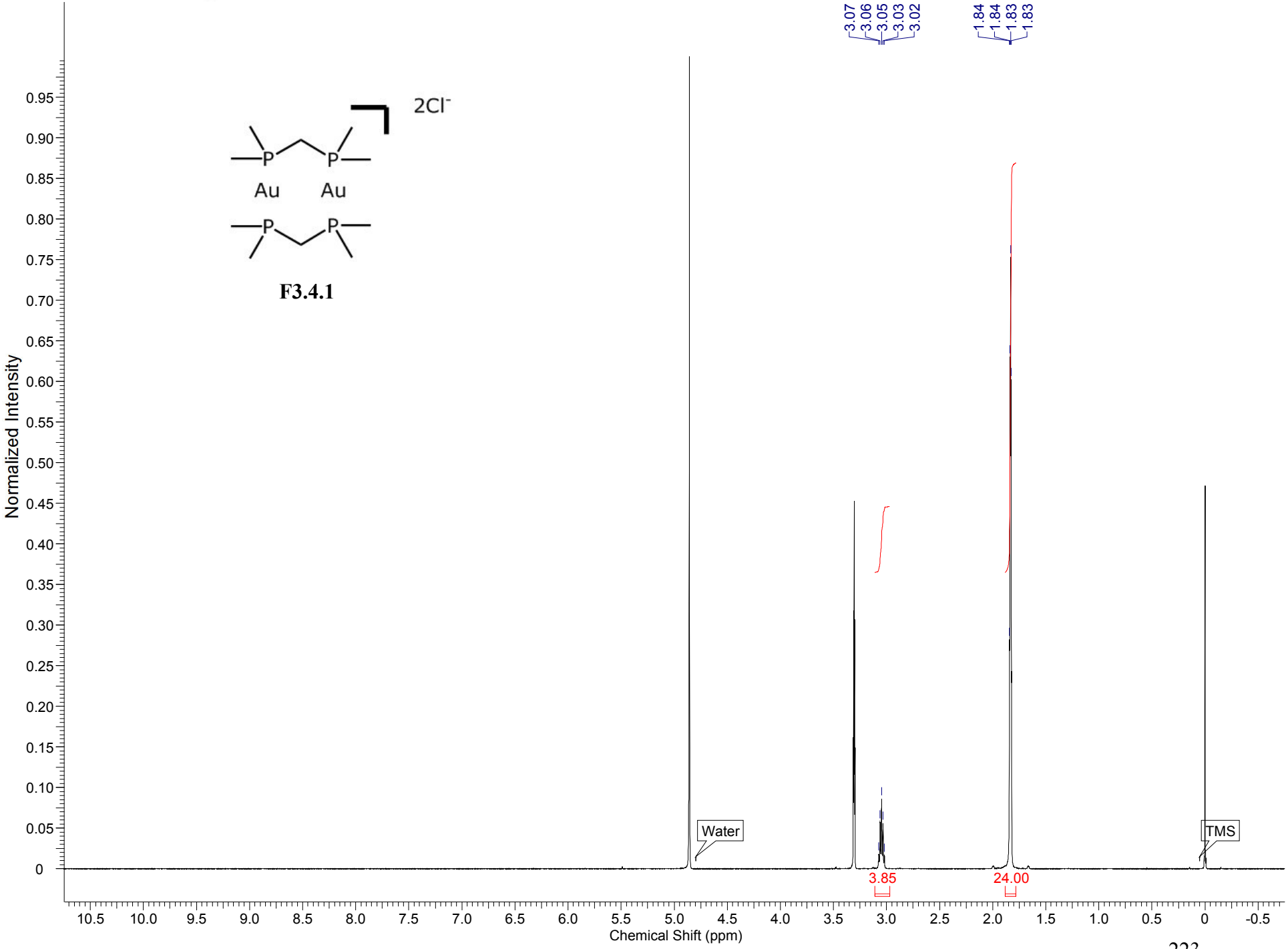
2Cl⁻
P
P
Au
Au
P
P
3.07
3.06
3.05
3.03
3.02
1.84
1.84
1.83
1.83
Water
TMS
3.85
24.00
Normalized Intensity
Chemical Shift (ppm)

F3.4.1

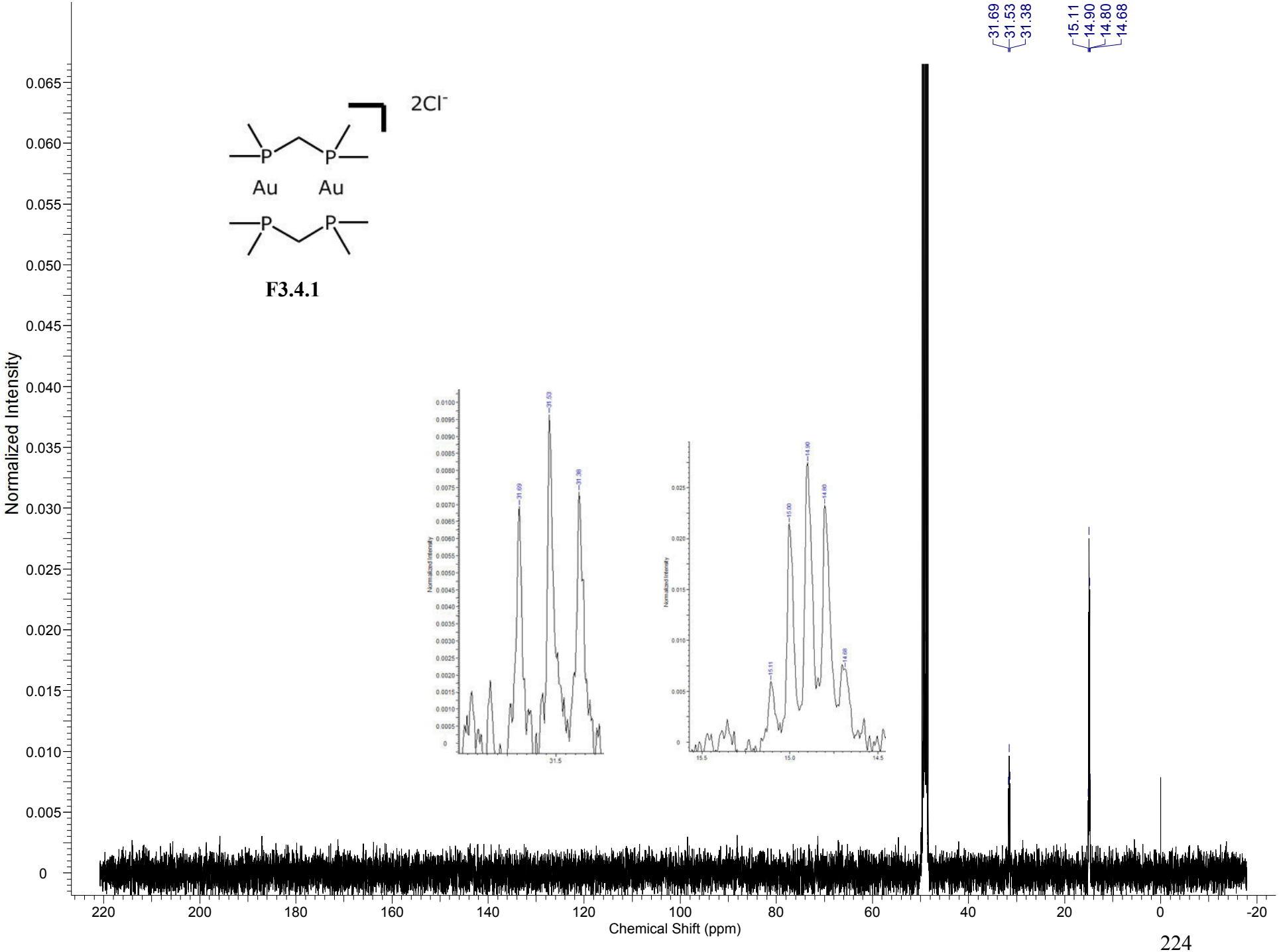
31.69
31.53
31.38
15.11
14.90
14.80
14.68
2Cl⁻
Au
Au
P
Normalized Intensity
Chemical Shift (ppm)

F3.4.1

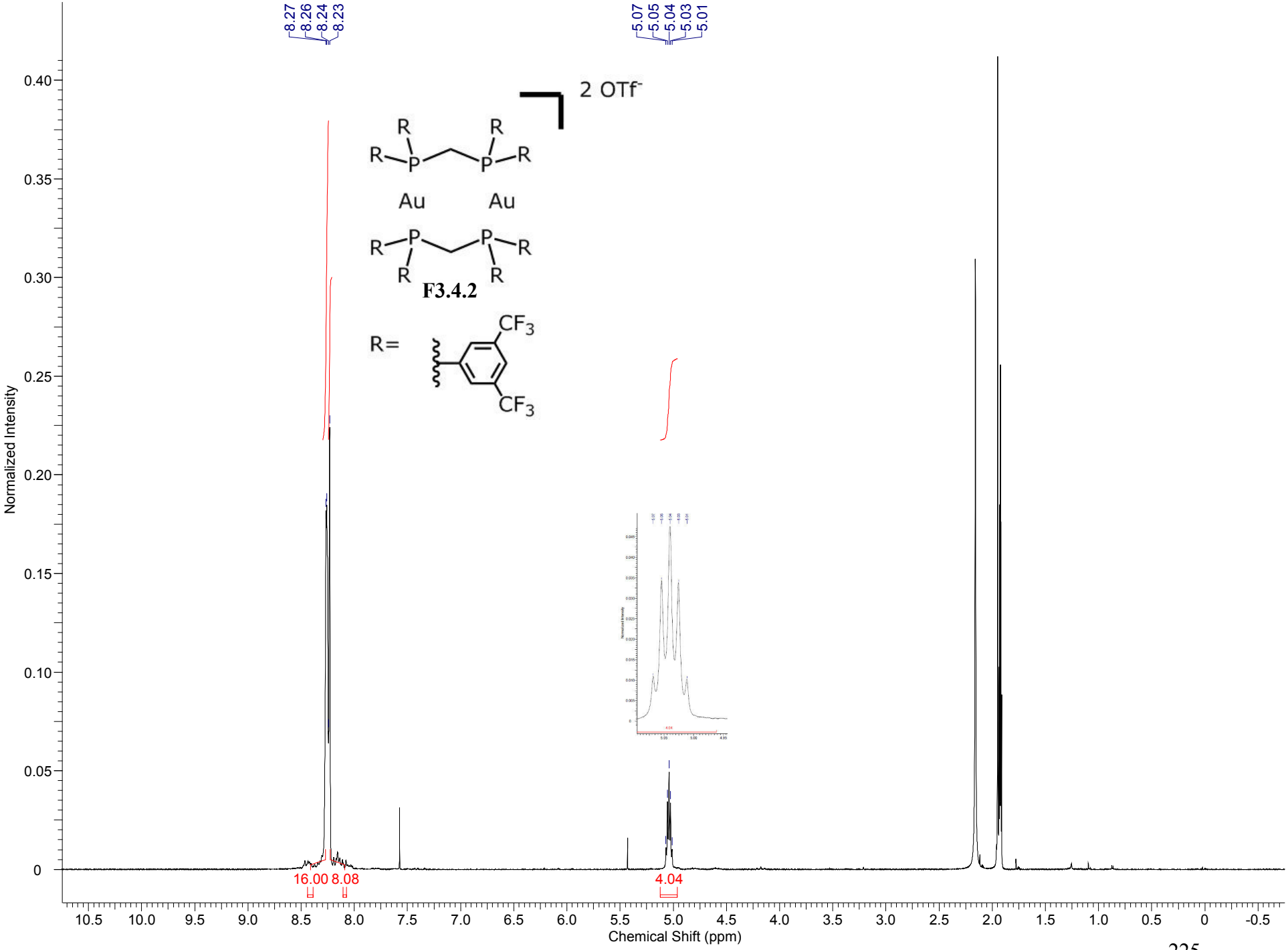
8.27
8.26
8.24
8.23
5.07
5.05
5.04
5.03
5.01
2 OTf⁻
R
P
Au
F3.4.2
R=
CF3
Normalized Intensity
16.00
8.08
4.04
Chemical Shift (ppm)

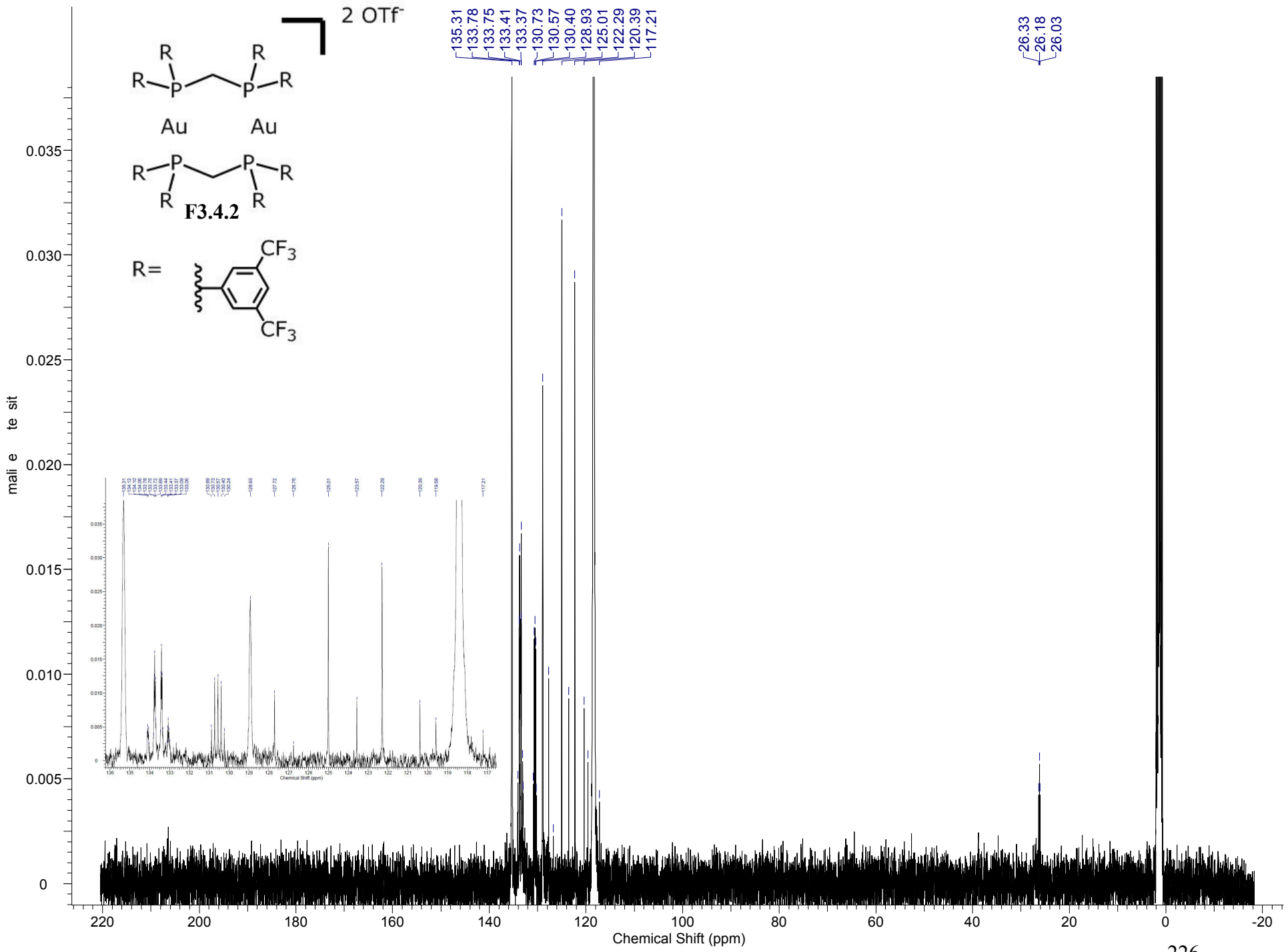
2 OTf-
135.31
133.78
133.75
133.41
133.37
130.73
130.57
130.40
128.93
125.01
122.29
120.39
117.21
26.33
26.18
26.03
Au
Au
R=
CF3
CF3
F3.4.2
mali e te sit
Chemical Shift (ppm)

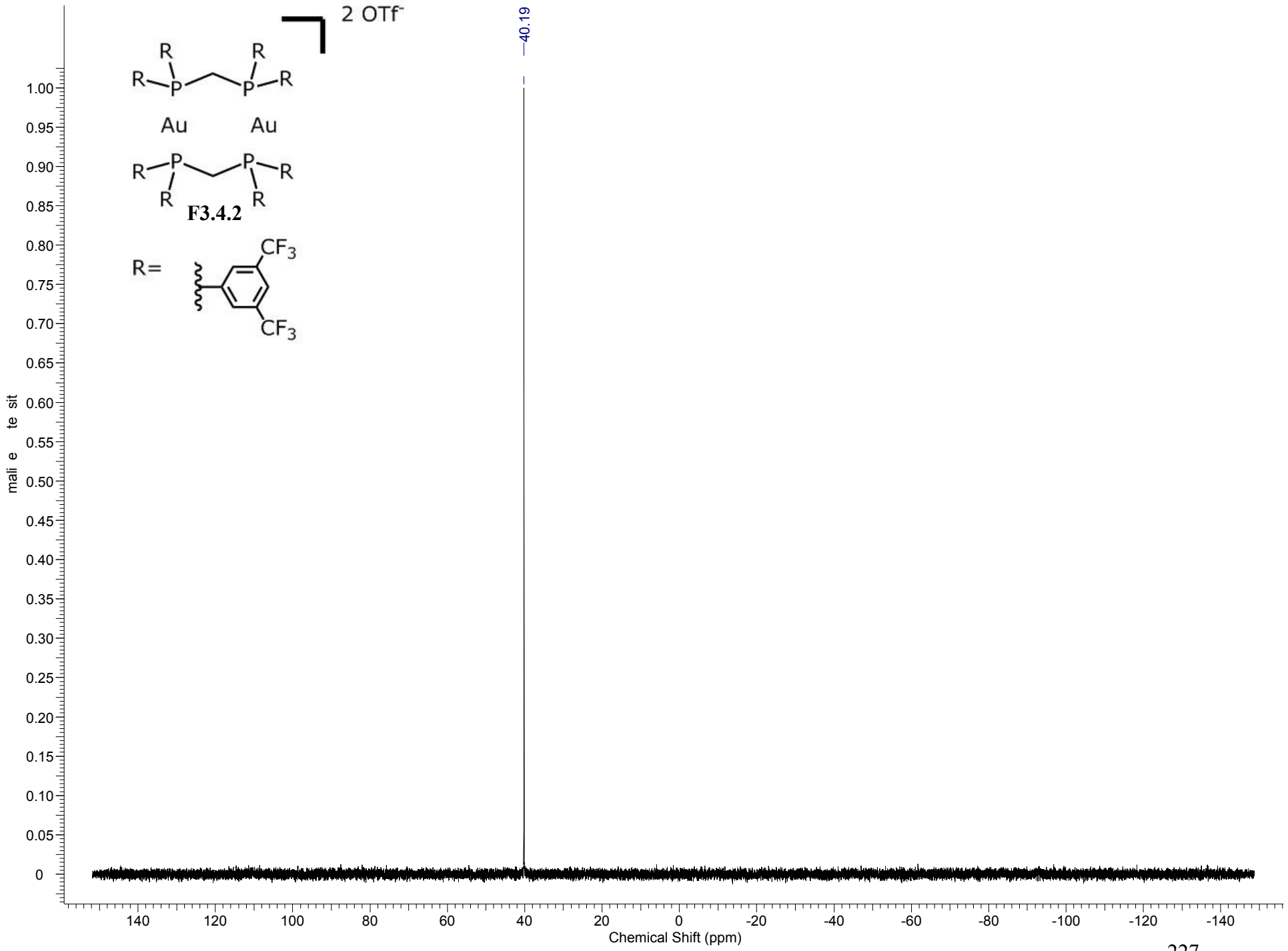
2 OTf-
40.19
R
R
R
R
P
P
R
R
Au
Au
P
P
R
R
R
R
F3.4.2
R=
CF3
CF3
mali e te sit
1.00
0.95
0.90
0.85
0.80
0.75
0.70
0.65
0.60
0.55
0.50
0.45
0.40
0.35
0.30
0.25
0.20
0.15
0.10
0.05
0
140
120
100
80
60
40
20
0
-20
-40
-60
-80
-100
-120
-140
Chemical Shift (ppm)

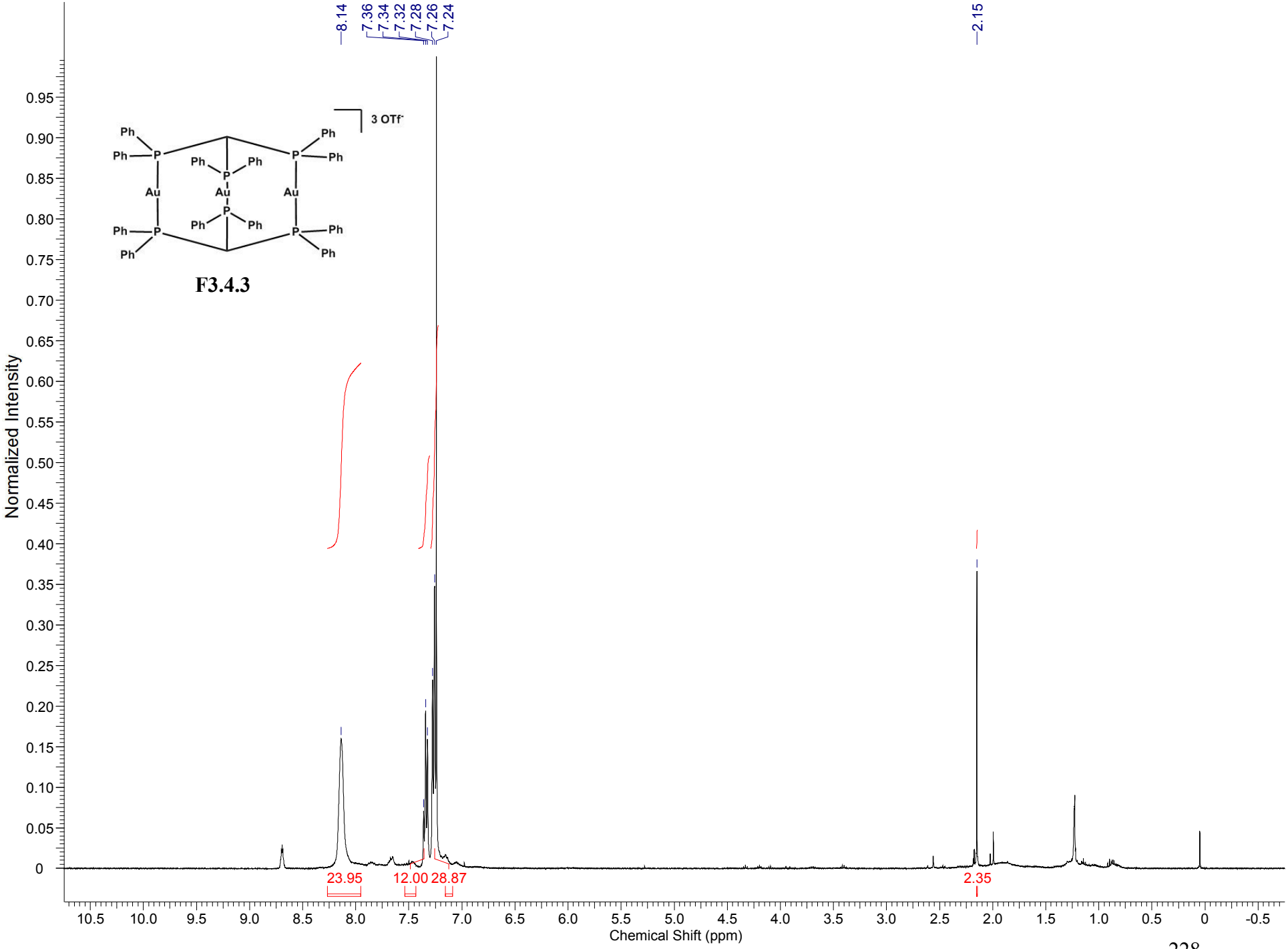
8.14
7.36
7.34
7.32
7.28
7.26
7.24
2.15
3 OTf⁻
Ph
P
Au
F3.4.3
Normalized Intensity
0.95
0.90
0.85
0.80
0.75
0.70
0.65
0.60
0.55
0.50
0.45
0.40
0.35
0.30
0.25
0.20
0.15
0.10
0.05
0
23.95
12.00
28.87
2.35
10.5
10.0
9.5
9.0
8.5
8.0
7.5
7.0
6.5
6.0
5.5
5.0
4.5
4.0
3.5
3.0
2.5
2.0
1.5
1.0
0.5
0
-0.5
Chemical Shift (ppm)

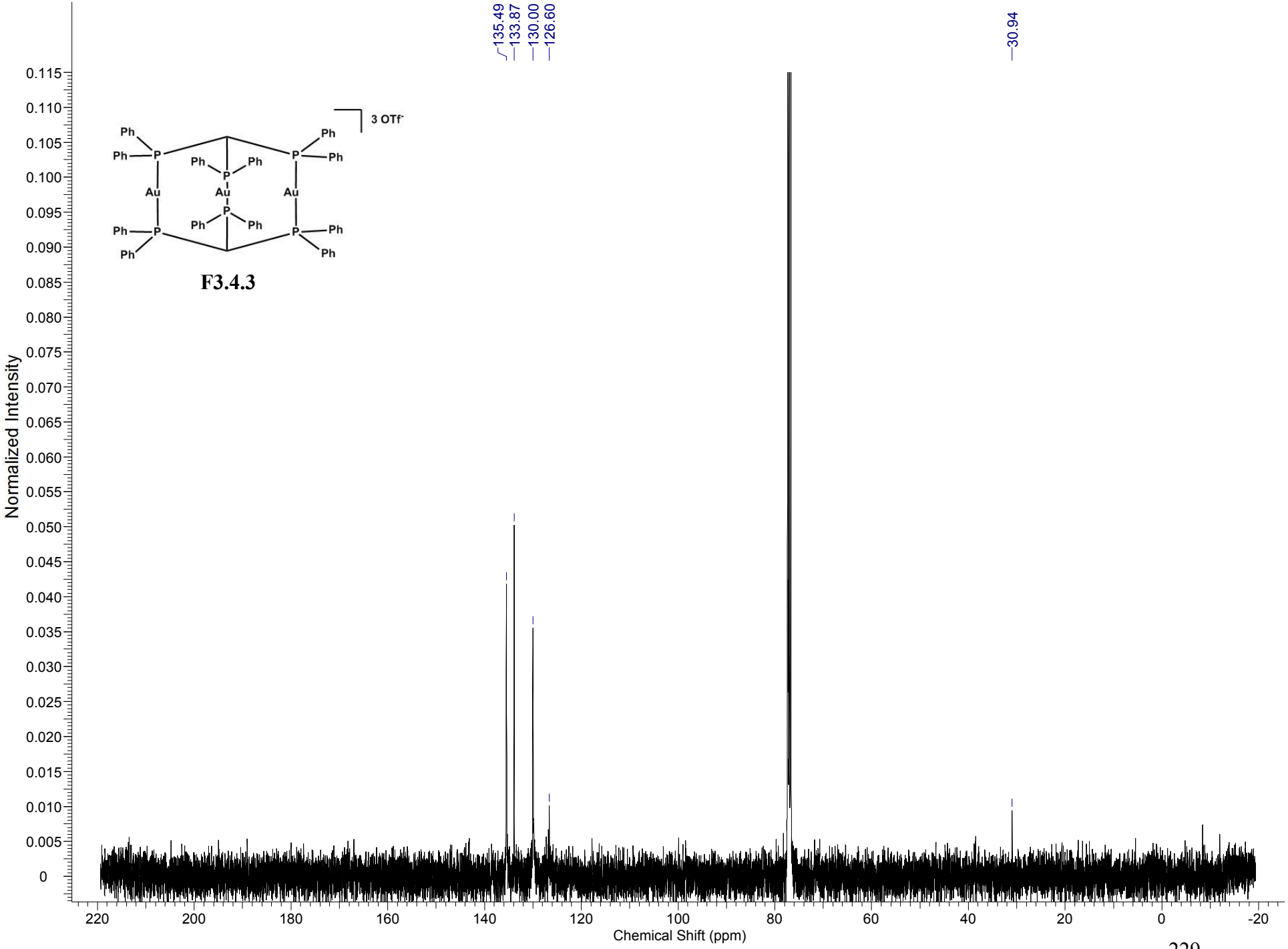
135.49
133.87
130.00
126.60
30.94
3 OTf-
Ph
P
Au
Normalized Intensity
Chemical Shift (ppm)

F3.4.3

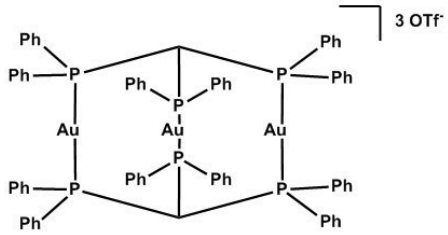
3 OTf-
Ph
P
Au

F3.4.3

45.79
Normalized Intensity
1.00
0.95
0.90
0.85
0.80
0.75
0.70
0.65
0.60
0.55
0.50
0.45
0.40
0.35
0.30
0.25
0.20
0.15
0.10
0.05
0
140
120
100
80
60
40
20
0
-20
-40
-60
-80
-100
-120
-140
Chemical Shift (ppm)

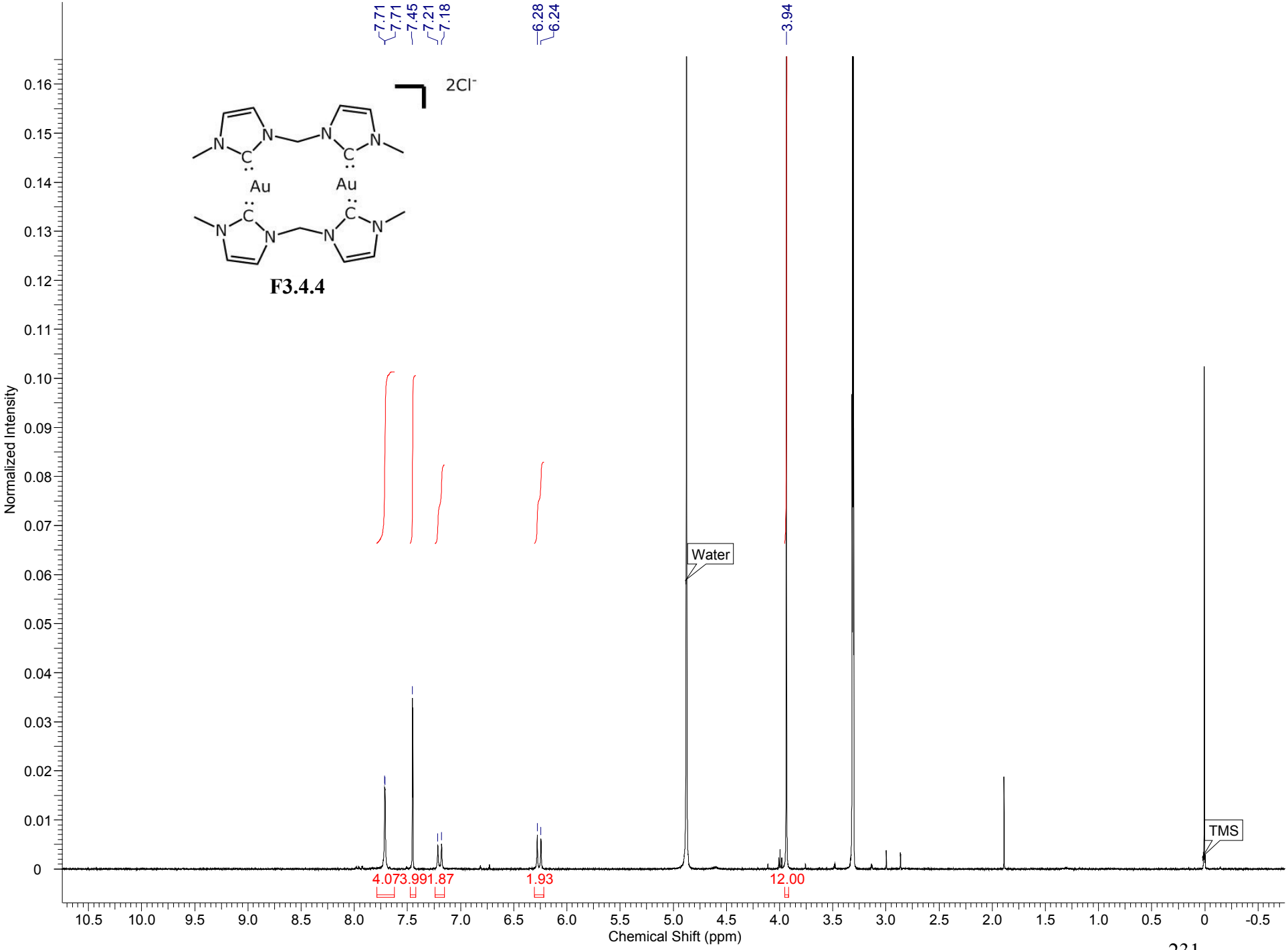
7.71
7.71
7.45
7.21
7.18
6.28
6.24
3.94
2Cl⁻
Au
Au
Water
TMS
4.07
3.99
1.87
1.93
12.00
Normalized Intensity
Chemical Shift (ppm)

F3.4.4

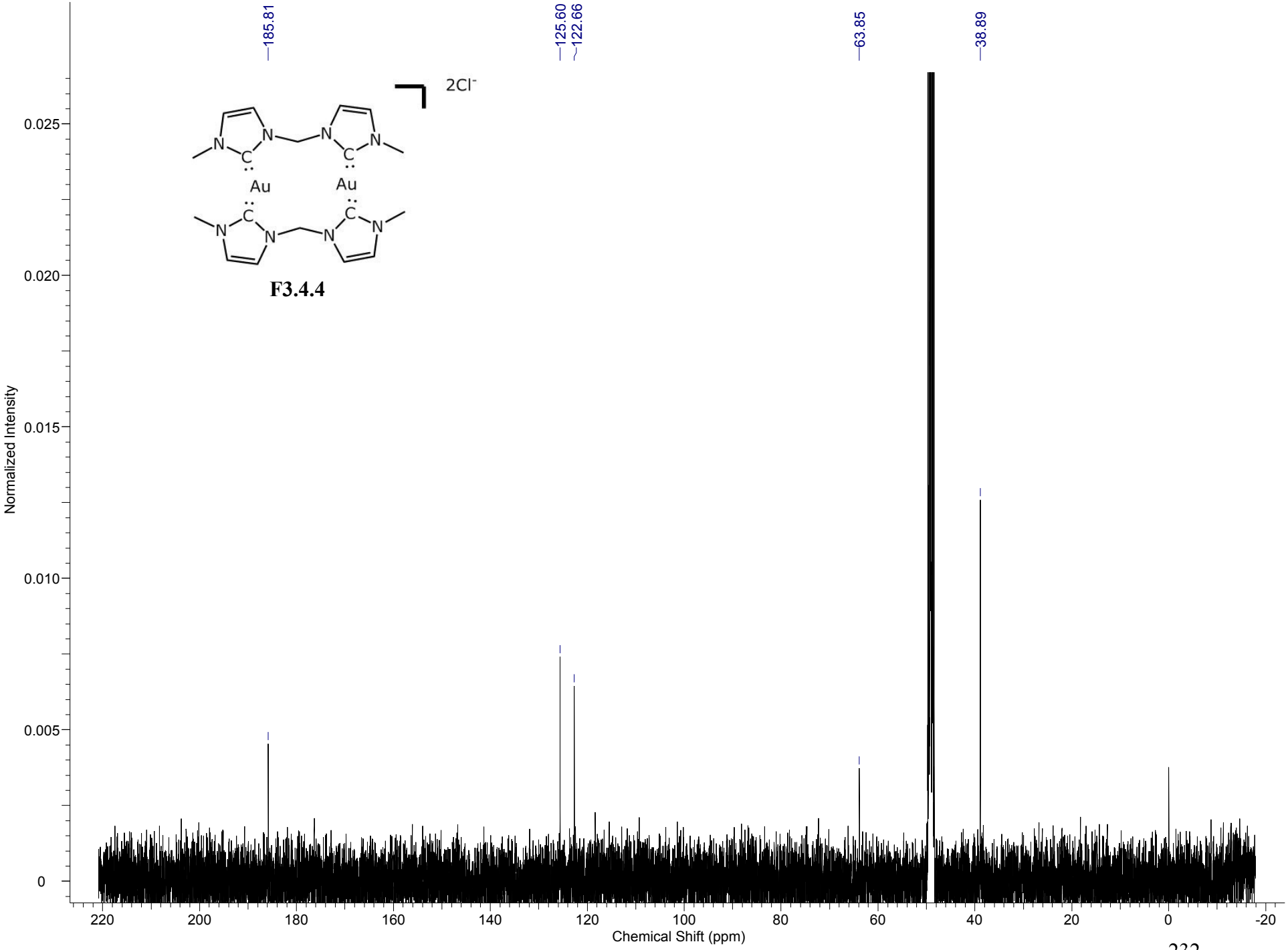
185.81
125.60
122.66
63.85
38.89
2Cl⁻
Au
Au
Normalized Intensity
0.025
0.020
0.015
0.010
0.005
0
220
200
180
160
140
120
100
80
60
40
20
0
-20
Chemical Shift (ppm)

F3.4.4

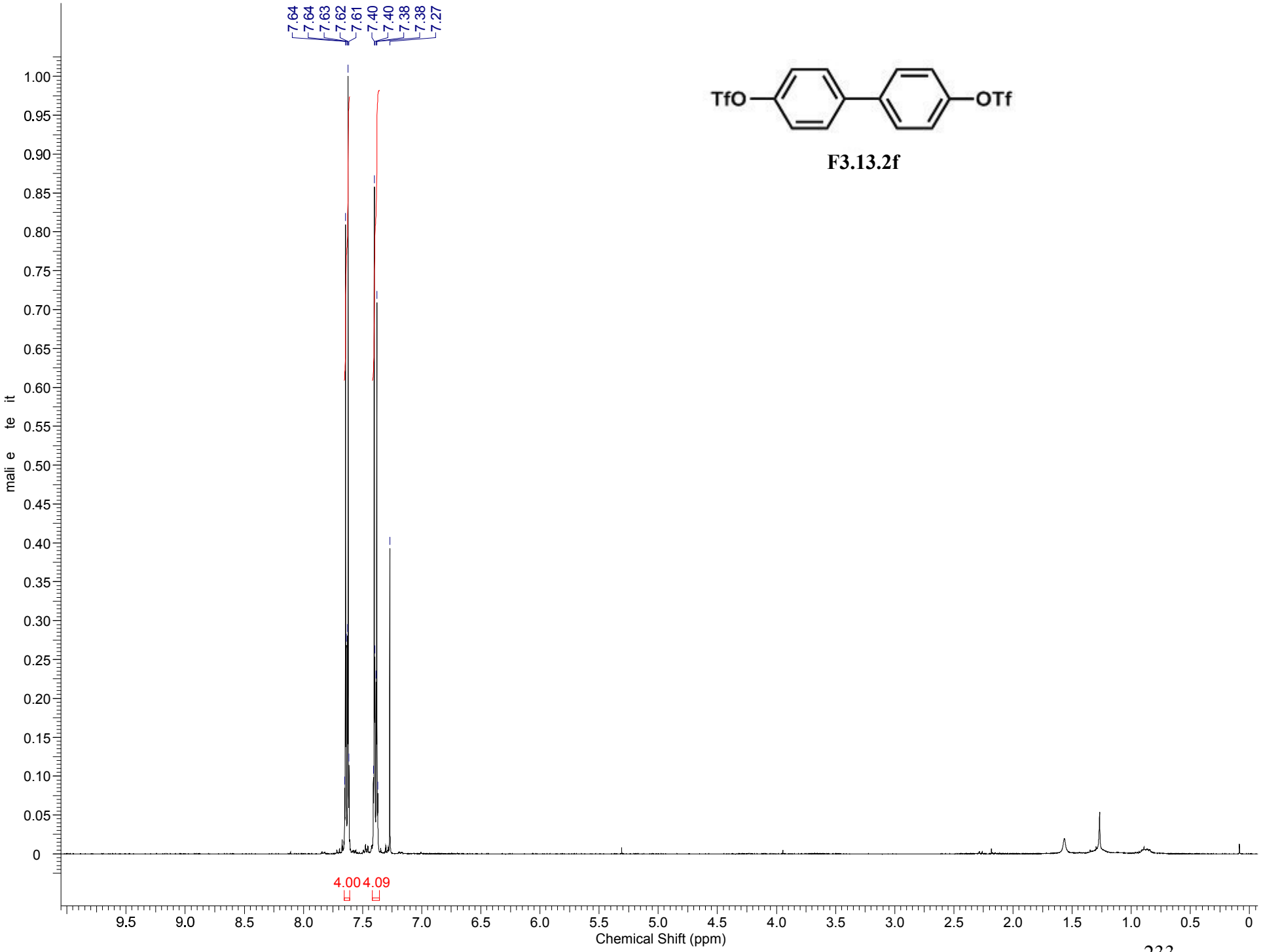
7.64
7.64
7.63
7.62
7.61
7.40
7.40
7.38
7.38
7.27
TfO
OTf
F3.13.2f
mali e te it
4.00
4.09
Chemical Shift (ppm)

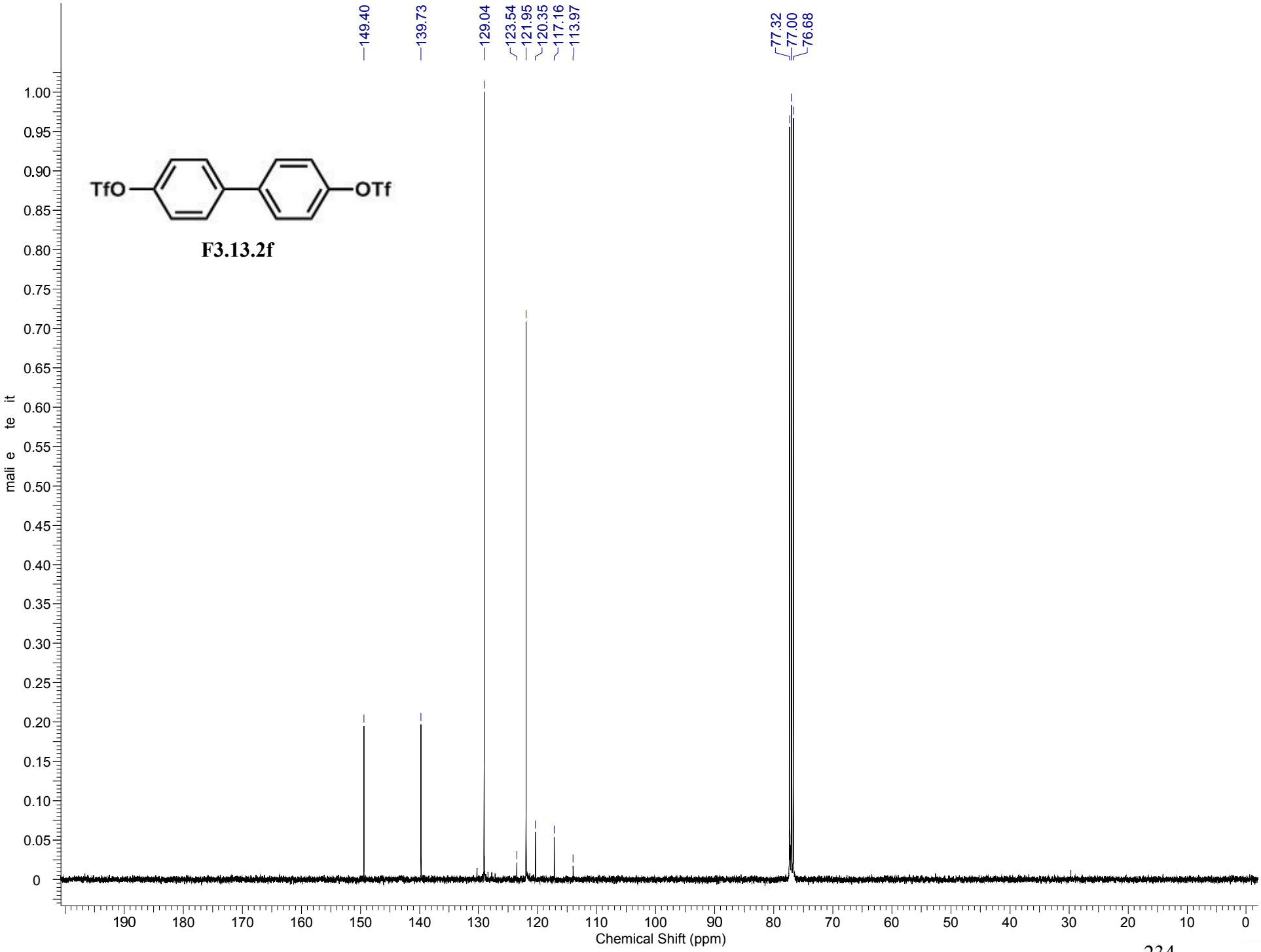
149.40
139.73
129.04
123.54
121.95
120.35
117.16
113.97
77.32
77.00
76.68
TfO
OTf
F3.13.2f
mali e te it
Chemical Shift (ppm)

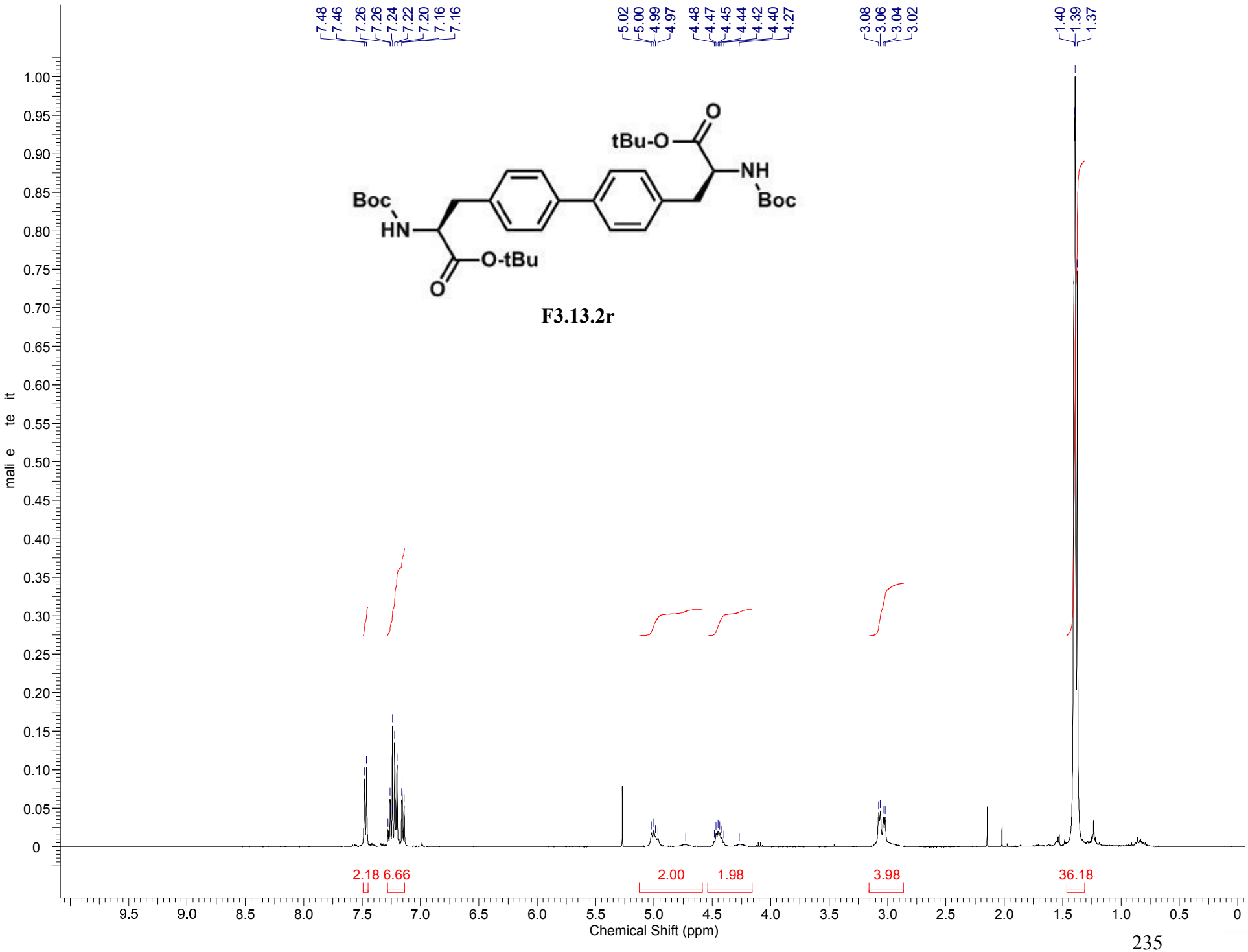
7.48
7.46
7.26
7.26
7.24
7.22
7.20
7.16
7.16
5.02
5.00
4.99
4.97
4.48
4.47
4.45
4.44
4.42
4.40
4.27
3.08
3.06
3.04
3.02
1.40
1.39
1.37
tBu-O
O
NH
Boc
Boc
HN
O-tBu
O
F3.13.2r
mali e te it
Chemical Shift (ppm)
2.18
6.66
2.00
1.98
3.98
36.18

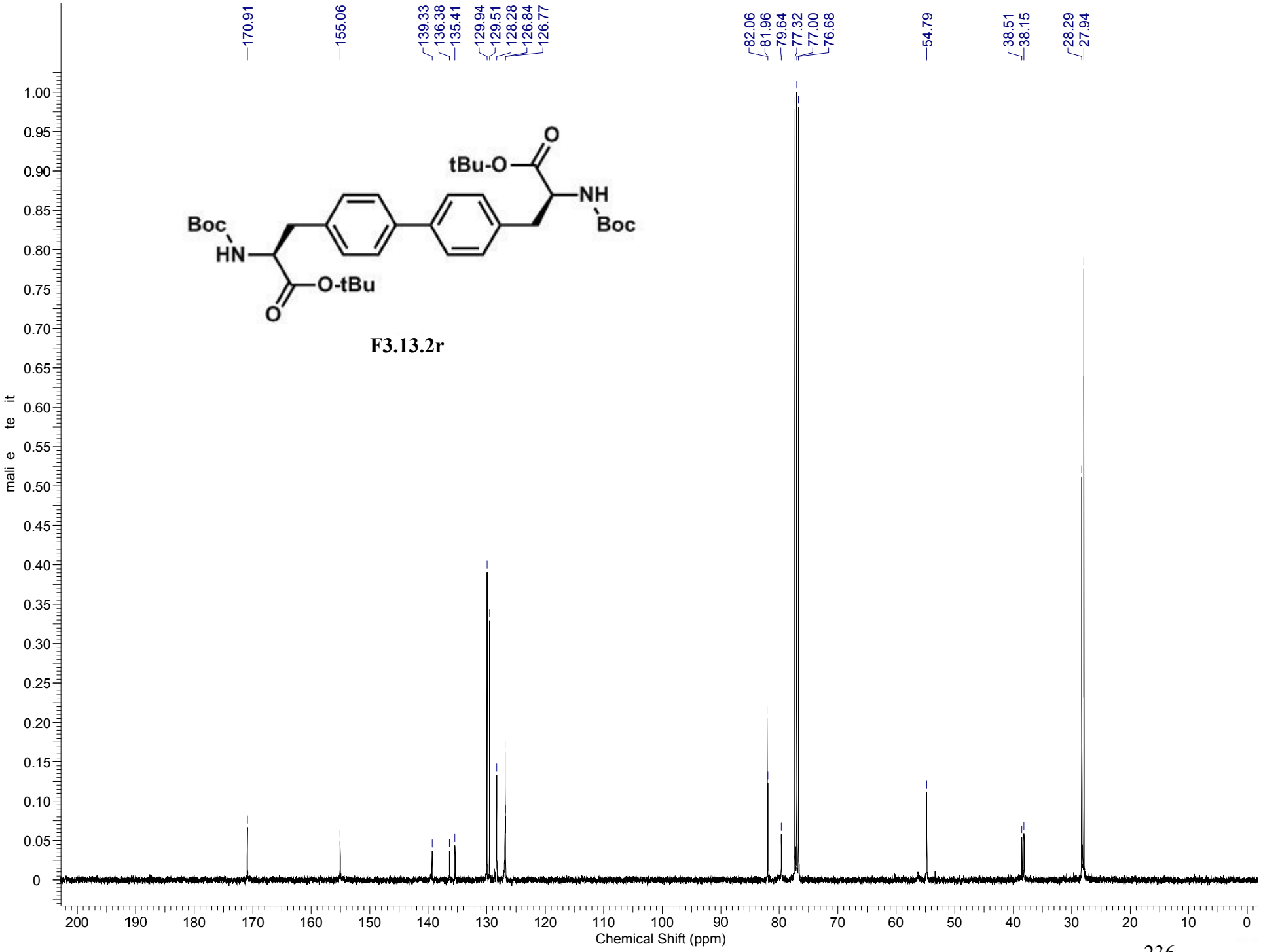
170.91
155.06
139.33
136.38
135.41
129.94
129.51
128.28
126.84
126.77
82.06
81.96
79.64
77.32
77.00
76.68
54.79
38.51
38.15
28.29
27.94
tBu-O
O
NH
Boc
Boc
HN
O-tBu
O
F3.13.2r
mali e te it
Chemical Shift (ppm)

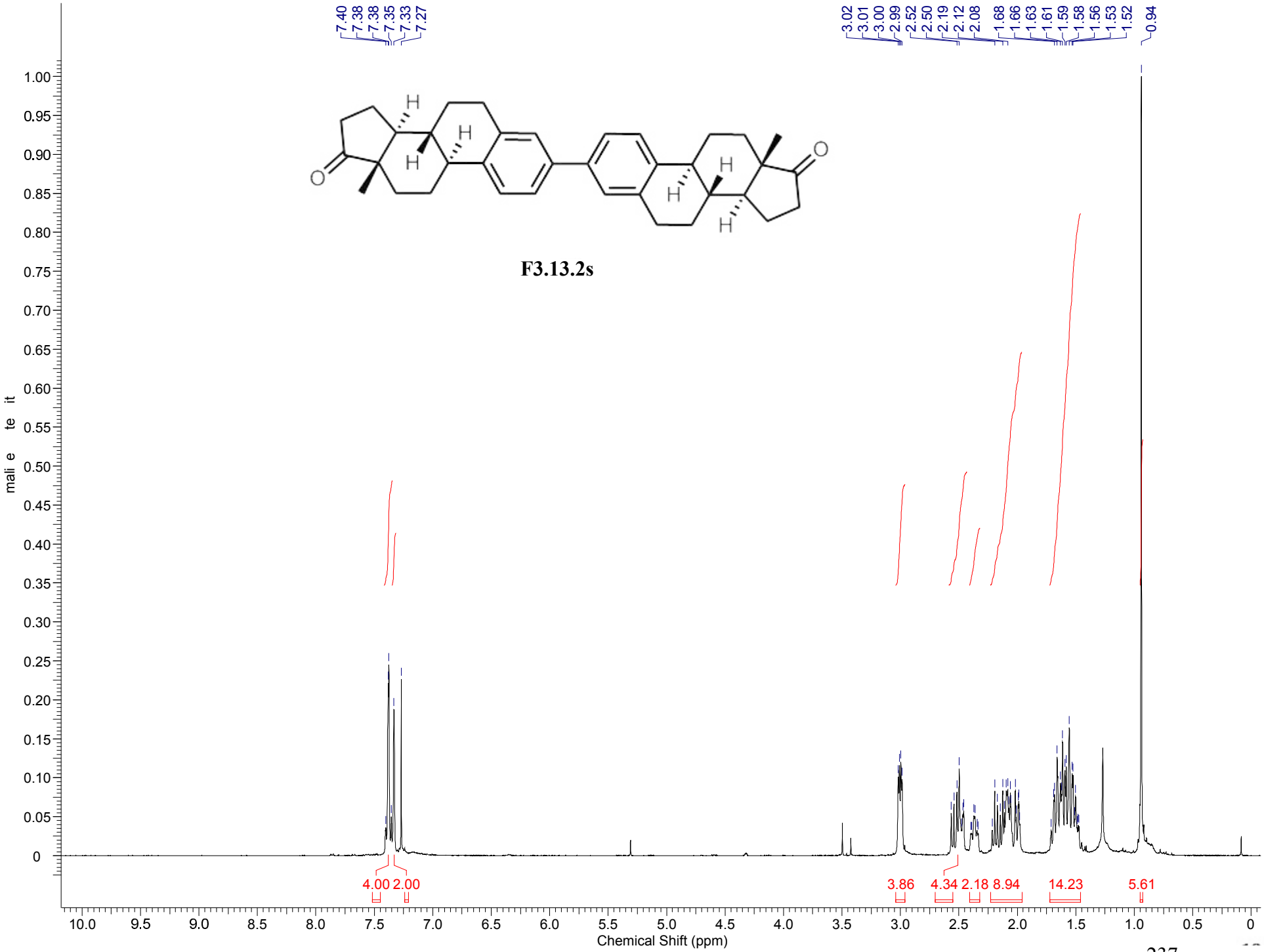
7.40
7.38
7.38
7.35
7.33
7.27
3.02
3.01
3.00
2.99
2.52
2.50
2.19
2.12
2.08
1.68
1.66
1.63
1.61
1.59
1.58
1.56
1.53
1.52
0.94
mali e te it
Chemical Shift (ppm)
4.00
2.00
3.86
4.34
2.18
8.94
14.23
5.61

F3.13.2s

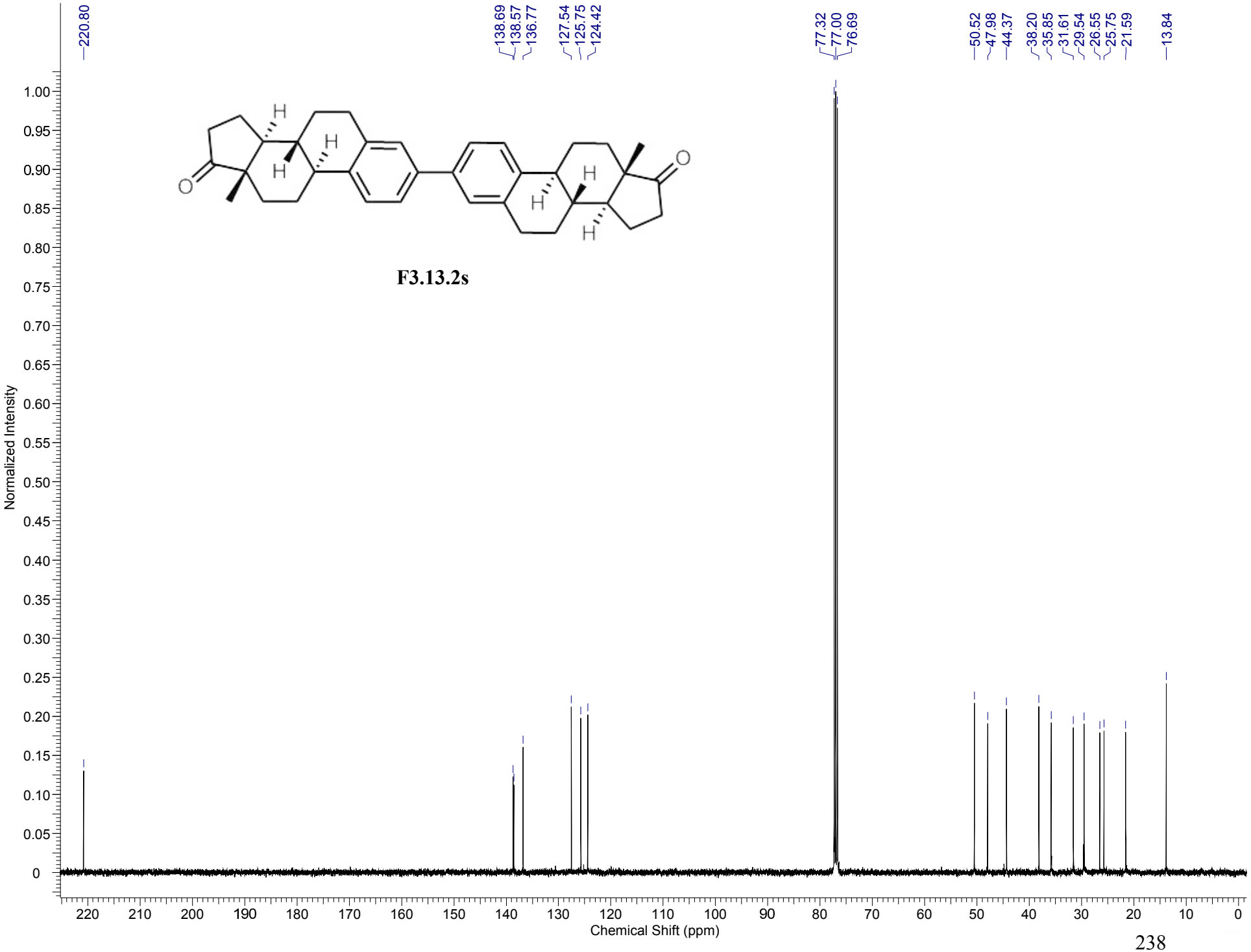
220.80
138.69
138.57
136.77
127.54
125.75
124.42
77.32
77.00
76.69
50.52
47.98
44.37
38.20
35.85
31.61
29.54
26.55
25.75
21.59
13.84
Normalized Intensity
Chemical Shift (ppm)

F3.13.2s

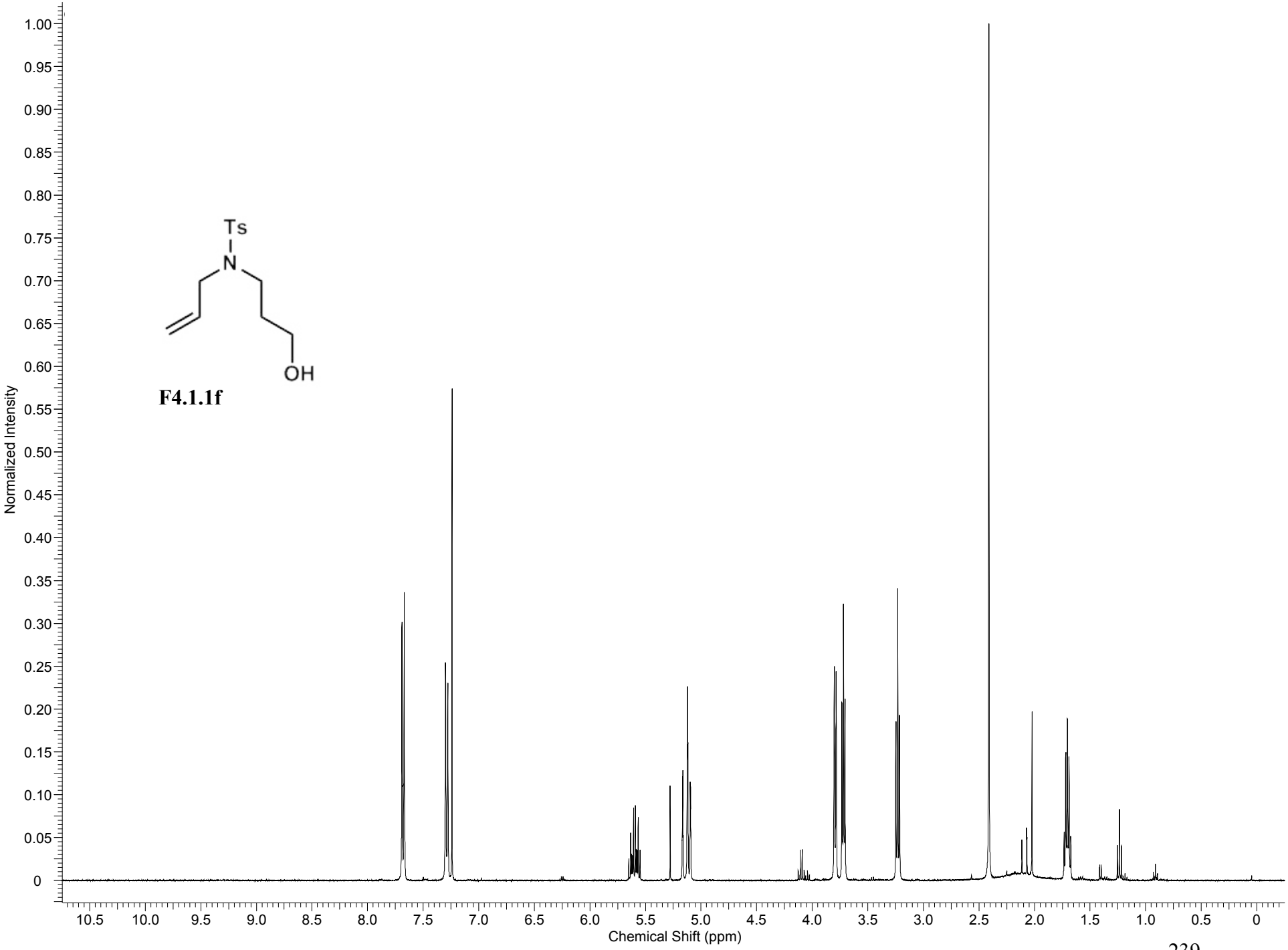
Ts
N
OH
F4.1.1f
Normalized Intensity
Chemical Shift (ppm)

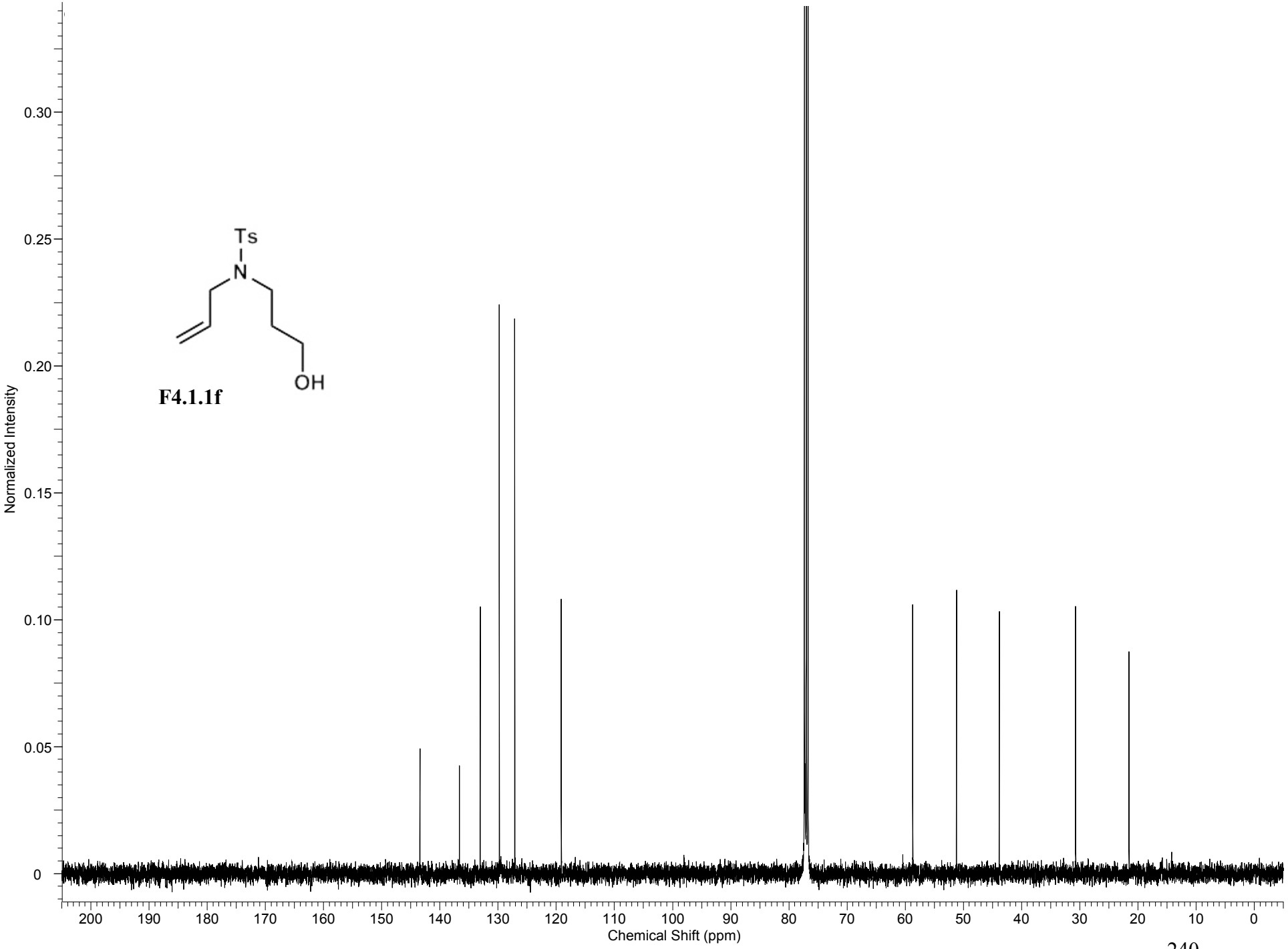
Ts
N
OH
F4.1.1f
Normalized Intensity
0.30
0.25
0.20
0.15
0.10
0.05
0
200
190
180
170
160
150
140
130
120
110
100
90
80
70
60
50
40
30
20
10
0
Chemical Shift (ppm)

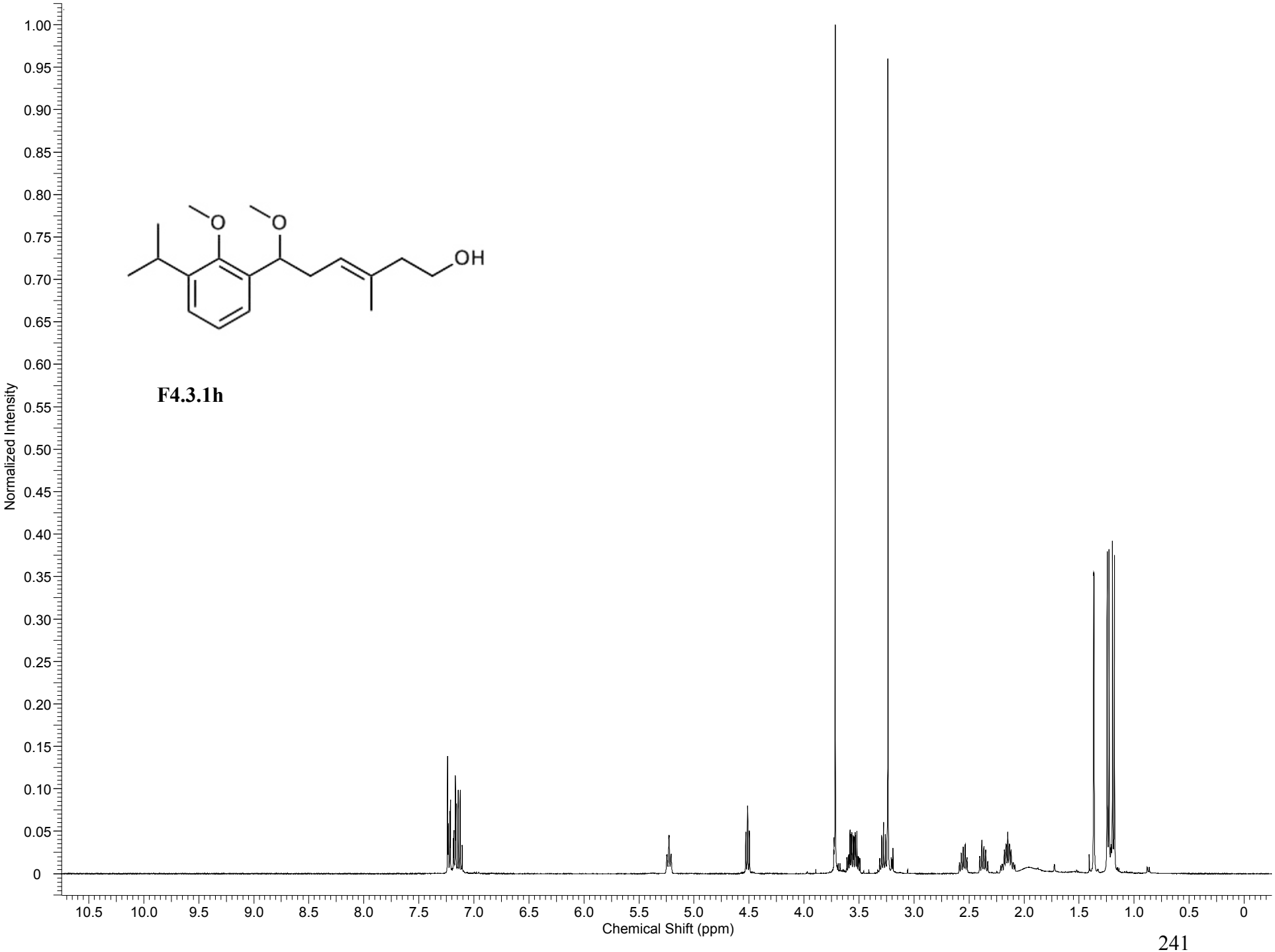
O
O
OH
F4.3.1h
Normalized Intensity
1.00
0.95
0.90
0.85
0.80
0.75
0.70
0.65
0.60
0.55
0.50
0.45
0.40
0.35
0.30
0.25
0.20
0.15
0.10
0.05
0
10.5
10.0
9.5
9.0
8.5
8.0
7.5
7.0
6.5
6.0
5.5
5.0
4.5
4.0
3.5
3.0
2.5
2.0
1.5
1.0
0.5
0
Chemical Shift (ppm)

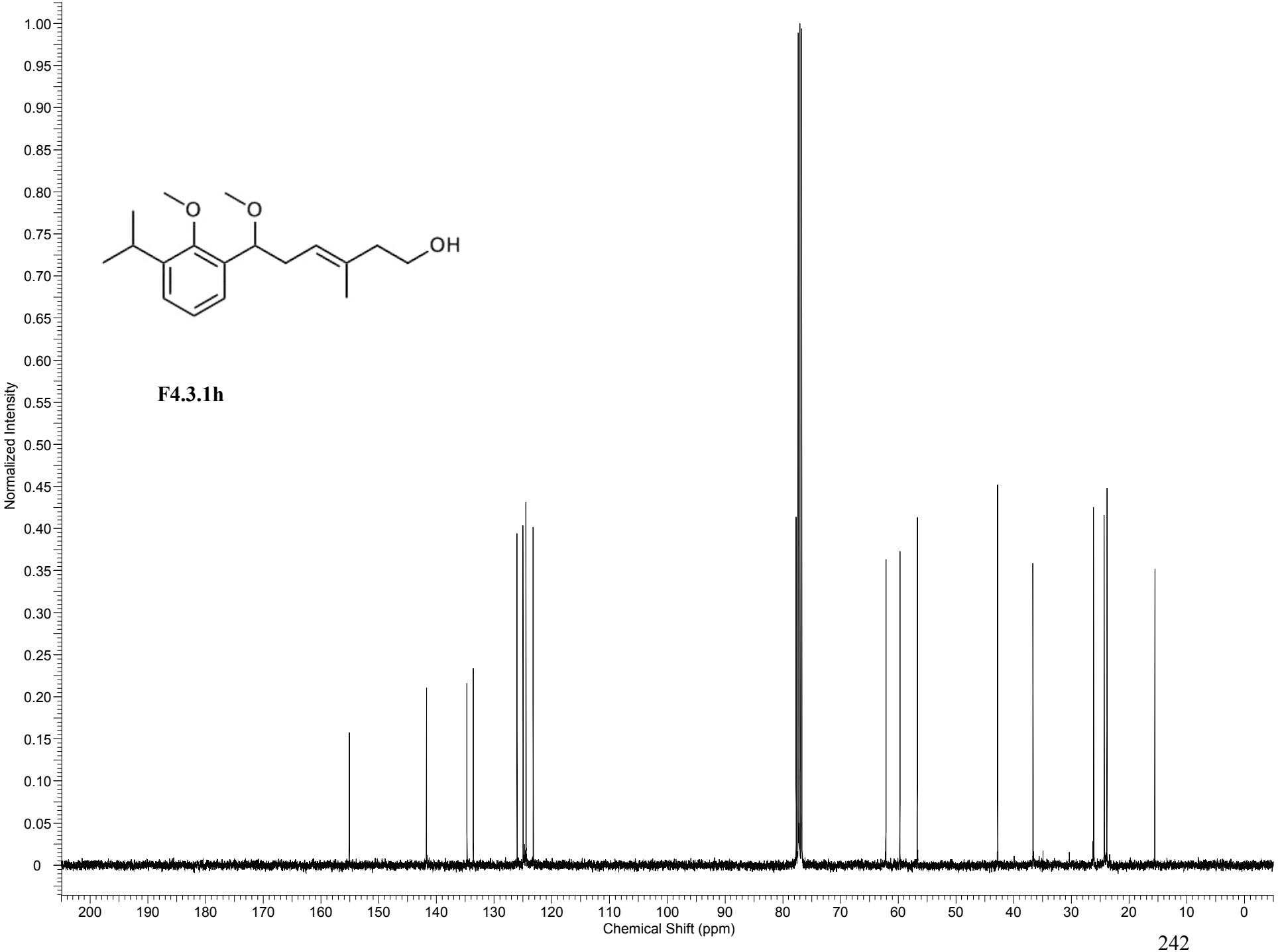
O
O
OH
F4.3.1h
Normalized Intensity
1.00
0.95
0.90
0.85
0.80
0.75
0.70
0.65
0.60
0.55
0.50
0.45
0.40
0.35
0.30
0.25
0.20
0.15
0.10
0.05
0
200
190
180
170
160
150
140
130
120
110
100
90
80
70
60
50
40
30
20
10
0
Chemical Shift (ppm)

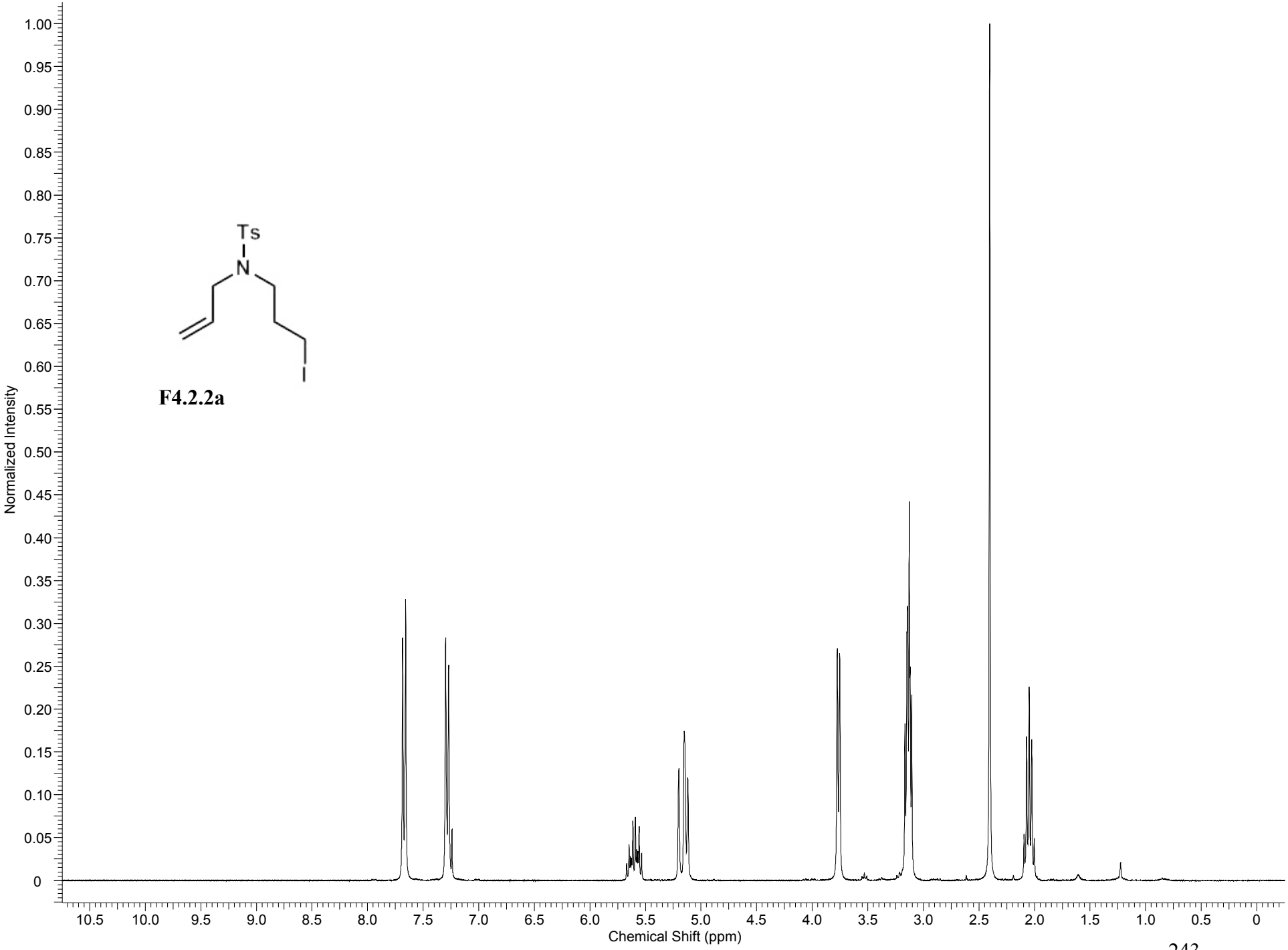
Ts
N
I
F4.2.2a
Normalized Intensity
1.00
0.95
0.90
0.85
0.80
0.75
0.70
0.65
0.60
0.55
0.50
0.45
0.40
0.35
0.30
0.25
0.20
0.15
0.10
0.05
0
10.5
10.0
9.5
9.0
8.5
8.0
7.5
7.0
6.5
6.0
5.5
5.0
4.5
4.0
3.5
3.0
2.5
2.0
1.5
1.0
0.5
0
Chemical Shift (ppm)

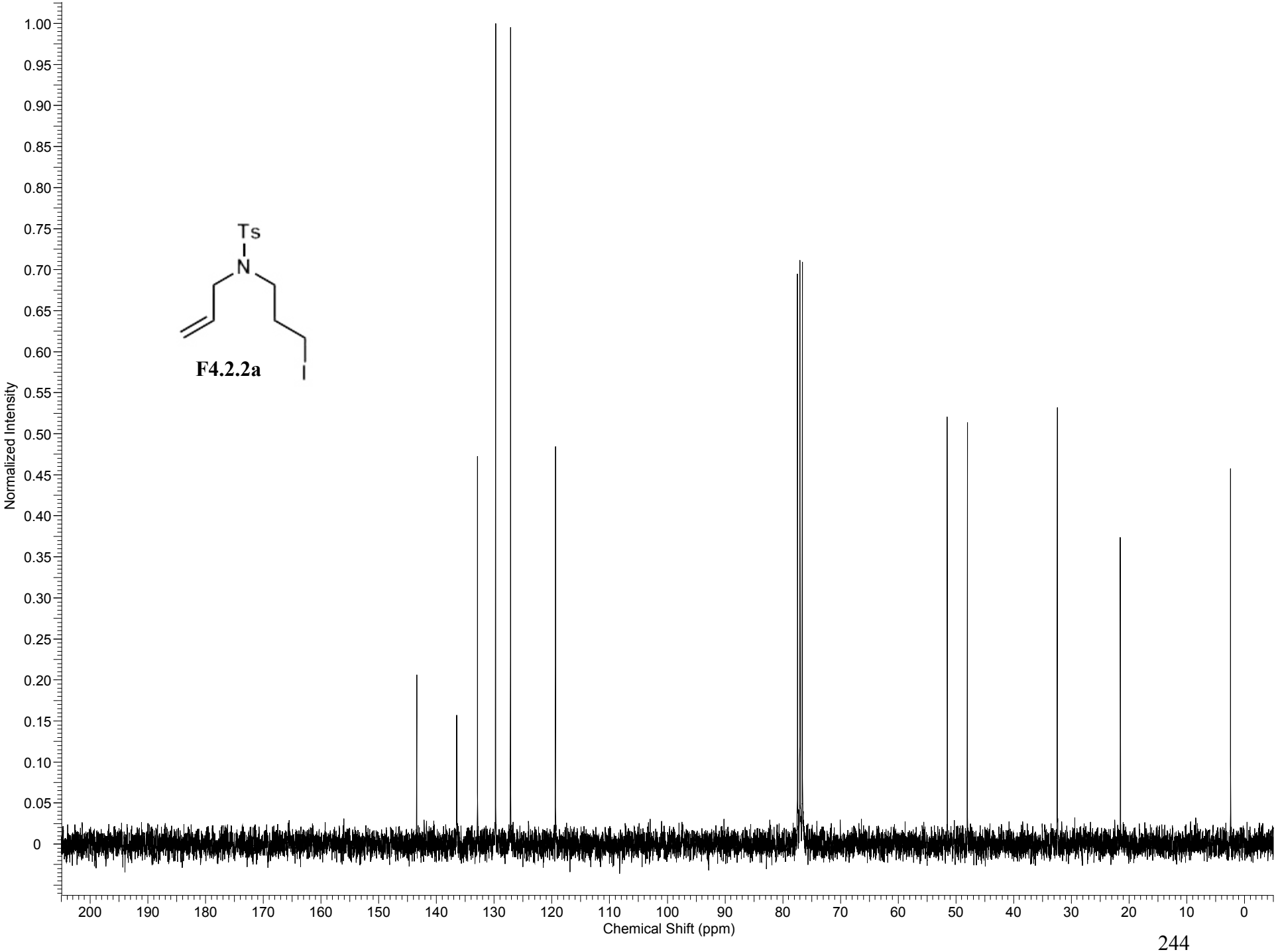
Ts
N
I
F4.2.2a
Normalized Intensity
1.00
0.95
0.90
0.85
0.80
0.75
0.70
0.65
0.60
0.55
0.50
0.45
0.40
0.35
0.30
0.25
0.20
0.15
0.10
0.05
0
200
190
180
170
160
150
140
130
120
110
100
90
80
70
60
50
40
30
20
10
0
Chemical Shift (ppm)

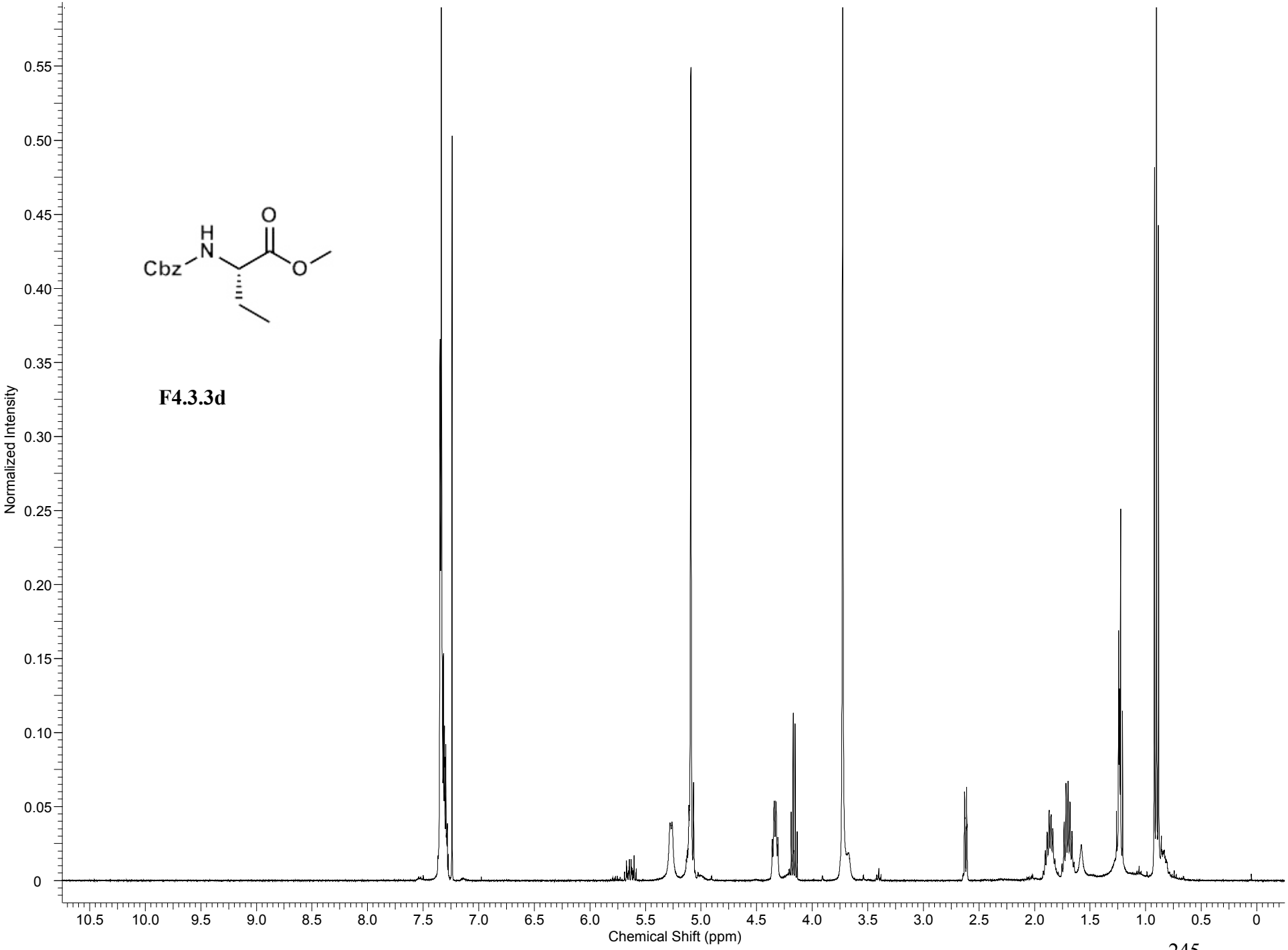
Cbz
H
N
O
O
F4.3.3d
Normalized Intensity
0.55
0.50
0.45
0.40
0.35
0.30
0.25
0.20
0.15
0.10
0.05
0
10.5
10.0
9.5
9.0
8.5
8.0
7.5
7.0
6.5
6.0
5.5
5.0
4.5
4.0
3.5
3.0
2.5
2.0
1.5
1.0
0.5
0
Chemical Shift (ppm)

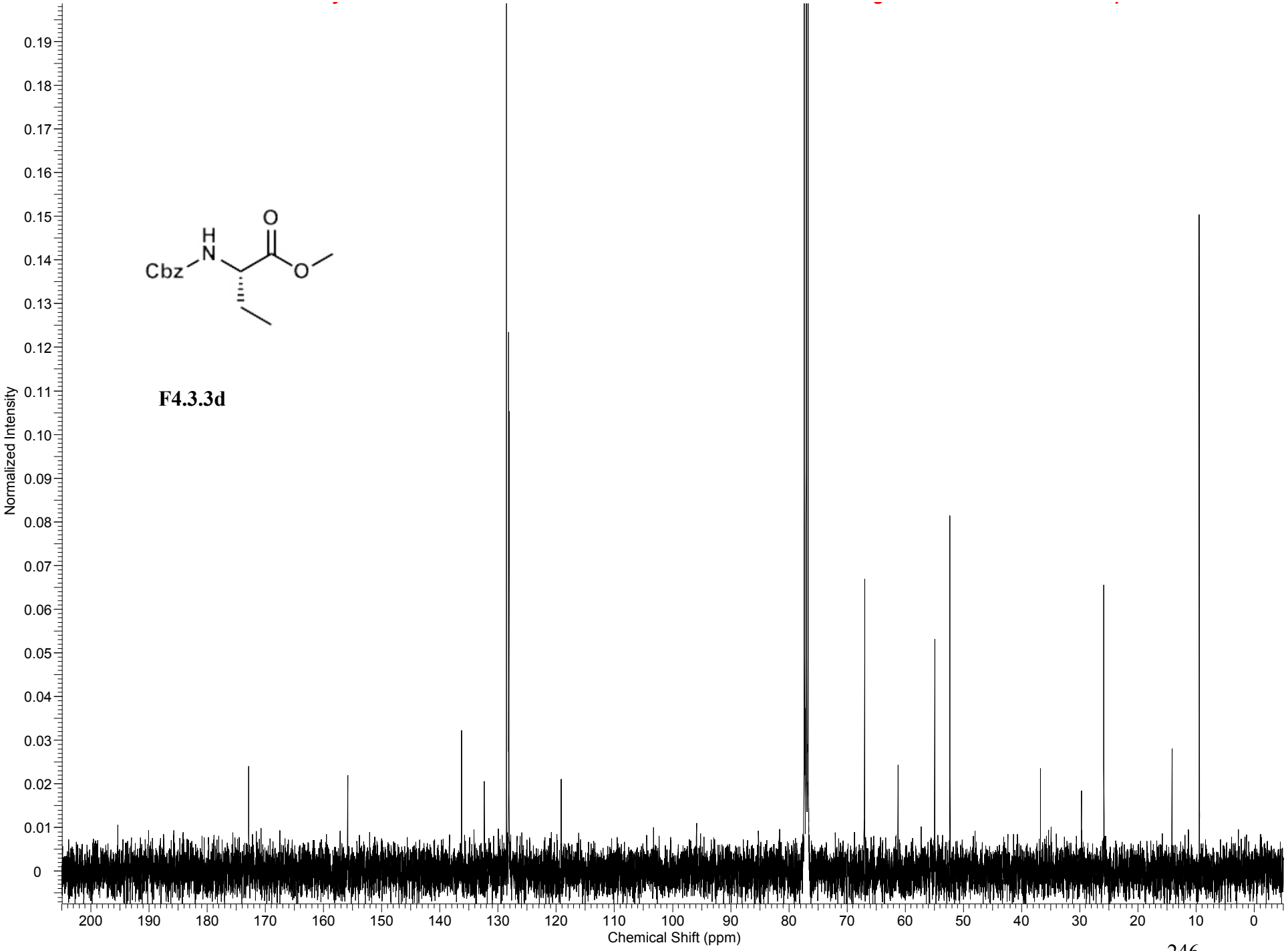
Cbz
H
N
O
O
F4.3.3d
Normalized Intensity
0.19
0.18
0.17
0.16
0.15
0.14
0.13
0.12
0.11
0.10
0.09
0.08
0.07
0.06
0.05
0.04
0.03
0.02
0.01
0
200
190
180
170
160
150
140
130
120
110
100
90
80
70
60
50
40
30
20
10
0
Chemical Shift (ppm)

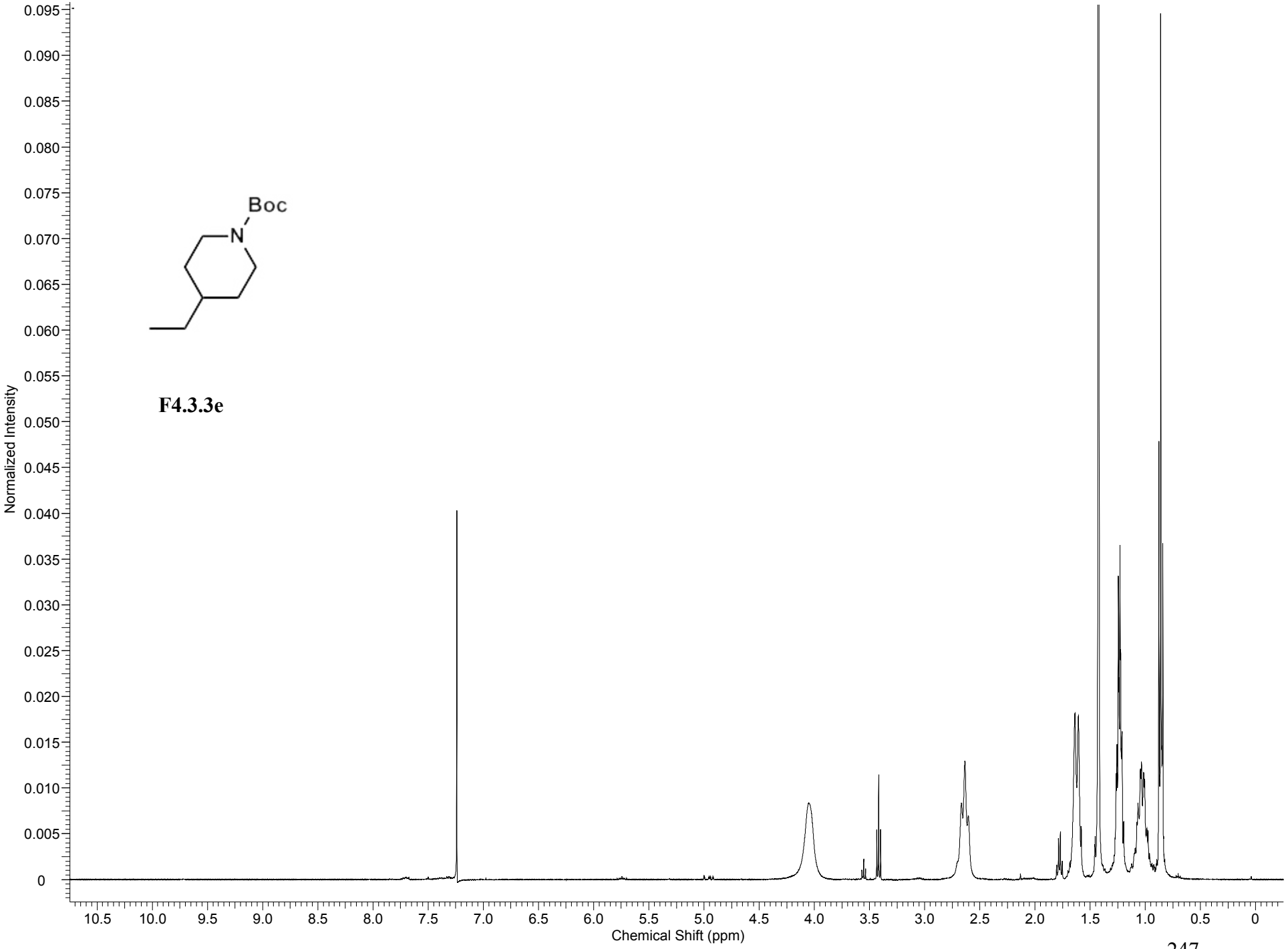
Boc
N
F4.3.3e
Normalized Intensity
0.095
0.090
0.085
0.080
0.075
0.070
0.065
0.060
0.055
0.050
0.045
0.040
0.035
0.030
0.025
0.020
0.015
0.010
0.005
0
10.5
10.0
9.5
9.0
8.5
8.0
7.5
7.0
6.5
6.0
5.5
5.0
4.5
4.0
3.5
3.0
2.5
2.0
1.5
1.0
0.5
0
Chemical Shift (ppm)

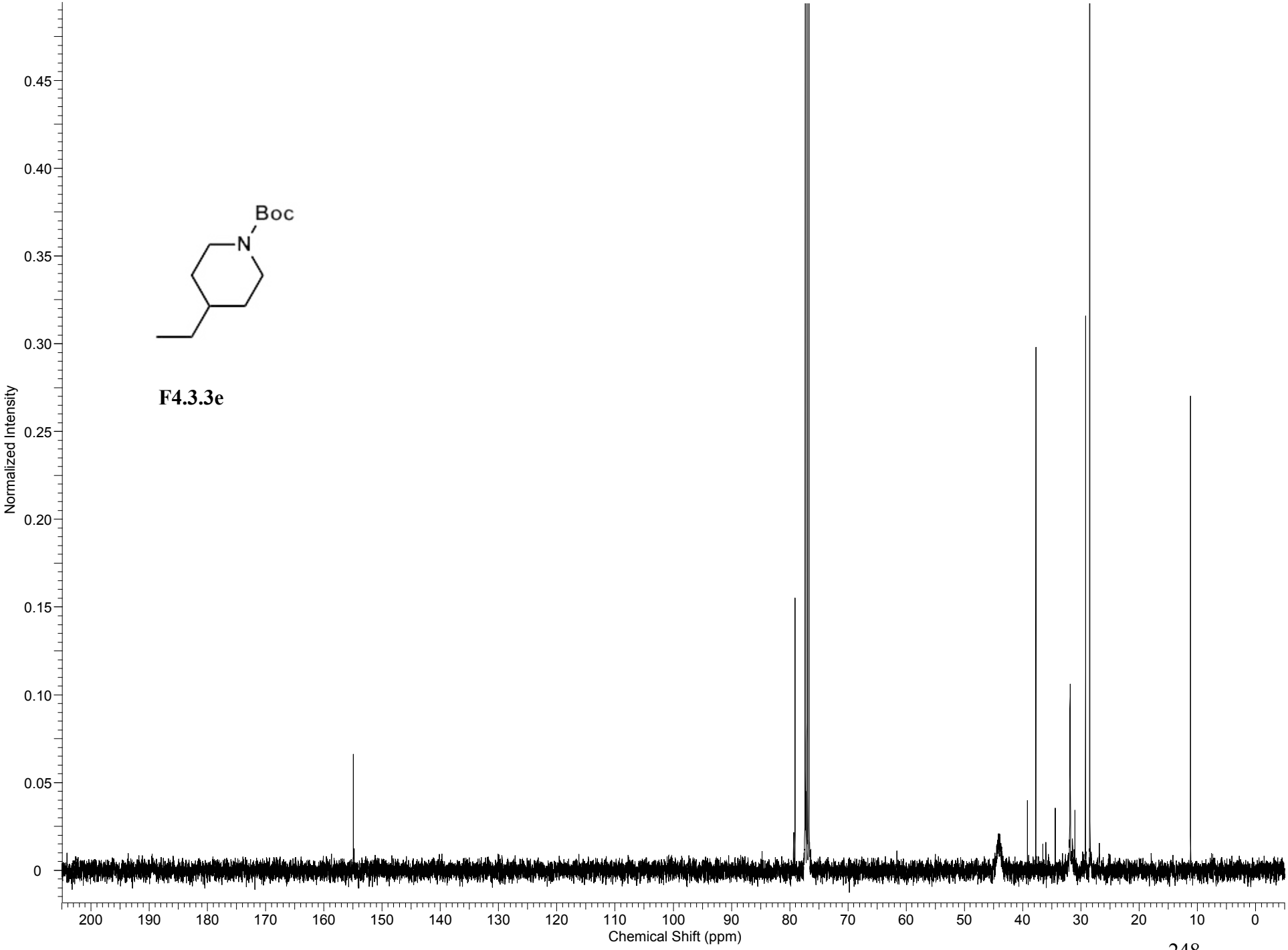
Boc
N
F4.3.3e
Normalized Intensity
0.45
0.40
0.35
0.30
0.25
0.20
0.15
0.10
0.05
0
200
190
180
170
160
150
140
130
120
110
100
90
80
70
60
50
40
30
20
10
0
Chemical Shift (ppm)

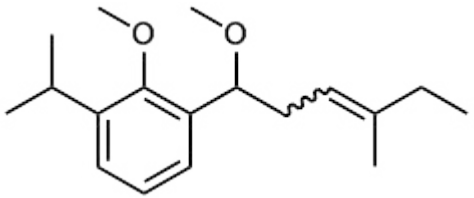

F4.3.3h

Normalized Intensity
1.00
0.95
0.90
0.85
0.80
0.75
0.70
0.65
0.60
0.55
0.50
0.45
0.40
0.35
0.30
0.25
0.20
0.15
0.10
0.05
0
10.5
10.0
9.5
9.0
8.5
8.0
7.5
7.0
6.5
6.0
5.5
5.0
4.5
4.0
3.5
3.0
2.5
2.0
1.5
1.0
0.5
0
Chemical Shift (ppm)

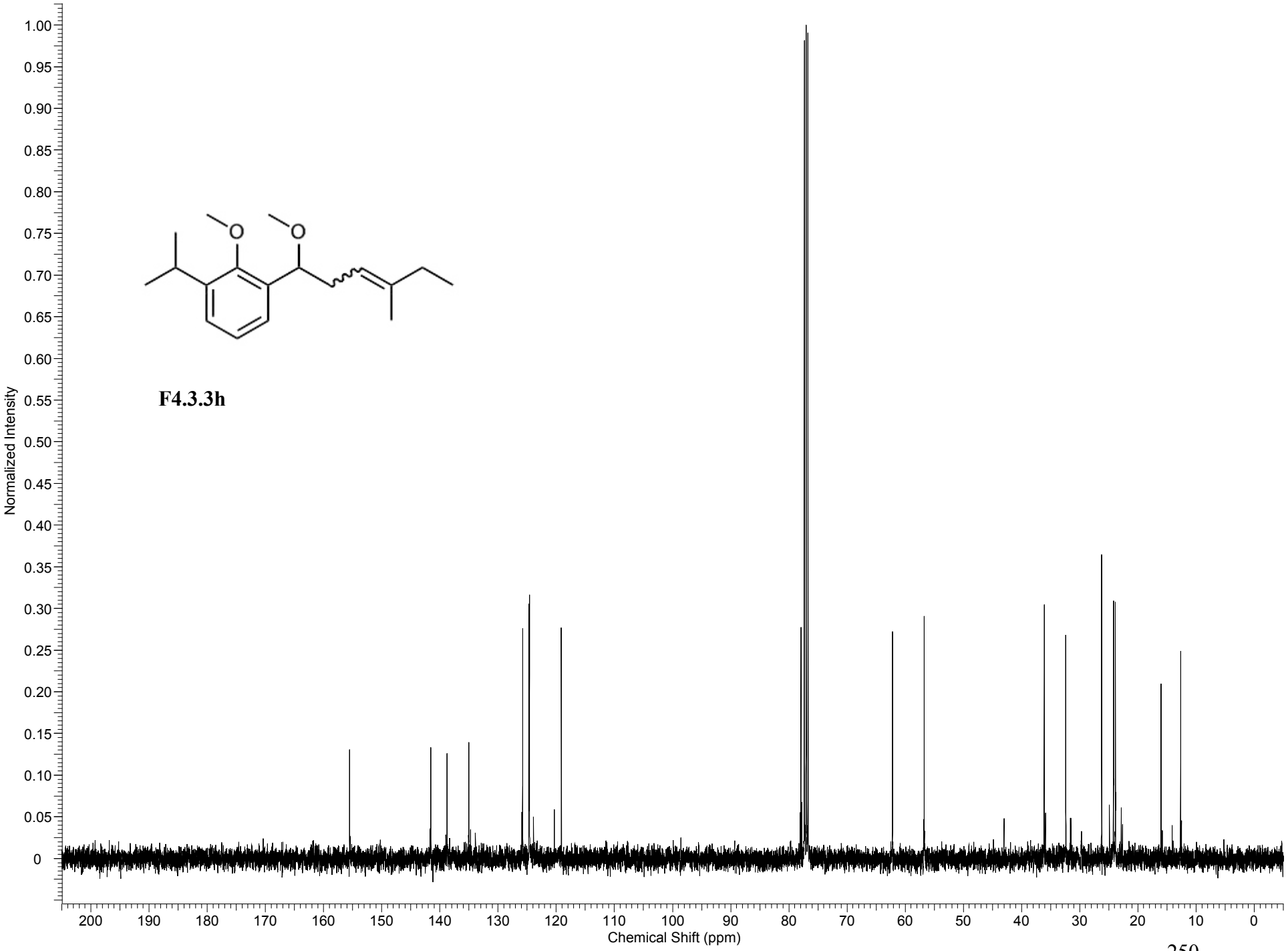
F4.3.3h
Normalized Intensity
1.00
0.95
0.90
0.85
0.80
0.75
0.70
0.65
0.60
0.55
0.50
0.45
0.40
0.35
0.30
0.25
0.20
0.15
0.10
0.05
0
200
190
180
170
160
150
140
130
120
110
100
90
80
70
60
50
40
30
20
10
0
Chemical Shift (ppm)